# CHARACTERIZATION OF THE TORSIONAL OPTOKINETIC RESPONSE TO ROLLING VISUAL FIELDS IN HUMANS

by

Dana Keoki Jackson

S. B., Massachusetts Institute of Technology, 1989

Submitted to the Department of Aeronautics and Astronautics

in Partial Fulfillment of the Requirements for the

Degree of Master of Science

in Aeronautics and Astronautics

at the

Massachusetts Institute of Technology

February 1992

Signature of Author

Department of Aeronautics and Astronautics
November 19, 1991

Certified by

Laurence R. Young, Thesis Supervisor
Professor of Aeronautics and Astronautics

Accepted by

Harold Y. Wachman
Professor of Aeronautics and Astronautics
Chairman, Departmental Graduate Committee

# CHARACTERIZATION OF THE TORSIONAL OPTOKINETIC RESPONSE TO ROLLING VISUAL FIELDS IN HUMANS

by

Dana Keoki Jackson

Submitted to the Department of Aeronautics and Astronautics
in Partial Fulfillment of the Requirements for the
Degree of Master of Science
in Aeronautics and Astronautics

## ABSTRACT

Due to the difficulty in accurately measuring torsional eye movements, virtually no experiments have studied the optokinetic responses to rolling visual fields in detail. This experiment had three aims: (1) Evaluation of the slow phase velocity (SPV) and tonic eye deviation during torsional optokinetic nystagmus (OKN); (2) Investigation of torsional optokinetic afternystagmus (OKAN); and (3) Comparison of eye movements with visually induced perception of self motion--roll vection.

Seven subjects were tested using a full field dome stimulus, covered inside with randomly placed dots, which rotated about the visual axis. Eye torsion was measured using a highly accurate magnetic search coil technique. Subjects were tested in erect and supine orientations using both counterclockwise and clockwise stimuli at four speeds between 15°/second and 60°/second. Aftereffects following optokinetic stimulation were recorded under three visual field conditions: in the light, in the dark with a fixation LED, and in complete darkness.

The SPV gain during OKN was shown to be quite low and highly variable, and to decrease with increasing stimulus velocity. Contrary to prior expectations, the majority of subjects demonstrated lower SPV gains supine than erect. This decline from erect to supine may have resulted from habituation, as adaptive effects were observed over the course of each session.

Contrary to previous studies, mean eye position was found to deviate in the direction of the fast phase during OKN. Tonic deviation increased with increasing SPV. While a single line through the origin best related ocular deviation to SPV for supine runs, the linear fits were translated in the direction of the slow phase for erect tests. The shift may have resulted from static ocular counterrolling induced by a central recomputation of the gravity vector.

Time constants of SPV decay during OKAN were found to average 2.4 seconds. OKAN time constants were shortened by both otolith suppression and visual information. The short time constant of SPV decay indicates that velocity storage is generally underdeveloped for torsion in human subjects.

Cross-correlation of roll vection with torsional SPV and eye position demonstrated that the perceptual and eye movement processes are not closely linked. Consistently greater eye deviation in the direction of the fast phase during vection indicated that vection and OKN may share some basic mechanisms.

Thesis Supervisor:    Laurence R. Young
                             Professor of Aeronautics and Astronautics

# ACKNOWLEDGEMENTS

My time at the Man-Vehicle Lab has been a "learning experience," with all of the ups and down the term implies. On the whole, I am grateful to Prof. Larry Young, who rescued me from the wasteland of the Engineering Internship Program and set me on the path of science (if not of righteousness) by granting me the opportunity to work on a shuttle Spacelab mission.

While many people have helped me to attain that coveted threshold of thesis completion, it is safe to say that nothing would have been completed without the assistance of Glenn Law. He helped me survive the desert, then ran all of my experiments (with the exception of the times he was the subject), while I punched computer keys and moaned about my broken arms. What can I say, except thanks--and may all your days be like Mardi Gras. Likewise, I wouldn't have made it this far without all the help and computer savvy that Nick Groleau provided.

I offer special thanks to Sherry Modestino, Jim Costello, Beverly Linton, and Kim Tseko; I have a feeling that you keep the world spinning on its axis. Dr. Dan Merfeld--lord of all you survey--you were virtually a surrogate advisor, and you even managed to keep us awake in those SLS-1 meetings. Jock Christie, MS--harvester of aluminum and scourge of the environmentally incorrect--you have been a model of virtue in an otherwise imperfect world. Wild and wacky Dava "Hotel" Newman, you've added color to my life, and gone far beyond the call of duty in keeping me under your roof. Thanks to all of you for keeping me going.

Mom, Dad, and the rest of the family--your love and support made everything possible. Dear Alissa--I don't know how you put up with me for so long, but you kept me mostly sane through qualifiers, busted limbs, and even this thesis. I think there's a special place in heaven (or Hawaii, at least) for people like you. Richard X. Seet--you've provided inspiration for a lifetime. Finally, many thanks to the beers, tunes, swimming, and the people who put it all together (Tina Grosskopf, Al Nash, Brad McGrath, Dave Seal, Glenn again, and all the rest)--you made it all worthwhile.

# CONTENTS

# FIGURES

8

# TABLES

# 1. INTRODUCTION

In 1820, Purkinje wrote that *Gesichtstäuschungen sind Sinneswahrheiten*--visual illusions reveal the truth about the senses. The illusions generated in man by large moving visual displays, as well as the accompanying interactions with the vestibular and postural control systems, remain active research topics today. Because these illusions generally result from the action of biologically adaptive mechanisms exposed to novel sensory inputs, they provide insight into the underlying neurologic organization. In turn, this basic research enables understanding of effects ranging from disorientation in high-performance aircraft to illusions and motion sickness in microgravity. Furthermore, appreciation of the functional capabilities and limits of the sensorimotor apparatus permits optimization of man-machine interfaces in areas such as visual displays, vehicle controls, and design of flight simulators.

The experiments detailed in this thesis deal specifically with the effects in humans of wide field displays rotating about the visual axis. Such displays cause reflex eye movements, known as torsional optokinetic nystagmus, which historically have proven difficult to measure accurately at high sampling rates. Postural reactions, possibly related to a central recalculation of the direction of the perceived gravity vector, result as well. Finally, the rotating visual field induces perceptual illusions, including roll vection--a visually induced sensation of full body rotation about the visual axis. Very little information has been collected to date on the compensatory eye movements induced by rolling visual fields. Furthermore, the interactions between reflexive responses and perceptual processes are not fully understood. The thesis experiments described here address these issues.

## 1.1. Motivation for the Experiment

There existed three main motivations for the experiments described in this thesis. First, the design was intended to allow adequate characterization of optokinetically induced torsional eye movements. Next, the experiments were constructed to examine torsional optokinetic

10

afternystagmus (OKAN).  The final purpose of the study was to investigate possible correlations between torsional eye movements and roll vection.

### 1.1.1.  Characterization of Torsional Optokinetic Nystagmus (OKN)

Because of the difficulties inherent in recording torsional eye movements, very little information exists on the properties of optokinetically induced torsion.  At this time only three studies of torsional optokinetic eye movements in humans have been reported which yielded accurate measurements at high sampling rates.  Although each of these experiments utilized a variation of the magnetic search coil technique, two were quite limited in the amount of data acquired and the scope of analysis performed, while the abstract describing the third study yielded little insight.

The first study, by Collewijn et. al. (1985), included only two subjects who were tested erect at stimulus rotation rates ranging from 1.2° to 30°/sec.  The average slow phase velocity (SPV) gain of the resulting torsional OKN was 0.11 at the lowest stimulus speed, and dropped to near 0.035 over the rest of the stimulus range.  The calculated gain was highly variable, and at all speeds the standard deviation of the gain exceeded the mean value.  Part of this variability was likely due to the grouping of results from both subjects and both rotation directions.  These tests indicated no prominent tonic deviation of the eye.

Malan (1985), who performed the second set of experiments, also tested only two subjects.  He recorded torsional OKN with the subjects in erect and supine positions at speeds from 10° to 30°/sec.  Malan's results, which were taken from a very small sample of slow phases, showed SPV gains considerably greater than those reported by Collewijn et. al.  Malan presented mean gains ranging from 0.07 to 0.23.  The variability in Malan's SPV data appears somewhat smaller than that seen by Collewijn, and he did not group results from different subjects or stimulus rotation directions.

However, his results were complicated by his grouping of the gains calculated at all stimulus speeds.  Although he did plot mean SPVs against stimulus speed for each subject, the

data coordinates were not tabulated and values had to be estimated from the graphs. He attempted no analysis of the dependence of SPV gain on stimulus rate. Also, Malan made no comparisons between the SPV erect and supine, although the gains appeared to be somewhat higher supine. Unfortunately, Malan presented no measures of the variability of his gain data, and even cautioned against drawing any conclusions from such a small sample. He did report that the eye appeared to be biased in the direction of the slow phase by approximately 2-3° for the erect trials, although this estimate was probably based on visual inspection of stripchart recordings. He observed no comparable tonic deviation for the supine condition.

The third study, by Morrow and Sharpe (1989), was published only in abstract form. The authors tested 5 subjects using a full-field dome stimulus, and found a decrease in gain from $0.23 \pm 0.09$ at 10°/sec to $0.06 \pm 0.03$ at 80°/sec. They also observed a variable afternystagmus with an SPV decay time constant of $1.3 \pm 1$ sec. No differences were noted between erect and supine conditions.

These three sets of experiments do provide an estimate of the strength of the torsional optokinetic reflex. However, few conclusions can be drawn due to the small sample sizes, grouping of data points, and lack of depth in the analysis. There are some notable differences between the results of the three studies, both in gain values and observed tonic eye deviation. Furthermore, comparisons are complicated by the fact that Malan's eye coil system allowed only monocular observation of the rotating stimulus, while the method used by Collewijn et. al. and Morrow and Sharpe permitted binocular viewing. Studies by Fox et. al. (1978), Wolfe and Held (1979), Wolfe et. al. (1980), and Crites (1980) suggest a binocular contribution to optokinetic nystagmus and ocular torsion.

One objective of the experiments performed for this thesis was a more comprehensive analysis of the torsional slow phase behavior and tonic eye deviation during binocular optokinetic stimulation. This required a subject sample larger than those included in the previous studies. The experimental paradigm was developed to consider the possible effects of

stimulus rotation direction, rotation rate, and the orientation of the subject with respect to the gravity vector. These three variables were deemed important for the following reasons:

- •Individual directional asymmetries frequently appear in the psychophysical responses to visual roll stimuli. (Dolezal and Held, 1975; cited in Henn et. al., 1980)

- •The SPV gain during horizontal OKN drops off at higher stimulus speeds in humans (Dichgans et. al., 1973) and other species (Collewijn, 1981). A similar saturation has been observed for torsional OKN in the rabbit (Collewijn, 1972). However, the results of Morrow and Sharpe (1989) included only 2 data points in describing the dependence of torsional SPV gain on stimulus velocity.

- •Otolith sensing of head tilt relative to the vertical is one cause of ocular counterrolling (Miller, 1961). Studies in both yaw and pitch OKAN have demonstrated decreases in SPV decay time constants for rotations about off-vertical axes (Lafortune et. al., 1990; Clément and Lathan, 1991). A study on torsional OKN and OKAN in the monkey (Schiff et. al., 1986) demonstrated a sharp suppression of both responses when the animal's orientation was changed from supine to upright.

## 1.1.2 Human Torsional Optokinetic Afternystagmus

Data on the eye movement aftereffects of torsional optokinetic stimulation are virtually nonexistent. Collewijn et. al. (1985) made no mention of recording eye movements after the cessation of stimulus rotation. Malan (1985) noted that the eye generally took 20 t o 30 seconds to return gradually to the rest position after the stimulus rotation stopped, but did not observe any afternystagmus. Two explanations for the failure of his stimulus to induce an OKAN seem plausible. First, OKAN is typically a weak and variable response in humans; Malan's small sample population did not preclude the existence of of torsional OKAN. In addition, a stationary visual surround is known to suppress OKAN, resulting in a rapid decrease in slow phase eye velocity (Cohen et. al., 1977). In Malan's experiment, the visual stimulus was still illuminated after the rotation stopped.

Despite the lack of prior evidence for torsional OKAN, a few nystagmic beats were occasionally observed after the stop of the rotating stimulus in preliminary tests for this thesis. These trial experiments, which were run on one subject (M) and were conducted entirely in the light, indicated the possible existence of torsional OKAN. Thus, the second main objective of

this study became an examination of the eye movements which occur following the removal of the rotating stimulus.

Studies on yaw OKAN suggested two important effects which could be evaluated within the framework of the experiments undertaken here. First, the possible suppression of torsional OKAN by a stationary visual field could be investigated by recording eye movement aftereffects both in the light and in darkness. Second, the influence of the relative direction of the gravity vector on torsional OKAN could be tested by comparing erect and supine runs. Several studies have demonstrated otolith involvement in regulation of the "velocity storage" integrator responsible for OKAN. These include the depressed post-rotatory nystagmus observed following longitudinal rotations about off-vertical axes and the "dumping" of central velocity storage caused by head tilts after yaw rotation (reviewed by Benson, 1974). More recently, Lafortune et. al. (1990) demonstrated that static tilts about the pitch axis produced a significant reduction in the decay time constant of horizontal OKAN slow phase eye velocity. Clément and Lathan (1991) observed a similar reaction for roll tilts during pitch OKAN, while Schiff et. al. (1986) found suppression of torsional OKAN in monkeys for roll stimuli about off-vertical axes.

## 1.1.3. Possible Correlation of Eye Torsion and Roll Vection

Two main groups of studies have attempted to relate the torsional eye movements and accompanying psychophysical responses induced by stimuli rotating about the visual axis. The first set (Finke and Held, 1978; Wolfe and Held, 1979; Merker and Held, 1980) compared visually induced tilt with ocular torsion measured using an afterimage method. The investigators concluded that eye torsion and the psychophysical responses were controlled by largely independent processes. However, the subjective afterimage technique has some critical deficiencies (Howard and Evans, 1963) and has never been validated as an accurate measure of ocular torsion. The efficacy of attempting to align a luminous rod with an afterimage during a

rapidly beating nystagmus seems dubious at best. An additional drawback to their method involved the inability to measure eye torsion and the induced tilt response simultaneously.

The second group of experiments, conducted through the MIT Man-Vehicle Laboratory, utilized the same rotating dome stimulus incorporated in this thesis. These tests relied on an objective still photography method to record ocular counterrolling, and compared eye torsion with the magnitude of roll vection. The extraction of torsion angles from the eye photographs proved accurate to within $0.5°$. Unfortunately, the camera system limited the sampling rate to 3 Hz.; while any truly tonic mean eye deviation could be measured with reasonable accuracy, the nystagmic beating of the eye could not be captured. Likewise, the low data rate prevented calculations of slow phase velocity.

Crites (1980) reported that "no direct correlation between vection and [the tonic portion of] OCR could be found." Interestingly, the eye deviation measurements collected by Crites demonstrated strong qualitative differences from those obtained in the afterimage experiments. Young et. al. (1981) found that the average ocular torsion shifted in the direction of stimulus rotation during periods of vection for some subjects, but concurred that ocular torsion and visually induced tilt represented essentially independent processes. In contrast, Lichtenberg (1979) suggested from unpublished experiments that a large torsional nystagmus occurred during periods of roll vection, but was absent during vection "dropouts."

In all, the experiments relating psychophysical responses to torsional eye movements have suffered from ocular torsion measurement techniques with questionable reliability and/or low sampling frequencies. The conclusions of the various studies regarding the correlation of the two phenomena also contain some unresolved contradictions. Furthermore, the torsional slow phase velocity or SPV gain might conceivably provide a more reasonable parameter than tonic deviation for comparison with roll vection, since vection describes a perceived rotation rate.

The magnetic search coil system provides an ideal tool for accurate high sampling rate measurement of torsional OKN simultaneous with subjective estimation of roll vection.

Although Collewijn (1985) stated that his stimulus induced a strong sense of vection, it appeared that no measurements of vection were taken during his torsion experiments. Malan (1985) did measure roll vection for his supine runs and visually induced tilt erect, but attempted no systematic correlation of the psychophysical reactions with the torsional eye movements. Thus, the final goal of the experiments reported here was to collect data on subjective roll vection and investigate possible correlations in time with torsional eye position or slow phase velocity.

## 1.2. Organization of the Thesis

Chapter II presents background information and pertinent previous research in the following areas: (1) the sensory end organs, especially in the visual and vestibular systems; (2) reflex eye movements induced by the visual and vestibular systems; (3) the psychophysical effects of wide field moving displays; and (4) possible connections between the compensatory eye movements and psychophysical responses. Chapter III is devoted to descriptions of the experimental apparatus--the vection stimulus, the magnetic search coil system for measuring eye movements, and the data acquisition equipment. Chapter IV describes the actual experiment in detail. A review of the experimental protocol is followed by an overview of the data analysis techniques.

The results of the study are presented in Chapter V. This chapter divides into three sections: (1) a characterization of the slow phase eye velocities during torsional optokinetic nystagmus; (2) an evaluation of torsional optokinetic after-nystagmus; and (3) an examination of tonic eye deviation under optokinetic stimuli. Comparisons of torsional eye movements with vection responses are dealt with in sections 1 (SPV vs. vection) and 3 (position vs. vection). A discussion of the results in the context of past studies and proposed models of visual-vestibular interaction follows each section. Chapter VI summarizes the conclusions and presents suggestions for further study.

16

The Appendices contain important supplemental information, including COUHES approval, subject consent documentation, and step-by-step descriptions of experimental procedures. Raw data parameters for each trial, summaries of subject comments, and hard copies of the computer programs used in the data analysis are presented as well.

# 2. BACKGROUND

## 2.1. Sensory End Organs

The sensory apparatus responsible for dynamic and static spatial orientation relies mainly on visual, vestibular, and to a limited extent somatosensory and proprioceptive inputs. The vestibular system encompasses the body's angular and linear accelerometers, while the visual system is sensitive to a wide variety of moving and static stimuli  Somatosensory and proprioceptive signals provide more limited information regarding tactile cues and joint positions.

### 2.1.1. The Vestibular System

The vestibular end organs, which provide the inertial guidance platform for the sensory system, consist of the vestibular labyrinth in each inner ear. The semicircular canals act as integrating angular accelerometers, while the otolith organs transduce linear acceleration.

#### 2.1.1.1. The Semicircular Canals

The semicircular canals are three nearly orthogonal membranous rings filled with endolymph, a fluid with properties similar to water. During head accelerations, the fluid is displaced relative to the canal walls due to its inertia. In turn, the fluid distorts the cupula, a gelatinous structure which obstructs fluid movement in the canal ampulla. Hair cells located in the crista beneath the cupula transduce this deformation. An overdamped second order torsion pendulum model provides a good first approximation to the semicircular canal dynamics (Steinhausen, 1931). For the human canal, the model estimates the two time constants at 0.0025 sec. (resulting in endolymph velocity proportional to head acceleration in 5-10 ms) and 12 sec. (reflecting the slow decay of cupula displacement for constant head velocity). Because the viscous drag of the canal walls on the endolymph is much greater than the restoring force exerted by cupular displacement over the normal spectrum of head movements, head accelerations are effectively integrated by the canal mechanics. Thus, the resulting primary

afferent discharges are roughly proportional to head angular velocity in the frequency range from 0.1 to 1 Hz.

## 2.1.1.2. The Otolith Organs

The otolith organs are made up of two roughly orthogonal structures: the utricle and the saccule. The dominant plane of the utricular macula is tilted approximately 25°-30° back from Reid's base line (Dai et. al., 1989), while the saccular macula lies largely in the saggital plane. The maculae support fibro-gelatinous membranes containing otoconia--calcium carbonate crystals with a density greater than the surrounding endolymph. Hair cells transduce displacement of the otolithic membrane due to the component of the specific force (gravito-inertial acceleration) vector lying in the dominant plane. Directional polarization of the hair cells allows each organ to perform as a two dimensional linear accelerometer.

Although no differences between utricular and saccular afferent units were seen in the monkey (Fernandez and Goldberg, 1976), only acceleration stimuli in the horizontal (utricular) plane give repeatable results in humans, while the precise function of the sacculus remains undetermined. The sensitivity of the otoliths to the specific force vector permits their operation as graviceptors, effectively signalling head tilt with respect to the gravity vector. Because of the geometry of the utricle, it becomes less sensitive to changes in the gravity vector with increasing lateral head tilt, and is most sensitive when the head is pitched 25° forward, bringing the dominant plane of the utricular macula approximately to the horizontal.

## 2.1.2. The Visual System

The separate visual functions of spatial orientation and object fixation and tracking, with their differing sensory requirements, have prompted a distinction between "ambient" and "focal" vision in primates (Held, 1970). Such a distinction may mirror functional divisions in the anatomy and physiology of the retina. Certain aspects of oculomotor function are also relevant. Eye movements in three dimensions, including ocular torsion, clearly depend on the structure and performance of the oculomotor plant. Additionally, proper interpretation of

retinal information, influencing perception of spatial constancy and self motion, relies on mechanisms for accurately sensing eye position and velocity.

### 2.1.2.1. The Primate Retina

As explained by "duplicity theory," primate vision divides functionally into two different systems relying on distinct groups of photoreceptors. The rods provide great sensitivity during low illumination, and subserve scotopic vision. Photopic vision, which depends on the cones, allows high acuity at high light levels. The differing characteristics of central and peripheral vision follow from the distribution of the two photoreceptor populations across the retina. The majority of cones are concentrated in a central area about 5.2° in diameter called the fovea. While the central island of the fovea contains no rods, the rod concentration rises sharply outside the fovea and reaches a peak approximately 20° from the center. Further into the periphery the rod density declines slowly.

Absolute threshold sensitivity of different parts of the retina correlates well with the distribution of rods. Sensitivity peaks at 20° nasal and 30° temporal are close to the rod density maxima. Likewise, the greatest acuity occurs at the highest cone concentration. Resolving power decreases with decreasing illumination, reflecting the lower sensitivity of the cone system. The tradeoff between sensitivity and acuity is mirrored in the spatial integration capabilities of the rod and cone systems. As the stimulus size is increased, thresholds for detection drop, indicating that spatial summation occurs. Ideal integration is more closely achieved at low illumination levels; good acuity is sacrificed by the rod system to allow spatial addition for higher sensitivity.

Another significant difference between rod and cone vision is seen in the critical fusion frequency, at which two images presented sequentially in time can no longer be distinguished. At high illumination levels, fusion at the fovea does not occur for presentation frequencies below 50 Hz.; frequencies of 10 to 20 Hz. are sufficient to prevent flicker away from the fovea or in dim light. Temporal integration is the functional inverse of the ability to resolve

successive stimuli. Part of the heightened sensitivity of the rod system is due to its high capacity to integrate photons over time. In contrast, the poor temporal integration ability of the cone system permits finer temporal resolution.

In many lower animals, such as the frog and pigeon, ganglion cells in the retina exhibit complex receptive field behavior. The cells may respond to unidirectional motion, the orientation of bars of light in the receptive field, or the number of edges within the field. In contrast, primates and other higher animals exhibit relatively simple concentric receptive field organization. Such animals rely on a highly developed visual cortex to perform much of the processing related to motion and orientation (Dowling and Dubin, 1984).

## 2.1.2.2. The Oculomotor Plant

The globe of the eye within its orbit comprises a heavily overdamped system. The main resistance to movement is generated by viscous rather than inertial forces. Six extraocular muscles work in synergy to permit rotational eye movements with three degrees of freedom (horizontal, vertical, and torsional). However, the muscles cannot be strictly grouped into orthogonally oriented opposing pairs.

Typically, horizontal and vertical eye movements can reach 40°-50° from the central rest position. The torsional range is much smaller, measuring only about 30° peak to peak (Balliet and Nakayama, 1978a). Torsion is probably limited by the mechanical properties of the oculomotor system, as experiments in forced cycloduction pointed toward a "leash" effect at approximately ±15° (Simonsz et. al., 1984).

With the exception of vergence movements, eye movements are generally conjugate and obey Hering's Law of Equal Innervation. "Slow" eye movements include voluntary pursuit of targets and the slow phases of vestibular and optokinetic nystagmus. "Fast" eye movements, consisting of tracking saccades and fast phases of nystagmus, follow a stereotyped "main sequence" relating size, duration and peak velocity. Overall, torsional saccades prove much slower than horizontal saccades of the same magnitude. Horizontal saccades of 5° have peak

velocities of 180°-260°/second, while the same size torsional saccades reach only 75°/second (Collewijn et. al., 1985).

### 2.1.2.3. Sources of Information about Eye Position and Velocity

Central representation of eye position and velocity in space requires a signal accurately representing the position and velocity of the globe in the orbit. There exist two possible sources for such information: proprioception or "inflow" and corollary discharge or "outflow" (Figure 2.1). While vision provides information about movement of images on the retina, such motion could result from changes in either eye or head position.

Efference copy or corollary discharge--the "outflow" hypothesized by Helmholz (1866)--permits differentiation between the retinal displacements due to object motion and eye movements through a comparison of the retinal signal and the corollary discharge. The existence of such a corollary discharge has been demonstrated by paralysis experiments (Matin, cited in Stark and Bridgeman, 1983) and by "eye press" studies (Stark and Bridgeman, 1983). These experiments cause a dissociation of eye motion from the efferent commands to the oculomotor muscles, resulting in an erroneous perception of visual world motion.

Leibowitz et. al. (1986) and Bridgeman (1986) have suggested that only activation of the voluntary pursuit system generates a corollary discharge, producing a perception of object motion. Eye movements caused by the compensatory stabilization system--VOR and OKN-- would not result in a corollary discharge. These investigators use the hypothesized dichotomy between a phylogenetically "old" stabilization system and a "new" pursuit system evolved later to explain several visual illusions, including the oculogyral illusion and concomitant motion of an illuminated point perceived during head translations.

Sherrington (1918) proposed that proprioceptive "inflow" eye position signals subserve discrimination between object motion and eye movement as causes of retinal motion. Because no eye muscle stretch reflex has been found, and the extraocular muscles operate under an unchanging load due to the symmetry of the nearly spherical globe, proprioception has been

22

**a. Outflow theory** (Helmholz, 1866)

Oculomotor
outflow

Corollary
discharge

Extraocular
muscle

Visual
scene

Visual motion
perception
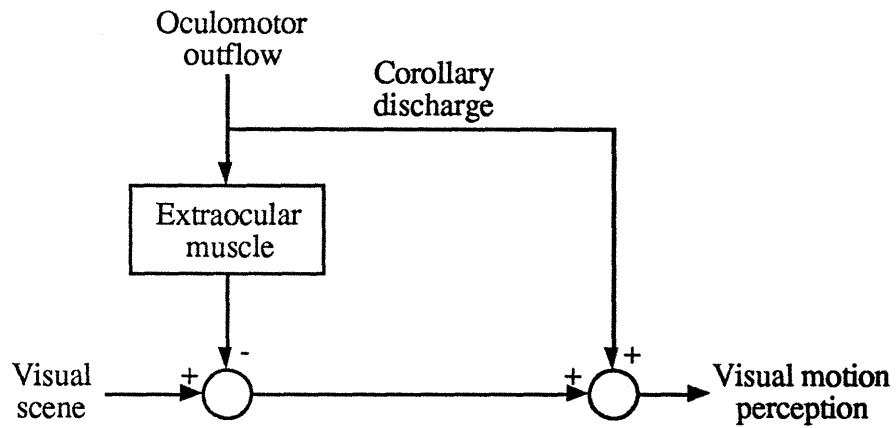
**b. Inflow theory** (Sherrington, 1918)

Oculomotor
outflow

Kinesthetic
inflow

Extraocular
muscle

Visual
scene

Visual motion
perception
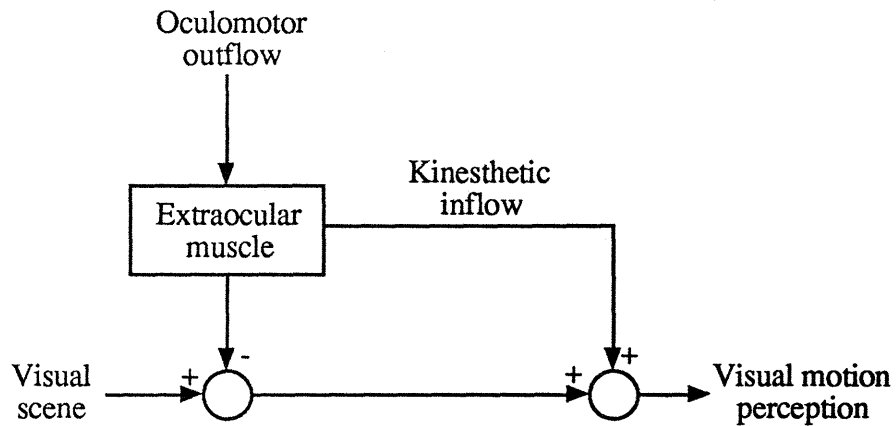
Figure 2.1. Two possible models describing visual motion perception. [a.] In the outflow theory, eye position is signalled by an efferent copy or corollary discharge. [b.] Inflow theory holds that eye position is sensed by receptors in the extraocular muscle. Evidence to date generally supports the outflow model (in Yasui, 1974).

discounted as an important source of eye position information. However, sensory receptors are incorporated in the eye muscles, including muscle spindles, Golgi tendon organs, and palisade endings located at the musculotendonous junction. Data reviewed by Steinbach (1987) indicate that proprioceptive inputs do exist and are probably necessary for the normal development of binocular function. Based on this evidence, outflow or corollary discharge probably provides instantaneous eye position readings while inflow serves as a slow calibrator of eye position with time constants measured in days.

### 2.1.2.4. Measurement of Eye Movements

Evaluation of the functional properties and importance of torsional eye movements requires a method of accurately recording the variety of movements which occur over a range of stimulus conditions. This section is not meant as a comprehensive discussion of eye movement measurement; Young and Sheena (1975) surveyed a wide variety of recording techniques while Law (1991) provided a more complete summary of methods applicable to the investigation of eye torsion. However, evaluation of the results from many previously published experiments relevant to this thesis must take into account the limitations of the eye movement methodologies employed: most often used were subjective afterimage alignment, still photographs, and magnetic induction coils.

In subjective methods, the subject estimates the angular deviation of a line either by direct inspection or alignment with an afterimage. The only advantages of subjective measures are the relative simplicity of the instrumentation and the limited data processing requirements. In contrast, a number of difficulties with subjective estimates have been documented by Howard and Evans (1963) and Fluur (1974):

- •Subjective techniques suffer from high variability--Fluur found an average measurement dispersion of 4.7°.

- •These methods require the use of a visual stimulus. Visual stimuli are know to induce eye torsion; Howard and Templeton (1964) observed torsional nystagmus in response to a rotating luminous line.

•Unavoidably low sampling rates prevent measurement of rapid changes in torsion, such as the nystagmus resulting from optokinetic stimuli.

•Variability in subjective judgment cannot be distinguished from fluctuations in torsion.

•There exists no innate capability for validation of the measure; apparently no validations using objective measures have been attempted.

•Eye torsion and perception of egocentric orientation cannot be recorded simultaneously.

Still photography of the eye has been used in a number of studies to calculate torsion from frame to frame by determining the change in position of iral, scleral, or contact lens landmarks. Torsion measurements generally display a repeatability on the order of 0.5° (Crites, 1980), although Balliet and Nakayama (1978a) claimed a better resolution of ±5 arc minutes. The main drawback of still photography is the low sampling rate (limited to about 3 Hz.), which precludes calculation of slow phase eye velocities. Unless specially marked contact lenses are incorporated, the technique relies on highly resolvable eye landmarks. Thus, some subjects may prove unsuitable for eye movement recording, and blinks interfere with data collection in any case. Finally, extracting torsion records from the series of photographs is an expensive, labor intensive, and time consuming process.

The magnetic induction eye coil method has produced by far the best eye torsion measurements to date. (Robinson, 1963; Collewijn et. al., 1975). Coils of insulated magnet wire can be permanently implanted in the eyes of laboratory animals using surgical techniques. For human subjects, specially wrapped coils fixed within silicone rubber rings may be temporarily mounted on the sclera. Oscillating magnetic fields generated about the subject's head induce signals in the eye coil proportional to the angular deviation of the eye. The capabilities of such a system are impressive. Eye torsion data is available in real time with noise levels as low as 1 arc minute. Measurement bandwidths up to 530 Hz. permit very high sampling rates using digital computer data acquisition. However, the search coil method does have some drawbacks:

•The procedure is somewhat invasive, and requires the use of topical anaesthesia.

•Test sessions are limited to 30 minutes in duration to avoid excessive irritation of the eye.

•A small possibility of corneal abrasion exists. Furthermore, the suction which causes the scleral ring to adhere to the eye contributes to a slight increase in intraocular pressure.

•No intrinsic method of absolute torsional calibration exists for a Robinson-style amplitude detection system (Robinson, 1963).

## 2.2. Reflex Visual Stabilization

The vestibulo-ocular reflex (VOR) and optokinetic nystagmus (OKN) together make up a postural reflex designed to stabilize visual scenes on the retina during movements of the head in space. At its most basic level the VOR relies on a phylogenetically old three-neuron arc consisting of a semicircular canal afferent, a single interneuron and an eye motoneuron. OKN, also referred to as the visual-ocular reflex, tracks large moving fields to augment visual stabilization. Other inputs exert a comparatively minor influence on compensatory eye movement. These include neck proprioception as well as aural (audiokinetic) and tactile (haptokinetic) cues. Reflex compensation can generally be overridden by voluntary fixation and target tracking eye movements.

Body or visual field rotations lasting longer than a few hundred milliseconds generate nystagmic eye movements. The nystagmus consists of compensatory "slow phase" tracking movements interspersed with oppositely directed saccadic "fast phases" which reset the eye position. By convention, the direction of nystagmus refers to the direction of the fast phase. The majority of research concerning compensatory eye movements relates to yaw rotations. Since the the properties of reflexive horizontal movements are generally representative of reflexive compensation about all three axes, yaw motion will be addressed first. The important differences seen for vertical (pitch) and horizontal (roll) compensation will then be discussed, as well as the need for three-dimensional representations to model adequately the visual-vestibular and oculomotor interactions.

### 2.2.1. Horizontal (Yaw) Compensatory Eye Movements
### 2.2.1.1. The Vestibulo-Ocular Reflex (Henn et. al., 1980)

The VOR depends largely on semicircular canal inputs to generate eye movements opposite to head rotations, keeping the visual axis stationary in space. Most natural head movements lie in the frequency range above 0.5 Hz., within which compensatory eye movements approach a gain of 1. Stabilization extends even into the higher frequency range

above 3 Hz. While the gain of the VOR for passive movements reaches a maximum of about 0.8, this value is brought near unity through the combined effects of high accelerations, otolith stimulation, alertness, and neck reflexes.

In response to a rotational velocity step, eye slow phase velocity (SPV) rises abruptly to stimulus velocity, plateaus at this peak value for several seconds, then decays slowly (Figure 2.2a). Neural activity in the vestibular nucleus represents an internal reconstruction of head velocity. The dominant time constant of SPV decay (15-28 sec) in a range of species is quite similar to vestibular nucleus time constants and appears considerably elongated compared to decay times of end-organ afferent activity. If a step from a constant velocity to zero occurs after the beginning of SPV decay, a post-rotatory nystagmus results in the direction opposite to that seen during rotation. If the sudden stop takes place after the SPV has decayed completely to zero, the post-rotatory eye movements approximately equal the per-rotatory response (Figure 2.2a).

The otolith organs also generate compensatory eye movements. During off-vertical axis yaw rotation, SPV decays to a non-zero steady state value. A modulation phase-locked to head orientation with respect to gravity appears superimposed on this tonic velocity component (Benson, 1974). Raphan and Schnabolk (1988) postulate that the steady-state component is generated by a centrally formed velocity estimate. The hypothesized central velocity reconstruction derives from the moving pattern caused by sequential excitation of otolith afferents with different polarization vectors exposed to the rotating gravity vector.

### 2.2.1.2. The Visual-Ocular Reflex and Optokinetic Nystagmus

Wide-field moving displays excite optokinetic eye movements which track visual field motion. In the laboratory, optokinetic nystagmus (OKN) can be generated by drums with various visual patterns rotating about the subject. (Figure 2.2b). Since opposite visual field motion normally accompanies head rotations, OKN usually complements the VOR in stabilizing images on the retina. As the VOR decays for extended rotations, OKN functions to

28
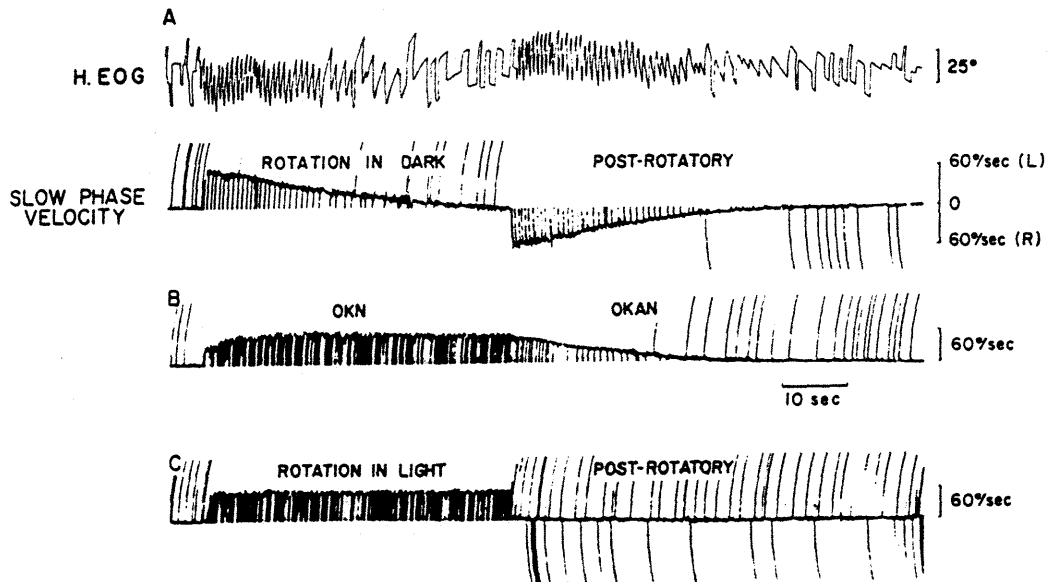
Figure 2.2. Horizontal nystagmus in the monkey induced by: [A] a velocity step of platform rotation in the dark; [B] a step in surround motion; and [C] a step of platform rotation in the light. For the same direction nystagmus during OKN and platform rotation, opposite direction aftereffects are observed. Following rotation in the light, the post-rotatory response was very slight. (in Raphan et. al., 1979)

maintain compensatory eye movements beyond the limits of vestibular sensing. OKN performs poorly for higher frequencies, but is superior to the VOR at low frequencies; when both systems are stimulated together the compensation gain curve remains flat and near unity over a wider range of frequencies (Collewijn, 1981).

In animals with afoveate, laterally placed eyes (such as the rabbit), the gain of OKN is near 0.8 up to about 20°/s and drops off sharply above this speed. For stimuli above a few deg/sec, OKN velocity builds up slowly to maximum over tens of seconds. OKN produced by monocular stimuli is highly asymmetric, with a strong preference for fields moving in the temporo-nasal direction. The lack of responsiveness to fields moving temporo-nasally permits suppression of signals generated during forward translation. A horizontal "visual streak" on the retina (subtending 175° horizontally and 60° vertically) is the area most sensitive to

optokinetic stimuli. In such animals, OKN is produced subcortically in the pretectal nucleus of the optic tract; decortication does not affect the optokinetic system (Collewijn, 1977).

In animals with foveas (primates), OKN gain remains high for much faster stimuli. This is true to a lesser extent for animals with an *area centralis*, such as cats and dogs. In primates, OKN demonstrates a fast rise upon stimulus onset; a slower rise to peak velocity follows in monkeys. For animals with a fovea or *area centralis*, monocular OKN remains generally symmetric. In foveate animals, OKN is probably generated by two processes. The first is a postulated primitive, sub-cortical OKN ("slow" system) similar to the rabbit's, supplemented by inputs fed through the visual cortex.

This old system is overlaid by a "fast," cortically controlled mechanism fed through the cerebellum and pontine nuclei (reviewed by Howard and Simpson, 1989). The "fast" mechanism is probably intimately related to the pursuit system, and presumably evolved to meet the needs of binocular vision by stabilizing visual scenes lying only within the plane of convergence It renders OKN bidirectional in each eye and increases OKN gain, especially for high stimulus velocities (Howard and Simpson, 1989). The two systems have been differentiated as "stier" (stare) and "schau" (look) nystagmus, or passive and active OKN respectively (Ter Braak; cited in Collewijn, 1981). Passive subcortical OKN can best be evoked in human subjects with the instruction "stare straight ahead at the stimulus," while instructions such as "follow the stripes" or "count the stripes" are used when active cortical OKN is desired. Active "look" OKN generally exhibits larger slow phase amplitudes and lower beat frequencies than "stare" OKN (Yasui, 1974).

In accord with the binocular function ascribed to OKN in higher mammals, Fox et. al. (1978) used random-element stereograms to demonstrate that purely stereoscopic contours could produce OKN. They hypothesized that the slower beat frequency observed in stereoscopic tracking compared with OKN from physical contours resulted from delays due to cortical processing. Wolfe et. al. (1980) also found a binocular contribution to OKN in both normal and stereoblind subjects using stroboscopic stimuli presented to the eyes individually.

30

In further studies, Howard and Gonzalez (1987) and Howard and Simpson (1989) found that OKN gain is inversely related to the magnitude of binocular disparity.

Various lesion and ablation experiments have explored the neurological basis of OKN in frontal eyed mammals, and support the existence of a primitive "slow" OKN mediated by the pretectum upon which a phylogenetically newer cortical process has been overlaid. Decortication in cats produces directional asymmetries similar to those in rabbits. Decorticate dogs still demonstrate OKN but with a slower saturation velocity, and lose smooth pursuit following cortical lesions. Lesion studies in monkeys provide further evidence for the existence of subcortical OKN in primates (reviewed by Collewijn, 1981). Infant primates (both monkeys and humans) exhibit directional asymmetries in monocular OKN for several months following birth, while cats deprived of binocular vision during development also demonstrate direction dependent OKN. Such asymmetries likely follow from slow development of cortical mechanisms subserving stereopsis.

For primates, some disagreement exists as to whether OKN is generated primarily by the central visual field or by peripheral stimuli. A study by Dichgans and colleagues (cited in Henn et. al., 1980) demonstrated a strong increase in OKN velocity when the stimulus was extended into the retinal periphery. However, for their narrower stimuli even relatively small eye movements would have effectively moved the fovea away from the moving field. Furthermore, the relative coarseness of the stimulus pattern probably resulted in significant deterioration of the motion stimulus for smaller visual angles

Dubois and Collewijn (1979) utilized a servo-controlled projection system to stabilize the projection area on a selected portion of the retina, effectively generating an open-loop OKN response. They found that diminishing the stimulus diameter decreased the response gain only moderately. However, deleting central portions of the stimulus caused a much more pronounced decline, indicating that the fovea was more powerful for producing OKN than the periphery. Dubois and Collewijn also found that peripheral stimulation elicited higher gains for temporal rather than nasal stimulus motion, a tendency which probably assists foveation.

Howard and Ohmi (1984) confirmed the greater efficacy of the foveal area, showing that occlusion of the central retina severely reduced OKN gain, but only for velocities above 30°/sec.

In the monkey, horizontal OKN peak velocity increases with gain close to 1 up to stimulus speeds of 180°/s. With the onset of field rotation, SPV rises quickly to approximately 60% of stimulus speed, followed by a gradual rise to peak velocity (Cohen et. al., 1977). The gain in humans remains close to unity only up to speeds of 60°-90°/sec. Furthermore, peak velocity is generally achieved within the first slow phase, and no slow increase is seen except in certain patients with malformed foveas (Cohen et. al., 1981).

## 2.2.1.3. Velocity Storage and Optokinetic Afternystagmus

The decay time constant of first-order semicircular canal afferent firing rates is approximately 5 seconds, while the corresponding time constant in humans has been estimated at 7-8 seconds from experiments in off-vertical axis rotation. For prolonged horizontal rotations, vestibular nucleus firing rates in the monkey have considerably longer decay time constants than end organ afferent rates. The decay of VOR slow phase eye velocity in monkeys and humans also displays longer decay time constants. This elongation in time constants is produced by a central "velocity storage" path, which has been modelled as a leaky integrator. Velocity storage lengthens the VOR response following a step velocity stimulus, producing a plateau where eye velocity closely matches the actual rotation rate. The VOR response for low frequency stimuli is similarly augmented.

The optokinetic system also participates in the central storage of eye velocity (Figure 2.3). The direct, cortically controlled "fast" path is responsible for the rapid jump in OKN velocity at the start of visual field rotation. In contrast, the "slow" subcortical OKN is characterized by a gradual speed increase, generated through an eye velocity storage pathway. A further consequence of this visually mediated velocity storage is the presence of an outlasting nystagmus following the cessation of optokinetic stimuli. This aftereffect, called optokinetic

32
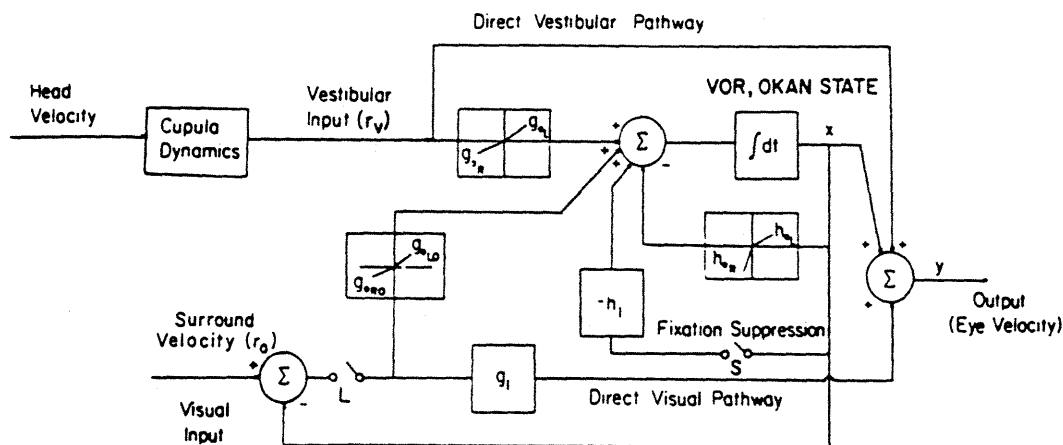
Figure 2.3. One dimensional model of the VOR, OKN, and velocity storage pathways. The model inputs are cupula deflection $r_V$ and visual surround velocity $r_O$; the output is eye velocity. In darkness, the switch L is open, and the system is driven only by $r_V$. Both vestibular and visual inputs are transmitted over direct pathways. Each input also feeds into the velocity storage integrator. Closing the switch S invokes suppression of nystagmus by fixation (in Raphan et. al., 1979).

after-nystagmus (OKAN), results from the slow discharge of the velocity storage integrator when the stimulus ends (Figure 2.2b).

The indirect velocity storage path for OKN has the effect of producing a smooth optokinetic response. Another functional purpose of velocity storage is to counteract anticompensatory post-rotatory vestibular nystagmus following body rotation in the light. After subject rotation in the light with a stationary visual field, post-rotatory nystagmus is reduced by an amount comparable to the OKAN observed in the dark after pure surround motion of equal velocity (Figure 2.2c). This dramatic reduction indicates an approximately linear summation of vestibular postrotatory and visually induced OKAN eye velocity components.

In the monkey, OKAN is related linearly to the prior stimulus velocity up to 90°-120°/sec, and peak OKAN SPV saturates at about 120°/sec (Cohen et. al., 1977). The charging time constant of velocity storage, calculated from the slow rise in OKN SPV, measures approximately 3-5 sec. At OKAN onset, the SPV drops immediately by about 10-20%, predicting a velocity storage gain of approximately 0.8. The velocity storage discharge time constant in the monkey in considerably longer, as the OKAN SPV decays with a time constant on the order of 10-30 sec.

In contrast to the monkey, velocity storage in humans appears to play a much more limited role. Human OKN shows no slow rise in SPV--peak velocity is achieved within the first slow phase. This immediate response upon stimulus onset indicates a gain in the direct OKN pathway near unity for speeds up to 60° - 90°/sec in humans. The increased gain of the "fast" component of OKN is accompanied by a decreased gain in the velocity storage pathway compared with the monkey, evidenced by maximum OKAN velocities of 15°-20°/sec. As a consequence, suppression of vestibular nystagmus following rotation in the light proves much less prominent in humans. The low OKAN gain suggests a much weaker coupling of the visual and vestibular systems than in the monkey (Cohen et. al., 1981).

Since human semicircular canal afferent dynamics or vestibular nucleus firing rates cannot be directly measured, OKAN provides a quantification of velocity storage. Cohen et. al. deduced a charging time constant of about 20 sec. and calculated a slightly longer OKAN decay time constant near 25 sec. Lafortune et. al. (1986) found saturation of peak OKAN velocity with 40 sec. of optokinetic stimulation, but proposed a somewhat longer charging time constant of 47 sec. Jell et. al. (1984) fit a double exponential model to the OKAN decay of SPV and found short and long time constants of approximately 1.2 and 49 sec.

OKAN also occurs when the eyes are kept stationary through fixation during stimulus rotation, demonstrating that tracking eye movements are not necessary to charge velocity storage. The cortical pathways are probably not responsible for velocity storage, since OKAN from central 30° stimulation alone is weaker and less regular than OKAN from exclusive

peripheral stimulation. Following the decay of OKAN, a secondary after-nystagmus or optokinetic after-after-nystagmus (OKAAN) may occur in the direction opposite to the initial OKAN. This later response, caused by a different mechanism from velocity storage, probably results from a central counterregulation to the main OKN effect during stimulation. Stronger and longer lasting than OKAN, OKAAN can completely suppress the occurrence of primary OKAN after continuous optokinetic stimulus durations of several minutes (Brandt et. al., 1974).

### 2.2.2. Vertical (Pitch) Compensatory Eye Movements

The properties of the vertical VOR were tested in both monkeys (Matsuo and Cohen, 1984) and humans (Baloh et. al., 1983) by rotation about a vertical axis in the dark with the head rolled 90° to the side. In both cases, the magnitude of the vertical VOR gain proved comparable to the gain observed for passive horizontal rotations. In response to a velocity step stimulus, monkey gains averaged 0.75 while humans displayed gains from 0.64 to 0.89. The monkey gain responses were symmetric with regard to rotation direction, and Baloh et. al. concluded that the vertical gains were symmetric in the majority of human subjects as well.

In contrast, distinct asymmetries were observed in the dynamic behavior of the vertical VOR. In monkeys, vestibular nystagmus with upward slow phases had a decay time constant of 15 sec. This value, close to estimates obtained for horizontal VOR, was nearly twice as long as the 8 sec. time constant measured for downward slow phases. A similar but less pronounced asymmetry pertained in humans: 8 sec. time constants were obtained for upward slow phases, compared with 6.4 sec for downward slow phases. Horizontal time constants averaging 17 sec were observed in the same human subjects. Consistent with the shortened time constants for vertical nystagmus, the phase lead for vertical sinusoidal oscillations was twice that seen in horizontal responses.

The asymmetry in vertical VOR time constants points to a much weaker influence of velocity storage for compensatory downward slow phases. This direction dependent reduction

also manifests itself in the asymmetric pitch OKN induced in monkeys lying on their sides in the 90° roll position. For upward slow phases, the gain approaches unity up to velocities of 60°/sec, and SPV saturates at stimulus velocities near 100°/sec. In contrast, downward slow phases demonstrate gains near 1 only up to 40°/sec, and eye velocity saturate for field rotation rates of only 60°/sec. Furthermore, the downward SPV is generally irregular. When the animals were tested upright, upward slow phases took on the characteristics of downward slow phase movements, with irregular velocities and diminished saturation speeds (Matsuo and Cohen, 1984).

For erect human subjects, the upward slow phase gain proved comparable to horizontal responses, but was approximately 0.15 higher than downward SPV gain (van den Berg and Collewijn, 1988; Murasugi and Howard, 1989). Several researchers have postulated that the upward preponderance in OKN probably developed in frontal-eyed animals to reduce the influence of the predominantly downward optic flow encountered during forward locomotion (Murasugi and Howard, 1989, among others). Paralleling the tendency toward similar upward and downward OKN responses in upright monkeys, Clément and Lathan (1991) found an increased vertical response asymmetry in humans for the 90° roll position. Interestingly, they also observed a clear asymmetry reversal in 2 of 6 subjects when tested in an inverted position. In support of a gravitational origin for the up-down asymmetry, Clément et. al. (1986) found a reversal in OKN gain asymmetry during the first 3 days of exposure to microgravity in spaceflight.

Like OKN, OKAN was asymmetric in monkeys lying in a 90° roll position. Upward (slow phase down) OKAN appeared generally weak or absent, and saturated at 10°/sec (Matsuo and Cohen, 1984). The stronger downward OKAN displayed a gain of 0.7 and increased peak velocity with stimulus speed up to a saturation velocity of 50°-60°/sec. The OKAN asymmetry was also reflected in uneven suppression of post-rotatory nystagmus following rotation in the light. While upward-beating nystagmus was cancelled or suppressed

following rotation, downward post-rotatory nystagmus showed no reduction. These results indicate further that velocity storage contributes little in upward nystagmus (slow phase down).

Humans exhibited similar OKAN asymmetries to monkeys: for pitch OKN stimuli with the head rolled 90° (Baloh et. al., 1983) or with the head erect (Murasugi and Howard, 1989), OKAN existed only in response to upward moving stimuli. Durations measured 3-25 sec. Murasugi and Howard (1989) investigated the source of the up-down asymmetry, and found that for OKN stimulated exclusively by periphery, the asymmetry increased for 6 of 9 subjects. Conversely, center-only stimuli resulted in the disappearance of any upward preponderance in OKN gain or asymmetry in OKAN. These results indicate that the asymmetry exists in the slow OKN system, a conclusion consistent with the apparent lack of velocity storage for upward OKN.

Head position with respect to gravity exerted a striking effect on downward OKAN in monkeys. With the head upright, saturation velocities were lower and the SPV decayed much more quickly. Likewise, Clément and Lathan (1991) discovered that the time constants of OKAN with upward slow phases increased with increasing head tilt. These facts, taken in conjuction with the difference in OKN asymmetry observed between subjects lying sideways and sitting erect, demonstrate a powerful conditioning role of otolith activation on velocity storage.

### 2.2.3. Torsional (Roll) Compensatory Eye Movements

For roll stimuli, both the otoliths and semicircular canals contribute to compensatory torsional eye movements. Static tilts result in a small otolith-induced torsional response directed in the sense opposite to head roll. This gain of this static counterroll generally reaches about 0.1° of eye torsion per degree of head tilt in humans (Collewijn et. al. 1985; Diamond and Markham, 1983), although Ferman et. al. (1987) found gains as high as 0.26.

To test the dynamic properties of the torsional VOR due to semicircular canal activation, Seidman and Leigh (1989) rotated human subjects sitting erect in the dark for 1 minute with the

head tilted back, facing the ceiling. Using off velocity steps of 50°/sec and 100°/sec, they found a mean peak SPV gain of 0.47 and a decay time constant of 4.0 sec. Similar values were found with the head tilted 90° toward the chest; the maximum gain was 0.37 and eye velocity decayed with a time constant of 5.9 sec. These time constants suggest that the duration of the post-rotational response was largely dictated by the mechanical properties of the labyrinth (Figure 2.4).

Several investigators have measured the positional gain of the torsional VOR during voluntary quasisinusoidal roll oscillations for upright subjects:

- Viéville and Masse (1987) found a dynamic OCR position gain of about 0.5 for ±20° head roll oscillations performed in the dark with a fixation point. Gain increased with increasing frequency, ranging from 0.3 at 0.1 Hz to 0.7 at 1 Hz. Phase lag decreased with increasing frequency. With the head pitched forward 90°, the gain decreased by about 0.2 to 0.16 at 0.1 Hz. and 0.35 at 0.4 Hz., and a phase lead of about 20° was observed.

- Leigh et. al. (1989) tested torsional VOR during active head roll rotations in the dark at approximately 0.5 Hz., observing gains with an average of 0.61. They found a mean increase in VOR gain from 0.61 in the dark to 0.72 when viewing a display fixed in space. When the visual stimulus was stationary with respect to the subject, gains dropped to 0.46. However, they found relatively weak optokinetic responses at this frequency, ranging between 0.05 and 0.12 for 2 subjects.

- Collewijn et. al. (1985) and Ferman et. al. (1987) observed frequency dependent gains similar to the results of Viéville and Masse, with an increase from 0.4 at 0.16 Hz. to 0.7 at 1.33 Hz. Collewijn's study confirmed the earlier results of Petrov and Zenkin (1973), who measured a 10% VOR gain increase from exposure to a stationary visual field.

These experiments revealed three main features of torsional VOR over the frequency range examined: (1) VOR gain increased with increased oscillation frequency; (2) otolith stimulation improved compensation; and (3) corroborating visual information increased the VOR gain.

The increased gain observed upon exposure to a fixed visual field presumably resulted from a torsional optokinetic mechanism. Schiff et. al. (1986) found a strong roll OKN supine and prone in monkeys, with saturation velocities from 40°-60°/s for full-field movement. The OKN response displayed a small, rapid rise in SPV at onset followed by a slow rise to steady state. However, when head orientation deviated more than 30° from supine, the peak OKN

38

## A



## B

## C
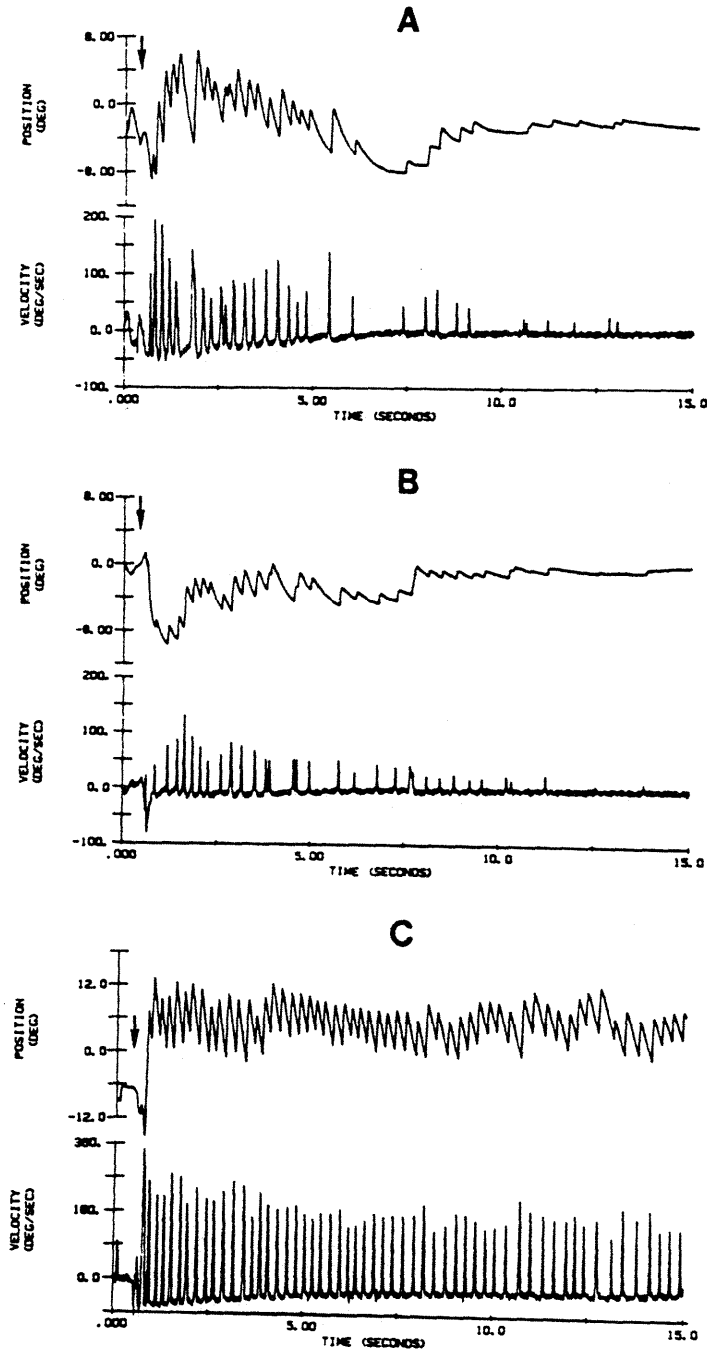
Figure 2.4. Post-rotational torsion responses to 100°/s off-velocity step stimuli in man. Arrows indicate chair stop. [a.] Torsional post-rotatory nystagmus after 1 minute rotation in darkness with face supine. [b.] Torsional post-rotatory response following 1 minute rotation in light. Duration is similar to (a), but response magnitude is less. [c.] Horizontal post-rotatory nystagmus in the same subject. Response exhibits greater strength and duration than torsion (in Seidman and Leigh, 1989).

39

velocity declined sharply; torsional OKN fully upright proved weak and irregular. The investigators concluded that no significant pathways for rapid torsional SPV changes existed implying that the main roll OKN and OKAN processing most probably occurred through the velocity storage mechanism.

Human OKN displayed considerably lower gains for torsion than for horizontal or vertical movement. Collewijn et. al. (1985) tested 2 subjects sitting upright under binocular viewing conditions with a rotating disk covered by a random dot pattern. The disk subtended 100° of visual angle and had a central fixation point. SPV gains reached only 0.035 for speeds from 6° - 30°/sec. At the lowest stimulus speed of 1.2°/s, the gains were highly variable and sometimes even negative. No prominent tonic deviation of the eye was detected. Malan (1985), who also reported on only two subjects, ran experiments in both the erect and supine conditions. He found slightly higher gains ranging from 0.1 - 0.2 for speeds from 3° - 30°/sec. His stimulus, viewed monocularly, consisted of an optokinetic drum with a vegetable pattern which covered the entire visual field. In addition to the nystagmic beating, visual inspection of the eye torsion traces revealed a 2-3° offset from the rest position in the direction of the slow phase for the upright trials. No such deviation for supine trials was reported.

Morrow and Sharpe (1989) conducted a considerably more complete study on 5 human subjects in both erect and supine orientations. Unfortunately, only an abstract describing their work was available in the literature. They made use of a striped, full-field drum stimulus rotating at 10°, 20°, 40°, and 80°/sec, and found a decrease in gain with increasing stimulus velocity, from $0.28 \pm 0.09$ at 10°/s to $0.06 \pm 0.03°$ at 80°/s. As with horizontal and vertical optokinetic movements in humans, torsional OKN exhibited a rapid rise to plateau velocity--the peak velocity was achieved within 500 ms. of stimulus onset. Peak SPV increased with stimulus velocity, but saturated in the range from 2.5°/sec to 8.1°/sec. In contrast to the monkey data, no OKN gain differences were observed between the erect and supine trials.

Published information on torsional OKAN is quite sparse, and exists only in abstract format. The monkey study by Schiff et. al. (1986) revealed a strong OKAN in the supine and

prone positions which lasted up to several minutes in darkness. For tilts greater than 30° from the horizontal, OKAN vanished. In humans, Seidman and Leigh (1989) found that the mean post-rotatory nystagmus SPV gain fell from 0.47 after rotation in the dark to 0.34 following rotation in the light, indicating an opposing velocity storage effect. The only additional human data (Morrow and Sharpe, 1989) showed that OKAN was poorly developed and frequently absent. When measurable, the SPV decay had a time constant of 1.3±1 sec. Unlike the monkey tests, the human study revealed no significant differences between erect and supine positions. This weak OKAN response, coupled with the extremely short post-rotatory nystagmus time constants found by Seidman and Leigh (1989), indicated that roll velocity storage is present only to a very limited extent. In comparison to the monkey, velocity storage plays relatively little part in the human roll OKN system.

### 2.2.4. Three Dimensional Velocity Storage Representation

Considerable evidence suggests that central velocity storage is represented three-dimensionally. Furthermore, the gravity vector assumes fundamental importance in imposing a spatial reference when the velocity storage integrator generates compensatory eye movements. In this manner, static tilt in pitch significantly shortened the yaw OKAN time constant in humans (Lafortune et. al., 1990); similar strong effects of the gravity vector on velocity storage have been demonstrated about the roll (Schiff et. al., 1986) and pitch axes (Matsuo and Cohen, 1984) in monkeys.

Along the same lines, Benson and Bodin (1966) found significantly faster post-rotatory nystagmus decays for horizontal axis yaw rotation. Similar "dumping" of velocity storage occurs for head tilts following yaw rotation. (Raphan et. al., 1981). This dumping of velocity storage in the subject's horizontal plane derives in part from cross-coupling with the other axes. Strong cross-coupling with the horizontal axis is seen for OKAN in both pitch (Clément and Lathan, 1991) and roll (Schiff et. al., 1986). Hain and Buettner (1990) measured time constants of subject-horizontal and subject-vertical VOR during yaw rotation about axes tilted

41

with respect to the vertical. They found decreased time constants for VOR decay with respect to the subject's horizontal, but the horizontal time constant with respect to space was not significantly different from measurements during vertical-axis rotations.

Such experiments show that head-horizontal and head-vertical components can decay at different rates. The similarity between cross-coupled time constants and decay rates observed for pure roll and pitch OKAN suggests that cross-coupling is an intrinsic property of a 3-dimensional velocity storage integrator. Cross-coupling acts as a gyroscopic mechanism, maintaining the principal axis of storage along the spatial vertical. The otoliths serve to reorient the velocity storage coordinate axes to remain coincident with those of the visual system for off-vertical head positions (Raphan and Cohen, 1988).

## 2.3. Psychophysical Responses to Moving Visual Fields

As might be expected from the close coupling of the visual and vestibular systems in the generation of compensatory eye movements, the visual system can also affect an observer's perception of both static and dynamic orientation. Static tilted visual scenes are known to alter subjective perception of the vertical (Witkin and Asch, 1948). More dramatic effects are produced by moving visual scenes: subjects perceive both self motion and tonic orientational bias.

### 2.3.1. Vection

A wide field, uniformly moving visual scene can induce a feeling of self-motion in the opposite direction in a stationary observer. The visual scene itself appears to slow down and even stop completely. This illusion occurs in response to such "natural" stimuli as waterfalls or moving trains (Mach, 1875); Mach was the first to reproduce the effect in the laboratory. This visually induced perception of self motion is termed "vection" (Tschermak, 1931). Circularvection refers to a sensation of angular motion caused by a field rotation about the subject. While circular vection is strongest for yaw rotations about a vertical axis, compelling motion sensations can also be evoked in pitch and roll. Likewise, a visually induced feeling of translation is known as linear vection.

This striking ability to induce motion perception by purely visual stimuli strongly suggests the convergence of visual inputs on vestibular structures, to be evaluated in turn by cortical areas nominally devoted to processing vestibular inputs (Dichgans and Brandt, 1978). In fact, such visual-vestibular interaction mimicking semicircular canal activation has been observed in the neuronal activity of several species. Large moving visual displays evoke direction-specific modulation of the vestibular nerve in the goldfish; various authors have observed similar modulation in the vestibular nuclei of the rabbit, guinea pig, cat, and monkey due to rotating visual scenes. Visual-otolithic convergence has been found as well: in the cat,

vestibular nucleus neurons which respond to linear acceleration also display direction
dependent sensitivity to visual field translations (studies cited in Henn et. al., 1981).

### 2.3.1.1. Yaw Vection

Following the onset of constant velocity field rotation in the yaw plane, the subject
generally perceives surround motion. After several seconds, the surround appears to slow
down and vection is sensed. This onset latency is generally attributed to a lack of confirming
semicircular canal cues (Dichgans and Brandt, 1978). Onset latencies evidently depend little on
the stimulus velocity for step inputs (Dichgans and Brandt, 1974). The perceived vection
velocity equals stimulus velocity up to speeds of $90°$ - $120°$/sec. Above $120°$/s, vection velocity
lags stimulus velocity and does not increase for stimuli above $180°$/s (Brandt et. al., 1973).
Overall, the sensation of steady rotation proves indistinguishable from actual body rotation,
although no sensations of acceleration or deceleration are noted.

Further evidence of a visual-vestibular convergence is provided by "pseudo-Coriolis"
effects induced by roll or pitch head movements during yaw vection. Such tumbling
sensations cannot be distinguished from vestibular Coriolis effects arising from cross-coupled
accelerations during body rotations (Dichgans and Brandt, 1978). Apparently, visually
induced vestibular excitation combines with actual vestibular information generated by the head
movements. Vection aftereffects also occur, in accord with the storage of visual inputs through
central vestibular excitation. Switching off the stimulus illumination generally results in
outlasting vection in the same direction for up to 30 sec., averaging about 10 sec. (Dichgans
and Brandt, 1974). In contrast, presentation of a stationary surround causes immediate
reversal of vection direction (Dichgans and Brandt, 1978).

Simultaneous visual and vestibular stimuli interact in a non-linear fashion to produce a
combined motion sensation which is closer to the actual stimulus than the perception evoked by
either system alone. Melcher and Henn (1981) compared self-motion perception latencies for
different accelerations of both visual and vestibular stimuli. They found the shortest vection

44

latencies at visual field accelerations of about $5°/sec^2$. Up to this acceleration, all surround movement created the perception of circular vection. In this low-acceleration range, vestibular detection latencies were longer than visual latencies, or no motion detection occurred. For higher surround accelerations, vection latency increased, until shorter vestibular latencies were observed above $10°/sec^2$. Rotation in light, resulting in a combined stimulus, produced the shortest latencies and widest range for correct velocity estimation.

Experiments by Wong and Frost (1981) supported the notion that onset latencies depended on the magnitude of visual-vestibular conflict. They found that corroborating vestibular stimulation at the beginning of the optokinetic stimulus significantly shortened onset latencies, although noncorroborating stimuli had little effect. In addition, asymmetric latencies were found in patients with unilateral Ménière's disease, which produces decreased vestibular sensitivity to rotation in one direction. The direction of asymmetry indicated shorter latencies in the case of lesser intersensory conflict.

Young et. al. (1973) provided further evidence for suppression of one sensory modality by other sources of conflicting information. Thresholds and detection times for angular body acceleration were raised for stimuli opposite the direction of circular vection. Rapidly occurring conflicts between visual and vestibular sensations, however, generally resulted in a precipitous loss of vection. Such a replacement of visual dominance by vestibular cues seems consistent with reliance on the vestibular system for stimuli of higher frequencies and accelerations.

The perception of vection depended strongly on movement in the retinal periphery. Thus, masking the central portion of a moving display up to 120° of visual angle scarcely weakened the vection response, while limiting the display to the central 30° produced a perception of display motion only (Brandt et. al., 1973). A central stimulus moving opposite to the peripheral field could weaken vection, but not to extent of reversal. In the presence of a stationary periphery, central motion induced vection only when the center was more distant than the surround (Howard et. al., 1987).

Vection perception changed little upon the reduction of luminance to levels barely

higher than the scotopic threshold, or the introduction of refractive errors above 16 diopters

(Leibowitz et. al., 1979). Although luminance and image sharpness are vital to focal vision,

these factors exert reduced influence in the retinal periphery . This dependence on the retinal

periphery for motion sensation agrees with the concept of two distinct modes for processing

visual information (Held, 1970; Leibowitz and Post, 1982). In this view, an "ambient" system

relies on the visual periphery for spatial orientation, while the "focal" system is dedicated to

visual tracking and object recognition.

Interestingly, vection has been induced in the central visual field for forward linear

vection (Andersen and Braunstein, 1985) and roll vection (Andersen and Dyre, 1987). Both

studies utilized a display with internal depth, created as a "volume" of points in a computer-

generated image. These studies suggested that ambient processing could also function in

central vision by taking advantage of internal display depth.

Several other studies have established the importance of depth cues in producing

vection. Visual scenes perceived to be in the background or most distant in depth dominate

self-motion perception. Brandt et. al. (1975) found that stationary contrasts in the background

of moving stimuli strongly inhibited vection, while similar contrasts in the foreground had only

a weak effect. Howard et. al. (1987) used monocular viewing of displays separated in depth to

eliminate the cue of binocular disparity. With this apparatus, occasional reversal of the

perceived depth order of the displays occurred. Vection was always controlled by the display

perceived to be most distant, even if it was actually nearer. Vection was not affected by plane

of focus or by which display was pursued or fixated. Such reliance on the visual background

and periphery for motion cues appears logical, since distant wide-field scenes would generally

not move with the observer.

## 2.3.1.2. Roll and Pitch Vection

Vection can also be induced about subject's pitch and roll axes by appropriate rotating visual fields (Figure 2.5). The saturation velocities for vection about horizontal axes are considerably lower than for comparable yaw stimuli. For roll and pitch vection, the response strength increases up to field velocities of 40° - 60°/sec (Held et. al., 1974; Young et. al., 1975). The response latency appears to decrease with increasing stimulus speed (Young et. al., 1973; Young et. al., 1975), indicating that faster stimuli produce a more compelling illusion of motion. As with yaw vection, peripheral stimuli prove dominant in roll and pitch vection. The effect increases with both field size and with increasing retinal eccentricity of a constant-area ring (Held et. al., 1974).

For visually induced rotation about earth-horizontal axes, the continuous rotation sensation is accompanied by a paradoxical perception of constant tilt angle (Dichgans et. al., 1972). The comparatively low saturation velocities and perception of constant angular displacement probably result from inhibitory otolithic inputs (Dichgans et. al., 1972). Thus, a sensation of full 360° rotation in roll is often generated when subjects lie supine, so that the vection axis aligns with the vertical and the otoliths provide no contradictory information (Crites, 1980; Young et. al., 1983). In like manner, Howard and Cheung (1987) found unimpeded vection in full circle for yaw, roll, and pitch vection whenever the vection axis was vertical. For all conditions where the vection axis lay in the horizontal plane, only partial rotation was experienced.

Studies of vection in bilaterally labyrinthine deficient subjects provide additional weight for inhibition of vection through otolithic sensing of orientation with respect to gravity (Cheung et. al. 1989). These tests showed that the labyrinthine deficient group experienced complete, unambiguous self-rotation through an upside-down orientation for both roll and pitch stimuli. In normal human subjects, short-term weightlessness made possible by NASA's KC-135 aircraft resulted in significantly shorter roll vection onset latencies (Young et. al., 1983).
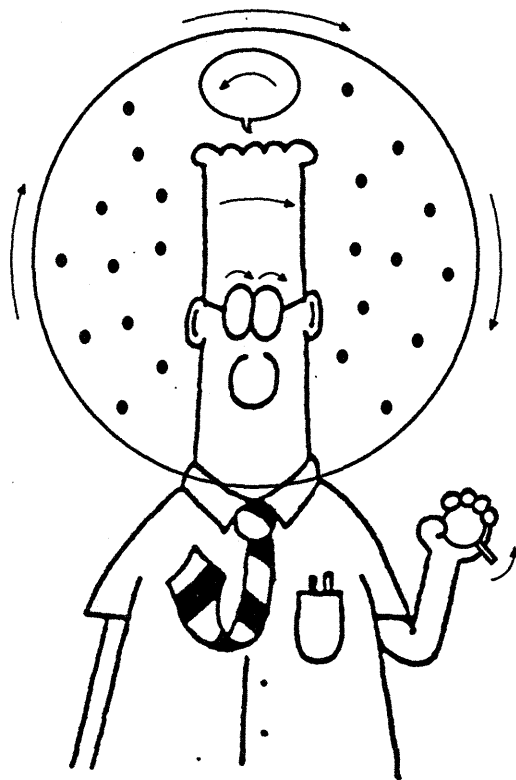
Figure 2.5.   Schematic representation of reactions to field rotation about the visual axis.   The stimulus rotates clockwise (from this view); after a few seconds, the subject begins to perceive counterclockwise self-rotation.   Roll vection is indicated by counterclockwise turn of the knob.   The subject also feels a counterclockwise tilt, resulting in a pseudo-vestibulocollic reflex which causes clockwise head sway.   Clockwise torsional optokinetic slow phases follow the field rotation (adapted from Young et. al., 1986; Adams, 1991).

Experiments performed on the space shuttle also demonstrated reduced onset latencies in microgravity (Young et. al., 1986). Furthermore, the astronauts displayed a greatly increased propensity toward fully saturated vection during spaceflight, a condition which occurred more rarely on the ground (Young and Shelhamer, 1990). These results indicated that the brain placed greater reliance on visual cues for dynamic orientation in flight, while less attention was paid to erroneous graviceptor inputs. The astronauts retained some carryover of increased visual dominance for a few days postflight, including shortened latencies to vection and greater static field effects for the rod-and-frame test (Young et. al., 1986). Further evidence of otolith suppression will be discussed below with regard to a closely related phenomenon, visually induced tilt.

Pitch vection exhibited a directional asymmetry (Young et. al., 1975; Howard and Cheung, 1987). Forward pitch vection proved stronger than backward pitch sensations. The asymmetry depended on the subject axes rather than gravitational orientation, since the same effect obtained for inverted subjects. Many subjects also displayed directional asymmetries for roll vection. However, no connection could be deduced between the directional dependence and either handedness or eye dominance (Held et. al., 1975). Such roll asymmetries might have related to vestibular imbalances which, although well compensated under normal circumstances, became apparent under unusual stimulation.

## 2.3.2. Visually Induced Orientation Bias

A static tilted visual scene can bias an observer's judgment of the gravitational vertical in the direction of field tilt. This effect can be produced by as simple a display as the "rod and frame" (Witkins and Asch, 1948), in which the perceived orientation of a luminous rod is influenced by tilting a surrounding luminous frame. Moving visual displays introduce similar but much stronger tonic deviations in the perception of orientation.

## 2.3.2.1. Shift of the Subjective Straight Ahead

Rotary full-body acceleration about the yaw axis is known to displace a subject's perception of the direction associated with "straight ahead." A purely egocentric definition, the subjective straight ahead appears displaced in a direction opposite to the angular acceleration, while a fixated point seems dislocated in the direction of acceleration so that it leads the subject. Interestingly, circular vection also displaces the subjective straight ahead in the direction opposite perceived motion, i.e. in the direction of visual field motion. This visual effect on the judgment of "straight ahead" is dramatically illustrated when subjects are instructed to walk straight forward while an optokinetic drum rotates about them--the subjects consistently deviate in the direction of field rotation. The phenomenon appears closely related to yaw vection, and like vection saturates at rotation rates near 100°/sec. (Dichgans and Brandt, 1978).

## 2.3.2.2. Central Recomputation of the Gravity Vector

Visual fields rotating about the roll and pitch axes also create an angular bias, this time in the perception of the vertical (Dichgans et. al., 1972). Unlike the subjective straight ahead, however, the vertical is not strictly egocentric since it is defined by the direction of the gravity vector. A few seconds after onset of stimulus rotation about the line of sight, a vertical contrast appears tilted in the direction opposite to field rotation. When instructed to set the contrast to the perceived vertical, the subject rotates the line several degrees in the direction of field rotation.

This illusion is closely linked to roll and pitch vection. During roll and pitch vection, visually tilt increases with stimulus velocity, saturating at field rotation rates of 40°-60°/sec. Maximum tilts found with the head erect average 15°-25°, but reach as high as 40°-60° in some subjects. (Dichgans et. al., 1972; Held et. al., 1974; Young et. al., 1975; Howard and Cheung, 1989) As with pitch vection, Young et. al. (1975) observed an asymmetry for tilts about the pitch axis: forward tilts were much larger than backward tilts. This asymmetry

appeared purely visual in origin, since the same asymmetry was observed with the subject inverted.

However, the perceived tilts are not strictly visual effects. Instead, they provide evidence for a central recalculation of the direction of gravity caused by visual field rotation. Dichgans et. al. (1972) tested this hypothesis by placing subjects in a moving base flight simulator. The subjects adjusted the position of the trainer to the subjective upright during the vection stimulus. As before, the subject perceived body tilt opposite the stimulus rotation and rotated the cab in the direction of field motion.

Like vection about the pitch and roll axes, visually induced tilt is apparently limited by conflict with otolith information signalling a constant orientation with respect to the gravity vector. Tests of roll and pitch vection were performed with the head rolled 90° to the side or inverted. When the utricular otoliths lay in such unfavorable geometries, the investigators observed heightened sensitivity to visually induced tilt. Pitching the head 25° forward to place the utricles in the plane of maximum sensitivity produced a corresponding decline in induced tilt (Young et. al., 1975; Dichgans et. al., 1974).

## 2.4. Possible Correspondence of Psychophysical Effects and Associated Eye Movements

Two mechanisms involving the visual system have evolved to respond to large moving visual displays: OKN helps to stabilize images on the retina, while the vection phenomenon aids in the maintenance of a veridical perception of self motion. Both mechanisms interact closely with the vestibular system and complement its performance. Although intracellular neural recordings are inappropriate in humans, the neuronal convergence of the visual and vestibular systems has been documented in many species including primates. It seems likely that the motion perception functions rely on the some of the same neurological structures which subserve the generation of compensatory eye movements.

On this basis, the possibility of a close correlation between the psychophysical effects and compensatory eye movements associated with moving visual fields cannot be ruled out.

51

Indeed, in certain cases eye movements might generate perceptual responses. Likewise, perceived self-motion might induce compensatory eye movements in a manner comparable to the stimulation of the pursuit system by perceived object motion (Yasui and Young, 1975). This section reviews the evidence both for and against a close linkage between eye movements and perceptual effects and evaluates some published models of the interaction between the visual, vestibular, and perception mechanisms.

### 2.4.1. Evidence for a Link between Eye Movements and Orientation Perception

The evidence for close links between eye movements and perception of static or dynamic self-orientation remains largely circumstantial. For instance, circular vection and OKN share many attributes in common. Both phenomena exhibit saturation at velocities near 120°/sec., and have similar time courses for rise (about 5 sec.) and discharge (20 - 30 sec.) (Brandt et. al., 1973). Schor et. al. (1984) examined smooth pursuit, OKN, and vection using a yaw stimulus illuminated stroboscopically at different frequencies. The investigators determined threshold illumination frequencies for perception of smooth continuous surround motion. While smooth pursuit occurred at all strobe frequencies, vection, OKN, and OKAN appeared only for frequencies above the smooth apparent motion threshold.

Furthermore, the perceptual and oculomotor aftereffects resulting from prolonged exposure to optokinetic stimuli display a positive correlation. Brandt et. al. (1974) studied the afternystagmus resulting from various durations of an optokinetic stimulus. The strength of the positive phase of OKAN increased for durations of up to 1 minute. Longer durations resulted in strengthening of the negative phase (OKAAN) antagonistic to the positive afternystagmus. Following stimuli of 15 minutes, the positive phase was no longer observed, and OKAAN began immediately when the lights were turned out. The direction of vection aftereffects generally followed the time course of optomotor aftereffects quite closely.

Zee et. al. (1976) compared aftereffects between normal subjects and bilaterally labyrinthine defective patients. Both normals and patients perceived vection during visual field

motion. Normals showed 20 - 50 sec. of OKAN and perceived up to 20 sec. of outlasting vection. One patient had a remnant of OKAN lasting 4-7 sec., and experienced only 2-3 sec. of continuing vection. The other two patients demonstrated an immediate negative afternystagmus (OKAAN); one of these felt a corresponding reversal of vection direction while the other had no motion aftereffects.

These experiments provide evidence for a brainstem mechanism capable of generating both self-motion sensation and the accompanying compensatory eye movements; normal functioning requires the presence of intact labyrinths. Cohen et. al. (1977) postulated that monitoring activity in the velocity storage integrators participated in the production of circular vection. Such activity cannot be solely responsible for vection, however, since velocity storage relies on a functioning peripheral vestibular system.

Brandt et. al. (1974) observed another correlation between perception and the characteristics of eye movements during long duration exposure to yaw field rotation (Figure 2.6). Following several minutes of constant velocity drum rotation, the subject experienced a slowing down in the perceived self-rotation velocity, with occasional reversals in vection direction. Concurrent with the episodes of inverted self-motion perception, the average eye position or *Schlagfeld* shifted from the direction of the fast phase toward the slow phase direction. However, voluntary deviation of the *Schlagfeld* in the slow phase direction did not produce vection reversal, and active attempts during reversal to move the average eye position toward the fast phase direction did not destroy the illusion.

Vertical OKN and pitch vection share a directional asymmetry. However, this connection seems rather tenuous. First, Clément and Lathan (1991) found evidence for reversal of the OKN asymmetry when subjects were inverted. Pitch vection, in contrast, generally exhibited a consistent asymmetry regardless of body orientation (Young et. al., 1975). Howard and Cheung (1987) compared vertical OKN and visually induced pitch angle. Although some of their subjects demonstrated opposite asymmetries in pitch perception, all subjects displayed stronger OKN with upward slow phases when tested upright.
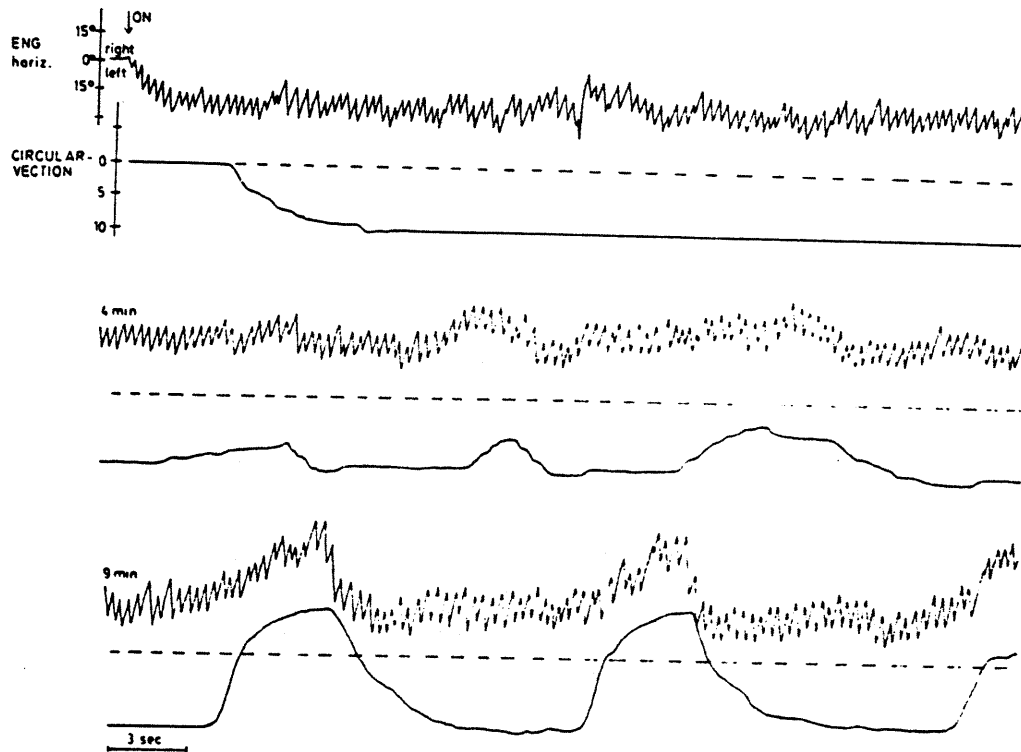
Figure 2.6. Breakdown and reversal of self-motion perception concurrent with a shift in average eye position in the direction of the slow phases. Effect intensity increases with stimulus duration; inverted motion perception is apparent in the bottom trace (in Brandt et. al., 1974).

Experiments performed by Balliet and Nakayama demonstrated a link between ocular torsion and perceived orientation. In one test, the investigators compared eye torsion predicted by Listing's Law with perception of the vertical (Nakayama and Balliet, 1977). According to Listing's Law, the vertical meridian of the eye does not remain aligned with the vertical axis of the head for oblique gaze positions. Eye torsion was measured for various gaze positions using an afterimage technique; comparison with the values expected from Listing's Law yielded a close fit (Figure 2.7a). For the same gaze deviations, subjects indicated the perceived vertical using an adjustable luminous line. The subjective vertical was consistently deviated in the same direction as eye torsion, although to a lesser extent (Figure 2.7b). The investigators concluded that some extraretinal signal provided information about eye torsion, albeit with a gain insufficient to ensure accurate perception of the vertical.

In further experiments, subjects were trained to make a repertoire of torsional voluntary eye movements, including pursuit and saccadic tracking and fixations within a 30° range (Balliet and Nakayama, 1978a). Eye torsion was documented using 16 mm. motion picture films. The eye movements were not visually induced, as they could be performed without any visual stimulus. During the training, subjects experienced a number of illusions including a feeling that their heads and bodies were "rolling laterally." Motion sickness symptoms consisting of nausea, headache and fatigue often accompanied these deviations in egocentric orientation. Sensations of "body flotation" and rapid falling in the direction of cyclotorsion also occurred.

To quantify the changes in perceived orientation induced by voluntary torsion, subjects were instructed to indicate their perception of the vertical during voluntary torsional deviations by pivoting a rod in the frontal plane (Balliet and Nakayama, 1978b). Subjects rotated their eyes torsionally to match an afterimage to specified tilts of a real line. Measurements of the perceived vertical were also taken with the head tilted to match the afterimage with the real line, and with full body tilt in complete darkness.

## a. Eye torsion (scleral coil)
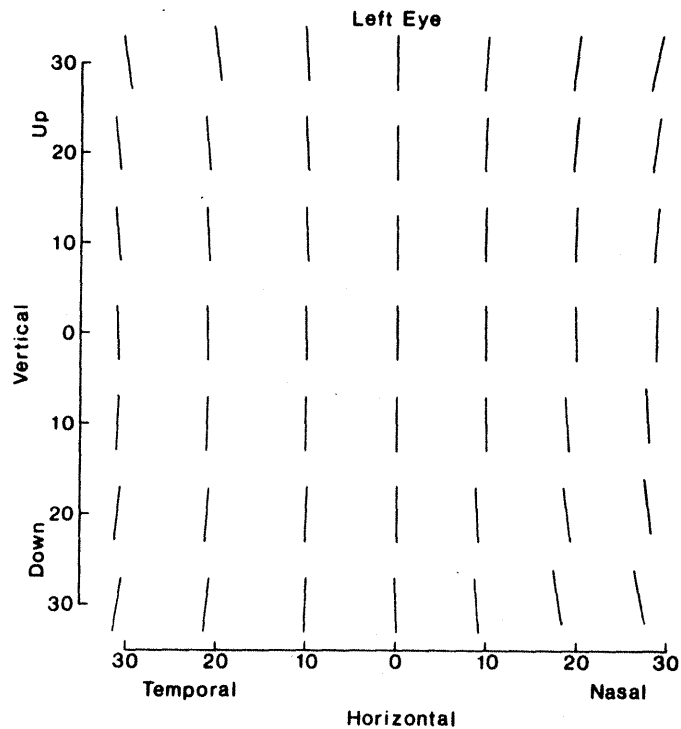
## b. Eye torsion and perceived vertical
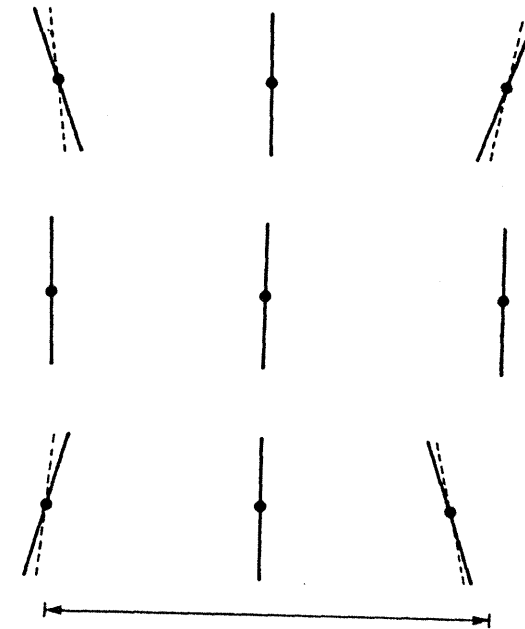


**Figure 2.7.** Eye torsion and perception of the vertical resulting from Listing's Law. (a.) Scleral coil measurements of eye torsion in oblique gaze positions demonstrate deviation in direction specified by Listing's Law which increases regularly with eccentricity (in Collewijn et. al., 1988). (b.) Superposition of perceived vertical settings (dashed lines) with eye torsion afterimage settings (solid lines). Angular deviations have been multiplied by three for clarity. Bottom line indicates 53° visual angle (in Nakayama, and Balliet, 1977).

The tilted line alone in the absence of voluntary torsion was demonstrated to have essentially no effect on the subjective vertical. In contrast, voluntary torsion, head tilts, and body tilts induced marked deviations of the perceived vertical: the rod was adjusted away from the vertical in a direction opposite eye tilt by nearly the same amount in all three conditions (Figure 2.8). The researchers postulated a signal determining egocentric orientation which overcompensated for eye tilt in space regardless of whether it resulted from voluntary torsion, head tilt, or full body rotation.

## 2.4.2. Evidence Against a Link between Eye Movements and Orientation Perception

Despite the observation that vestibular nucleus firing rates, self-motion perception, and compensatory eye movements correlated closely under some conditions, several important dissociations between optokinetic eye movements and psychophysical responses have been documented.

- •Brandt et. al. (1973) demonstrated the occurrence of saturated yaw vection for angular velocities below 90°/sec regardless of whether the subject fixated a stationary point or allowed the eyes to pursue the field through OKN.

- •OKN was most strongly induced by moving fields in the plane of binocular convergence. Vection depended on the stimulus perceived as most distant, regardless of the state of vergence. (Howard, 1990).

- •Peripheral moving fields generated the strongest vection and visually induced tilt (Brandt et. al., 1973; Held et. al., 1975). OKN gains were highest for stimuli on the central part of the retina (Dubois and Collewijn, 1979).

- •Vection and OKN slow phases can be generated in the same direction simultaneously (compensatory eye movements would oppose head motion). During conflicting central and peripheral optokinetic stimuli, OKN followed the central stimulus while circular vection direction depended on motion in the periphery (Brandt et. al., 1973).

These instances could be interpreted as the dominance of a cortically dependent "fast" OKN system evolved to maintain stabilization of scenes under binocular viewing. Closely tied to the pursuit eye movement system, the phylogenetically newer fast system could suppress or override "slow" subcortical OKN which might otherwise be strongly linked to perceptual responses. Since torsional smooth pursuit is underdeveloped or absent in most individuals
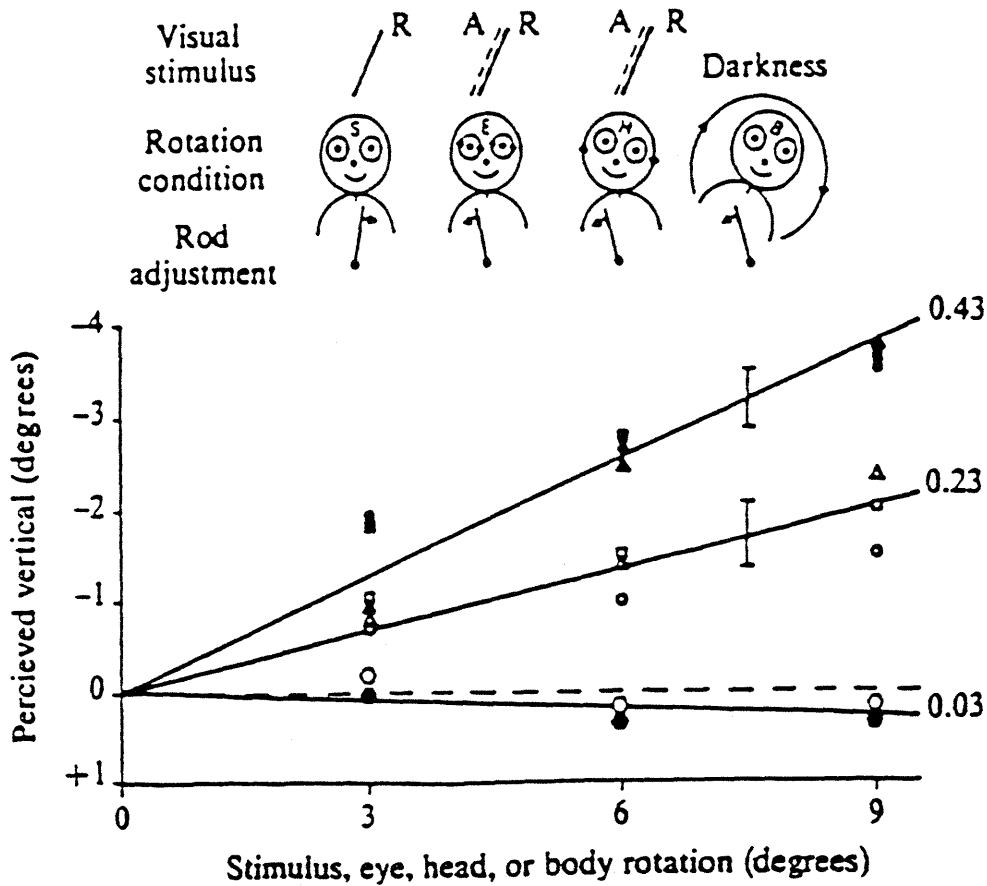
Figure 2.8. Deviation in the perceived vertical resulting from voluntary eye torsion. Changes in perception of the vertical are also shown for head and body tilts. In each case, rotations were in range ±9°. Visual stimulus for each condition is shown: R, real stimulus line; A, afterimage line. R and A set to vertical with eyes at rest and straight ahead. Rotation conditions depicted below visual stimuli: S, real stimulus line rotation only; E, voluntary eye torsion to align afterimage with stimulus line; H, head tilt to align afterimage with stimulus line; B, full body tilt in complete darkness. Graph shows change in perceived vertical as function of rotation magnitude. Filled and open symbols display results for two different subjects; error bars show standard error of mean for combined subject data. Symbols indicate the following: ▲ = E; ■ = H; ● = B. Hexagons near abcissa denote 'S' condition (in Balliet and Nakayama, 1978b).

(the subjects of Nakayama and Balliet required tens of hours of training over a period of months), one might expect torsional eye movements and egocentric roll perception to display a closer correlation.

It has been suggested that tonic eye deviation during roll vection might account for the phenomenon of visually induced tilt. However, the size of the two effects differed by an order of magnitude: torsion usually amounted to a few degrees while tilt could approach 60°. A series of experiments performed by Held, Wolfe, and colleagues indicated further dissociations between eye torsion and perceptual effects. All of these experiments utilized an afterimage technique to measure eye torsion; the severe deficiencies associated with this method should be kept in mind.

Wolfe and Held (1979) examined a binocular contribution to eye torsion and displacement of the vertical during optokinetic roll stimuli. The test was based on the observation that tilt and torsion both increase with flash frequency for stroboscopic illumination of a roll stimulus. Two stroboscopes were used to illuminate the stimulus pattern; one was covered with a red filter while the other used a green filter. The subject viewed the pattern through goggles with one red and one green lens, allowing stimulation of each eye independently. The pattern could be illuminated by simultaneous flashes ("in phase" stimulus) or by the strobes flashing at the same rate but 180° out of phase ("cyclopean" stimulus--the individual eyes still received the original flash rate, but stimulus frequency was effectively doubled if binocular integration occurred).

Normal subjects demonstrated binocular summation for both eye torsion and visually induced tilt, i.e. the cyclopean stimulus induced greater tilt and torsion than did the in phase illumination. Stereoblind subjects also showed an increase in torsion under cyclopean stimulation, but did not exhibit binocular summation for tilt (Figure 2.9). The investigators concluded that the two effects depended in part on different binocular processes in normal subjects. Stereodeficiency impaired the binocular mechanism for tilt but left the torsion process unaffected.

59
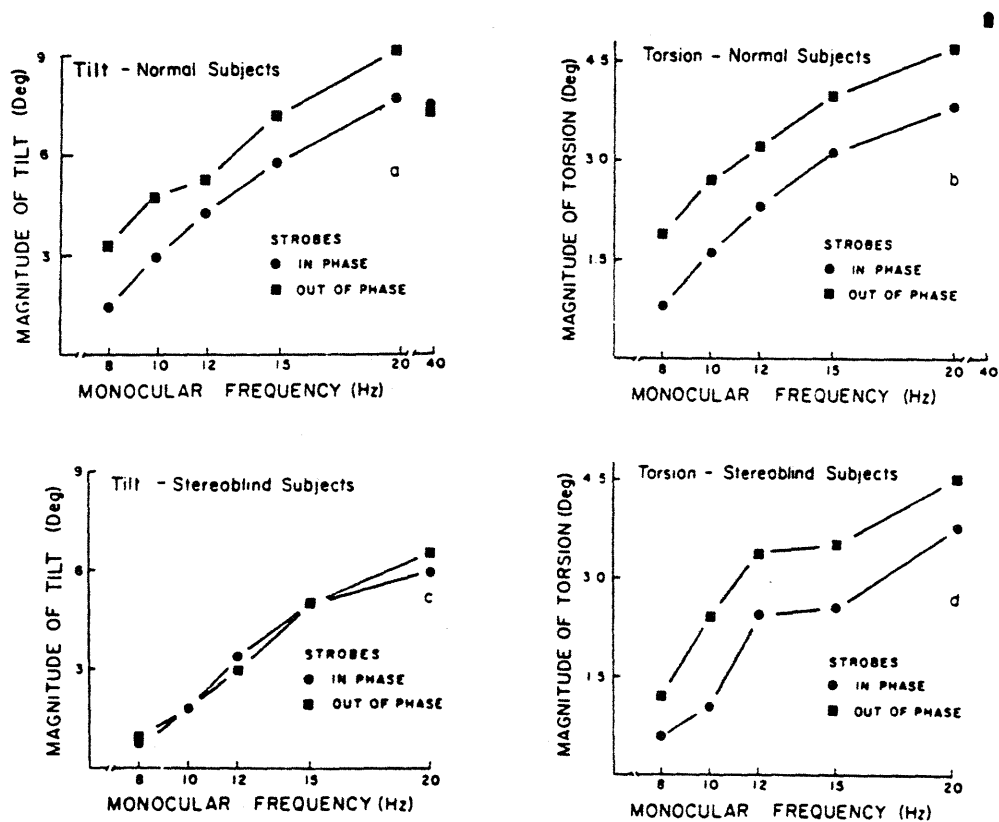
Figure 2.9. Eye torsion and visually induced tilt in normal and stereoblind subjects. Stimulus presented to eyes separately for "in phase" and "out of phase" conditions. In "out of phase" condition, torsion increases for all subjects, while tilt increases only for normals (in Wolfe and Held, 1979).

Merker and Held (1980) compared the influence of combined head tilt and visual roll stimuli on eye torsion and induced tilt. Eye torsion due to field rotation appeared to sum linearly with counterrolling from head tilt. Perceived tilt displayed a different and more complex interaction between the two factors, providing evidence for independent processes mediating torsion and tilt. Finke and Held (1978) measured eye torsion and visually induced tilt during differing states of roll vection. In State 1, the subject felt body rotation, while State 2 was marked by perception of surround motion only.

Noting that State 1 induced larger tilts but evidenced a smaller amount of eye torsion, Finke and Held argued for separate tilt and torsion processes (Figure 2.10). Their second experiment contrasted the effect of the gravity vector on tilt and torsion. Subjects indicated

60
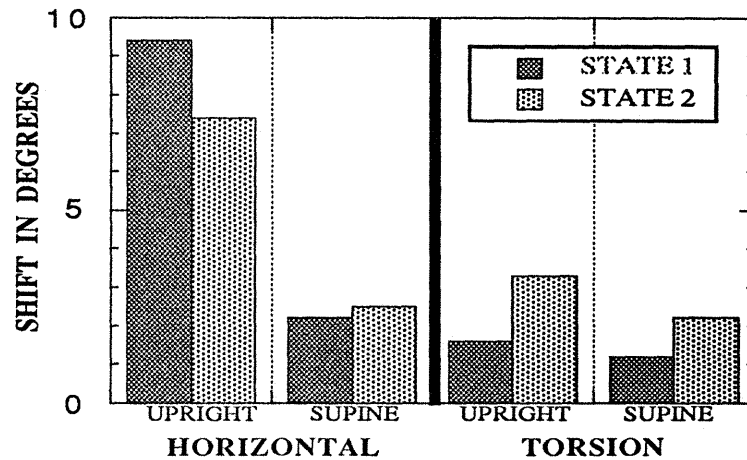
**Figure 2.10.** Mean shifts in visually induced tilt and ocular torsion as a function of vection state and subject orientation. State 1 = self-rotation; State 2 = surround rotation (in Finke and Held, 1978)

significantly greater tilt supine than erect, but showed little difference in torsion between the two orientations. Since aligning the field rotation axis with gravity enhanced one effect but not the other, the case for dissociation between eye torsion and visually induced tilt was strengthened.

### 2.4.3. Models of Visual-Vestibular Interaction

Figure 2.11 presents in block diagram format the interaction of various elements which underlie models of visual-vestibular interaction. Such models attempt to explain and predict the compensatory eye movements and motion sensations resulting from a range of vestibular and visual stimuli using physiologically plausible combinations of sensory inputs, internal feedback signals, and central computation.

Two important blocks deal with internal models of plant dynamics and combination of visual and vestibular signals. Internal models use prior knowledge of plant (head and body; semicircular canal) dynamics to produce a best estimate of head or eye velocity; representations may range from velocity storage integrators to actual realizations of dynamic equations

61

RETINAL SLIP          ADAPTIVE GAIN       EYE VELOCITY
                        OF VOR
          HEAD VELOCITY      (FLOCCULUS?)        ?
              ?

EYE VELOCITY                                              EFFERENT COPY
WRT HEAD                                                  OF EYE VELOCITY
                  COPY OF EYE                             COMMAND
                  VELOCITY COMMAND
                                                VOR GAIN

         RETINAL
         SLIP         RECREATED          VISUAL ESTIMATE OF
FIELD    VELOCITY     TARGET VELOCITY    HEAD VELOCITY WRT TGT
VELOCITY             WRT HEAD    INTERNAL
(WRT HEAD)                       MODEL OF
         MOVEMENT                CANALS OR
         DETECTORS               BODY DYNAMICS

                                        ADDITION OR    VOR        OCULOMOTOR         OCULOMOTOR         EYE VELOCITY
                                        NONLINEAR      COMMAND    COMMAND            PLANT              WRT HEAD
                                        COMBINATION -             GENERATION
                                        V.V.I.

                          VESTIBULAR EFFERENTS                               INTERNAL MODEL
HEAD         CANAL                                                           FILTER-ESTIMATOR    SUBJECTIVE ROTATION
VELOCITY     DYNAMICS                                                        (INCLUDES "PATTERN  WRT SPACE
                          "OTHER KNOWLEDGE OF SITUATION"                     CENTER")
                          (ACTIVE MOVEMENT, PREDICTABLE
                          INPUT OR ACCURATE ESTIMATE OF PLANT)

Figure 2.11.    General block diagram depicting arrangement of elements in models for eye movements and motion perception.    TGT = target, VOR = vestibulo-ocular reflex, VVI = visual-vestibular interaction, WRT = with regard to (Young, in Henn et. al., 1980).

incorporated into Kalman filter gains. Visual and vestibular signals must be combined to evaluate head velocity; such a block could rely on simple linear summation or represent complex nonlinear interactions.

Post et. al. (1986) and Wertheim (1990) have proposed models somewhat different from each other, both of which explain many observed interactions between circular vection and optokinetic nystagmus. These models also provide possible explanations for several unusual visual effects, including the oculogyral illusion, center-surround induced motion, and the Filehne illusion. Both models can be summarized by the representation in Figure 2.12.

According to Wertheim's model, a retinal slip signal is compared with a "reference" signal to generate a perception of either visual field motion or stationarity. The reference signal consists of a vestibular component, an efference copy representing all slow phase eye motion, and an optokinetic component. Wertheim postulated that the optokinetic component was built up slowly from the retinal slip signal, accounting for the slow onset and decay of vection. This model had difficulty explaining how the optokinetic signal was built up when the eyes tracked the stimulus during vection, since retinal slip was minimal in this case. Wertheim solved this problem by proposing that retinal smear during the fast phase of OKN produced the necessary optokinetic component. However, the phenomenon of saccadic suppression renders this explanation rather unlikely.

For the model of Post et. al., the reference signal in Figure 2.12 would consist solely of a corollary discharge component. They suggest that the compensatory eye movements of VOR and OKN result from a phylogenetically "old" system which does not produce a corollary discharge signal. Only pursuit eye movements, presumably evolved later, would contribute to the reference signal. Since their model relies on cancellation of reflex eye movements by the pursuit system during fixation conditions, a corollary discharge could result even in the absence of manifest eye motion. This model adequately predicted perceived surround stationarity during circular vection, independent of subject fixation or tracking eye movements. However, it too had difficulty in explaining the gradual onset and decay perceived for vection.
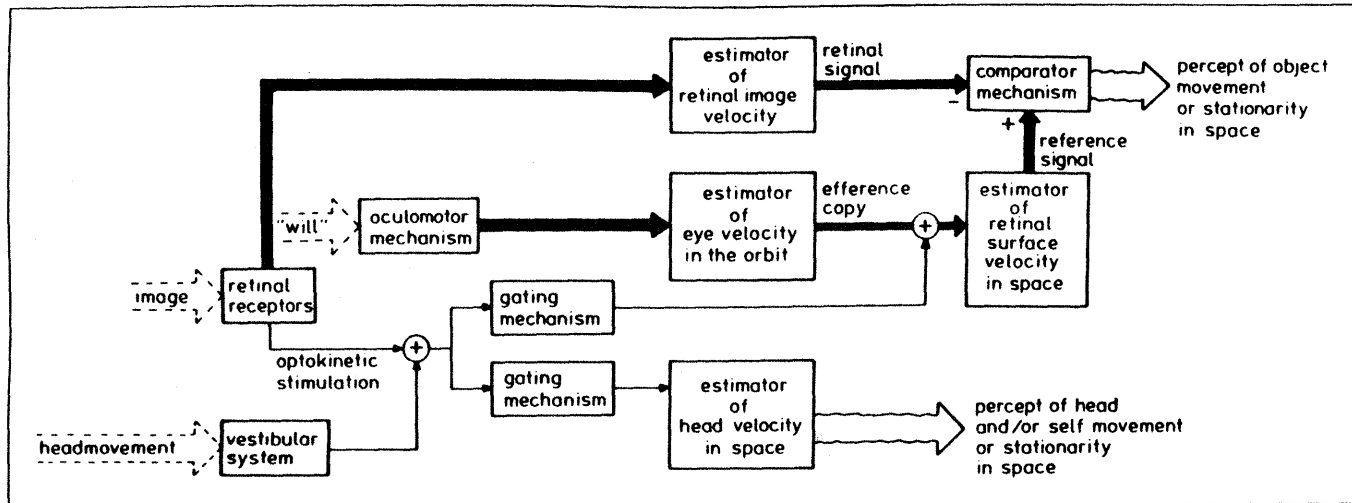
Figure 2.12. Model describing the generation of reference signals and the interrelationships between object- and self-motion perception. Thick lines denote traditional pathways for "inferential" theories; thin lines indicate standard visual-vestibular interaction paths. (in Wertheim, 1990).

# 3. EXPERIMENTAL APPARATUS

## 3.1. Rotating Dome

The rotating dome stimulus incorporated in these experiments was originally constructed by Troy Crites in preparation for the visual-vestibular interaction experiments aboard the 1983 shuttle Spacelab-1 mission, STS-9 (Crites, 1980). After refinement and verification in a series of parabolic flight tests on NASA's KC-135 aircraft, the design formed the basis for the domes used on that flight and subsequent Spacelab missions D-1 (61-A, 1985) and SLS-1 (STS-40, 1991). The dome consisted of a cylindrical drum with one end open (Figure 3.1). The subject viewed the interior of the drum with its center at eye level, so that the drum rotated about the subject's line of sight. The dome measured 13.5" in depth and 17" in diameter. When the subject's head was fixed in place by the dental biteboard mounted within the dome, the distance from the subject's eyes to the rear of the dome measured approximately 12.5". The lateral distance from the eye to the wall of the drum was about 7.5". Thus, the dome subtended a visual angle of 195°.

The pattern on the dome interior was made up of circular colored dots on a white background. The dots were 0.75" diameterAvery labels distributed randomly at a density of 800/m$^2$ to cover approximately 20% of the dome area. Six different colors were utilized: light blue, dark blue, light green, dark green, fluorescent red, and dark red. Crites (1980) felt that this pattern created the most compelling vection sensation of the 9 variations he tested. Brandt et. al. (1975) found that visually induced tilt reached saturation when approximately 30% of the visual field was moving, a value comparable to the dot concentration used here.

The rear of the dome shell contained a central hole 4" in diameter designed to accommodate a camera lens and ring flash for recording eye position. However, eye photographs were not needed for the current experiment, and stationary background visual cues have been demonstrated to inhibit vection (Brandt et. al., 1975). The hole was
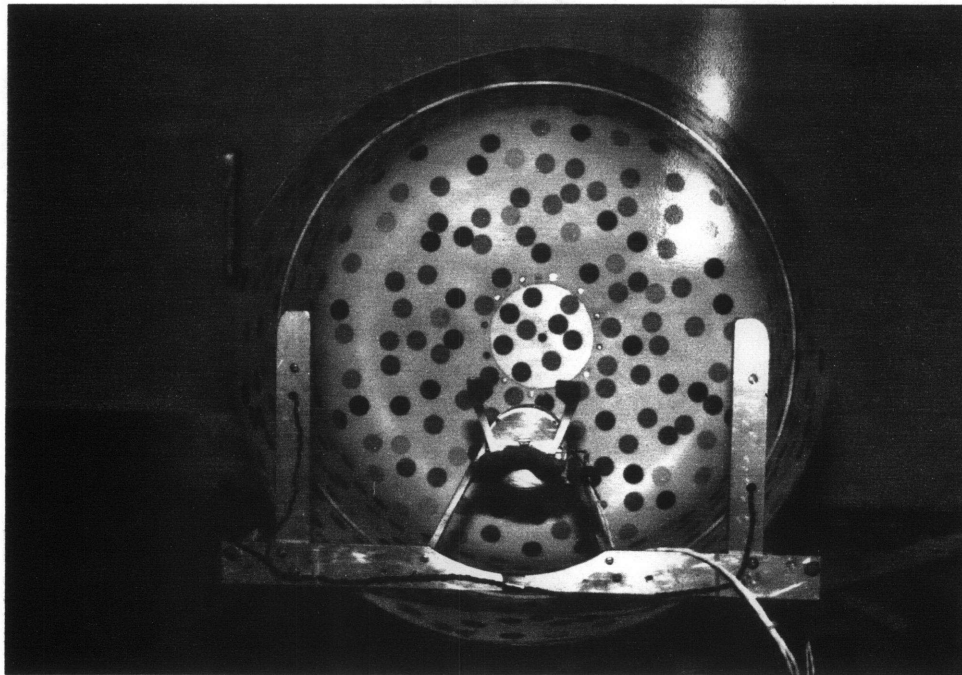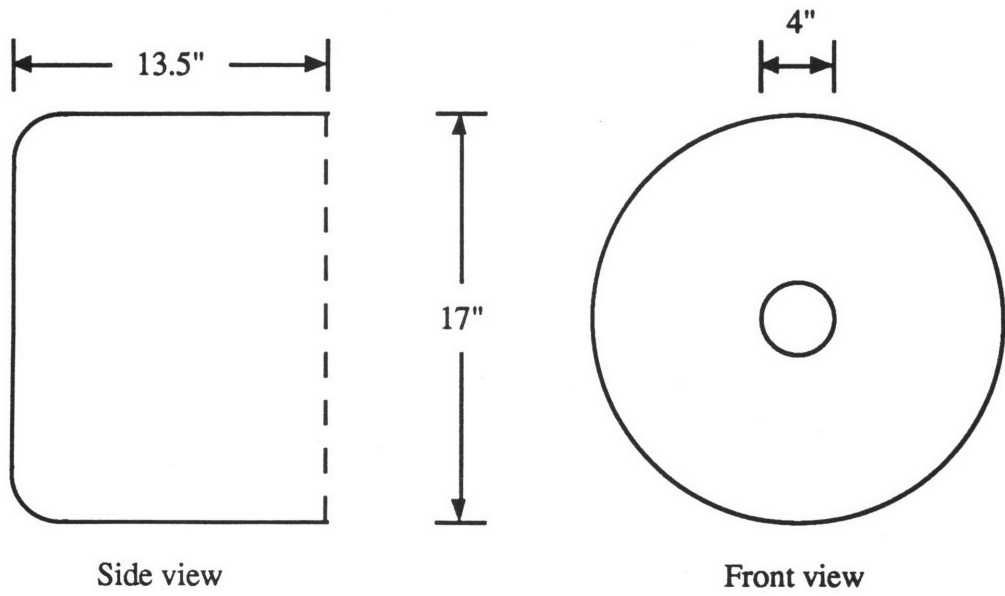
**Figure 3.1.** Rotating dome. Upper schematics depict dome dimensions. Lower photograph shows visual stimulus pattern, fixation point, and biteboard position.

covered by a disk with the same dot pattern as the rest of the dome interior, providing uniform rotation of the full visual field. A red LED was mounted at the center of the disk, coincident with the dome rotation axis. This LED, which subtended a visual angle of 0.5°, provided a fixation point for the subject during the dome trials. A fixation point was necessary to avoid induction of erroneous scleral coil torsion signals by oblique eye movements. The LED was very dimly lit and was mounted within a black holder to prevent any illumination of the dome interior during fixation periods in the dark. Power to the LED was provided by a 9 V battery mounted on the back of the central disk.

### 3.1.1. Drive System

The rotating dome was driven by a DC electric motor with maximum ratings of 24 rpm and 0.002 horsepower (Figure 3.2). The dome was linked to the motor with a toothed belt incorporating a gear reduction ratio of 32:72. This arrangement provided a predicted maximum dome speed of 64°/sec. The dome speeds selected for the experiment ranged from 15° to 60°/sec, although 4 trials for one subject were run at 72°/sec. A unidirectional 30V supply provided power, so dome rotation direction was selected with a manual switch which reversed the polarity of the output voltage to the motor. The data acquisition computer automatically controlled dome speed by outputting a signal proportional to the required motor voltage. A diagram of the dome driver circuitry is included in Appendix A.

An optical encoder linked to the dome motor provided a measure of dome rotation rate. The encoder output a square wave consisting of 256 cycles per encoder axle revolution. The linkage about the motor and encoder axles resulted in one encoder square wave half-cycle for each 0.43° of dome rotation. Given a 200 Hz. sampling rate and the need for at least one sample per half-cycle to adequately characterize the encoder signal, the encoder system could function as as meter of rotation rate up to a theoretical maximum dome speed of 86°/sec.

Figure 3.3 shows the dome speed variation over a typical 30 second trial duration for trials at speeds from 15° to 60°/sec. Speeds were calculated at 1 second intervals by counting
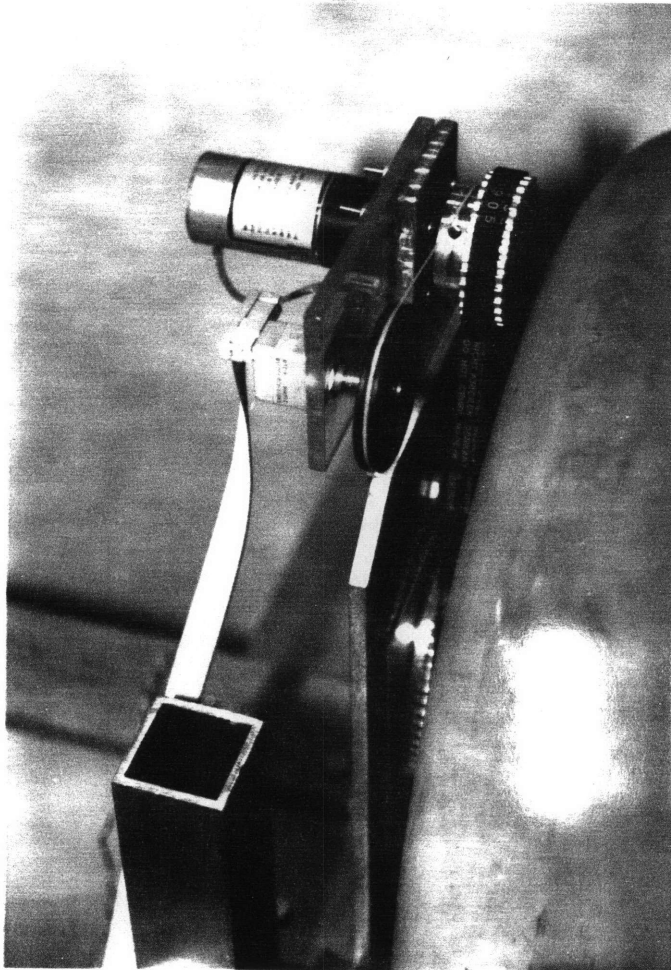
**Figure 3.2.** Dome motor drive mechanism. The DC drive motor is linked to the dome axle by a toothed belt. The black disk in the foreground links the optical encoder to the drive motor via a narrow band.

## Dome speed variation in time
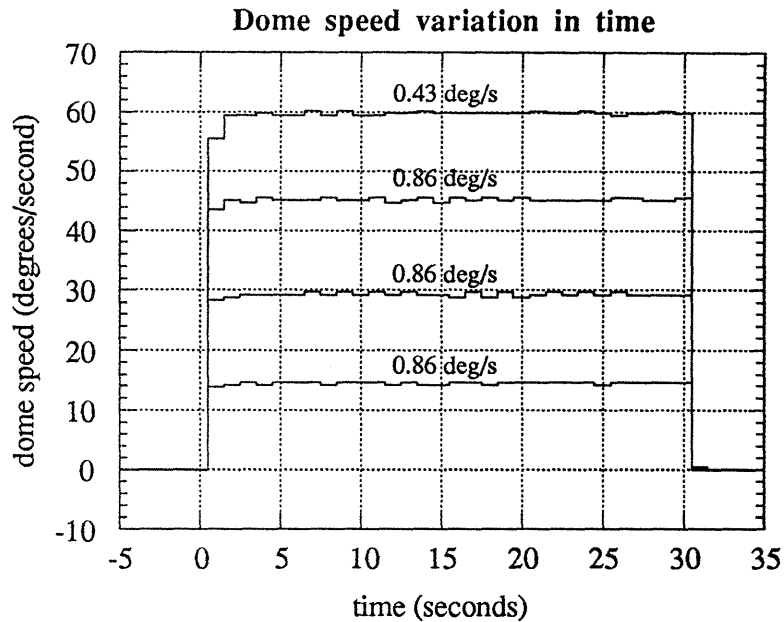


**Figure 3.3.** Variability in dome speed over time for the four speeds tested, measured from optical encoder output. Values above traces indicate peak-to-peak variation during steady state.

## Samples per encoder half-cycle vs. time
## 60 deg/sec velocity step



response time = 0.065 seconds
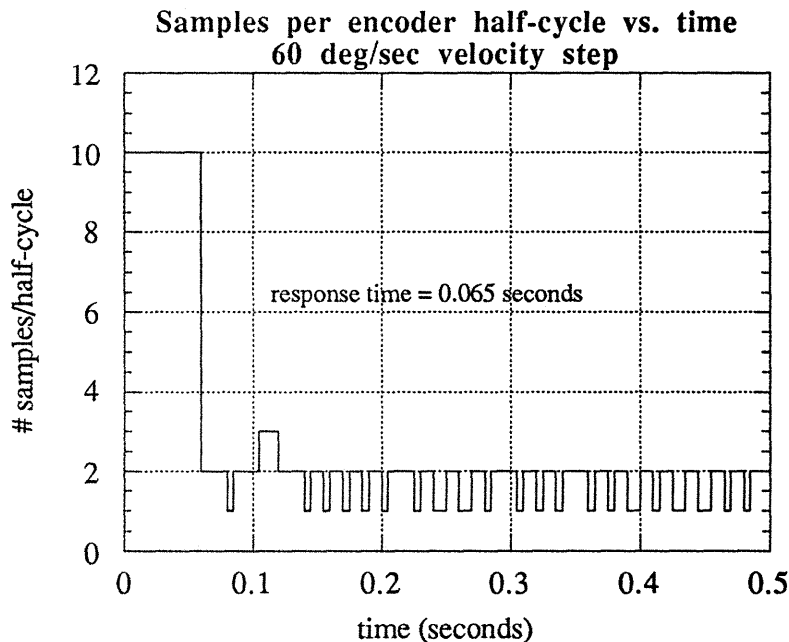
**Figure 3.4.** Time response of dome speed to motor voltage step input. Number of 200 Hz. samples per time encoder square wave half-cycle vs. time for typical trial (60°/s). Motor voltage step applied at time 0. Full velocity (steady state) reached within approximately 0.065 seconds.

the number of square wave half cycles recorded each second. These plots show that the speed generally remained constant to within ±0.43°/sec, the resolution of the optical encoder system based on a 1 second window. Since the desired stimulus constituted a velocity step, the response time for attainment of the steady-state dome velocity became an issue. The velocity rise time was determined by counting the number of samples recorded for each encoder half-cycle. As the dome accelerated, the number of samples per half-cycle dropped to a fairly steady value. By evaluating the time required to reach steady state, the rise time was almost always found to measure less than 0.1 seconds. Figure 3.4 displays the number of samples per cycle versus time for a typical 60°/sec trial with a calculated response time of 0.065 seconds.

### 3.1.2. Dome Lighting

Crites (1980) found that 24 foot candle incandescent lighting gave good pattern illumination while minimizing eyestrain. In the current experiments, two 1.9 W incandescent bulbs provided illumination at approximately one half the power level (measured with a camera lightmeter) used for the Spacelab stimulus. Subjects tested on both dome configurations reported equally strong vection at the lower light intensity; Leibowitz et. al. (1979) found that vection remained largely independent of changes in lighting even when illumination was reduced to near the scotopic threshold. The bulbs were mounted at eye level on either side of the subject's head approximately 2.25 inches from the inside wall of the dome, just outside the dome mouth. The mount design shaded the subject's eyes from the direct glare of the lamps.

Since the experimental trial protocol required a period of complete darkness (other than the LED fixation point), the room lights were turned off and the doors were closed for the duration of the experiment. Dome illumination was controlled solely by the dome lamps, which could be turned on and off using either a manual switch or a computer-controlled relay. Although some small light leaks were present in the test room, the dome shell itself occluded virtually all of the stray light. Subjects reported that even after dark-adapting for 1 - 2

70

minutes, nothing was visible within the visual field when the dome lights were off. Furthermore, the fixation LED proved too dim to provide any illumination.

### 3.1.3. Biteboards

The subject's head was fixed within the dome by a dental biteboard. Each subject constructed a personal custom-fit biteboard, which consisted of dental impression material molded over a flight-reject biteboard blank designed for the Spacelab missions. The impression material used was Express™ STD vinyl polysiloxane putty manufactured by 3M. This two part (base/catalyst) putty required an oral setting time of 5 minutes, during which the subject bit down continuously until the putty reached its final firmness. The biteboard was mounted in a holder specially instrumented with strain gages to transduce neck torque exerted by the subject.

### 3.1.4. Vection Measurement

Subjects indicated their vection sensations with a rotary joystick using a magnitude estimation technique (Young et. al., 1986; Young and Shelhamer, 1990). The joystick (Figure 3.5) consisted of a spring-loaded knob mounted on the shaft of a potentiometer. The knob had a central rest position and hard stops at deflection angles of $\pm 45°$. When powered by a $\pm 15$ V supply, the joystick output ranged from 0 V in the center to $\pm 5$ V at full deflection.

### 3.2. Scleral Search Coil Eye Movement Measurement System

Ocular torsion was measured using a magnetic induction method first described by Robinson (1963). An oscillating magnetic field composed of both horizontal and vertical components was induced about the subject's head, while a specially wound coil rested on the sclera of the subject's eye. According to Faraday's law of induction, an electric potential was induced in the eye coil proportional to the rate of change of magnetic flux across the coil. Therefore, the oscillating signal induced in the scleral coil had an amplitude proportional to the coil area lying perpendicular to the magnetic field. A phase-sensitive detector extracted only the

71

Figure 3.5.  Rotary joystick used to signal estimated magnitude of vection velocity scaled to dome rotation rate.  Subject holds box in non-dominant hand with the point on the knob directed downward. Dominant hand is used to turn joystick knob.

signals in synchronization with the driving frequency of the magnetic field, rejecting all random and non-synchronous interference signals. The phase detector produced a DC voltage in proportion to the area of the coil perpendicular to the field vector. The perpendicular area depended on the sine of the torsion angle. No correction for this nonlinearity was required, however, since the torsion angle measure in radians deviated from the sine of the angle by less than 2% for angles below 20°.

### 3.2.1. Magnetic Field Generation Coils

The magnetic field generator and phase detection electronics were purchased from C-N-C Engineering (Seattle, Washington). Specifications on this equipment are included in Law (1991). The field generation system consisted of two orthogonally mounted coil pairs. Each coil measured 2 feet on each side, and was imbedded within a square wooden frame. One pair lay in the horizontal plane, while the other was mounted vertically in the subject's pitch plane; the set described the outline of a cube about the subject's head. The horizontal coils produced a magnetic field with a vertical component at the center of the cube, while the vertical pair generated a horizontal component in the subject's frontal plane. The peak magnetic field strength generated at the cube center reached 0.3 gauss and 0.4 gauss for the horizontal and vertical coils respectively.

To differentiate between the horizontal and vertical components, the two coil pairs were driven at different frequencies between 60 kHz and 135 kHz, selected with a ratio of 3:2. The coil pairs made up series resonant tuned circuits; for this particular coil system at resonance, the horizontal and vertical pairs operated at respective frequencies of about 122 kHz and 83 kHz. Peak to peak system noise typically fell below 1 arc minute given a measurement bandwidth of 530 Hz.

Dual Phase Detectors, one for the torsion channel and one for the horizontal/vertical channel, broke down the eye coil signals into horizontal, vertical, and torsional eye position

components. Four main controls were used to adjust each Phase Detector during coil system calibration:
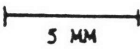
1. Offset control: adjusted the zero of the scleral coil output to match the zero degree eye position.

2. Gain control: adjusted the output gain to a nominal value of 2 V per 10° of eye rotation.

3. Meter sensitivity switch: set the eye position indicator to either ±5° or ±50° full scale. The 5° range was used only for fine zero adjustment; all measurements were conducted using the ±50° range.

4. 0° / 180° switch: reversed the phase of the analog output signal.

### 3.2.2. Scleral Search Coil

The scleral coils used in these experiments were manufactured by Skalar Inc. of the Netherlands, based on a design by Collewijn (1975). Each scleral ring, depicted schematically in Figure 3.6a, contained two separate coils imbedded in silicone rubber. The coils employed nine windings of 0.05 mm insulated copper wire. One coil was wound just within the outer margin of the ring, and transduced horizontal and vertical eye position. The second coil, designed to detect torsional movements, required a more complicated winding in which the wire crossed between the inner and outer margins of the ring every 180°. The torsion coil had a plane of symmetry defined by the diametrically opposed wire crossing points; the projection of the coil onto this plane effectively produced a flattened vertical coil wound consistently in one direction.

The silicone rubber ring (Figure 3.6b), which had an inner diameter of approximately 11.3 mm, rested completely on the sclera. The central hole was considerably larger than the maximum pupil diameter, so vision was not obscured. The ring was aligned on the eye with the coil leads exiting at the inner canthus. The concave inner surface had a radius of curvature smaller than that of the globe of the eye. By pressing the coil down firmly to evacuate bubbles and fluid from the space between the ring and the eye, a suction effect was created to fix the

74

## a. Scleral coil winding schematic



SCALE: |————————| 
5 MM

ALL DIMENSIONS IN MM

COIL 2

COIL 1

COIL 2        COIL 1

1/2 EFFECTIVE
AREA OF COIL 2
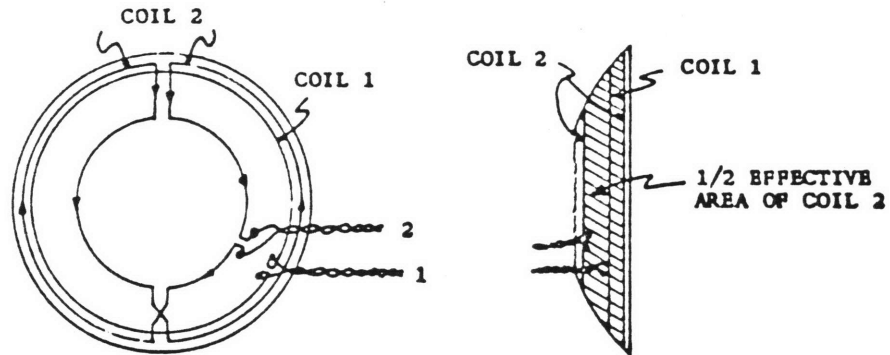
## b. Actual scleral coil in silicone ring
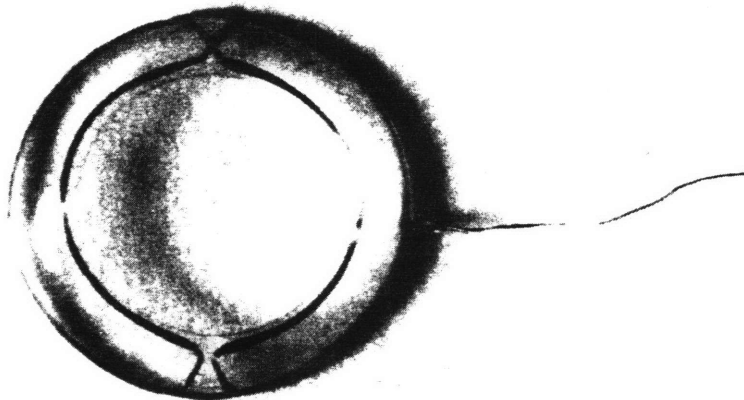


Figure 3.6.   Scleral search coil.   [a.]   Diagram depicting winding scheme for coils transducing horizontal/vertical (coil 1) and torsional (coil 2) eye movements.   Diagram on left is a frontal view; right picture shows side view of effective coil area (in Robinson, 1963).   [b.]   Skalar scleral coil imbedded in silicone rubber ring (in Ferman et. al., 1987).

coil to the eye. This evacuation raised the intraocular pressure slightly to a level regarded as "high normal."

Use of the scleral coil required prior numbing of the subject's eye with a topical anaesthetic, proparacaine HCl 0.5% (brand name Ophthetic). The coil could remain in the eye no longer than 30 minutes; further anaesthetic was administered as requested by the subject. Hydrogen peroxide solution ($H_2O_2$ 3%) provided a means of sterilizing the coil before use. Sterile saline solution was used to rinse the hydrogen peroxide from the coil before insertion into the eye.

### 3.2.3. Mounting the Field Coils and Dome

Optimal coil system performance required centering the subject's head within the field generation coils. For proper presentation of the rotating stimulus, the dome shell had to project through the front opening of the coil frame. Furthermore, this subject-dome-coil relationship had to be preserved in both the erect and supine orientations.

For the upright runs (Figure 3.7a), the field coils were supported by two tables, one in front of and one behind the subject. Neither table touched the subject. The dome was mounted on an adjustable stand resting on the front table. With the coil and dome positions fixed, metal plates and boards of the necessary thickness were placed beneath the subject's feet to permit a comfortable erect stance with the head centered in the coils. The supine sessions incorporated the chair from the MIT linear acceleration sled (Figure 3.7b), which was constructed and described in detail by Law (1991). This chair was designed to accommodate the coil system, and allowed the subject to lie supine with the coils mounted about the head. The relative distance from the coil frame to the seat of the chair was adjustable for subjects of different sizes. The dome support stand rested atop the wooden coil frame, suspending the dome shell above the subject's head. Cushions raised the subject's head to the proper position within the mouth of the dome.

**a. Erect dome**

**b. Supine dome**

Figure 3.7. Rotating dome and magnetic field coils in erect and supine orientations. [a.] In the erect position, the coil system rests on two tables, and the subject stands within the coil frame. [b.] For the supine runs, the coils are supported by the chair designed for the MIT linear acceleration sled, and the subject lies in the chair.

### 3.3. Dome Controller and Data Acquisition Computer

A Macintosh computer running LabView software was used for both data acquisition and control of stimulus presentation. The actual input/output interface utilized a 12 bit MacAdios I/O board with a ±10 V range. Four signals (torsional eye position, joystick vection indication, biteboard torque, and optical encoder output) were sampled at 200 Hz. Two output channels were also utilized: one controlled the dome speed while the other turned the dome lights on and off.

The LabView programs for the dome experiment were written by Nick Groleau. Figure 3.8a shows the panel display for the virtual instrument **Keoki.Thesis**. The right half of the panel allowed definition of the data sampling rate and trial duration, divided into pre-, per-, and post-rotation segments. Before each run, the appropriate subject code letter and run order number were also selected. Upon starting the program, the computer proceeded automatically through the preselected trial sequence. Input and output signals were displayed in real time inside the plot windows at the left. After each trial, the operator was given the option of repeating the trial or saving the data and proceeding to the next trial. The panel display for **cread-cwrite Demo** is presented in Figure 3.8b. This virtual instrument served as a computerized stripchart recorder, allowing the operator to check the computer interface with each of the input and output channels.

A stripchart recorder also plotted four channels of data, serving as a backup and quick reference. The eye movements in all three planes (horizontal, vertical, and torsional) were output. By recording the horizontal and vertical channels, it was possible to look for large oblique eye movements which would have coupled with the torsional channel. The fourth stripchart channel consisted of the joystick vection indication.

Front Panel
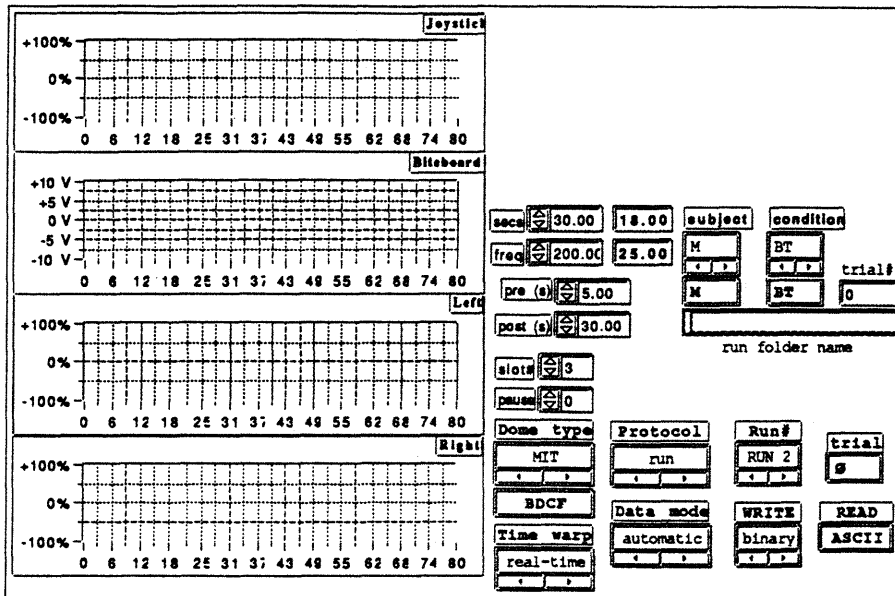
Front Panel
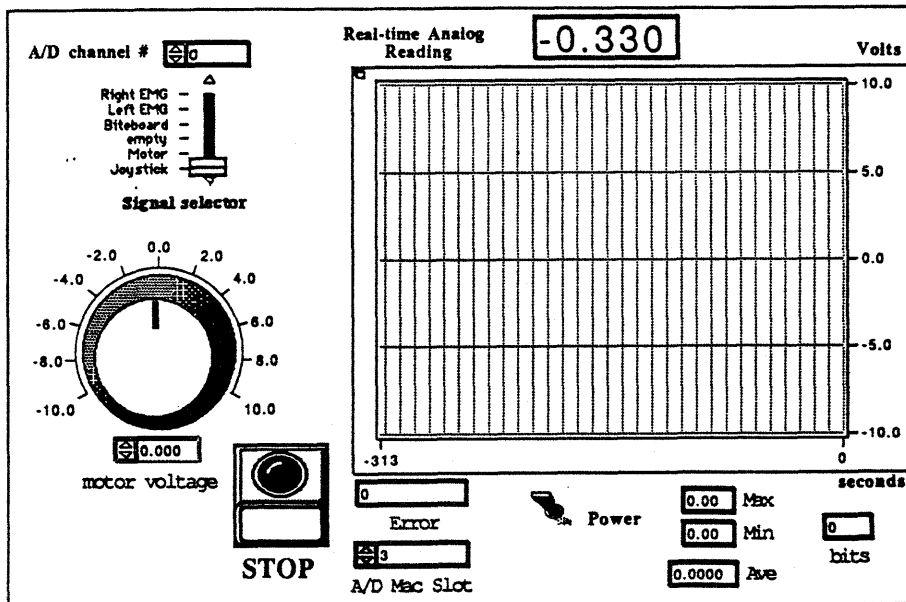


**Figure 3.8.    LabView virtual intrument panels for data acquisition.   [a.] LabView dome controller and data acquisition virtual instrument.   [b.]   Instrument for input/output signal check.**

# 4. THE EXPERIMENT

## 4.1. Experimental Design

This section describes the design of the experiment, guided by the stated objectives of the study, which took place at three different levels: (1) organization of the runs for different experimental conditions; (2) construction of test runs by selecting the number and order of trials, as well as their stimulus speeds and directions; and (3) designation of the length of an experimental trial, including pre-, per-, and post-stimulus-rotation periods. Selection of test subjects followed the development of the experimental procedure. Relevant information concerning each of the seven subjects is presented. Finally, the actual order of trials and runs used for each subject is summarized, and all anomalies or deviations from the experimental procedure are noted.

### 4.1.1. Definition of Experimental Paradigm

The objectives of the study called for comparison of optokinetically induced ocular torsion erect and supine, as well as an examination of the effects of different visual fields on OKAN. It was decided that each subject would take part in four experimental runs representing the four possible combinations of the variables of interest (2 orientations, 2 post-stimulus visual fields). To allow for a reasonable number of trials per run, the four runs were split into two sessions of two runs each, and the sessions took place on different days. Two of the runs had the subject standing erect, and in the other two the subject lay supine. Because of the time consuming process involved in changing the experimental equipment setup between orientations, both runs for a given orientation occurred within the same session. To avoid continuous switching of the equipment orientation, all subjects were first tested erect. The dome and coil system were then moved to the supine orientation, and all subjects were run again in this position.

Within each session, the pre- and per-stimulus-rotation segments of each run were identical. In contrast, the post-stimulus period in each run incorporated one of two different

visual fields. The initial design called for leaving the dome illuminated after the end of rotation in half of the trials, providing a stationary visual field. In the other half, the dome lights would be extinguished, leaving the subject in complete darkness except for a dim central LED fixation point.

Subject M was tested in upright and supine orientations under these conditions. Visual inspection of the optokinetic torsion traces revealed little difference between the aftereffects in the light and dark. It was thought that the fixation LED might have inhibited afternystagmus, even though it subtended only 0.5° of the subject's visual field and its radial symmetry provided no orientation cues. For this reason, the trials with the post-stimulus segment in the light were replaced with a condition of total darkness during the post-rotation period. Because the fixation LED was no longer lit in these trials, the danger existed that measurements of eye torsion would suffer contamination from coupling with large oblique eye movements. To minimize this possibility, the subjects were instructed to fixate on an "imagined" central LED during the period when aftereffects were measured.

Turning off the fixation LED involved turning on the room lights, unplugging the 9 V battery which powered it, and ascertaining that the middle dome section and LED remained centered about the dome rotation axis. Since the experiment time was strictly limited, the decision was made to perform all the trials in the first run with the LED illuminated. Then the LED would be unplugged, and the fixation LED would not be visible in the dark for the second run. Because the fixation LED condition was always tested before the non-LED condition, and erect tests always preceded supine tests, there was a risk that the influence of these two variables might be confounded with any habituation or exposure-related effects. This possibility will be discussed later in the context of the experimental results and the relevant literature.

Having defined the experimental conditions, the next step in the design of the experiment involved selecting the combination of stimulus rotation speeds which would comprise a run. Ideally, the test speeds would cover a range likely to generate both strong

optokinetic and vection responses. Collewijn et. al. (1985) observed a largely constant torsional SPV gain for stimulus speeds above 6°/sec, while the psychophysical responses to visual roll stimuli saturate at rates from 40 to 60°/sec (Dichgans et. al., 1972). Based on these figures, an initial decision was made to retain the stimulus speeds selected for the shuttle Spacelab missions: 30°, 45°, and 60°/sec (Young et. al., 1986; Young and Shelhamer, 1990). LabView software written by Nick Groleau for baseline data collection connected with the Spacelab Life Sciences 1 shuttle mission was readily available; this program provided data acquisition and control of the rotating stimulus for experimental runs of 6 trials (3 speeds, 2 directions). The stimulus control program provided for two different run sequences, in which the order of the trials was randomized by rotation speed and direction. The randomized presentation served two purposes: it (1) minimized confounding of legitimate directional or speed dependencies with possible effects of presentation order, and (2) prevented the subject from anticipating the trial order.

Two runs of six trials (lasting approximately 110 sec each, including pre- and post-rotation recording intervals, for a total of 22 minutes) were completed for subject M in the upright orientation using the speeds ±30°, ±45°, and ±60°/sec. Even with the 8 spare minutes, the session lasted the entire allowable 30 minutes, demonstrating that a time "overhead" of approximately 35% was needed to complete a two run protocol. Analysis of the OKN from these runs indicated a saturation of the SPV at the two higher speeds. To characterize better the speed dependence of the OKN SPV, two more trials at ±15°/sec were added to each run for the remainder of the experiment. The stimulus duration for each trial was reduced by 1/3 to 30 seconds to accommodate the increase in trials from 6 to 8 per run. Table 4.1 shows the 2 finalized run orders; the key to the trial letter codes is included.

The main constraint on the length of a session was determined by guidelines for use of the scleral search coil. To avoid excessive irritation of the eye, the coil could remain in a subject's eye for a maximum of 30 minutes. This hard limit created a clear tradeoff between

82

| Trial | 1 | 2 | 3 | 4 | 5 | 6 | 7 | 8 | | | CW | CCW |
|---|---|---|---|---|---|---|---|---|---|---|---|---|
| Run | | | | | | | | | | | (+) | (-) |
| 1 | E | A | F | B | H | C | D | G | | 15°/s | A | E |
| 2 | B | H | E | C | A | F | D | G | | 30°/s | B | F |
| | | | | | | | | | | 45°/s | C | G |
| | | | | | | | | | | 60°/s | D | H |

**Table 4.1.** The two randomized run orders of 8 trials (4 speeds, 2 directions) used for stimulus presentation. A key to trial letter codes is included at right.

the length of an experimental trial and the number of trials which could take place in one session. Observation of OKAN provided the driving criterion in selection of an appropriate trial length. The duration of the stimulus rotation was chosen to allow for adequate charging of the "velocity storage" integrator, which in turn would presumably generate a strong afternystagmus.

Brandt et. al. (1974) found that the peak velocity of horizontal OKAN increased with stimulus duration to a maximum obtained with a stimulus lasting about 60 seconds. Cohen et. al. (1981) estimated the charging time constant of OKAN at 20 seconds, while Lafortune et. al. (1986) proposed a value of approximately 49 seconds. The latter estimate seems quite high, since the authors stated in the same paper that " 'saturation' levels for this parameter [the 'stored' velocity] were presumably attained by 40 sec." A tentative stimulus duration of 45 seconds was selected to permit maximal charging of velocity storage. This duration was shortened to 30 seconds after the first session with subject M in order to allow an increase in the number of trials per session from 12 to 16. Assuming a time constant of 20 seconds, this stimulus duration would still allow charging of velocity storage to about 80% of saturation.

Next, the length of time post-stimulus for which eye movements would be sampled was selected to enable observation of the major features of the aftereffects. Cohen et. al. (1981) found a horizontal OKAN discharge time constant near 25 seconds; Jell et. al. (1984)

83

used a double exponential fit to their data and obtained a mean long time constant for OKAN decay of 49 seconds. However, the torsion records accumulated by Malan (1985) indicated the return of the eye to rest within 20 to 30 seconds; these results were corroborated by the author in preliminary tests on subject M. Based on a horizontal OKAN decay time constant of 25 seconds and the available torsion data, a post-stimulus recording period of 30 seconds was chosen.

Also, an interval of five seconds prior to the onset of stimulus rotation was established to measure the baseline eye position. A total of 65 seconds of data were sampled per trial. The computer needed approximately 20 seconds to save the data and set up for the next trial, giving the subject some additional recovery time to relax between trials. The total minimum trial length thus came to 85 seconds (Figure 4.1). A total of 16 trials per session (2 runs of 8 trials each) resulted in 22.7 minutes dedicated solely to data acquisition and computer setup time, leaving approximately 7 minutes (30%) leeway. In practice, the coil sessions virtually always required the entire half hour.

In order to familiarize the subjects with the experiment, each subject completed a training run before any eye movements were recorded. The run consisted of several trials prior to coil insertion, with the intent of allowing the subject to become adept at indicating vection with the the joystick and eliminating any learning effects during the actual data-taking runs. With the exception of M, all subjects performed the training run at the beginning of the first session (upright). Subject M, who had served several times as a test subject in the dome, did not take part in a training run during any of the sessions recorded for this thesis.

### 4.1.2. Subject Selection

A sample population of 6 subjects was selected as a reasonable balance between the desire for a large sample and the limited time and resources available for the study. The subjects, 4 male and 2 female, were chosen from the students associated with the MIT Man-Vehicle Laboratory. Because one subject (R) perceived almost no vection during his first

## Dome Trial Event Sequence
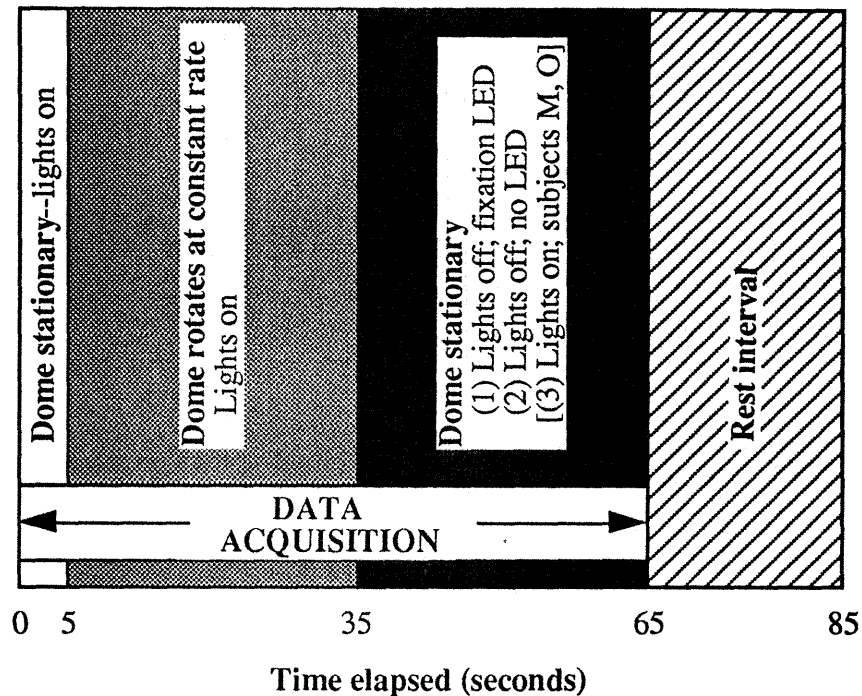


**Figure 4.1. Standard trial sequence of events.**

experimental session, he was not tested again and a third female subject was added. The

subjects ranged from 19 to 26 years of age. Two of the subjects had taken part in a similar

rotating dome experiment about 18 months previously. Relevant information concerning each

of the subjects is listed in Table 4.2. The subject codes range from M through S because the

data acquisition software was designed for the SLS-1 crewmembers designated in this fashion.

Subject M took part in all of the tests during the design definition phase. He was first run in

September 1990; the data from this session were not included in the thesis results due to a low

sampling rate of 25 Hz.

### 4.1.3. Summary of Individual Experimental Runs

The actual experimental runs performed by each subject are presented in Table 4.3.

Trials are designated by the letter codes defined earlier in Table 4.1 to denote the nominal dome

speed. Actual mean dome speeds for each trial are tabulated in Appendix D. The run series for

three subjects included some differences from the final experiment protocol. As explained

85

| Subject | Sex | Age | Handedness | Eye dominance | Uncorrected vision | Prior dome experience? |
|---------|-----|-----|------------|---------------|--------------------|-----------------------|
| M | M | 23 | right | left | | yes |
| N | F | 21 | right | left | 20/20 | no |
| O | M | 26 | right | left | | no |
| P | M | 23/24 | right | right | 20/20 | yes |
| Q | F | 19 | right | left | 20/24 l 20/35 r | no |
| R | M | 24 | right | left | 20/20 | no |
| S | F | 23 | right | right | 20/200 | no |

**Table 4.2. Summary of relevant subject information.**

above, subject M's tests took place during the design definition phase of the experiment, and therefore were somewhat different from those of the other subjects. Due to a computer problem and time constraints, subject N's erect session included 12 trials in the fixation LED condition and only 4 trials in complete darkness following stimulus rotation. The test battery for subject O included two erect sessions over which 3 runs were performed. During his first erect run, O developed severe motion sickness symptoms and the session was ended after that run. During his second erect session O felt no motion sickness, and a run with the lights left on following dome rotation was included rather than a repetition of the trials under the fixation LED condition.

These subjects (M, N, and O) represented the major deviations from the experimental design. However, some minor differences were introduced by the propensity of the data acquisition computer to "hang" or "crash" in the middle of a run. The dome controller was programmed to step through 1 of 2 specific pseudorandom trial sequences for each run; restarting the LabView program required starting from the beginning of one of the predefined trial orders. Thus, computer difficulties created irregularities in the trial sequences for some runs. These runs are marked in Table 4.3 by a '†' symbol at the trial after which the computer crashed. Other trials, marked with an '*' in the table, represent cases where the dome lights were inadvertently left on during the post-rotation phase of eye movement recording.

| | | | | Trial number | | | | | | | |
|---|---|---|---|---|---|---|---|---|---|---|---|
| Subject | Session Date | Postural Orientation | Post-rotation visual field | 1 | 2 | 3 | 4 | 5 | 6 | 7 | 8 |
| M | 4/19/91 | erect[a] | dark; LED | B | G | H | C | F | D | -- | -- |
| | 4/19/91 | erect | light | B | G | H | C | F | D | -- | -- |
| | 5/3/91 | supine[b] | dark; LED | G† | G† | G | E† | B | F | -- | -- |
| | 5/6/91 | supine | dark; LED | A | E | F | B | D | C | H | G |
| | 5/6/91 | supine | light | A | E | F | B | H | C | D | G |
| N | 7/12/91 | erect | dark; LED | E | A | F | B† | E | A | F | B |
| | | | | H | C* | D | G | -- | -- | -- | -- |
| | 7/12/91 | erect | dark; no LED | B | H | E | C | -- | -- | -- | -- |
| | 7/18/91 | supine | dark; LED | B | H | E | C | A | F | D* | C |
| | 7/18/91 | supine | dark; no LED | E | A | F* | B | H | C | D* | G |
| O | 7/12/91 | erect | dark; LED | B | H | E | C | A | F | D | G |
| | 7/15/91 | erect | dark; no LED | F | D | E | C | A | B | H | G |
| | 7/15/91 | erect | light | E | A | F | B | H | C | D | G |
| | 7/19/91 | supine | dark; LED | E | A | F | B† | B | H | E | C |
| | 7/19/91 | supine | dark; no LED | A | F | D | G | B | H | E | C |
| P | 7/15/91 | erect | dark; LED | B | H | E | C | A | F | D | G |
| | 7/15/91 | erect | dark; no LED | E | A | F | B | H | C | D | G |
| | 7/23/91 | supine | dark; LED | E | A† | B | H* | E | C | A | F |
| | 7/23/91 | supine | dark; no LED | D | G | B | H | E | C | A | F |
| Q | 7/16/91 | erect | dark; LED | E | A | F | B | H | C | D | G |
| | 7/16/91 | erect | dark; no LED | B | H | E | C | A | F | D | G |
| | 7/19/91 | supine | dark; LED | B | H | E | C | A | F | D | G |
| | 7/19/91 | supine | dark; no LED | E | A | F | B | H | C | D | G |
| R | 7/17/91 | erect | dark; LED | B | H | E | C | A | F | D | G |
| | 7/17/91 | erect | dark; no LED | E | A | F | B | H | C* | D | G |
| S | 7/18/91 | erect | dark; LED | E | A | F | B | H | C | D | G |
| | 7/18/91 | erect | dark; no LED | B | H | E | C | A | F | D | G |
| | 7/19/91 | supine | dark; LED | B | H | E | C | A | F | D | G |
| | 7/19/91 | supine | dark; no LED | E | A | F | B | H | C | D | G |

[a] Duration of dome rotation was 45 seconds for subject M erect. Dome rotation lasted 30 seconds for all other sessions.
[b] Dome rotation speeds for subject M supine were ±21°, ±41°, ±56°, and ±72°/sec due to a calibration error.
* Dome lights inadvertently left on after dome stopped rotating.
† Computer crash caused irregularity in trial sequence.

**Table 4.3.** Run conditions and trial sequences for which eye torsion was recorded.

## 4.2. Experimental Procedure

Each experimental session included four main phases. The first segment was devoted to preparing the subject for the experiment. Second, the coil system was readied for collection of eye movement data. The actual experimental runs and data collection made up the third phase. Finally, the subject was debriefed following completion of the tests. Appendix B contains detailed outlines of the protocol for each part of the session.

### 4.2.1. Subject Preparation

Since the erect and supine runs were identical except for subject orientation, most of the subject preparation took place during the erect session, which was scheduled first. The session began with a description to the subject of the nature of the experiment. The experimental apparatus was shown to the subject, the test procedures were reviewed, and the subject's task was explained. The function of the scleral search coil system was briefly described, and the possible risks to the subject associated with use of the eye coil were clarified. The subject was informed that the experiment would take place in two sessions on different days, and that he or she could withdraw from the experiment at any time. The subject then signed a statement agreeing to participate in the experiment as described. Copies of the human use applications for the rotating dome experiment and the scleral coil system, as well as a sample informed consent statement, are included in Appendix C.

Next, the experimental test apparatus was adjusted for the individual subject. First, the subject made a personal biteboard to hold the head in place during the experiment. Approximately 5 minutes were required for the dental impression compound to set. Then the biteboard was fixed into the instrumented biteboard support contained within the dome shell. At this point, the subject was positioned so that the eyes were close to the center of the field generation coils and the subject was able to remain comfortable while biting on the biteboard.

When the apparatus was properly adjusted for the size of the subject, specific instructions were given to the subject on how to perform the experimental trials. The rotary

88

joystick was given to the subject, who turned the knob to either side in order to determine its range of motion. The subject was given roughly the following instructions:

> Stand with your feet together at all times [erect runs only]. Before the beginning of each trial, you will be instructed to fixate on the central LED at the rear of the dome. Bite down on the biteboard hard enough to keep your head from moving. You are to continue fixating on the LED during and after dome rotation, until the operator instructs you to relax. For some of the trials, the fixation LED will be turned off and you will be in complete darkness after the dome rotation. At these times, imagine the central LED and try to fixate on this point. When the operator instructs you to relax, you may stop fixating or close your eyes. You may also let go of the biteboard. If you experience any discomfort, eye irritation, or motion sickness symptoms, feel free to ask the operator to stop the experiment at any time.

> Hold the joystick box in your left hand [all subjects were right handed] with the knob toward your body and the rod projecting from the knob pointed down, so that the knob rotates about your body's roll axis. Turn the knob with your right hand to indicate your feeling of subjective vection. Turn the knob in the direction toward which you feel you are rotating; do not indicate the direction of field rotation. Scale your perceived velocity by the rotation rate of the dome, so that you indicate your vection velocity as a percentage of the dome speed. Thus, full deflection of the joystick means that you feel saturated vection--the dome appears stationary while you have taken on its full rotation velocity. Likewise, zero deflection means that you feel yourself stationary and sense only the dome rotation. Remember to indicate your rotation rate and not your perceived tilt angle. Stationary objects [primarily the biteboard holder] in your field of view may appear to rotate with you during vection. You may use such a perception as another cue about vection onset and magnitude. If you feel a vection dropout--a period when your perception of self-motion stops--return the joystick to the central zero position until vection returns. If you perceive any outlasting self-rotation or reversal of self-rotation direction after the dome rotation stops, indicate such vection aftereffects with the joystick.

After receiving these directions, the subject completed one training run before actually being tested erect. The purpose of this run was to make sure the subject fully understood all of the instructions and was comfortable with the proper use of the joystick. The joystick trace was monitored, and questions were asked of the subjects between trials to ascertain that their vection indications were consistent with their actual perceptions. Table 4.4 displays the sequence of trials for each subject's training run. Subject M had been tested several times previous to his data acquisition sessions, and did not require a training run.

| | Training run trial # | | | | | | | |
|---|---|---|---|---|---|---|---|---|
| Subject | 1 | 2 | 3 | 4 | 5 | 6 | 7 | 8 |
| N | B | H | E | G | A | F | D | C |
| O | B | H | A | -- | -- | -- | -- | -- |
| P | E | A | F | B | -- | -- | -- | -- |
| Q | B | H | E | C | A | F | -- | -- |
| R | E | A | F | B | H | C | D | G |
| S | B | H | E | C | A | F | D | G |

**Table 4.4. Training runs performed during test session upright prior to data collection runs.**

### 4.2.2. Coil System Preparation

The power to the coil system was turned on at least one half hour before use to allow the electronics to warm up. After this settling time, the calibration jig was mounted within the field coils and the scleral coil to be used was taped onto the calibration jig. The coil output was zeroed, then calibrated for horizontal, vertical, and torsional rotations. The calibration device was removed and the eye coil was placed in a sterilizing hydrogen peroxide solution ($H_2O_2$ 3%) for at least 10 minutes prior to insertion in the subject's eye, then rinsed thoroughly with sterile saline solution. When the subject was properly positioned within the field coils, the subject's right eye was anesthetized using a topical 0.5% solution of proparacaine HCl (brand name Ophthetic®).

The search coil was inserted under the eyelids so that it rested on the sclera with the leads exiting nasally. The lead wire was taped to the subject's forehead and cheek to prevent it from interfering with vision. At this point a stopwatch timer was started to ensure the coil did not remain in the subject's eye for longer than 30 minutes. Before starting the experiment, the coil output was zeroed again in all three axes while the subject fixated on the central LED. If necessary, the output was also zeroed between the two experimental runs. Additional anaesthetic was provided upon request. When the tests were completed, the coil was immediately removed from the eye and placed into a hydrogen peroxide bath. Drops of sterile

saline solution were dropped into the eye after coil extraction. None of the subjects complained of any irritation other than dryness due to the anaesthetic.

### 4.2.3. Experimental Test Procedure

As described above, each session consisted of 2 runs of 8 trials each. The 2 runs were identical except for the post-rotation phase. With the exceptions noted for subjects M and O, the first run utilized a central fixation LED during the post-rotation period; for the second run the LED was extinguished. Except for the LED, this segment of each trial took place in complete darkness. At the start of each run, the doors to the test room were closed and the room lights were extinguished. The brightness of the computer monitor was lowered to the minimum setting, and flashlights were used by the test operators. Flashlights were not used during the post-rotation data collection period in darkness. A stripchart recorder was utilized throughout both runs to provide a backup record of the subjective vection and eye movements in three dimensions.

At the beginning of each trial, the dome lights were turned on and the subject was instructed to fixate on the central LED. Five seconds of eye movement data were sampled prior to the onset of dome rotation. The computer then initiated dome rotation at a constant speed for 30 seconds* , at which time it halted the dome rotation and extinguished the dome lights simultaneously. The computer continued to sample data for 30 seconds† after the lights were turned off. When the program signalled the completion of data acquisition, the subject was instructed to relax. The subject received approximately 20 seconds of rest between trials while the computer stored the data and allocated memory for the next trial.

---

* The duration of dome rotation for subject M's erect trials was 45 seconds.
† For subject M's supine trials on 5/6/91, 30 seconds of post-rotation data were sampled but only the first 13.75 seconds were stored on disk due to a software bug.

### 4.2.4. Subject Debrief

Following removal of the scleral coil, the subject was asked a number of questions regarding the qualitative nature of his or her self motion perceptions. Comments were requested on the following:

•maximum amount of vection perceived; occurrence of saturated vection
•presence of paradoxical vection or perception of unambiguous 360° rotation
•amount of body tilt perceived
•postural imbalance or body sway
•perceived directional asymmetries in vection magnitude
•dependence of vection magnitude on dome speed
•differences between quality of vection erect and supine [following supine runs]
•presence of visual or self-motion aftereffects following the end of dome rotation
•motion sickness symptoms

The subject comments are summarized in Appendix E.

### 4.3. Data Analysis

Figure 4.2 contains an overview of the main elements in the data analysis pathway. The LabView data acquisition program sampled 4 signals simultaneously and saved the time series in four binary files per trial. These binary files were converted to MatLab variable format using **dome_convert**, a C program written by M. D. Balkwill and modified slightly by the author. The majority of the analysis was then performed using a number of MatLab scripts. Printouts of the primary analysis programs and scripts are located in Appendix F. Analysis of the data divided into three segments. The first step simply involved calculating the dome speeds from the optical encoder output. By far the largest amount of processing time was required by the second stage--analysis of the eye torsion. The third segment was devoted to evaluation of the subjective vection responses.

### 4.3.1. Dome Speed Calculation

The optical encoder output a 5 volt square wave when the dome rotated. The pulse width varied inversely with the dome speed. The dome rotation rate was calculated with the script **enc_speed**, which counted the number of rising and falling edges within successive
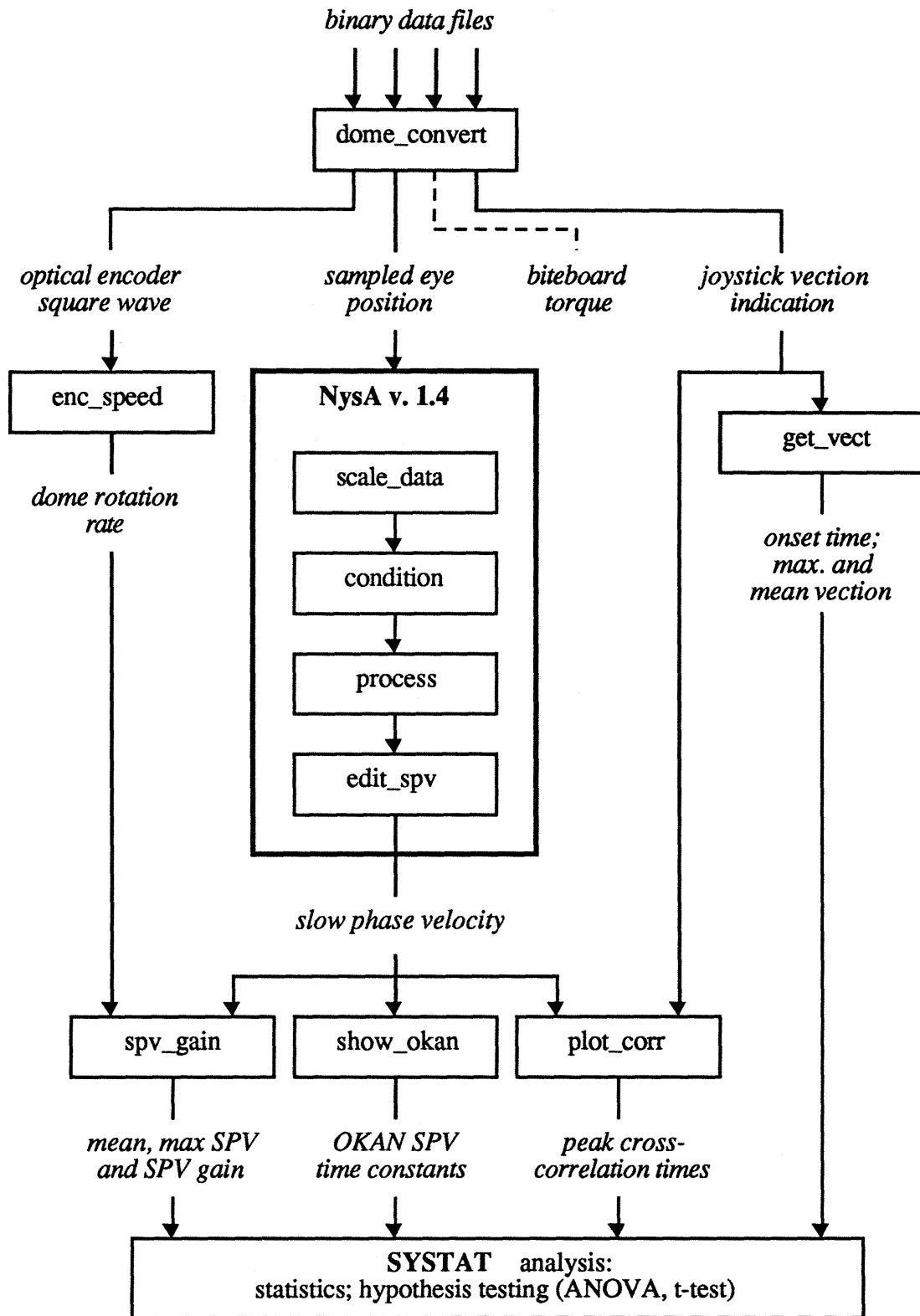
**Figure 4.2.** **Flowchart of data processing and analysis. Boxes denote programs and MatLab scripts. Italics indicate output products and parameters.**

time windows. There existed an inherent tradeoff in the selection of the window length: a shorter window improved the temporal resolution of the speed estimate but reduced the resolution of the velocity calculation. The optical encoder axis was linked to the dome driver motor with a belt such that each full revolution of the dome produced 309.82 cycles, giving a factor of 0.43 degrees per edge. A 1 second window was selected for the speed calculation, resulting in a resolution of 0.43°/sec for a measurement rate of 1/sec. Thus, the worst-case resolution equalled about 2.9% of the lowest dome speed utilized--15°/sec.

### 4.3.2. Eye Movement Processing

The first and most time consuming step in the eye movement analysis was the extraction of slow phase velocities from the position traces obtained using the scleral coils. Calculating the slow phase velocity sequences effectively required removal of all fast phases of nystagmus. This task was performed using **NysA v. 1.4** (for <u>Nys</u>tagmus <u>A</u>nalysis), a set of MatLab scripts designed and implemented at the MIT Man-Vehicle Laboratory by D. J. Merfeld and M. D. Balkwill (Balkwill, 1991). First, the torsional eye position data was converted from A/D units (2048 / 10 V) to degrees using **scale_data**. Next, the data was smoothed by the **condition** script. The smoothing process utilized a predictive finite impulse response (FIR)-median hybrid filter, described by Engelken and Stevens (1990). This filter modeled the nystagmus signal as a piecewise continuous sequence of second order polynomials; its main advantage lay in the preservation of the sharp transitions between slow and fast phases of nystagmus.

The heart of the fast-phase removal algorithm was incorporated in the **process** script, which implemented a version of the acceleration peak detection method used by Merfeld (1990). Velocity and acceleration were obtained by twice differentiating the position series with a Remez equal ripple filter made up of a first order derivative and low-pass filter. The acceleration trace was scanned for values greater than a specified peak threshold; upon detecting a peak the acceleration series was scanned backward and forward until values lower

than a second "end" threshold were detected. These values represented the beginning and end of the fast phase; the slow phase velocity was interpolated across the gap using a zero-order hold. The entire NysA procedure through this script was configured to run in batch mode.

The automated fast phase removal algorithm performed quite well for most trials, and correctly detected approximately 90-95% of saccades. However, each trial had to be manually edited to remove small undetected fast phases. Also, intensive manual editing was required for a few trials with unusually high noise levels; in such cases the automated algorithm excised large portions of the velocity trace. In the **edit_spv** script, the beginning and end points of undetected saccades were selected by the operator. The velocity during the saccade was replaced with a first order interpolation between the two endpoints. Manual editing completed the computation of the slow phase velocity traces.

Mean and maximum slow phase eye velocities (during the duration of dome rotation only), as well as mean and maximum SPV gains, were calculated for each trial in the script **spv_gain**. The dependence of SPV gain on stimulus speed was modeled with a relationship of the form

$$\text{Gain}_{SPV} = \left| \frac{G_0}{\dfrac{jV_{corner}}{V_{dome}} + 1} \right| \tag{4.1},$$

where $V_{dome}$ was the dome rotation rate, $V_{corner}$ gave the "break" velocity, and $G_0$ represented the SPV gain as the dome speed approached zero. This model was suggested by plots of SPV gain versus stimulus speed for horizontal OKN in several species (Collewijn, 1981) and torsional OKN in the rabbit (Collewijn and Noorduin, 1972). The torsional SPV gains collected in this experiment were fit to the model in **fit_gains**. This script employed a Nelder-Mead simplex algorithm for nonlinear optimization to minimize the norm of the error vector between the model predictions and the actual data points.

After Jell et. al. (1984), the decay in slow phase eye velocity during OKAN was fit to a double exponential of the form

$$SPV_{OKAN} = V_{short}e^{-t/\tau_s} + V_{long}e^{-t/\tau_l} + V_{bias} , \quad (4.2)$$

where $\tau_l$ and $\tau_s$ represented the long and short decay time constants, and $V_{long}$ and $V_{short}$ were the respective magnitudes of the decay terms. A constant term, $V_{bias}$, was included because some subjects displayed a spontaneous directional drift in eye torsion. The fit was performed by the script **show_okan**, which used the Nelder-Mead algorithm as well.

### 4.3.3. Analysis of Subjective Vection

The script **plot_corr** was used to evaluate the correlation between subjective self-motion sensations and involuntary torsional eye movements. First, the eye position record was low-pass filtered forward and backward using a 2 pole Butterworth filter with a corner frequency of 0.5 Hz. The eye position, eye SPV, and vection time series were then decimated by a factor of 20. The decimation routine first employed an $8^{th}$ order Chebyshev type 1 low pass filter with a break frequency of 5 Hz. Unbiased cross-correlation functions were calculated between the decimated series for subjective vection and both torsional SPV and torsional eye position. The time corresponding to the peak of the cross-correlation function was stored for each correlation.

Parameters characterizing the vection for each trial were also extracted using the script **get_vect**. The three parameters of interest were vection onset latency, maximum vection, and average vection. The onset latency was defined as the time at which vection reached and maintained a specified threshold level for at least 0.5 seconds. Because there was a certain amount of play in the joystick at its central position, the zero position was defined as the halfway point between the two extreme positions (indicating saturated vection in either direction). The onset thresholds were defined as 4% beyond the points at which a restoring force could be felt from the spring-loaded knob. Thus, the thresholds for CCW and CW

96

vection became -10.4% and 4.8% respectively. Maximum vection for a trial was defined as the maximum of the absolute value of the vection indications; average vection was simply the mean of the vection indications taken over the duration of dome rotation.

# 5. RESULTS

## 5.1. Analysis of Slow Phase Eye Velocity during Torsional OKN

The functional characteristics of the smooth tracking eye movements observed during torsional optokinetic stimulation were examined. This section presents an analysis of SPV dependence on stimulus speed and direction, subject orientation, and repeated exposures. Furthermore, the possibility of a link between roll vection and torsional SPV is explored.

### 5.1.1. Eye Movements Generated during Torsional Optokinetic Stimulation

The reflex eye movements produced by exposure to the rotating dome took the form of torsional nystagmus, with slow phases in the direction of rotation and fast resetting phases in the opposite direction (Figure 5.1; Figure 5.2a). The eye began following the dome's rotation after a latency of approximately 150 - 250 ms., and reached a large fraction of the ultimate maximum SPV within the first slow phase. The individual slow phases often exhibited a concave shape, such that the eye velocity was highest at the beginning of a segment and decreased toward the end.

In addition to the velocity decline within slow phases, the SPV varied considerably in magnitude over the duration of a trial (Figure 5.2b), never achieving a true steady state. The highest slow phase velocities observed were approximately $12° - 15°$/sec, and are listed by subject in Table 5.1. The nystagmic beats were generally accompanied by a more tonic torsional deviation of the eye. The direction and magnitude of this bias varied from subject to subject. During OKN the maximum peak-to-peak range of motion was on the order of $12°$, although the largest slow phases were almost always less than $7°$ (Table 5.1).

#### 5.1.1.1. Relationship of SPV Gain to Stimulus Speed

Higher dome rotation rates produced higher SPVs (Figure 5.3). However, the increase in SPV with increasing dome speed was less than linear. Mean SPV gain decreased with increasing dome speed for the range of speeds tested (Figure 5.4). This decrease occurred

## Torsional optokinetic nystagmus
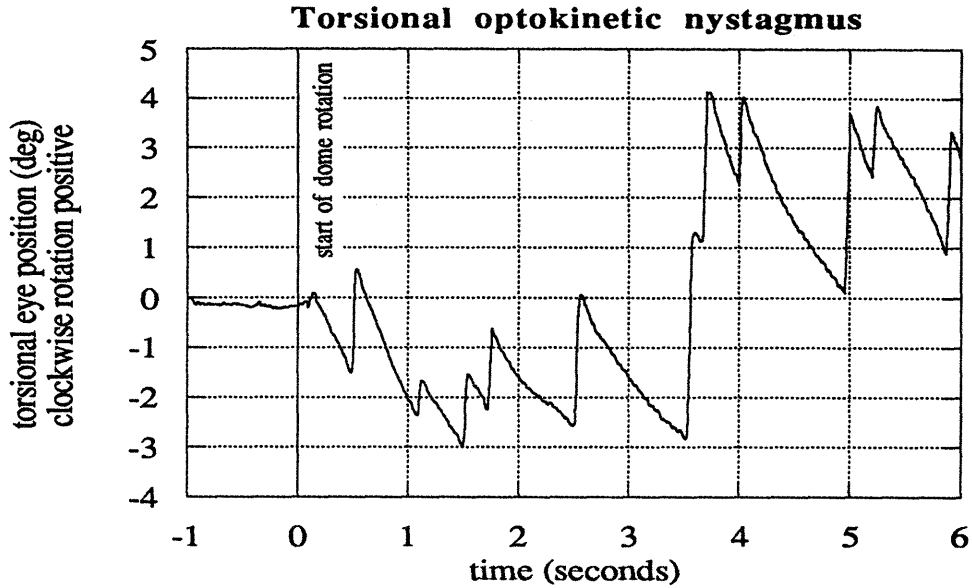


Figure 5.1. Torsional optokinetic nystagmus (Subject P; 60°/sec CCW stimulus). Dome rotation begins at time 0.

| Subject | Maximum SPV (°/sec) | | Peak-to-peak OKN range (°) | | Peak slow-phase magnitude (°) | |
|---|---|---|---|---|---|---|
| | peak | mean (top 5) | peak | mean (top 5) | peak | mean (top 5) |
| M | 13.6 | 12.5 | 9.2 | 8.5 | 4.8 | 4.0 |
| N | 10.9 | 9.2 | 12.1 | 10.4 | 6.4 | 6.0 |
| O | 15.8 | 13.2 | 11.8 | 11.0 | 7.1 | 5.9 |
| P | 13.0 | 11.8 | 14.3 | 12.0 | 7.6 | 5.9 |
| Q | 8.0 | 6.8 | 12.0 | 10.1 | 5.3 | 4.9 |
| R | 11.9 | 11.1 | 10.3 | 9.2 | 6.3 | 5.1 |
| S | 20.8 | 16.7 | 13.7 | 11.2 | 5.5 | 5.3 |

Table 5.1. Maximum OKN responses (SPV, torsional range, slow-phase magnitude) by subject for roll stimuli from 15°/sec - 60°/sec. Overall peaks and averages of the highest five samples recorded are presented.

99

**a. Torsional optokinetic nystagmus**

**b. Torsional slow phase velocity**
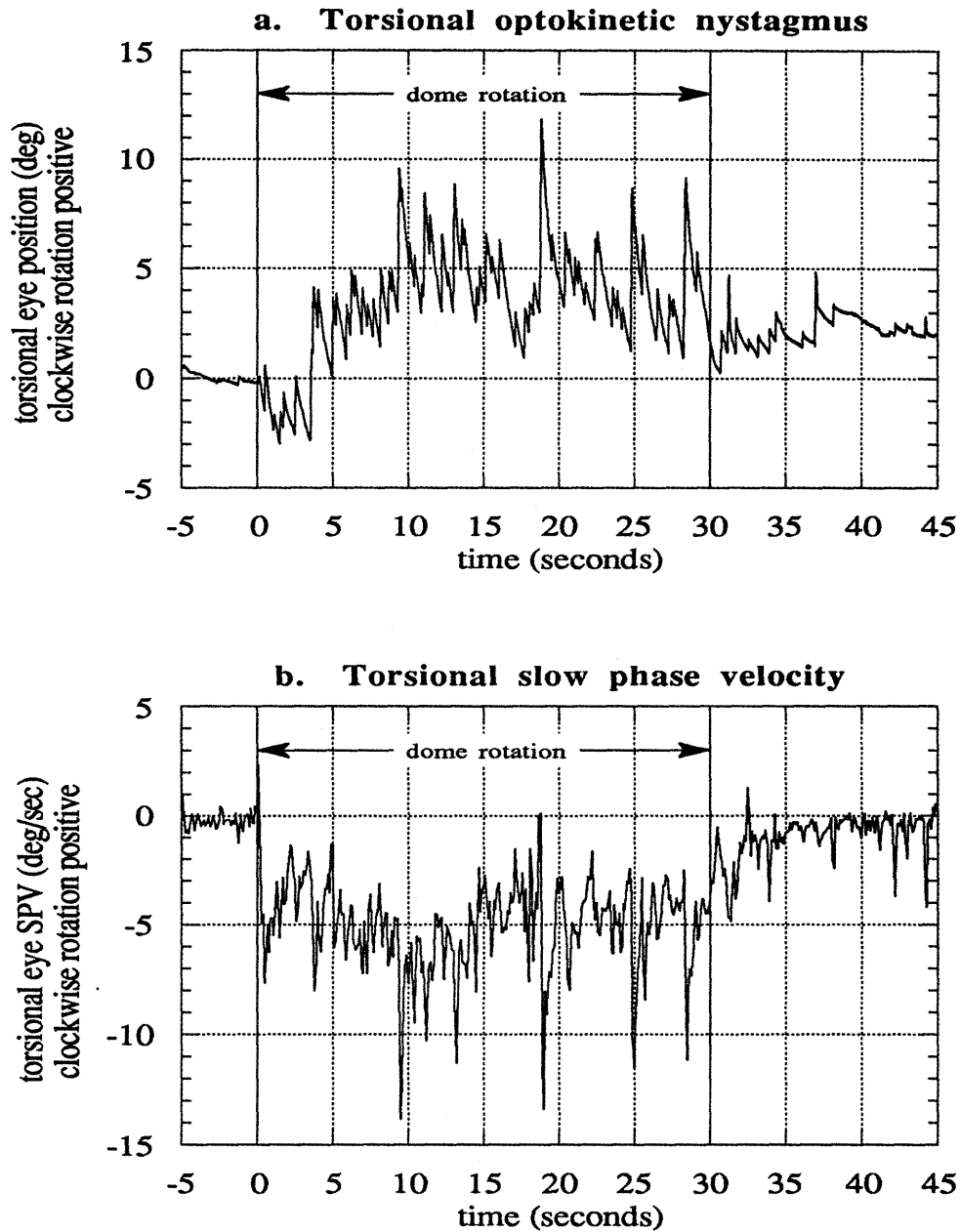
Figure 5.2. Torsional optokinetic nystagmus and calculated slow phase velocity. [a.] Torsional eye position. [b.] Torsional SPV. Dome rotation begins at time 0 and ends at a time of 30 seconds.

**a. Erect dome: all subjects
Slow phase velocities**

**b. Supine dome: all subjects
Slow phase velocities**
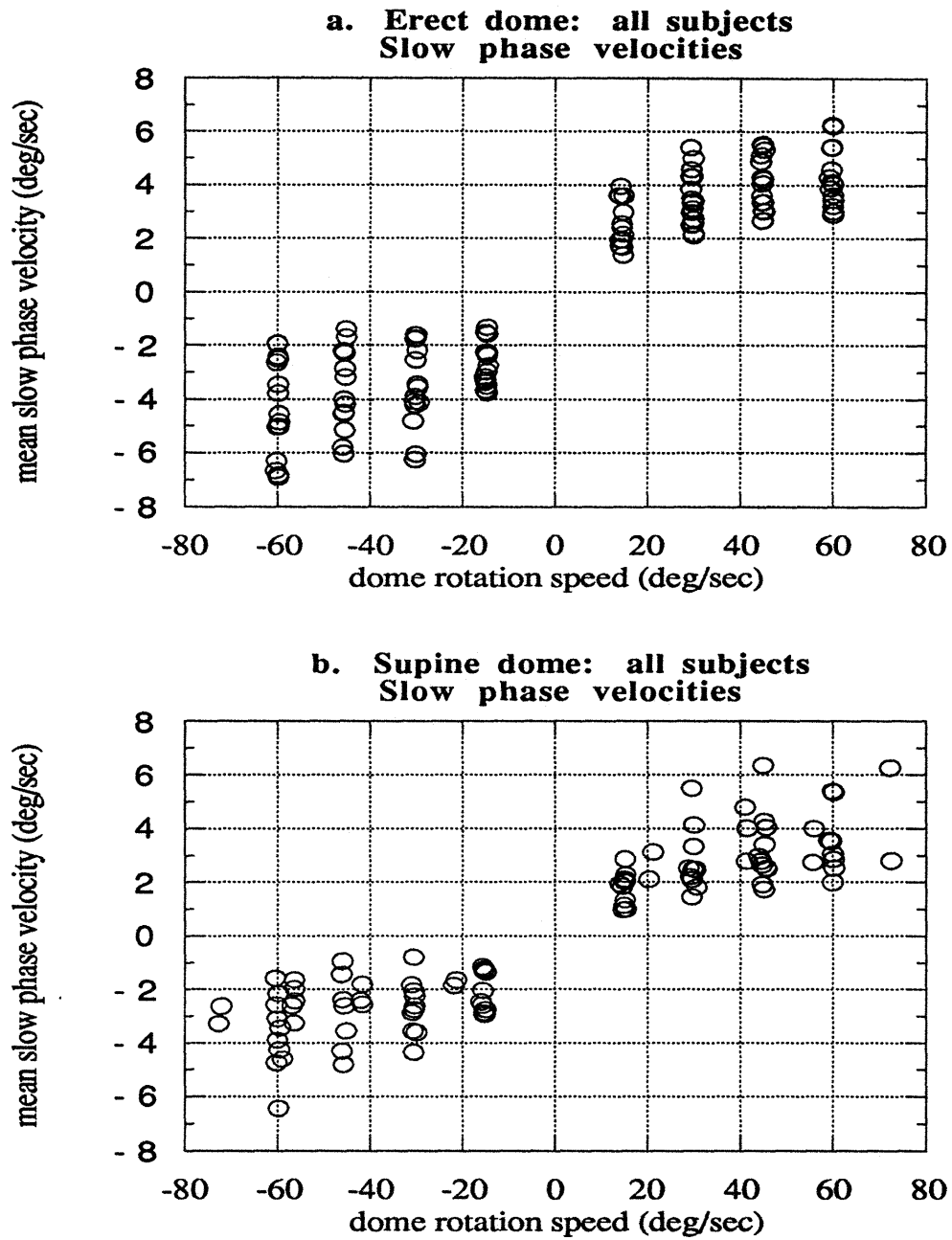
Figure 5.3. Mean SPV for all subjects. [a.] Erect dome. [b.] Supine dome. Each data point represents a single trial

**a. Erect dome: SPV gain (all subjects)**

**b. Supine dome: SPV gain (all subjects)**
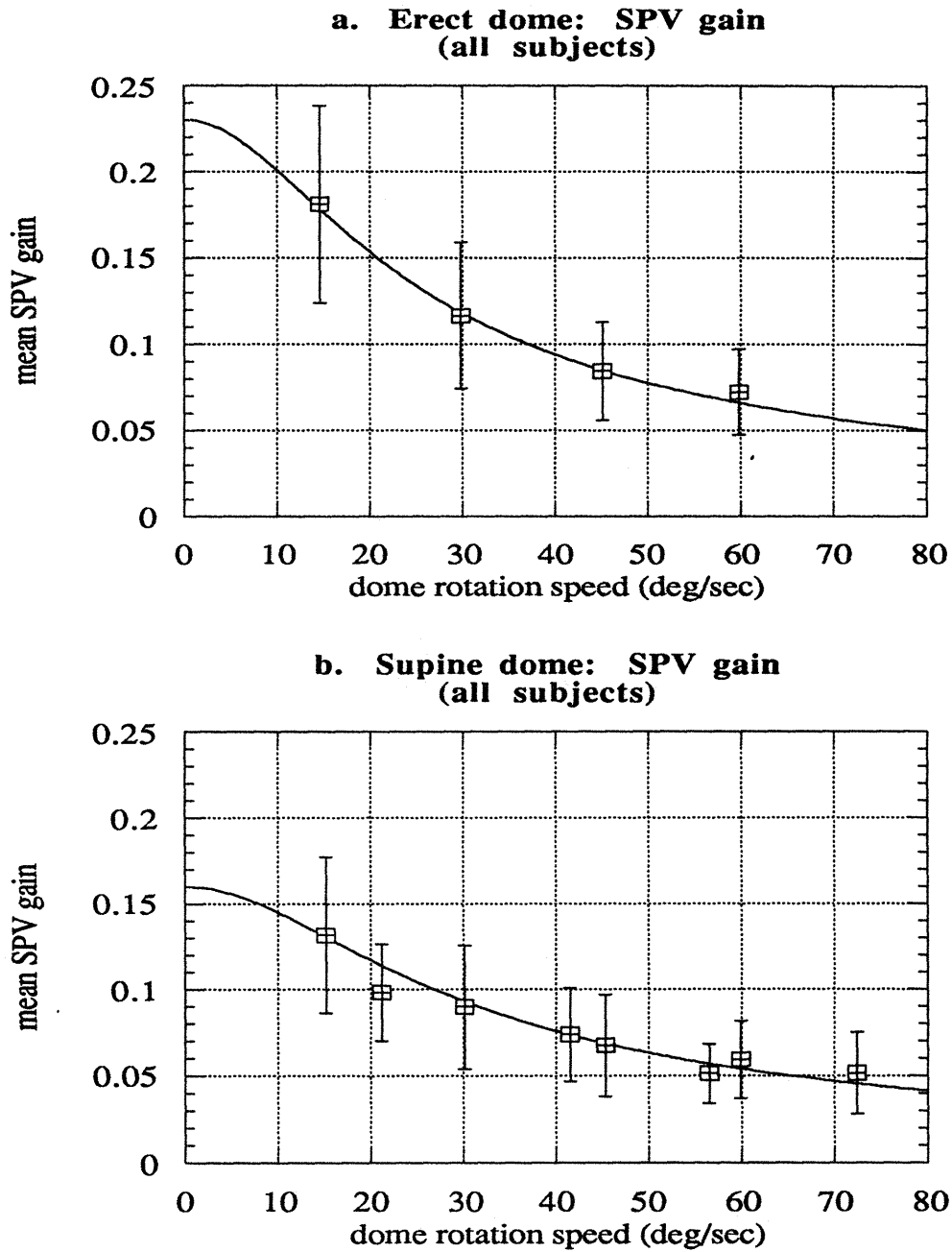
Figure 5.4. Mean SPV gain for all subjects. [a.] Erect dome. [b.] Supine dome. Data points indicate mean values ± 1 standard deviation. Curve fits from Eq. 5.1, using parameters from Table 5.4.

consistently for all subjects, regardless of subject posture or dome direction (Figure 5.5). The magnitude of the decrease varied among subjects, as well as within a single subject's data set for different directions and postures. For all subjects and conditions grouped, the average decrease in gain was approximately 57%, from 0.15 at a dome speed of 15°/s to 0.065 at 60°/s. When the subjects were taken individually and their gains grouped according to posture and dome direction, the reductions in gain ranged from 21% to 76% (Table 5.2).

As described earlier, the SPV gains for each run were separated by dome direction and fit to functions of the form shown in Eq. 1, where $v_{corner}$ represents a "corner" rotation rate similar to the corner frequency of a Bode plot and K provides an estimate of the OKN gain at very low stimulus rates.

$$G_{SPV} = \left| \frac{K}{\dfrac{j v_{dome}}{v_{corner}} + 1} \right| \qquad (5.1)$$

Average values of the parameters across all subjects, as well as parameter values calculated for all subjects and runs grouped, are listed in Table 5.3. The parameters for the single run fits, as well as for fits obtained by grouping each subject's runs according to posture, are presented in Table 5.4. In the great majority of cases, these curves provided better fits than either linear or exponential expressions. Overall, these fits indicated that the maximum gain likely to be observed even at very low speeds is less than 0.3. Furthermore, OKN gain dropped off sharply above a "corner" dome rotation rate of approximately 15° - 30°/sec.

## 5.1.1.2. Exposure-Related Effects on SPV Gain

For each subject, SPV gain appeared to decrease with increasing exposure to the dome stimulus within a single experimental session. Unfortunately, this gain decrease could not be tracked within an individual run, because each speed-direction combination was generally
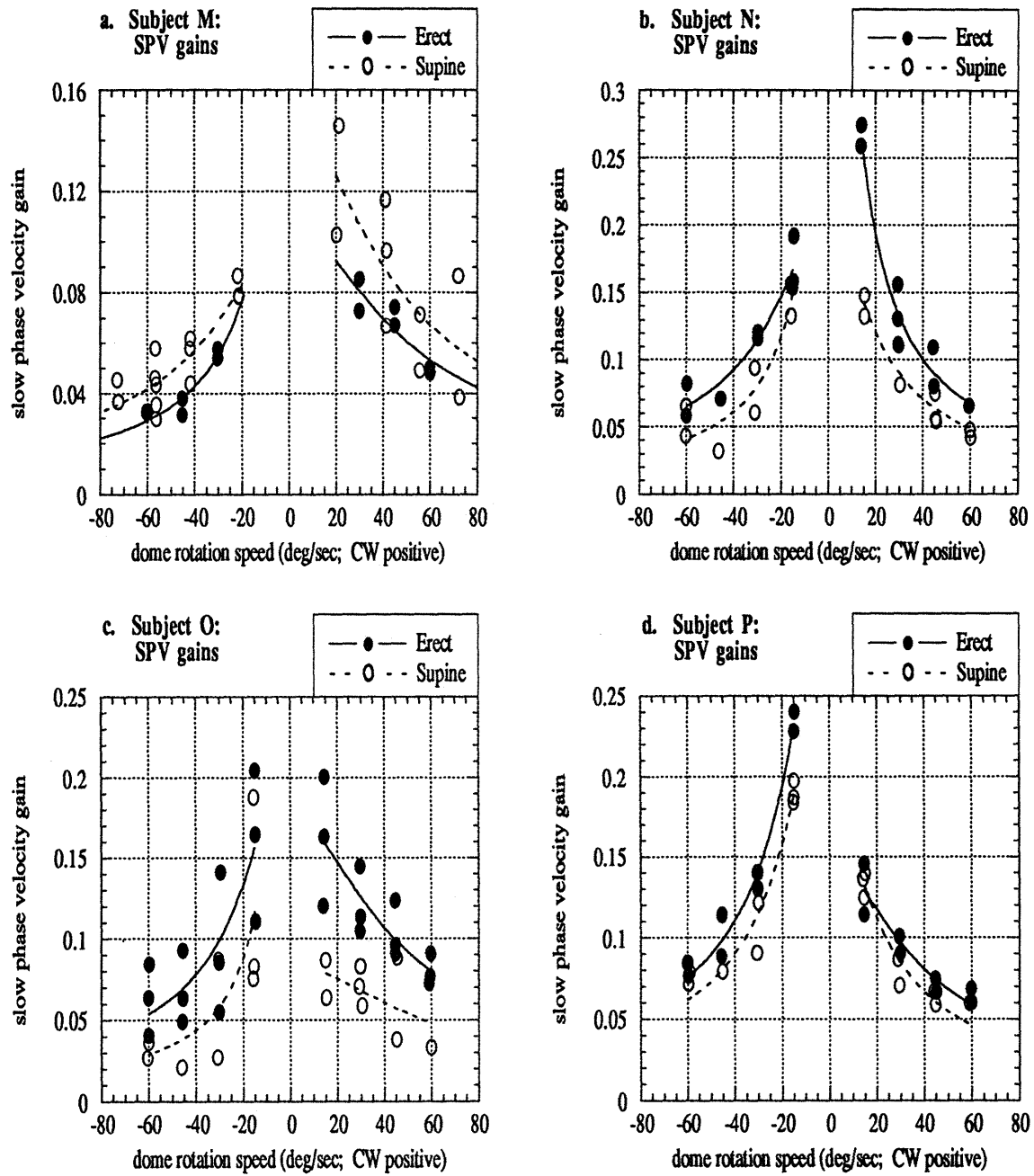
Figure 5.5. SPV gains erect and supine for individual subjects. Curve fit parameters are listed in Table 5.3. [a.] Subject M. [b.] Subject N. [c.] Subject O. [d.] Subject P.
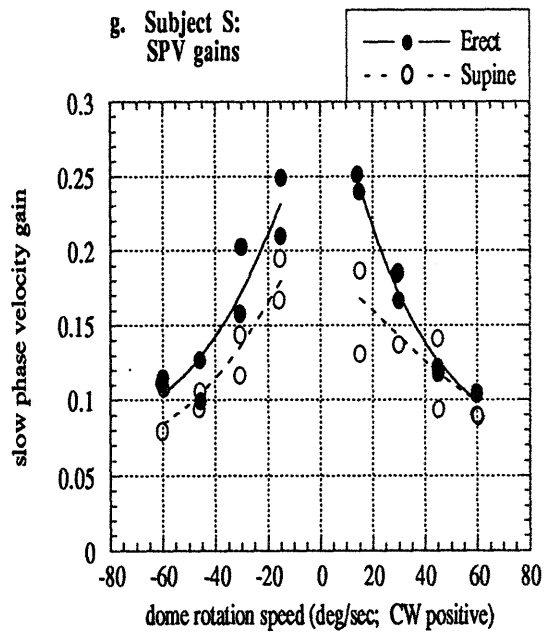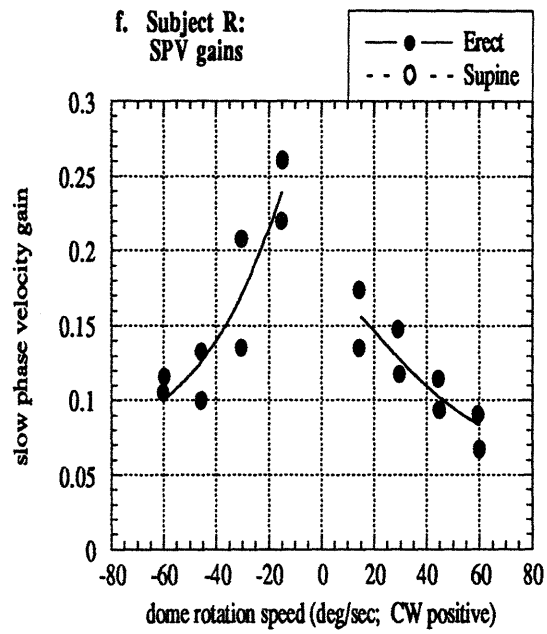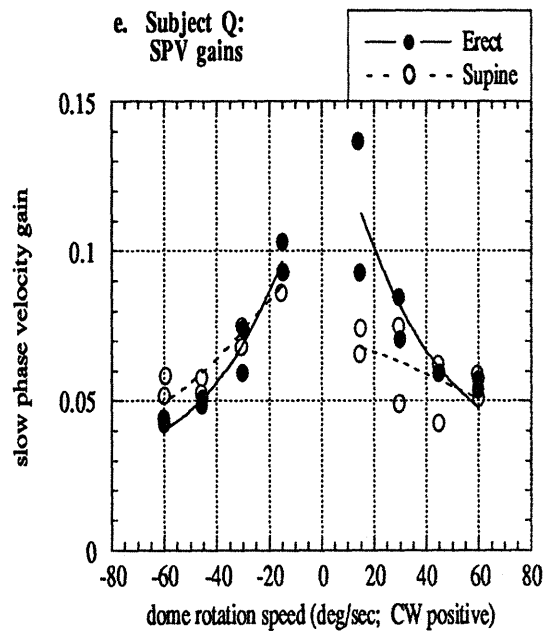
e. **Subject Q:**
   SPV gains

Erect
O Supine

slow phase velocity gain

0.15

0.1

0.05

0

-80 -60 -40 -20 0 20 40 60 80

dome rotation speed (deg/sec; CW positive)

f. **Subject R:**
   SPV gains

Erect
O Supine

slow phase velocity gain

0.3

0.25

0.2

0.15

0.1

0.05

0

-80 -60 -40 -20 0 20 40 60 80

dome rotation speed (deg/sec; CW positive)

g. **Subject S:**
   SPV gains

Erect
O Supine

slow phase velocity gain

0.3

0.25

0.2

0.15

0.1

0.05

0

-80 -60 -40 -20 0 20 40 60 80

dome rotation speed (deg/sec; CW positive)

**Figure 5.5.** SPV gains erect and supine for individual subjects. Curve fit parameters are listed in Table 5.3. [e.] Subject Q. [f.] Subject R (erect only). [g.] Subject S.

105

| Subject | CCW or CW | Erect | | | Supine | | |
|---|---|---|---|---|---|---|---|
| | | mean gain 15°/sec | mean gain 60°/sec | gain ratio 60°/s÷15°/s | mean gain 15°/sec | mean gain 60°/sec | gain ratio 60°/s÷15°/s |
| M | CCW | 0.056* | 0.033 | 0.58 | 0.081† | 0.041† | 0.51 |
| | CW | 0.079 | 0.049 | 0.62 | 0.125 | 0.062 | 0.50 |
| N | CCW | 0.168 | 0.070 | 0.42 | 0.145 | 0.054 | 0.37 |
| | CW | 0.267 | 0.065 | 0.24 | 0.140 | 0.045 | 0.32 |
| O | CCW | 0.160 | 0.053 | 0.33 | 0.115 | 0.031 | 0.27 |
| | CW | 0.161 | 0.080 | 0.50 | 0.076 | 0.033 | 0.44 |
| P | CCW | 0.234 | 0.081 | 0.34 | 0.189 | 0.075 | 0.40 |
| | CW | 0.130 | 0.065 | 0.50 | 0.133 | 0.060 | 0.45 |
| Q | CCW | 0.098 | 0.043 | 0.44 | 0.090 | 0.055 | 0.48 |
| | CW | 0.115 | 0.056 | 0.48 | 0.070 | 0.055 | 0.79 |
| R | CCW | 0.241 | 0.111 | 0.46 | -- | -- | -- |
| | CW | 0.155 | 0.079 | 0.51 | -- | -- | -- |
| S | CCW | 0.230 | 0.113 | 0.49 | 0.181 | 0.094 | 0.52 |
| | CW | 0.245 | 0.104 | 0.42 | 0.159 | 0.090 | 0.56 |
| All subjects | both | 0.181 | 0.072 | 0.40 | 0.132 | 0.059 | 0.45 |

*The lowest speed used in the erect runs for subject M was 30°/sec
†The low and high speeds used in the supine runs for subject M were 21°/sec and 72°/sec

Table 5.2. Mean gains for the highest and lowest speed stimuli, separated by subject, orientation, and dome direction. Magnitude of decrease in gain over speed range tested is indicated by the ratio of fast-stimulus to slow-stimulus gains.

| | K | | $\omega_c$ | |
|---|---|---|---|---|
| | mean (subject fits) ± 1 st. dev. | fit--all subjects, all trials | mean (subject fits) ± 1 st. dev. | fit--all subjects, all trials |
| erect | 0.24 ± 0.15 | 0.23 | 21.7 ± 8.2 | 17.92 |
| supine | 0.17 ± 0.09 | 0.16 | 28.8 ± 16.3 | 21.47 |

Table 5.3. Erect and supine gain-SPV curve fit parameters for all subjects grouped.

## a. Curve fit parameters for erect dome runs.

| Subject | Run # | CCW dome Single run K | $\omega_c$ | Grouped runs K | $\omega_c$ | CW dome Single run K | $\omega_c$ | Grouped runs K | $\omega_c$ |
|---|---|---|---|---|---|---|---|---|---|
| M | 1 | 0.15 | 12.8 | | | 0.13 | 27.7 | | |
|   | 2 | 0.15 | 11.0 | 0.15 | 12.0 | 0.09 | 44.0 | 0.11 | 34.7 |
| N | 1 | 0.22 | 18.7 | | | 0.51 | 8.7 | | |
|   | 2 | 0.18 | 22.4 | 0.21 | 19.6 | 0.16 | 30.6 | 0.70 | 5.8 |
| O | 1 | 0.73 | 4.2 | | | 0.23 | 26.4 | | |
|   | 2 | 0.20 | 24.9 | | | 0.19 | 24.7 | | |
|   | 3 | 0.17 | 12.2 | 0.22 | 15.1 | 0.13 | 46.2 | 0.18 | 30.4 |
| P | 1 | 0.36 | 13.2 | | | 0.17 | 22.6 | | |
|   | 2 | 0.33 | 13.8 | 0.35 | 13.5 | 0.13 | 30.2 | 0.15 | 26.0 |
| Q | 1 | 0.11 | 25.9 | | | 0.18 | 16.5 | | |
|   | 2 | 0.13 | 17.4 | 0.12 | 21.8 | 0.10 | 37.7 | 0.14 | 22.9 |
| R | 1 | 0.31 | 24.5 | | | 0.19 | 33.3 | | |
|   | 2 | 0.27 | 19.4 | 0.29 | 22.2 | 0.15 | 33.9 | 0.17 | 33.5 |
| S | 1 | 0.31 | 21.3 | | | 0.30 | 21.3 | | |
|   | 2 | 0.23 | 30.5 | 0.27 | 24.8 | 0.30 | 20.7 | 0.30 | 21.0 |

## b. Curve fit parameters for supine dome runs.

| Subject | Run # | CCW dome Single run K | $\omega_c$ | Grouped runs K | $\omega_c$ | CW dome Single run K | $\omega_c$ | Grouped runs K | $\omega_c$ |
|---|---|---|---|---|---|---|---|---|---|
| M | 1 | 0.13 | 15.6 | | | 0.22 | 20.6 | | |
|   | 2 | 0.09 | 46.7 | | | 0.11 | 75.1 | | |
|   | 3 | 0.12 | 24.1 | 0.10 | 26.3 | 1.08E+5 | 2.76E-5 | 0.15 | 29.6 |
| N | 1 | 0.15 | 26.2 | | | 0.21 | 15.8 | | |
|   | 2 | 9.98E+4 | 2.29E-5 | 0.35 | 7.0 | 0.21 | 12.6 | 0.20 | 14.9 |
| O | 1 | 0.21 | 12.9 | | | 0.11 | 25.0 | | |
|   | 2 | 6.77E+5 | 1.64E-6 | 1.21E+6 | 1.44E-6 | 0.07 | 69.2 | 0.08 | 42.6 |
| P | 1 | 0.25 | 17.7 | | | 0.16 | 18.7 | | |
|   | 2 | 0.30 | 11.6 | 0.28 | 13.6 | 0.22 | 12.3 | 0.18 | 16.1 |
| Q | 1 | 0.10 | 37.5 | | | 0.07 | 93.2 | | |
|   | 2 | 0.09 | 35.2 | 0.10 | 36.3 | 0.07 | 38.6 | 0.07 | 63.8 |
| R | --- | --- | --- | --- | --- | --- | --- | --- | --- |
|   | --- | --- | --- | --- | --- | --- | --- | --- | --- |
| S | 1 | 0.22 | 28.5 | | | 0.21 | 35.8 | | |
|   | 2 | 0.19 | 25.1 | 0.21 | 26.8 | 0.14 | 46.5 | 0.18 | 39.5 |

Table 5.4. Parameters for curve fits relating SPV gain to dome velocity. Values are given for each dome run and for runs grouped by subject. [a.] Erect dome. [b.] Supine dome.

presented only once per run. Thus, the dependence of gain on dome speed as well as directional asymmetries within subjects made within-run comparisons problematic. However, a gross measure of this gain decrease was obtained by dividing the SPV gain obtained in the second run by that obtained in the first for trials corresponding in speed and direction. On the occasions where a certain speed and direction were repeated within a single run, the ratio of the later gain to the earlier was calculated as well.

Figure 5.6 shows the mean of the ratios for each subject. In this figure, the values obtained from both sessions (erect and supine) have been combined. The mean gain decrease attributed to stimulus exposure ranges from 8% to over 30%. In Table 5.5, the statistics for the gain ratios have been tabulated for the erect and supine cases separately, and the percentages of comparisons giving ratios less than 1 (signifying a gain decrease over time) have been included. In five of the six subjects tested both erect and supine, the gain decrease was more pronounced supine. However, the difference was significant only for subject S (p < 0.05, independent samples t-test).

## 5.1.1.3. Directional Asymmetry in SPV Gain

Highly individual-specific directional asymmetries were observed in the OKN gain. In order to quantify the asymmetries, ratios of mean SPV gain for trials of the same speed but opposite direction were calculated. Thus, this procedure generally gave one ratio per dome speed for each run. The logarithm of each ratio was taken to facilitate comparison of ratios greater and less than one. Mean values for the erect and supine runs are presented in Figure 5.7.

Subjects M, P, and R showed very consistent asymmetries. Subject M exhibited significantly higher SPV gains for CW dome rotation both erect (p = 0.001) and supine (p = 0.002). In contrast, subject P had a much stronger response for CCW rotation erect (p = 0.001) and supine (p = 0.003). Subject R's torsion also favored the CCW direction (p = 0.01), although data were taken only for the erect condition.

**Exposure effect on SPV gain**
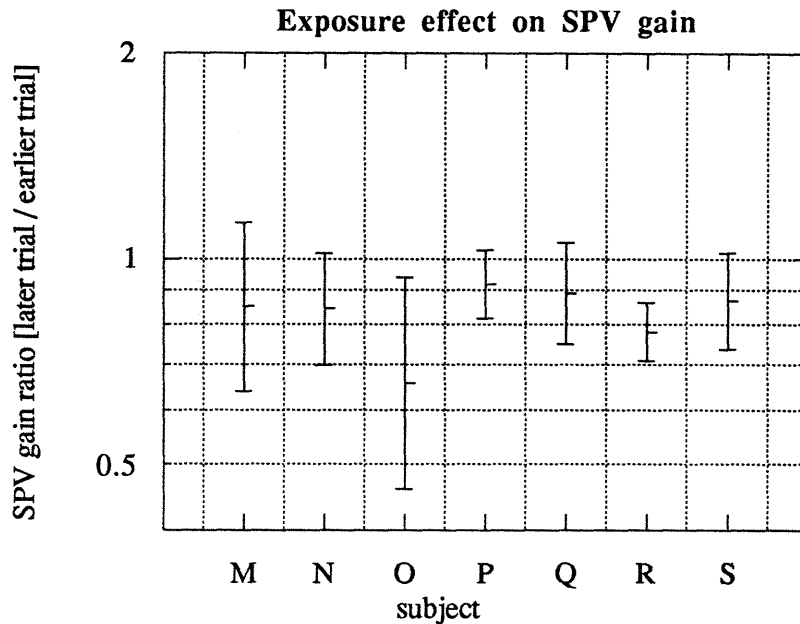
Figure 5.6. Effect of repeated stimulus exposure on SPV gain. Geometric mean of gain ratios (later / earlier trial) for each subject (erect and supine runs combined). Error bars indicate ±1 standard deviation of logarithms of gain ratios.

| Subject | ERECT | | | SUPINE | | |
|---|---|---|---|---|---|---|
| | Mean ratio | st. dev. | % vals < 1 | Mean ratio | st. dev. | % vals < 1 |
| M | 0.93 | 0.09 | 67 | 0.85 | 0.31 | 75 |
| N | 0.89 | 0.16 | 80 | 0.83 | 0.18 | 78 |
| O | 0.74 | 0.23 | 88 | 0.66* | 0.22 | 100 |
| P | 0.92 | 0.12 | 75 | 0.93 | 0.11 | 80 |
| Q | 0.94 | 0.15 | 50 | 0.87 | 0.15 | 88 |
| R | 0.79 | 0.08 | 100 | -- | -- | -- |
| S | 0.96 | 0.15 | 88 | 0.80 | 0.11 | 100 |

*one comparison (ratio = 2.3) of the 10 was omitted from the calculations as it fell over 7 standard deviations from the mean

Table 5.5. Effect of stimulus exposure on SPV gain. Statistics are for ratios of SPV gain calculated from corresponding trials (later / earlier). Percentages denote number of comparisons with results smaller than 1.
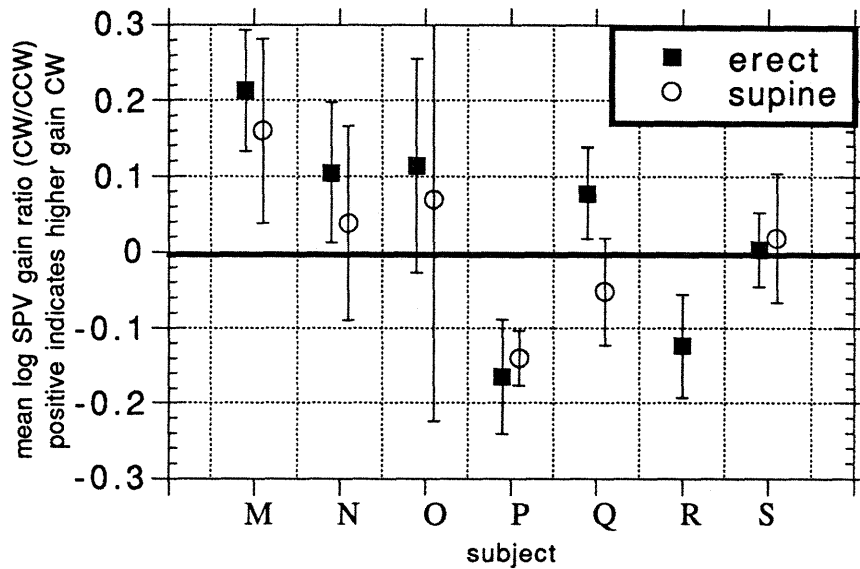
**Figure 5.7.** Directional asymmetry in SPV gain. Plot shows means of log(CW SPV / CCW SPV) for corresponding dome speeds. Error bars indicate ±1 standard deviation of logarithms of gain ratios.

Other subjects presented more ambiguous responses. When erect, subject N had significantly higher gains for CW dome rotations (p = 0.01); the supine trials showed no strong asymmetry. Subject Q, who also demonstrated markedly larger gains in the CW direction for the erect runs (p = 0.084), actually had stronger OKN for CCW trials when supine (not significant). Finally, neither O nor S had particularly asymmetric OKN.

The directional asymmetries in SPV gain could not be related to either handedness or eye dominance. All of the subjects were right handed, yet not all subjects shared the same direction asymmetry. Five of the subjects were left eye dominant; of these subjects, three exhibited higher gains for CW rotation (M, N, O), one had higher CCW gains (R), and one exhibited opposite asymmetries erect and supine (Q). One of the two right eye dominant subjects showed higher gains for CCW rotation (P), while the SPV gains for the other were nearly symmetric (S).

### 5.1.1.4. Effects of Orientation with Respect to Gravity on SPV Gain

In order to quantify the effects of subject posture (erect or supine) on SPV gain, the ratio of gain erect to gain supine was calculated for trials corresponding in dome speed and direction (Figure 5.8). Because of the decrease in gain seen between the first and second runs within a session, a subject's first run erect was compared only with the first run supine, and likewise for the second runs. Subjects M and O each had a third session consisting of one run; such a run was compared with the first run from the session of the other postural orientation. The logarithm of the gain ratio was used as the measure of asymmetry--positive values indicated higher gains erect, while negative values were obtained for higher supine gains.

Table 5.6 presents significance levels by subject for the erect-supine gain comparison, based on an ANOVA with three variables: stimulus speed, stimulus direction, and subject orientation. Four of the six subjects tested both erect and supine (N, O, P, and S) had significantly higher SPV gains erect than supine. In these subjects, the dependence of gain on posture showed no clear relationship to either dome speed or direction, so all speeds and directions were lumped together. For these subjects the gain increase erect ranged from 15% to 75%. In contrast, only subject M demonstrated consistently and significantly higher gains in the supine position. On average, this subject's erect gains were 25% lower than corresponding supine values. The SPV gains for the sixth subject, Q, were generally higher erect for CW dome rotations, but the reverse held for CCW rotations. In subject Q's case, significant interactions were observed between (1) posture and direction ($p = 0.019$), and (2) posture and speed ($p = 0.048$).

### 5.1.2. Comparison of Torsional SPV and Psychophysical Responses

The possible relationship between the perceptual responses and the slow phase eye velocities caused by the rolling visual field was investigated. In an attempt to compare directly the SPV and vection responses, cross-correlations of the two time sequences were performed
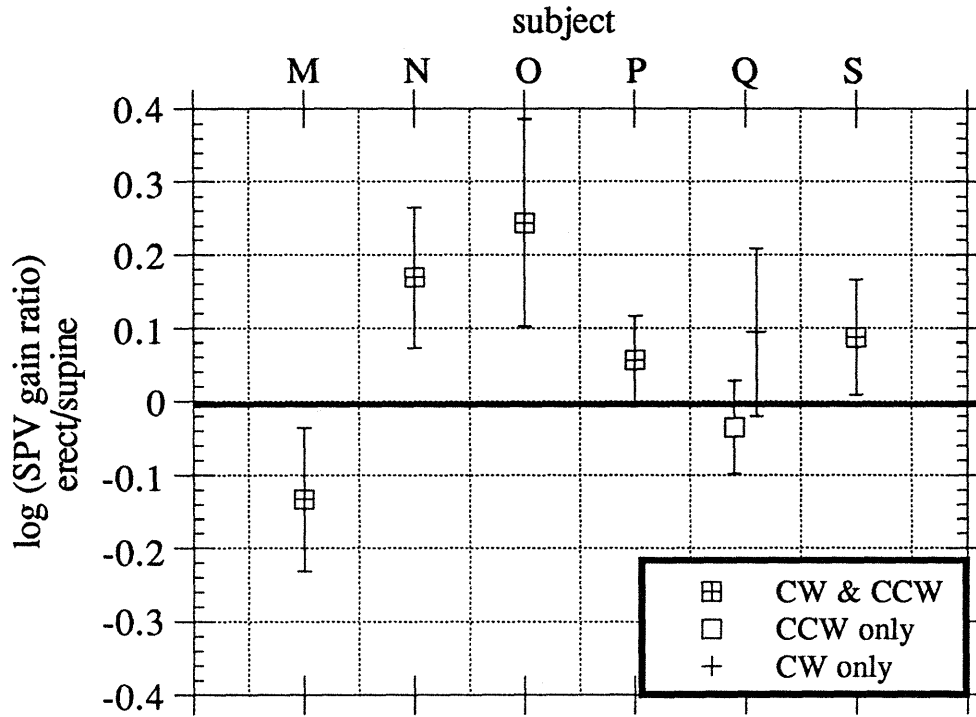
Figure 5.8. Comparison by subject of SPV gain erect vs. supine. Data points represent the mean log (ratio of erect gain/supine gain). Positive values indicate higher gain erect. Ratios were taken for trials corresponding in speed and direction. Error bars represent ±1 sd. CW and CCW results were grouped for all subjects but Q.

| | Significance level (p < ?) | | | | | | |
|---|---|---|---|---|---|---|---|
| | Main variables | | | Cross terms | | | |
| Subject | Posture | Direction | Speed | Posture *direction | Posture *speed | Direction *speed | Posture *direction *speed |
| M | 0.001 | 0.001 | 0.001 | ns | ns | ns | ns |
| N | 0.001 | 0.005 | 0.001 | 0.1 | 0.05 | 0.1 | 0.05 |
| O | 0.001 | ns | 0.001 | ns | ns | ns | ns |
| P | 0.001 | 0.001 | 0.001 | 0.05 | ns | 0.001 | ns |
| Q | ns | ns | 0.001 | 0.05 | 0.05 | ns | ns |
| R | -- | 0.05 | 0.005 | -- | -- | ns | -- |
| S | 0.001 | ns | 0.001 | ns | 0.1 | ns | ns |

Table 5.6. Results of ANOVA on mean SPV gain for each subject. Variables tested were postural orientation, rotation direction, and stimulus velocity.

112

for each trial. Comparing the traces only during the period of dome rotation was largely

unsuccessful, since the peaks in the cross-correlation function often were not sharp, and the

times of the peaks varied over a ±20 sec. range.

Cross-correlation of vection and SPV for entire trials, including periods before and

after dome rotation, yielded times associated with the correlation peaks which grouped much

more tightly. Unfortunately, a closer look revealed that the peaks in these cross-correlation

functions did not imply a strong correspondence between the SPV and joystick traces. Rather,

the timing of the peaks reflected the latency in vection onset relative to the immediate jump in

SPV at the start of dome rotation. Figure 5.9 depicts the relation between mean timing of the

cross-correlation peaks and mean onset times. Each data point represents a single subject; most

of the points lie almost precisely on a line with a slope of 1.
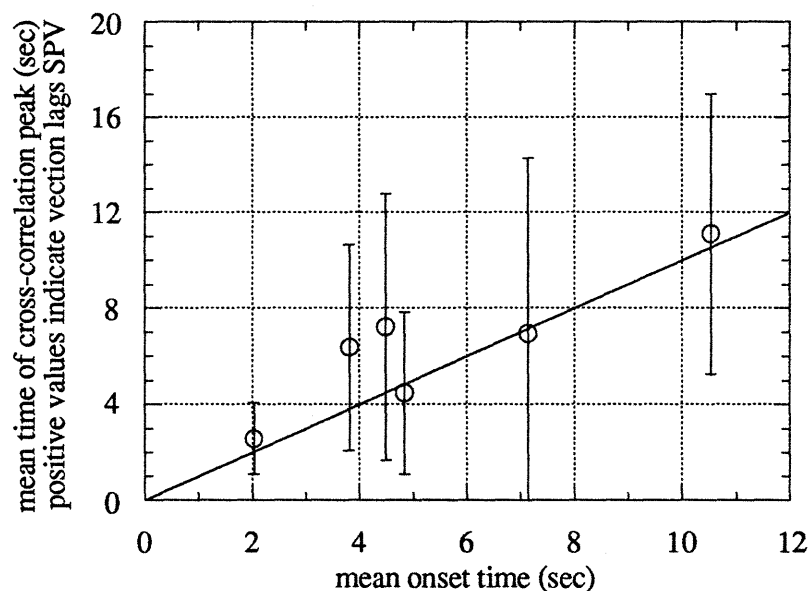


Figure 5.9. Mean time of SPV-vection cross-correlation peaks
shown against mean onset times. Each data point represents an
individual subject (correlations were not computed for subject R).
Positive times for peak correlation indicate that the vection
response is delayed with respect to the SPV trace.

### 5.1.2.1. Comparison of Asymmetries in SPV and Vection Responses

Various parameters describing the OKN (mean SPV gain) and vection (onset latency, maximum and average vection) were extracted from the time sequences recorded for each trial; evaluation of their interrelationships provided an alternative to performing correlations of the vection and SPV traces. However, simply comparing the OKN and vection parameters yielded little information due to the complex dependence of both phenomena on dome speed and direction. Instead, the directional asymmetries and postural differences in OKN and vection were compared.

For each parameter, the directional asymmetry was represented by the ratio of the CW value to the CCW value for trials of the same dome speed. Again, logs of the ratios were taken to permit easier comparison of results above and below 1. Thus, a positive coordinate indicated a larger value for the CW parameter of the CW-CCW pair. Comparisons are presented for subjects M, N, and P, who demonstrated the most consistent directional asymmetries in SPV gain. (Although subject R had a clear directional preponderance in OKN, this subject's very limited sensation of vection prevented meaningful comparisons.) Figure 5.10 shows directional asymmetries in both average vection and onset time plotted against SPV gain asymmetry.

Subjects M and N, who generated higher SPV gains for CW dome rotation, both perceived stronger average vection for CW rotation as well. Although the onset times for subject M indicated little difference due to direction, subject N's shorter vection onset latencies for CW rotation were consistent with stronger vection for this direction. In contrast, subject P consistently demonstrated higher OKN gains for CCW trials. However, like M and N, subject P felt stronger average vection for CW rotations. Furthermore, the vection onset latencies recorded by subject P were always shorter for the CW direction. In summary, two subjects achieved enhanced vection for trials in the same direction that produced higher SPV gains, while another reported the opposite: less vection for the direction associated with higher SPV gain.
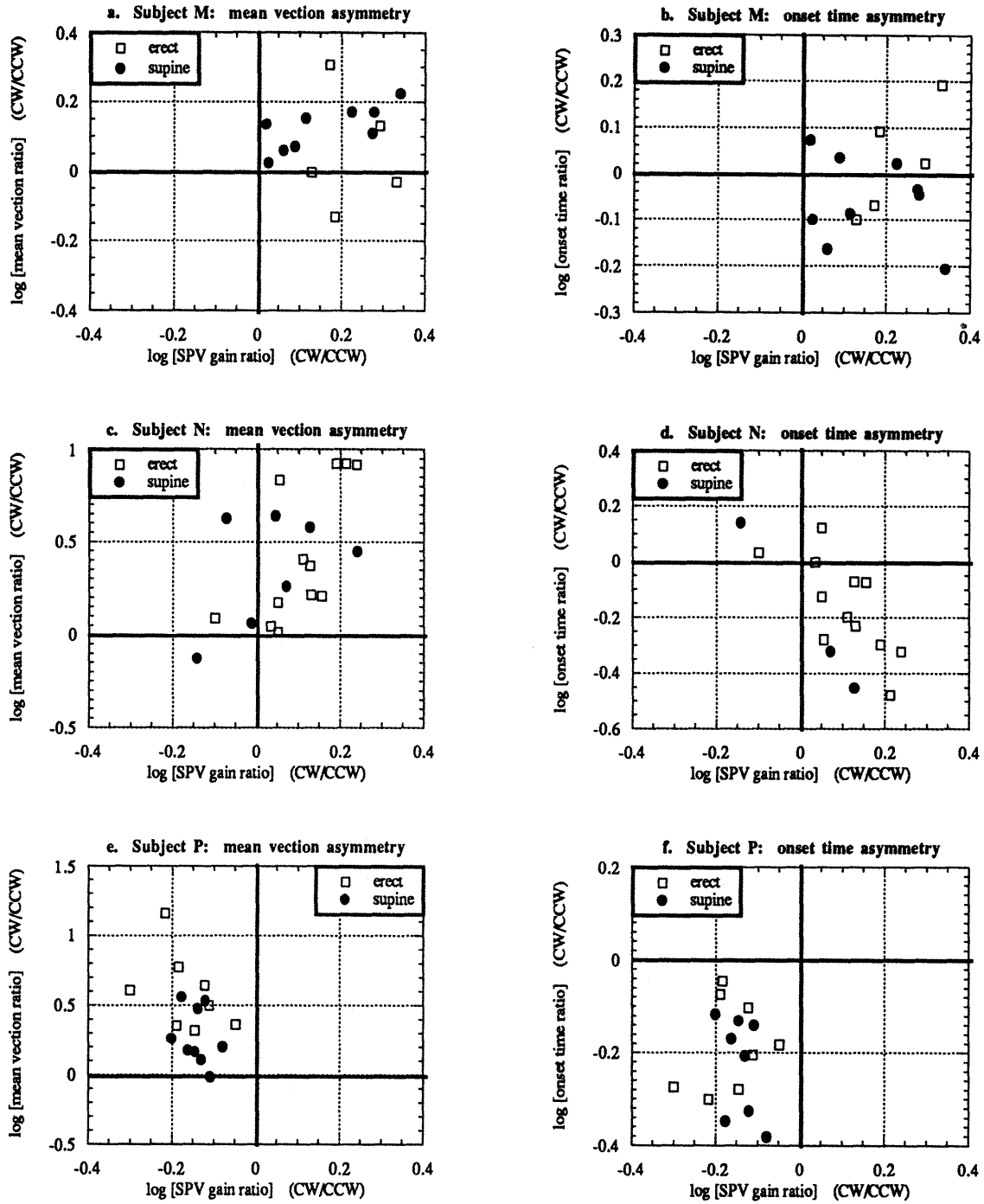
Figure 5.10. Comparison of directional asymmetries in vection and SPV gain. Plots [a], [c], and [e] show asymmetries in average vection against asymmetries in SPV gain. Plots [b], [d], and [f] show onset time asymmetries versus SPV gain asymmetries. Positive values indicated larger CW results.

115

A similar technique was employed to investigate the differences in vection and OKN gain seen between the erect and supine trials. As with the directional asymmetries, subjects M, N, and P demonstrated the clearest differences in vection strength between the two postural conditions. For this comparison, the ratios of the erect parameters to the supine parameters were computed for each trial matching in stimulus speed and direction. Figure 5.11 presents the postural asymmetries in average vection and onset time for subjects M, N, and P. Again, logarithms of the ratios were plotted; positive values indicate a greater parameter value erect.

Subjects N and P both exhibited consistently higher SPV gains erect. However, these two subjects displayed opposite asymmetries in vection. While subject P perceived stronger vection and indicated shorter onset times in the supine position, subject N's responses demonstrated decreased self-rotation and extended onset latencies lying down. Furthermore, subject M was the only subject to display an increase in SPV gain supine, but like N he reported greater vection erect than supine. Interestingly, subject M's directional asymmetries implied greater vection during trials with higher SPV gains, but his postural asymmetries seemed to show the opposite relation.

### 5.1.2.2. Mean SPV Gain Across Vection State Transitions

Comparison of mean SPV during OKN periods with and without vection provided a further means of testing whether or not vection and eye velocity were related. For each trial, the mean SPV was calculated for periods during which the subject experienced vection (State 1). Another mean SPV value was calculated for the combined periods without vection (State 2, comprising the time between stimulus onset and the beginning of vection, as well as vection dropout intervals). A ratio of mean SPV in State 1 to the corresponding value in State 2 was computed for each trial, providing a measure of the the difference in SPV magnitude between the vection and no-vection states. Figure 5.12 shows the geometric means of the ratios calculated for each subject.
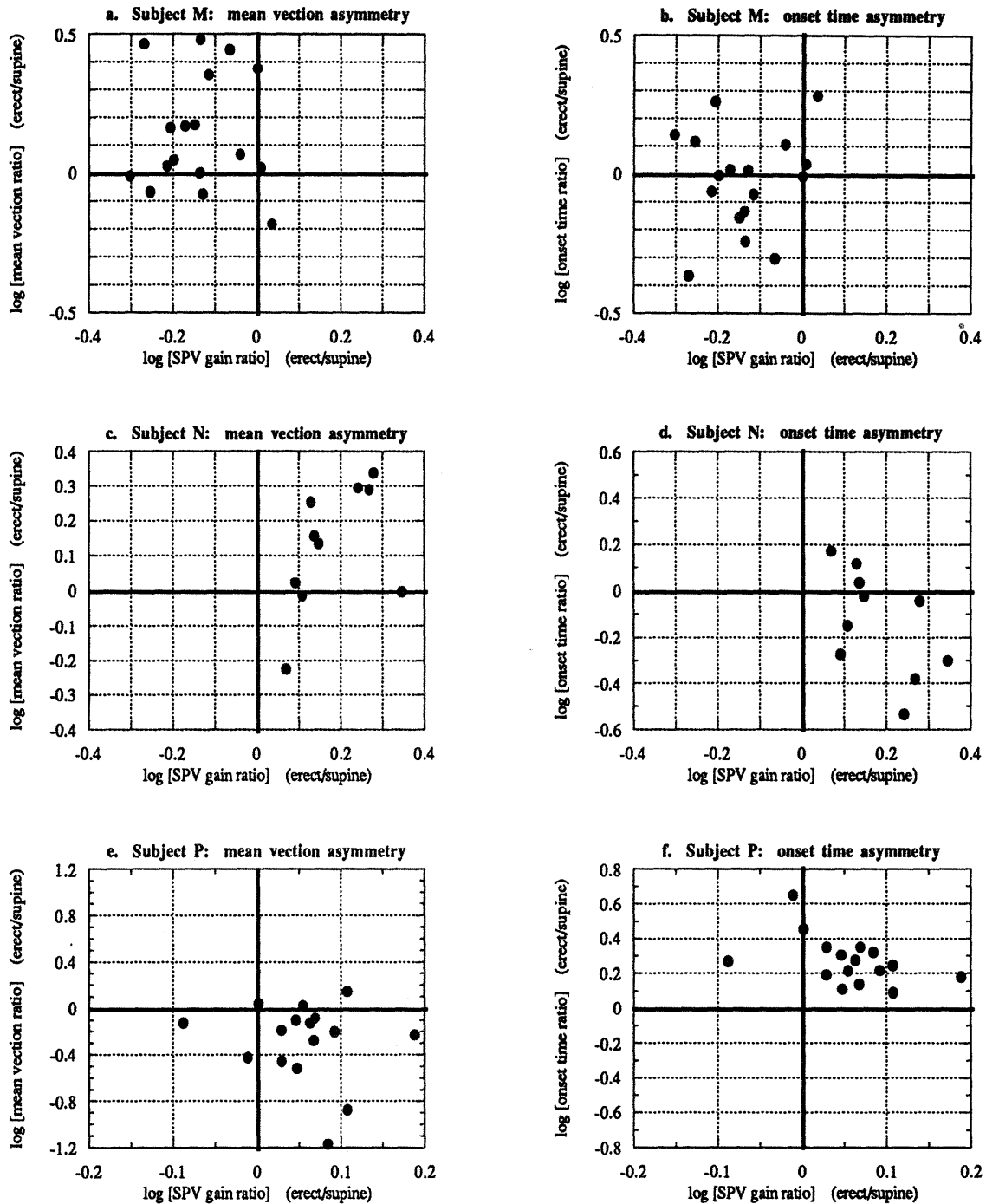
Figure 5.11. Comparison of postural asymmetries in vection and SPV gain. Plots [a], [c], and [e] show asymmetries in average vection against asymmetries in SPV gain. Plots [b], [d], and [f] show onset time asymmetries versus SPV gain asymmetries. Positive results indicated larger values erect.
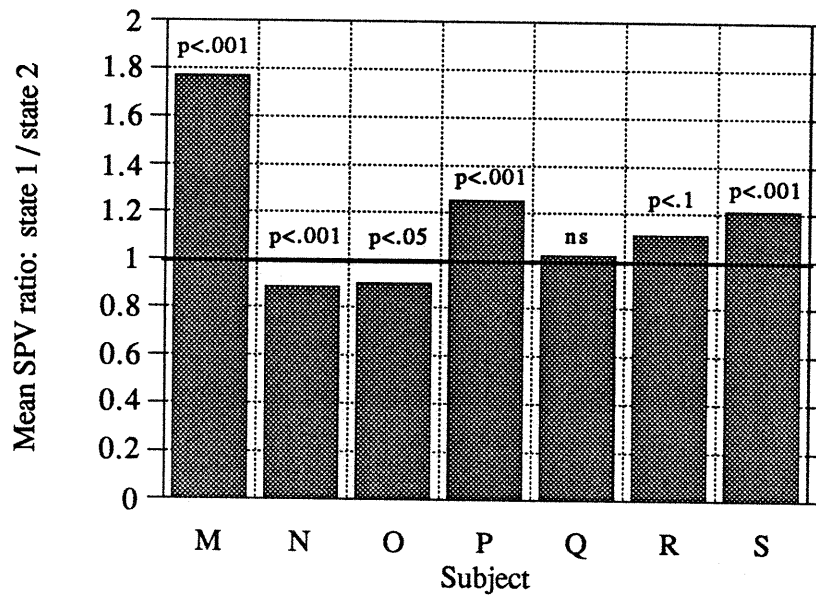
**Figure 5.12.** Mean ratios of OKN SPV in State 1 (vection) to corresponding value in State 2 (no vection). Ratios greater than 1 indicate a tendency toward increased SPV during vection.

The mean ratios were significantly different from unity for 5 of the subjects, indicating that OKN SPV was consistently higher in one of the two states for this group. However, the state exhibiting higher SPVs was not uniform among these subjects. Three of the subjects demonstrated higher SPVs during vection ($p < 0.001$ for M, P, S), while N ($p < 0.001$) and O ($p < 0.05$) displayed decreased eye velocity during self-motion perception.

## 5.2. Discussion of OKN SPV Characteristics

The overall OKN SPV gain results from the present study are plotted together with data from other torsional OKN experiments in Figure 5.13. The most prominent characteristic of torsional OKN is the low gain of the slow phase eye velocity response. The maximum SPV gains observed in this study did not exceed 0.3, even at the slowest stimulus rate of 15°/sec, and on average dropped by a factor of two from the slowest stimuli employed to the fastest. In comparison, yaw OKN in humans exhibits a gain near unity up to speeds of 60°-90°/sec. Thus, it appears that torsional OKN is of secondary importance in stabilizing images on the retina.

Ocular torsion is irrelevant in positioning the center of the fovea. In addition, Collewijn et. al. (1988) cited evidence that retinal slip velocities of up to 2.5°/sec in the fovea do not appreciably decrease visual acuity. Visual fields rotating at 60°/sec about the visual axis would induce linear retinal slip velocities above 2.5°/sec only at eccentricities greater than about 2.3°, an angle comparable to the foveal radius. Thus, even relatively high rates of visual field roll may not contribute much to loss of acuity in foveal vision, rendering torsional OKN relatively insignificant. While maintaining orientational stationarity of the retinal image is clearly desirable, fast visual field rolling motion generally results from head rotations, which can generate vestibularly induced eye torsion with gains above 0.7. These considerations appear to account for the comparatively minor role played by torsional OKN.

### 5.2.1. Comparison with Prior Studies

The most complete prior study of torsional OKN was conducted by Morrow and Sharpe (1989). Unfortunately, their abstract only stated the gains observed at their extreme stimulus velocities (10°/sec and 80°/sec), which lie outside the stimulus range tested here. Nonetheless, their reported values do fall quite near the gain curve suggested by the present study (Figure 5.13).

119

## a. Human torsional OKN SPV gains: all studies to date (erect orientation)



- present study
- Collewijn (1985)
- Malan (1985)
- Morrow and Sharpe (1989)

mean SPV gain

stimulus rotation speed (deg/sec)

## b. Human torsional OKN SPV gains: all studies to date (supine orientation)



- present study
- Malan (1985)
- Morrow and Sharpe (1989)

mean SPV gain

stimulus rotation speed (deg/sec)
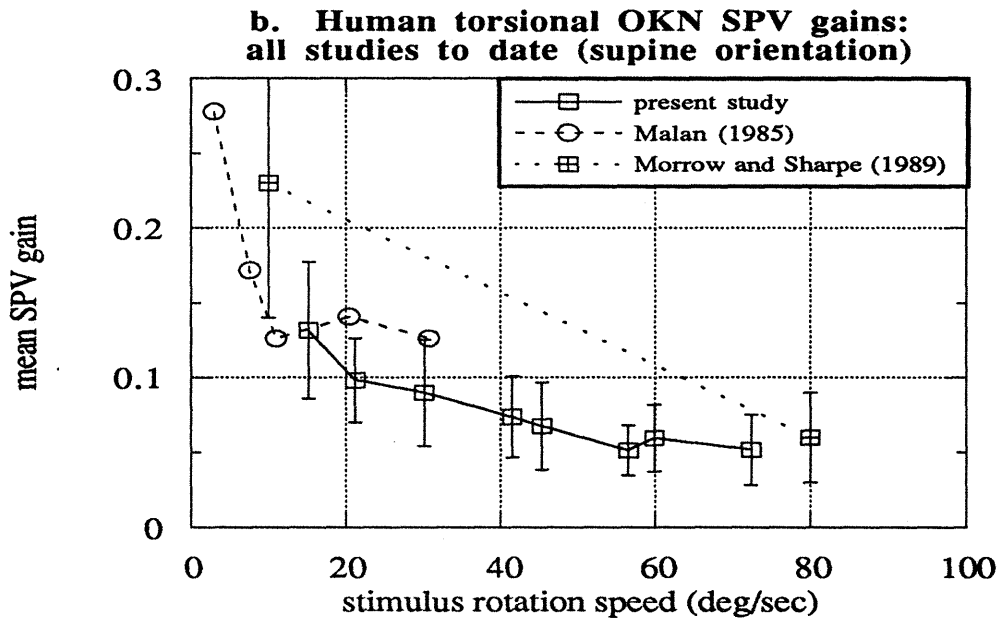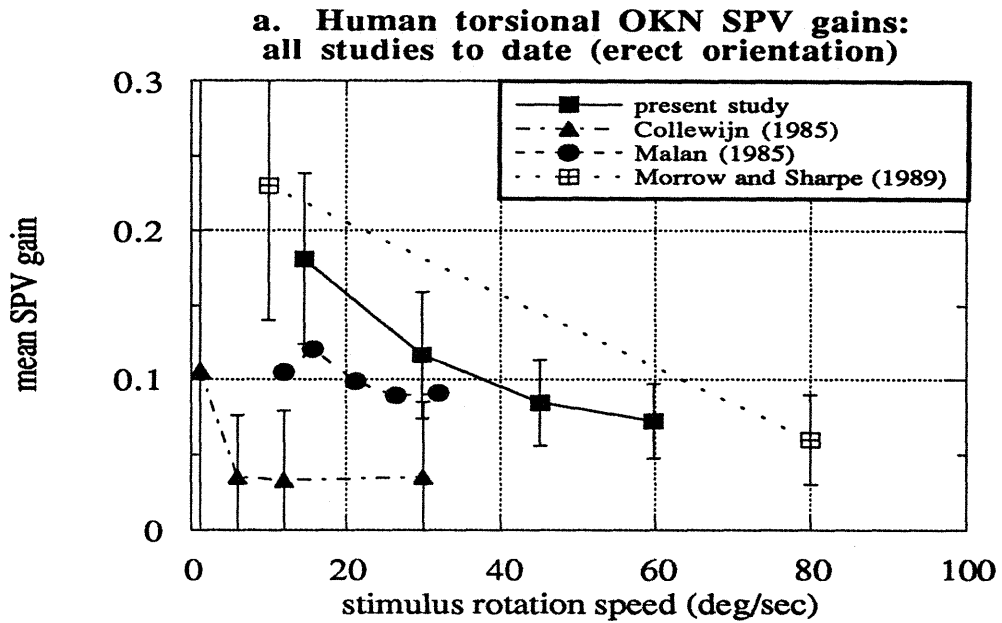
**Figure 5.13.** Comparison of SPV gains from present study with prior torsional OKN studies.

For the erect case, the average gains measured here were somewhat higher than those observed by Malan (1985). However, his data points fall within the range of gain responses observed in the present subjects, and information on the variance of his measurements was not available. His slightly reduced gains may have resulted from the restriction to monocular viewing by his eye coil device. A number of studies have reported a binocular contribution to the generation of OKN (Fox et. al., 1978; Wolfe et. al., 1980; Howard and Gonzalez, 1987; Howard and Simpson, 1989).

The OKN gains observed by Collewijn et. al. (1985) proved considerably lower than the present findings. Their much smaller gains may have been due to the optokinetic stimulus they employed, which consisted of a rotating disk subtending less than 100° of visual angle. Thus, a large proportion of the visual periphery was not stimulated in their experiment. While stimulation of the central retina generates the strongest horizontal and vertical OKN, peripheral motion may prove more important in the torsional case. Because the actual linear slip rate of images on the retina is proportional to the eccentricity for torsional stimuli, objects in the periphery move across the retina much faster than central objects rolling at the same rate.

### 5.2.2. Influence of gravitational orientation on torsional OKN

Of the six subjects tested both erect and supine, four demonstrated significantly lower OKN SPV gains supine, while only one demonstrated a significant increase in SPV gain supine. This surprising result ran contrary to prior expectations. Otolith information is known to exert a strong conditioning effect on eye movements induced by various body and visual field rotations about non-vertical axes. Schiff et. al. (1986) observed vigorous OKN for monkeys lying supine and prone, but the OKN velocity dropped sharply when the monkeys were tilted more than 30° from the horizontal. In addition, otolith stimulation has been shown to suppress down-beating pitch OKN in monkeys (Matsuo and Cohen, 1984), with a less pronounced effect in humans (Clément and Lathan, 1991).

121

On the basis of the demonstrated effects of otolithic inhibition, an increase in human torsional OKN SPV gain from the erect to the supine orientation might have been expected. Although Malan (1985) warned that no conclusions should be drawn from his SPV gain data due to the small sample sizes, his results did indicate somewhat higher SPV gains in the supine position. In contrast, Morrow and Sharpe (1989) found no differences between their erect and supine data.

The ambiguity concerning effects of orientation with respect to gravity on torsional OKN appears to signify that visual mechanisms are not as closely coupled to the vestibular (otolithic) system in humans as they are in monkeys. Interestingly, Clément and Lathan (1991) reported large decreases in both horizontal and vertical OKN gains from an upright position to a 90° roll orientation. They speculated that the global reductions in OKN gain resulted from subject disorientation rather than a specific gravitational effect on OKN mechanisms.

### 5.2.3. Possible habituation of OKN SPV gain responses

Comparison of later trials to earlier trials within a test session demonstrated a decline in SPV gain over the course of the session. While this effect may have resulted from subject boredom or fatigue, the possibility exists that repeated exposure to the rotating dome caused habituation to the stimulus and a concomitant reduction in SPV gain. Furthermore, the hypothesized habituative effect may have carried over from the first to the second test session. Since the supine session was conducted after the erect session for every subject, such habituation could explain the observed decrease in SPV gain supine for 4 of the subjects.

Two of the subjects were tested in one orientation on two separate days: subject M participated in two supine sessions, and subject O was tested erect on two occasions. By comparing the second session to the first session in the same orientation, the possibility of habituation could be examined without the complication of orientation influences. Ratios of mean SPV gain were calculated by dividing the SPV gains found in the second session by the
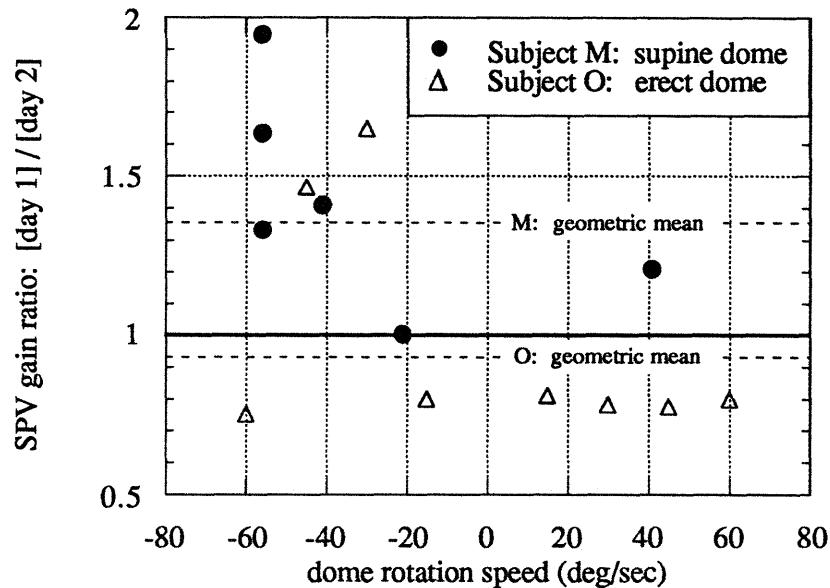
**Figure 5.14.** Comparison of SPV gains for runs in the same orientation performed on different days (subject M supine; subject P erect). Ratios of mean gain on day 2 to mean gain on day 1 are plotted for corresponding trials. Dashed lines indicated geometric means of ratios for each subject.

gains of the corresponding trials in the first session. Figure 5.14 shows the computed SPV gain ratios for both subjects.

The ratios for subject M were uniformly greater than 1, indicating increased gains during the second session. For subject P, however, the majority of the gain ratios were below 1, demonstrating a tendency toward reduced gains in the second session. The fact that M showed consistently higher gains in his second session, combined with the observation that P did not demonstrate a uniform decrease in SPV gain, may indicate that habituation to the stimulus does not have an important effect from day to day.

On the other hand, the direction of the gain alteration from the first to the second session of the same orientation is consistent with the change in gain from the erect (earlier) session to the supine (later) session for each subject. Subject M was the only one to

demonstrate higher gains supine, while P showed a decrease in supine gains which was shared by the remaining subjects. Thus, the gain changes observed between the two consecutive sessions for the same orientation might actually mirror opposite individual responses to repeated stimulus exposures. Subject M's gains may increase with additional exposures, while subject P (and others) may show a progressive decline in OKN gains associated with habituation.

There exists little evidence in the literature to support the habituative decline of OKN SPV gain upon repeated stimulus exposure. Kornhuber (cited in Miyoshi et. al., 1973) stated that habituation of optokinetic nystagmus does not exist. In support, Miyoshi et. al. (1973) found a "constant and definite increase of optokinetic response, interpreted as the result of a *positive learning process*" when they repeated optokinetic trials on 15 subjects for 10 consecutive days.

## 5.2.4. Lack of correlation between vection and OKN SPV

All of the tests performed in this study failed to reveal a link between vection and the slow phase eye velocity during OKN. Cross-correlations of vection and SPV yielded highly variable and generally inconsistent results, while comparisons of asymmetries in vection and SPV gain produced mutually contradictory patterns across the subject pool and even within a single subject's data set. Finally, direct comparison of SPV magnitude during periods with and without vection divided the subject population into two separate groups: one groups evidenced higher SPVs during vection, while the other demonstrated lower SPVs during periods of perceived self-rotation.

In all, these results point to a significant dissociation between optokinetic eye movements and the perceptual processes subserving vection. Thus, this study adds additional evidence to the many experiments which have rejected a close link between OKN and vection. In the most dramatic of these earlier demonstrations, Brandt et. al. (1973) proved that appropriate stimuli could even evoke horizontal OKN and yaw vection in opposite directions.

124

## 5.3. Eye Movement Aftereffects Following Visual Field Roll Stimulation

In addition to the optokinetic responses observed during visual field rotation, a broad range of eye movement aftereffects were recorded following the cessation of dome rotation. These aftereffects varied from person to person, and depended on the experimental conditions as well. Figure 5.15 shows examples of two different responses often seen after the dome stopped. The upper plots show a distinct optokinetic after-nystagmus (OKAN), which continued in the direction of the preceding OKN and had a slow phase component whose velocity decayed over time. The lower panels demonstrate a smooth return of the eye back to a rest position, during which no nystagmic beats occurred. Although an individual subject's eye movement traces tended to conform to one or the other of these response types, all subjects did demonstrate an after-nystagmus lasting for several beats in at least a few trials.

As described earlier, the slow phase velocity of the post-field-rotation response for each trial was fitted to a double exponential function of the form

$$SPV\ (t)\ =\ V_s e^{-t/\tau_s}\ +\ V_l e^{-t/\tau_l}\ +\ V_{bias}\ ,\qquad\qquad (5.2)$$

where $\tau_s$ and $\tau_l$ are the short and long decay time constants, and $V_s$ and $V_l$ are the magnitudes of the short and long components at $t = 0$. A constant term, $V_{bias}$, was included in the fit because some subjects appeared to exhibit a slow, spontaneous torsional drift in one direction which was interrupted by blinks or small saccades in the opposite direction. The fit parameters for each trial are tabulated in Table 6 in Appendix D. Of the 207 trials for which reasonable fits of this form could be determined, 109 (approximately 53%) were best approximated by a combination of fast and slow exponential decays. In the remainder of the cases, the fits for the two time constants converged to the same value.

Figure 5.16 shows frequency histograms of the fitted short and long time constants when all trials were grouped. In both histograms, the time constants appear to fall into two
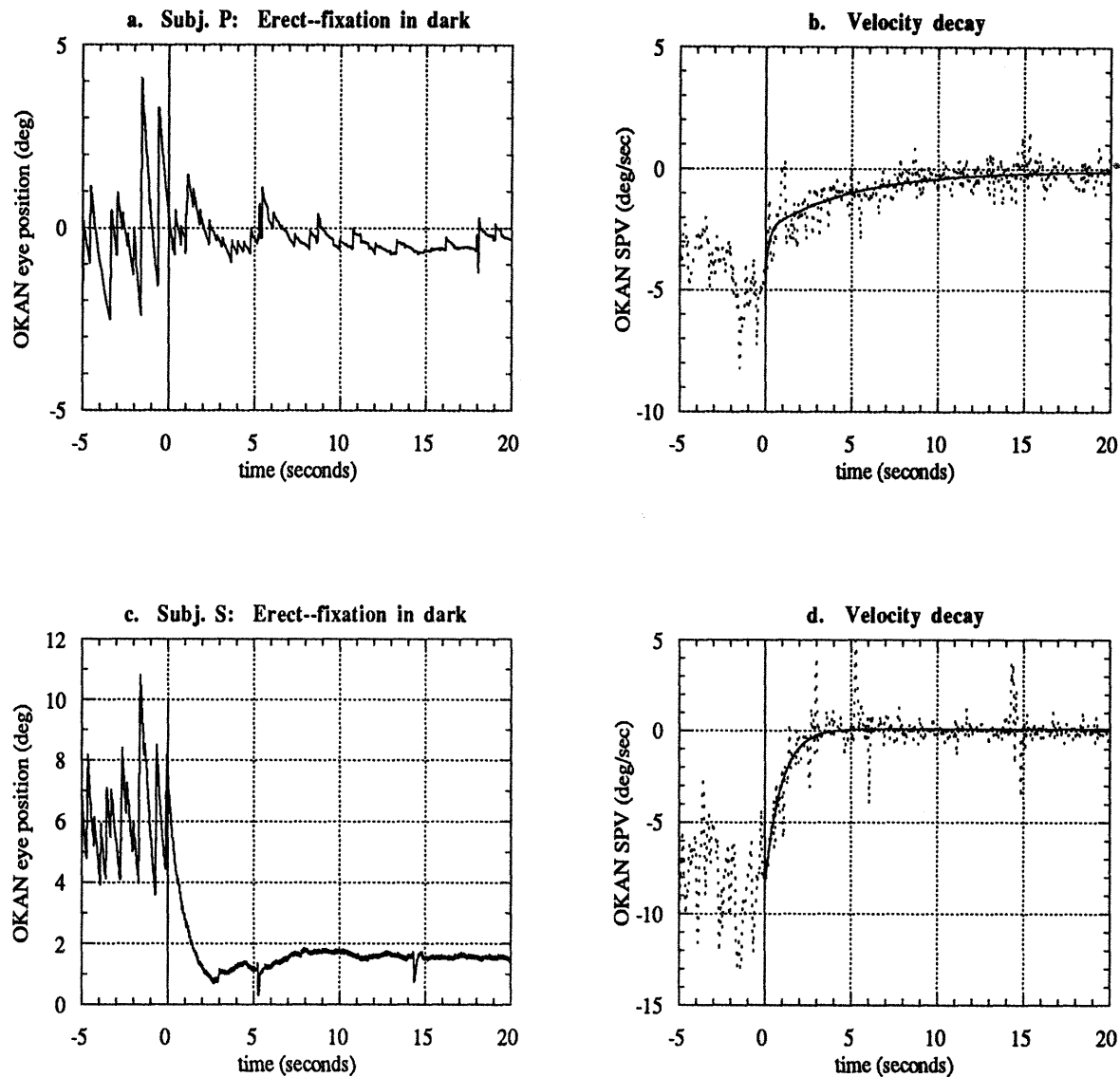
**Figure 5.15.** Different types of post-rotation responses to torsional optokinetic stimulation. Plots [a, b] show a true torsional after-nystagmus and the associated SPV decay. In [c, d], a smooth return of the eye to its rest position occured and no nystagmus was present. The lights were turned off at time 0. In the velocity plots [b, d] the solid lines represent fitted exponential decays.
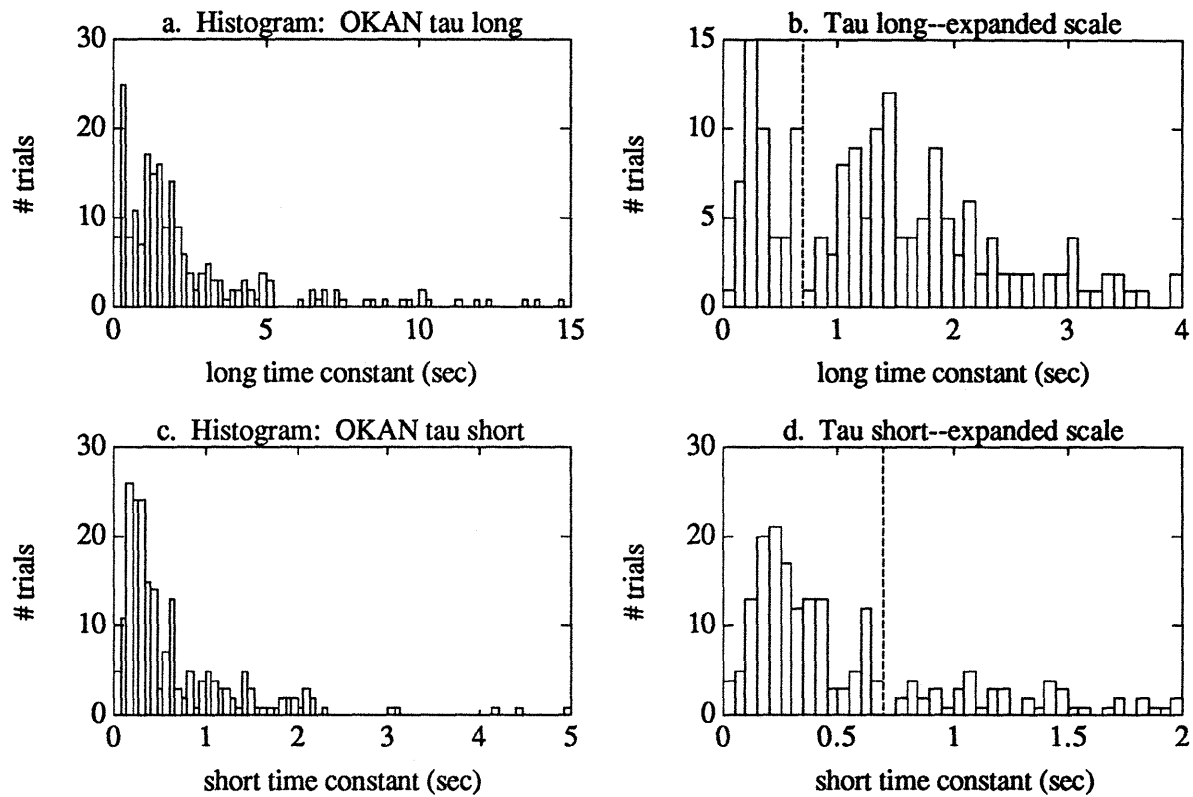
**Figure 5.16.** Frequency histograms showing distribution of time constants associated with OKAN SPV decay (double exponential fit). Plots [a, b] give distribution of longer time constants; [c, d] contain distribution of shorter time constants. Expanded views of the lower ranges in plots [a, b] are shown in [c, d]. Dashed lines drawn in [c, d] indicate apparent separation of time constants into two distinct groups at approximately 0.7 seconds.

distinct groups, with the dividing line at approximately 0.7 seconds. ("Short" values appear in the "long" time constant group, and vice versa, because of the overlap introduced by the cases best fitted with single exponentials.) Thus, it appears that the post-stimulus response consisted of two phases: (1) a rapid deceleration of the eye immediately following removal of the stimulus, and (2) a slower decay of slow phase velocity which often took the form of a nystagmus. For the 98 trials where a single exponential provided the best fit, one of the phases predominated: the eye either came rapidly to a stop (49 cases) or the SPV decayed slowly without an appreciable sharp decline when the dome stopped (49 cases).

When the calculated time constants were sorted into "short" ($\tau < 0.7$ sec.) and "long" ($\tau \geq 0.7$ sec.) response categories, the median decay time constants were 0.28 sec. and 2.0 sec., respectively. The mean[*] short and long time constants for each subject are presented in Table 5.7. The mean ratio of the magnitude of the slow decay to the initial SPV at the time the dome stops,

$$r = \frac{V_l}{V_l + V_s} , \qquad\qquad (5.3)$$

is also tabulated in Table 5.7. This ratio is generally near 0.5, and provides a measure of the strength of the slow response in relation to the magnitude of the OKN SPV during dome rotation.

## 5.3.1. Characteristics of Slow SPV Decay during OKAN

In order to characterize the behavior of the slow OKAN SPV decay process, the long decay time constants must be compared for different experimental conditions. However, for some subjects a large percentage of the trials did not exhibit a slow velocity decay during OKAN. Simply comparing the long time constants ($\tau \geq 0.7$ sec.) across conditions does not account for such "fast" velocity decay cases. To examine the processes underlying inhibition

---

[*] The geometric mean was used because all time constants are positive with a distribution skewed heavily toward the low end of the range.

| | | $\tau_l$ (sec) | | $\tau_s$ (sec) | | | $V_l/V_0$ | |
|---|---|---|---|---|---|---|---|---|
| Subject | # trials | geom. mean | st. dev. log $(\tau_l)$ | geom. mean | st. dev. log $(\tau_s)$ | % trials $\tau_l{\geq}0.7$ s. | geom. mean | st. dev. log$(V_l/V_0)$ |
| M | 32 | 1.78 | 0.26 | 0.31 | 0.23 | 97 | 0.51 | 0.35 |
| N | 29 | 2.49 | 0.22 | 0.31 | 0.22 | 55 | 0.38 | 0.41 |
| O | 34 | 2.96 | 0.31 | 0.22 | 0.21 | 62 | 0.38 | 0.39 |
| P | 32 | 2.89 | 0.27 | 0.28 | 0.23 | 94 | 0.48 | 0.23 |
| Q | 32 | 1.93 | 0.20 | 0.35 | 0.21 | 66 | 0.61 | 0.26 |
| R | 16 | 3.62 | 0.41 | 0.23 | 0.34 | 69 | 0.42 | 0.29 |
| S | 32 | 2.28 | 0.35 | 0.25 | 0.29 | 81 | 0.43 | 0.31 |

Table 5.7. Characteristics of post-dome-rotation eye movements. Geometric mean of short and long decay time constants. The standard deviation of the logarithms of the time constants is given as a measure of their variability. Also included is the percentage of trials exhibiting a "slow" SPV decay, and the ratio of the magnitude of the "slow" response ($V_l$) to the initial post-stimulus SPV. Again, the geometric mean of these ratios is given, along with the standard deviation of the logarithm.

of the slow velocity decay, the distribution of trials lacking "long" time constants is presented in Table 5.8. For each subject, the number of trials with time constants below 0.7 seconds is shown according to dome direction, postural orientation, and post-field-rotation visual surround.

As was done for SPV gain, the longer time constants were compared by direction and by postural orientation. Also, the effect of the different visual field conditions during the post-rotation period was examined. The non-normal distribution of the time constant values, as seen above in the frequency histograms, complicated comparisons between sets of trials. First, the velocity traces took the form of decaying exponentials, so all time constants were positive. Furthermore, the time constants had a distribution skewed toward the low end. For these reasons, the logarithms of the time constants were compared rather than the time constants themselves, and the graphs of time constant comparisons present the geometric means[*]

---

[*] The logarithm of the geometric mean is equal to the mean of the logarithms.

| Subject | # trials $\tau_1 < 0.7$ s. | Directional distribution | | Postural distribution | | Visual field distribution | | |
|---|---|---|---|---|---|---|---|---|
| | | proportion of CCW | proportion of CW | proportion of erect | proportion of supine | proportion in light | proportion in dark; fixation | proportion in dark; no fixation |
| M | 1 | 0/18 0% | 1/14 7% | 0/12 0% | 1/20 5% | 0/13 0% | 1/19 5% | -- |
| N | 13 | 10/13 77% | 3/16 19% | 9/15 60% | 4/14 29% | 1/4 25% | 10/17 59% | 2/8 25% |
| O | 13 | 3/15 20% | 10/19 53% | 7/19 37% | 6/15 40% | 2/6 33% | 3/14 21% | 8/14 57% |
| P | 2 | 0/16 0% | 2/16 13% | 1/16 6% | 1/16 6% | -- | 1/15 7% | 1/16 6% |
| Q | 11 | 7/16 44% | 4/16 25% | 8/16 50% | 3/16 19% | -- | 7/16 44% | 4/16 25% |
| R | 5 | 1/8 13% | 4/8 50% | 5/16 31% | -- | -- | 3/8 38% | 1/7 14% |
| S | 6 | 1/16 6% | 5/16 31% | 4/16 25% | 2/16 13% | -- | 2/16 13% | 4/16 25% |

Table 5.8. Distribution of trials lacking an outlasting "slow" velocity decay during OKAN. Only trials which permitted reasonable fits to the SPV decay were included. Frequency of occurrence of "fast decay" trials is shown grouped by dome rotation direction, subject postural orientation, and post-dome-rotation visual field. Dashes indicate experimental conditions for which no trials were performed.

(Figures 5.17 - 5.22). The error bars represent the exponentiation of values one standard deviation on either side of the mean of the logarithms; they appear symmetric about the geometric mean when the y-axis is drawn on a logarithmic scale.

### 5.3.1.1. OKAN Directional Asymmetries

First, CCW and CW trials were compared to test for directional asymmetry in the slow decay of SPV during OKAN. Only trials with decay time constants longer than 0.7 seconds were included in this comparison (Table 5.9a). Six of the subjects (N through S) exhibited somewhat longer time constants for CCW dome rotations, but none of the six comparisons proved statistically significant. (When these six were grouped together, the increase in time constants for CCW rotations was significant, with $p < 0.05$.) In contrast, CW rotations

induced slower SPV decays in only one individual subject (M), and the directional difference was significant ($p < 0.05$). No consistent asymmetry for the subject population was indicated when all subjects were grouped.

While the within-subject directional differences were largely insignificant for trials exhibiting a slow decay, the proportion of trials actually resulting in such outlasting eye movements was much more dependent on stimulus direction. As shown in Table 5.8, the trials with OKAN time constants below 0.7 seconds were distributed quite unevenly by direction. Subjects N and Q had a higher percentage of trials with slowly decaying SPVs for CW dome rotations; CCW stimuli produced more instances of gradual velocity decay in subjects O, R, and S.

When the comparison of long decay time constants was expanded to include the trials with only a fast decay, the effect of the their asymmetric distribution became clear (Figure 5.17). Table 5.9b contains the new time constant statistics--four subjects in addition to M now show significant directional asymmetries. The trend observed above earlier longer decay time constants for CCW SPV in subjects O, P, R, and S became significant when all trials are included. Of the five subjects with significant OKAN time constant asymmetries, three (M, P, and R) demonstrated consistent and significant asymmetries in OKN SPV gain. In all three cases, the stimulus direction producing higher SPV gain also resulted in elongated SPV decay time constants.

### 5.3.1.2. Torsional OKAN Dependence on Postural Orientation

Table 5.10 contains geometric mean values of the long decay time constants for the erect and supine runs grouped separately. In Table 5.10a, only the time constants corresponding to slow SPV decays ($\tau \geq 0.7$ sec.) were included in the calculations. Because only one of the subjects displayed a pronounced directional asymmetry for this set of trials, both stimulus directions were grouped. (Subject M showed no significant postural effects even when the trials were separated by direction.) As with the directional comparisons on the slow

**a.  Directional Comparison for Long Time Constants ($\tau_l \geq 0.7$ sec. only)**

| Subject | CCW rotation | | CW rotation | | mean ratio CW/CCW | p < ? (t test) |
|---|---|---|---|---|---|---|
| | geometric mean ($\tau_l$) | st. dev. log ($\tau_l$) | geometric mean ($\tau_l$) | st. dev. log ($\tau_l$) | | |
| M | 1.46 | 0.13 | 2.33 | 0.35 | 1.60 | 0.05 |
| N | 4.17 | 0.40 | 2.21 | 0.38 | 0.53 | ns |
| O | 3.33 | 0.32 | 2.53 | 0.31 | 0.76 | ns |
| P | 3.30 | 0.25 | 2.48 | 0.28 | 0.75 | ns |
| Q | 2.04 | 0.11 | 1.86 | 0.25 | 0.91 | ns |
| R | 4.66 | 0.44 | 2.32 | 0.33 | 0.50 | ns |
| S | 2.51 | 0.38 | 2.00 | 0.31 | 0.80 | ns |
| All subjects | 2.57 | 0.32 | 2.23 | 0.31 | 0.87 | ns |
| Subs. N through S | 3.03 | 0.32 | 2.20 | 0.30 | 0.73 | 0.05 |

**b.  Directional Comparison for Longer Time Constants (includes $\tau_l < 0.7$ sec.)**

| Subject | CCW rotation | | CW rotation | | mean ratio CW/CCW | p < ? (ANOVA) |
|---|---|---|---|---|---|---|
| | geometric mean ($\tau_l$) | st. dev. log ($\tau_l$) | geometric mean ($\tau_l$) | st. dev. log ($\tau_l$) | | |
| M | 1.46 | 0.13 | 2.13 | 0.37 | 1.46 | 0.050 |
| N | 0.75 | 0.48 | 1.52 | 0.49 | 2.04 | ns |
| O | 2.09 | 0.51 | 0.78 | 0.55 | 0.37 | 0.005 |
| P | 3.30 | 0.25 | 1.84 | 0.44 | 0.56 | 0.100 |
| Q | 0.94 | 0.43 | 1.22 | 0.40 | 1.29 | ns |
| R | 3.49 | 0.54 | 0.96 | 0.47 | 0.28 | 0.050 |
| S | 2.21 | 0.43 | 1.03 | 0.56 | 0.47 | 0.050 |

Table 5.9.  Directional comparison of slow velocity decay component of OKAN.  [a.]  Comparison using only trials with "long" decay time constants ($\tau \geq 0.7$ sec.)  [b.]  Comparison using all trials, including those lacking a "slow" decay component ($\tau < 0.7$ sec.)
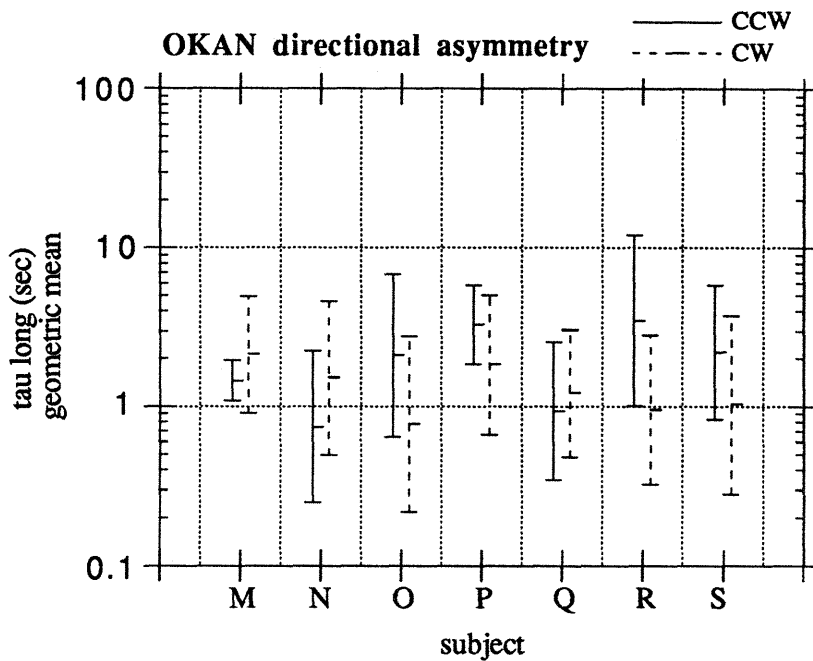
Figure 5.17. Comparison of long time constants of OKAN SPV decay for CCW and CW dome rotation. Geometric means are plotted because the distribution of time constants is highly skewed toward the low end. Differences are significant for: M (p < 0.05); O (p < 0.005); P (p < 0.1); R (p < 0.05); S (p < 0.05).

decay time constants alone, the postural comparisons yielded ambiguous results. Although significant differences between positions were found for two subjects, N had longer decay time constants supine while P's SPV decay proved elongated for the erect runs. When the subjects were grouped, the mean long time constants were identical in both orientations.

Table 5.8 also includes the breakdown by postural orientation of trials lacking a slow SPV decay. Such trials occurred at least twice as often erect as they did supine for subjects N, Q, and S. For the other subjects, trials missing long decay time constants occurred either infrequently (M, P) or at approximately the same rate both erect and supine (subject O). The longer time constants for all trials were included in the means calculated for Table 10b, effectively accounting for the trials in which the slow decay response was completely inhibited.

| a. long SPV decay only ($\tau_l \geq 0.7$ sec) | | | | | | |
|---|---|---|---|---|---|---|
| | Erect | | Supine | | | |
| Subject | Geometric mean ($\tau_l$) | st. dev. log ($\tau_l$) | Geometric mean ($\tau_l$) | st. dev. log ($\tau_l$) | supine/erect | p = ? (t test) |
| M | 2.00 | 0.31 | 1.65 | 0.23 | 0.83 | ns |
| N | 1.44 | 0.15 | 3.46 | 0.41 | 2.41 | 0.05 |
| O | 2.79 | 0.35 | 3.21 | 0.27 | 1.15 | ns |
| P | 3.60 | 0.25 | 2.31 | 0.25 | 0.64 | 0.05 |
| Q | 1.81 | 0.25 | 2.02 | 0.18 | 1.12 | ns |
| S | 2.02 | 0.37 | 2.54 | 0.33 | 1.26 | ns |
| All subjects (except R) | 2.34 | 0.32 | 2.32 | 0.29 | 0.99 | ns |

| b. all trials (including $\tau_l < 0.7$ sec) | | | | | | |
|---|---|---|---|---|---|---|
| | Erect | | Supine | | | |
| Subject | Geometric mean ($\tau_l$) | st. dev. log ($\tau_l$) | Geometric mean ($\tau_l$) | st. dev. log ($\tau_l$) | supine/erect | p = ? (t test) |
| M | 2.00 | 0.31 | 1.57 | 0.24 | 0.79 | ns |
| N | 0.65 | 0.33 | 1.94 | 0.54 | 2.96 | 0.008 |
| O | 1.08 | 0.62 | 1.37 | 0.52 | 1.27 | ns |
| P | 2.95 | 0.42 | 2.006 | 0.32 | 0.70 | ns |
| Q | 0.71 | 0.47 | 1.60 | 0.27 | 2.25 | 0.01 |
| S (CCW) | 1.95 | 0.52 | 2.50 | 0.33 | 1.28 | ns |
| S (CW) | 0.59 | 0.60 | 1.81 | 0.42 | 3.08 | 0.08 |
| All subjects (except R) | 1.19 | 0.53 | 1.75 | 0.38 | 1.47 | 0.01 |

Table 5.10. Long time constants of OKAN SPV decay: erect vs. supine. [a.] includes only trials with $\tau_l \geq 0.7$ sec. [b.] includes all trials. The time constants for subject S have been subdivided by dome rotation direction, because S has significant directional asymmetries. (Although O and P also exhibit directional asymmetries, neither displays significant postural effects when the trials are separated by direction.)

When the subjects were grouped together, their slow decay time constants were significantly longer supine than erect (p = 0.01). The comparisons for three individuals--N, Q, and S-- showed significant differences: in each case the supine time constants were elongated with respect to their counterparts erect (Figure 5.18).

As noted earlier, the proportion of subject S's trials lacking long decay responses was much higher for CW dome rotations; the postural difference for this subject was significant only for SPVs in the CW direction. Although subjects O and P also displayed marked directional asymmetries, their postural comparisons revealed no significant results even when separated by direction.
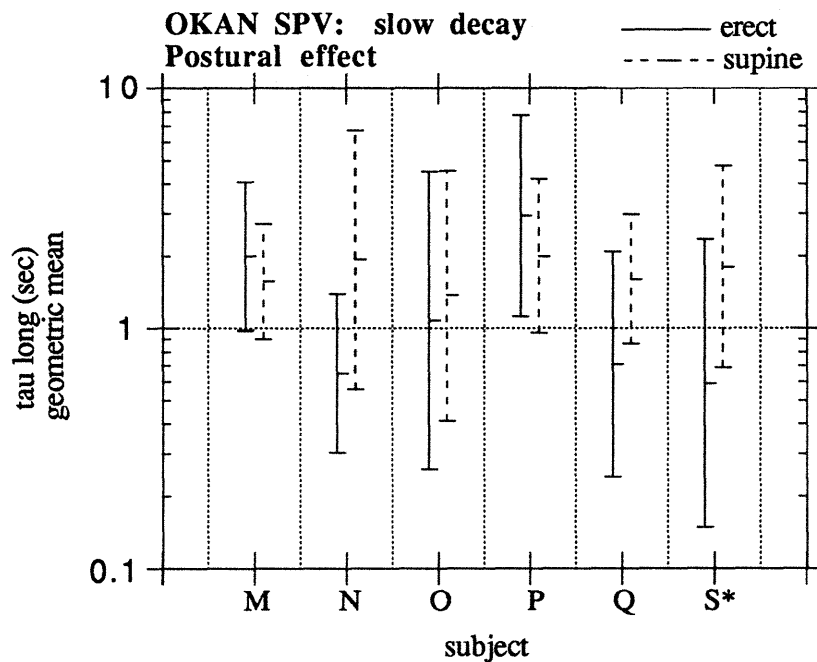


*The plot for subject S includes CW dome rotation trials only.

**Figure 5.18. Long time constants of OKAN SPV decay for erect and supine positions. Includes longer time constants from all trials. Differences significant for N (p = 0.008), Q (p = 0.01), S* (p = 0.08)**

135

### 5.3.1.3. Visual Field Effects on Slow OKAN Decay Process

The long time constant of SPV decay was compared for the different visual conditions tested following the end of the dome rotation (Figure 5.19). Only trials displaying a slow velocity decay ($\tau > 0.7$ sec) were included in this analysis. Table 5.11a compares the time constants obtained in the darkness while the subject fixated on an "imagined" LED with those realized when an actual fixation LED was in place. Half of the 6 subjects tested in these two conditions demonstrated significant differences; all three of these (P, Q, S) had a slower SPV decay when no visual information was present. Furthermore, a comparison for subjects N through S combined indicated that the group exhibited a significantly slower velocity decay without the fixation LED ($p < 0.05$).
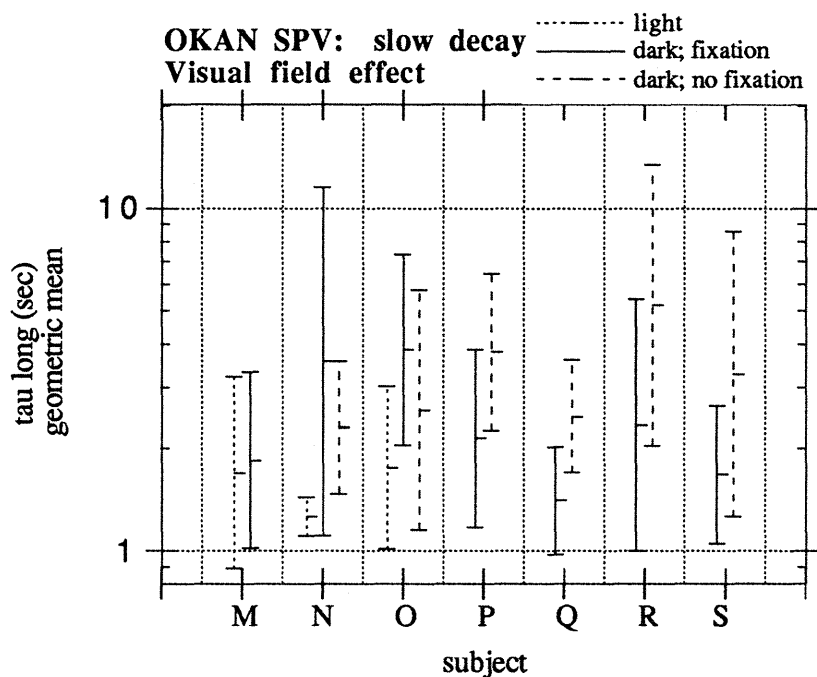


**Figure 5.19.** Time constants of slow OKAN SPV decay for different post-rotation visual conditions: (1) in the light (full visual field), (2) in the dark with a central LED fixation point, and (3) in complete darkness; subject instructed to fixate on an "imagined" LED. Includes only trials with long time constants greater than 0.7 seconds.

**a. Comparison by post-rotation visual field: fixation vs. no fixation in darkness**

| Subject | Dark; fixation geometric mean ($\tau_1$) | st. dev. log ($\tau_1$) | Dark; no fixation geometric mean ($\tau_1$) | st. dev. log ($\tau_1$) | mean ratio no fix./ fix. | p < ? (t test) |
|---|---|---|---|---|---|---|
| M | -- | -- | -- | -- | -- | -- |
| N | 3.57 | 0.51 | 2.29 | 0.19 | 0.64 | ns |
| O | 3.87 | 0.28 | 2.57 | 0.35 | 0.66 | ns |
| P | 2.13 | 0.26 | 3.81 | 0.23 | 1.79 | 0.01 |
| Q | 1.40 | 0.16 | 2.47 | 0.16 | 1.76 | 0.005 |
| R | 2.33 | 0.37 | 5.21 | 0.41 | 2.23 | ns |
| S | 1.67 | 0.20 | 3.28 | 0.42 | 1.96 | 0.05 |
| All subjects (N - S) | 2.25 | 0.32 | 3.17 | 0.31 | 1.41 | 0.05 |

**b. Comparison by post-rotation visual field: in light vs. fixation in darkness**

| Subject | Lights on geometric mean ($\tau_1$) | st. dev. log ($\tau_1$) | Dark; fixation geometric mean ($\tau_1$) | st. dev. log ($\tau_1$) | mean ratio fix./ light | p < ? (t test) |
|---|---|---|---|---|---|---|
| M | 1.69 | 0.28 | 1.84 | 0.26 | 1.09 | ns |
| N | 1.26 | 0.06 | 3.57 | 0.51 | 2.84 | ns* |
| O | 1.75 | 0.24 | 3.87 | 0.28 | 2.22 | 0.05 |
| All subjects (M - O) | 1.63 | 0.25 | 2.63 | 0.35 | 1.61 | 0.05 |

*For subject N, if inhomogeneous variances are assumed across the two conditions (light, darkness with fixation) the difference is significant at p = 0.06.

**Table 5.11. Comparison of slow OKAN SPV decay for different post-dome-rotation visual field conditions. Results include trials with $\tau_1 \geq 0.7$ seconds only. [a.] Decay time constants in darkness: fixation LED vs. "imagined" fixation LED. [b.] Decay time constants: in light vs. fixation LED in darkness.**

Trials with the lights left on following dome rotation were available for three subjects: M, N, and O. The slow decay time constants from these trials were compared with the trials utilizing a fixation LED in the dark (Table 5.11b). All three subjects displayed more slowly decaying SPV in the dark, and the difference in time constants was significant for subject O. (If inhomogeneous variances were assumed for subject N, that difference also proved significant with p = 0.06.) Again, grouping these three subjects revealed significantly longer time constants (p < 0.05) for the condition with less visual information (fixation in the dark).

## 5.3.2. Characteristics of Fast SPV Decay Following End of Field Rotation

A systematic comparison of the short SPV decay time constants ($\tau_s$), similar to the analysis performed for the slower process of OKAN decay, was made across the set of experimental conditions. Decay time constants shorter than 0.7 seconds were considered representative of the "fast" segment of post-rotatory SPV decay; the following tests included only trials exhibiting such a quick decline in velocity. Appropriate comparisons were made to examine directional asymmetries, postural influences, and effects of the post-stimulus visual field.

Figure 5.20 shows the short time constants grouped according to rotation direction. The geometric means are tabulated in Table 5.12. Of the 7 subjects, all but R showed longer time constants for CCW dome trials. Combining all the subjects revealed a significant tendency toward elongated decays following CCW rotations for the group ($p < 0.02$). The increase in the short time constants for CCW rotations was significant for two individuals: N and S. This directional preponderance for the group mirrors the slight asymmetry seen in the long decay time constants, where 6 of the 7 demonstrated slower decays for CCW trials (the exception was M for the long OKAN time constants).

Comparisons of the fast SPV decay erect versus supine exposed the same trend observed in the case of the slow decay time constants: the decay time constants were generally longer with the subject supine (Figure 5.21). Table 5.13 displays the mean short time constants according to orientation. In subjects O and P the increase in tau supine was significant; the elongation supine was also significant for the group at the level $p < 0.02$. It is important to note, however, that the apparent increase in slow decay time constants for supine trials really resulted from more prevalent inhibition of the slow decay response erect. In contrast, the magnitude of the fast time constant actually depended on subject orientation.

Although the makeup of the visual field after the dome stopped rotating appeared to affect the short time constant of SPV decay for a number of the individual subjects (Figure 5.22), it was difficult to discern any consistent trends. Two of the subjects (Q and R)
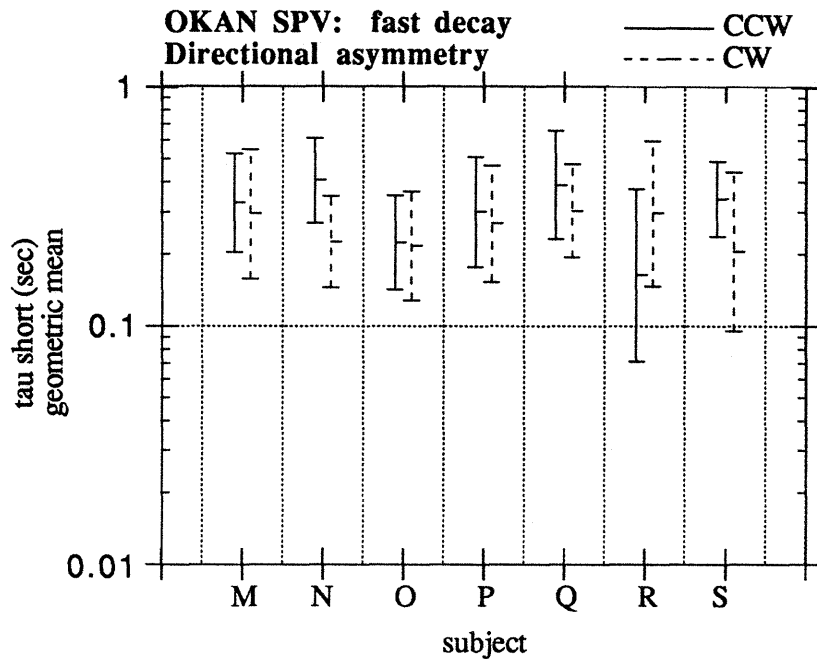
**Figure 5.20.** Short time constant of OKAN SPV decay: CCW vs. CW dome rotation. Differences significant for: N (p < 0.05); S (p < 0.1).

| Subject | CCW rotation | | CW rotation | | mean ratio CW/CCW | p < ? (ANOVA) |
|---|---|---|---|---|---|---|
| | geometric mean ($\tau_S$) | st. dev. log ($\tau_S$) | geometric mean ($\tau_S$) | st. dev. log ($\tau_S$) | | |
| M | 0.33 | 0.21 | 0.29 | 0.27 | 0.90 | ns |
| N | 0.41 | 0.18 | 0.22 | 0.19 | 0.55 | 0.05 |
| O | 0.22 | 0.20 | 0.22 | 0.23 | 0.97 | ns |
| P | 0.30 | 0.23 | 0.27 | 0.24 | 0.90 | ns |
| Q | 0.39 | 0.23 | 0.30 | 0.19 | 0.78 | ns |
| R | 0.16 | 0.36 | 0.30 | 0.30 | 1.81 | ns |
| S | 0.34 | 0.16 | 0.21 | 0.33 | 0.61 | 0.1 |
| All subjects | 0.31 | 0.24 | 0.25 | 0.26 | 0.80 | 0.02* |

*Probability p = 0.02 for all subjects combined was generated from independent samples t test.

**Table 5.12.** Comparison of short SPV decay time constants by direction. Includes trials with time constants below 0.7 sec. only.
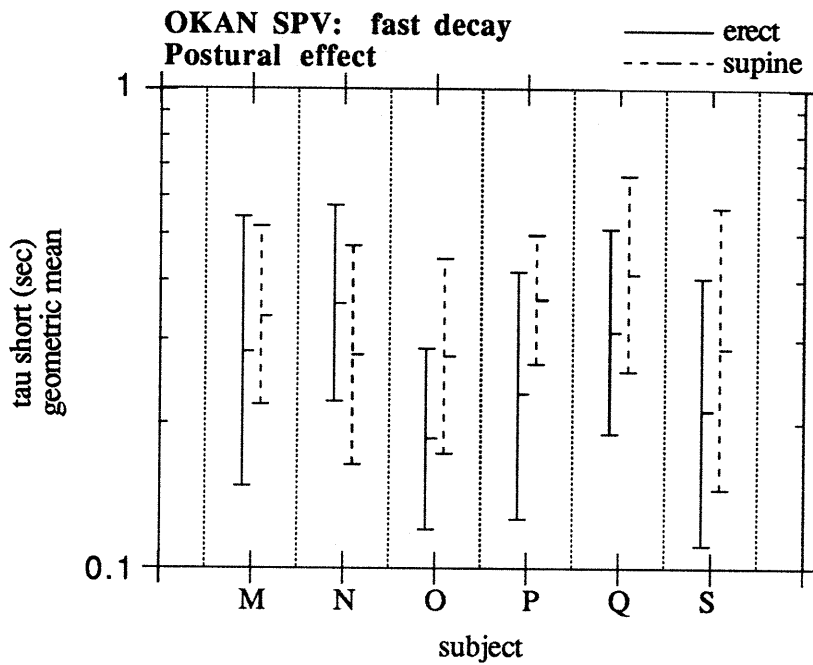
Figure 5.21. Short time constant of OKAN SPV decay grouped according to erect and supine positions. Differences significant for: O (p < 0.01), P (p < 0.05)

| Subject | Erect dome | | Supine dome | | mean ratio supine/erect | p < ? (ANOVA) |
|---|---|---|---|---|---|---|
| | geometric mean ($\tau_s$) | st. dev. log ($\tau_s$) | geometric mean ($\tau_s$) | st. dev. log ($\tau_s$) | | |
| M | 0.28 | 0.28 | 0.34 | 0.19 | 1.19 | ns |
| N | 0.36 | 0.21 | 0.28 | 0.23 | 0.78 | ns |
| O | 0.19 | 0.19 | 0.28 | 0.21 | 1.49 | 0.01 |
| P | 0.23 | 0.26 | 0.36 | 0.14 | 1.58 | 0.05 |
| Q | 0.31 | 0.22 | 0.41 | 0.21 | 1.32 | ns |
| S | 0.21 | 0.28 | 0.29 | 0.30 | 1.35 | ns |
| All subjects (except R) | 0.25 | 0.25 | 0.31 | 0.22 | 1.26 | 0.02* |

*Probability p = 0.02 for all subjects combined was generated from independent samples t test.

Table 5.13. Comparison of short SPV decay time constants by postural orientation. Includes trials with time constants below 0.7 sec. only.
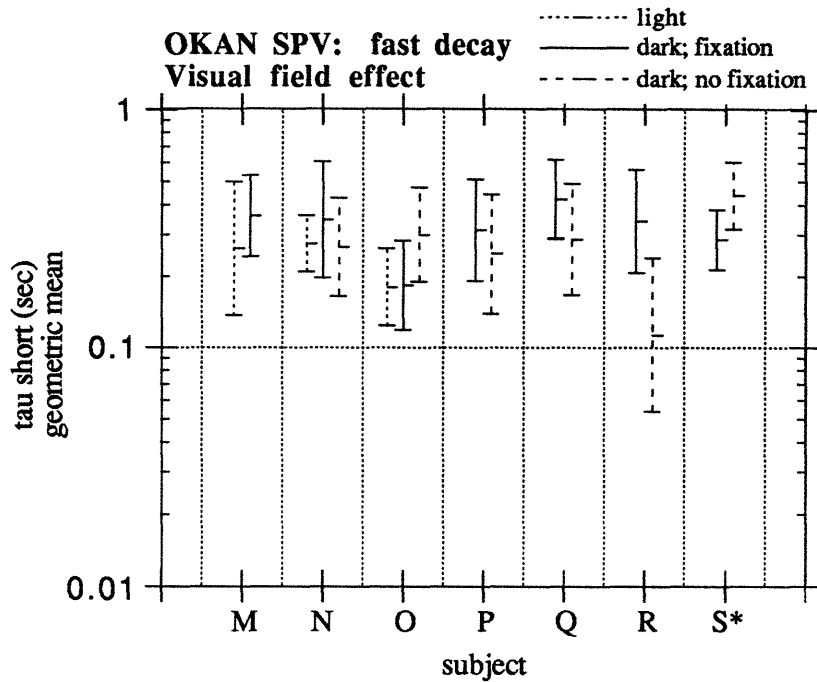
Figure 5.22. Short time constants of OKAN SPV decay for different post-rotation visual conditions: (1) in the light (full visual field), (2) in the dark with a central LED fixation point, and (3) in complete darkness; subject instructed to fixate on an "imagined" LED. Differences significant for: M (p < 0.1); O (p < 0.005, between dark conditions); Q (p < 0.1); R (p < .05).

exhibited significantly longer time constants with the fixation LED present in the dark, while two others (O and S) recorded the opposite behavior (Table 5.14a). Overall, the group tended weakly toward longer time constants with the LED lit when the values for subjects N through S were combined (p < 0.1). Of the 3 subjects who were also tested post-rotation in the light, 2 displayed faster SPV decays in the light than in the dark while the third showed no change. The quicker decay in the light approached significance only for subject M (p < 0.1).

**a.** Comparison by post-rotation visual field: fixation vs. no fixation in darkness

| Subject | Dark; fixation | | Dark; no fixation | | mean ratio no fix./ fix. | p < ? (ANOVA) |
|---|---|---|---|---|---|---|
| | geometric mean ($\tau_S$) | st. dev. log ($\tau_S$) | geometric mean ($\tau_S$) | st. dev. log ($\tau_S$) | | |
| M | -- | -- | -- | -- | -- | -- |
| N | 0.35 | 0.24 | 0.27 | 0.21 | 0.77 | ns |
| O | 0.18 | 0.19 | 0.30 | 0.20 | 1.63 | 0.005 |
| P | 0.31 | 0.21 | 0.25 | 0.25 | 0.80 | ns |
| Q | 0.42 | 0.17 | 0.29 | 0.23 | 0.68 | 0.1 |
| R | 0.34 | 0.22 | 0.11 | 0.33 | 0.33 | 0.05 |
| S (CCW) | 0.29 | 0.13 | 0.44 | 0.14 | 1.53 | 0.1* |
| S (CW) | 0.27 | 0.31 | 0.17 | 0.34 | 0.61 | ns |
| All subjects (N - S) | 0.30 | 0.24 | 0.24 | 0.28 | 0.82 | 0.1* |

*Probabilities p generated from independent samples t test..

**b.** Comparison by post-rotation visual field: in light vs. fixation in darkness

| Subject | Lights on | | Dark; fixation | | mean ratio fix./ light | p < ? (ANOVA) |
|---|---|---|---|---|---|---|
| | geometric mean ($\tau_S$) | st. dev. log ($\tau_S$) | geometric mean ($\tau_S$) | st. dev. log ($\tau_S$) | | |
| M | 0.26 | 0.28 | 0.36 | 0.17 | 1.37 | 0.1 |
| N | 0.28 | 0.12 | 0.35 | 0.24 | 1.26 | ns |
| O | 0.18 | 0.16 | 0.18 | 0.19 | 1.02 | ns |
| All subjects (M - O) | 0.24 | 0.23 | 0.28 | 0.25 | 1.17 | ns |

Table 5.14. Comparison of fast OKAN SPV decay for different post-dome-rotation visual field conditions. Results include trials with $\tau_S$ < 0.7 seconds only.
[a.] Decay time constants in darkness: fixation LED vs. "imagined" fixation LED. Comparisons for subject S were separated by rotation direction, because this subject demonstrated a significant directional asymmetry. (Subject N also exhibited a directional asymmetry, but showed no significant dependence on visual field when the trials were grouped by direction.)
[b.] Decay time constants: in light vs. fixation LED in darkness.

142

## 5.4. Discussion of Torsional Optokinetic Afternystagmus

The decay in SPV during OKAN consisted of two separate processes, each with a characteristic time constant. The initial rapid drop in SPV, which had a time constant with a geometric mean of 0.26 sec across all subjects, probably reflected the response of the "fast" cortical OKN pathway upon cessation of the optokinetic stimulus. The slower decay in eye velocity (characterized by a time constant with a geometric mean of 2.4 sec) was most likely mediated through the "slow" velocity storage path.

The mean value of the torsional SPV long decay time constant--2.4 sec--was extremely short compared to the 25 sec discharge time constant observed for horizontal OKAN in humans (Cohen et. al., 1981). Likewise, durations of up to 25 sec have been reported for vertical OKAN with slow phases upward. The comparatively fast decay in torsional OKAN, together with the short 4.0 sec decay time constant for roll post-rotatory nystagmus and the weak and variable nature of torsional OKN, indicates that velocity storage about the roll axis is extremely underdeveloped in humans. This finding contrasts sharply with evidence that torsional OKN in the monkey is mediated almost solely throught the velocity storage pathway, with no significant pathways for rapid change in torsional SPV (Schiff et. al., 1986).

## 5.4.1. Gravitational Suppression of Velocity Storage in Torsion

Three subjects demonstrated significant decreases in mean OKAN long decay time constants from the supine to the erect orientation. Furthermore, when all subjects were grouped, the erect time constants were significantly shorter than the supine time constants. These results implied suppression of torsional velocity storage activity by otolithic inputs. Although Morrow and Sharpe (1989) did not find any differences between erect and supine time constants, many experiments in humans and animals predict that velocity storage suppression should occur in roll for erect subjects.

Lafortune et. al. (1990) showed that static tilts in pitch suppressed velocity storage for yaw OKAN, leading to decreased decay time constants. Furthermore, pitch and roll rotations

are comparable in the sense that both normally occur about earth-horizontal axes, bringing the otolith organs into play. Roll of the head moves the utricular maculae out of their dominant plane, resulting in increased decay time constants for vertical OKAN in both monkeys (Matsuo and Cohen, 1984) and humans (Clément and Lathan, 1991).

By extension, moving the head to either the supine or prone position should increase the decay time constants for torsional OKAN. Such an orientational dependence has been observed for torsional OKAN in the monkey: Schiff et. al. (1986) found that tilting the head more than 30° from the supine position nearly abolished the previously vigorous OKAN response. All of these studies verified the attenuation of velocity storage about off-vertical axes through the influence of the otoliths, supporting the notion that otolithic suppression accounted for the reduced time constants in SPV decay observed for the erect runs.

### 5.4.2. Suppression of OKAN by Visual Information

All three subjects who underwent OKAN testing in the light exhibited shorter decay time constants compared to the values obtained during OKAN in the dark with a fixation point. The decrease in mean decay time constant during pattern illumination was significant for two individuals, as well as for the three as a group. Similar "dumping" of velocity storage has been studied more extensively for horizontal OKAN in humans and monkeys. Cohen et. al. (1981) found that exposure of the subject to a stationary visual surround resulted in a loss of stored activity combined with an attenuation of the response when compared with the control OKAN response in the dark.

One important difference between the horizontal and torsional cases involved fixation suppression. When the stationary surround was illuminated during horizontal OKAN in humans, eye velocity declined rapidly to zero. If the lights were turned out before the velocity storage was completely discharged, OKAN resumed, although with a lower velocity than would be expected for the control case in the dark. However, in the torsional case OKAN SPV declined at a faster rate in the light than in darkness, but did not drop immediately to zero with

the lighted stationary surround. This difference from the horizontal case was probably due to the absence of a well-developed fixation mechanism for torsion.

Interestingly, even the fixation LED alone contributed to suppression of velocity storage. Although the round LED subtended only 0.5 degrees and provided no orientational cues, 3 of the 6 subjects tested in complete darkness exhibited significantly longer decay time constants when no visual information was present. The same effect also proved significant when all subjects were grouped. Collewijn et. al. observed a somewhat similar phenomenon: torsional VOR gains during head rotations in darkness increased significantly when the subject viewed a fixation point projected by a helium-neon laser beam. Both observations indicated that even small visual stimuli lacking features which could provide orientational information had significant effects on reflexive compensatory eye movements.

### 5.4.3.  Possible Effects of Habituation on OKAN

Since the supine runs always followed the erect runs, and runs in total darkness always followed the runs with the fixation LED, the existence of exposure effects on OKAN might generate questions concerning the actual origin of the changes in SPV decay time constants observed for the supine and darkness conditions. Studies in monkeys indicated that repeated exposures to optokinetic stimuli caused decreases in OKAN discharge time constants. Cohen et. al. (1977) found that time constants became shorter with repeated testing over a 6 month period. A possibly more relevant test by Skavenski et. al. demonstrated that 20 1-minute exposures to a spinning drum reduced OKAN time constants by half.

These studies demonstrate habituative effects of OKN exposure, which cause a decrease in the time constant of OKAN response. However, the later runs in the present study (supine runs and runs in darkness) displayed increased time constants. Thus, the increase in time constants seen in the supine orientation and in complete darkness cannot be attributed to habituation.

## 5.5. Deviation of Nystagmus Beating Field during Optokinetic Stimulation

During OKN, the mean eye position frequently deviated in the direction of the fast phase of nystagmus. This tonic bias in the nystagmus beating field, or *Schlagfeld*, could measure over 5° and appears clearly in the OKN in Figure 5.2. The amount of deviation toward the fast phase direction generally increased with higher slow phase eye velocities. To quantify the bias in the *Schlagfeld*, a measure of mean eye reset position was defined. After Yasui (1974), the mean reset position for a single trial was calculated as the average of the final positions of the individual fast phases during optokinetic stimulation. A mean reset value of zero would therefore indicate that the fast phases brought the eye back to the central rest position, while a value opposite in sign to the SPV would demonstrate a shift toward the fast phase direction.

In Figures 5.23 - 5.29, mean reset positions are plotted against mean SPVs for each trial. The supine and erect cases are shown separately by subject. For each orientation, regression lines were fit to the data points using a least-squares technique. Separate fits were computed for CCW and CW dome rotations. The calculated slopes and y-intercepts for each orientation and rotation direction are presented by subject in Table 5.15. Of the 26 regression lines, 24 exhibited negative slopes, indicating greater deviation in the fast phase direction with increased SPV. The mean of the slopes for all subjects combined measured -0.92 °/(°/sec) with a standard deviation of 0.70.

For every individual subject, the slopes of the regression lines (in both orientations and directions) were found not to be significantly different from each other based on 90% confidence intervals. In the supine orientation, none of the subjects exhibited a significant difference at the 90% level between the y-intercept values for CCW and CW rotations. However, for 4 of the 7 subjects tested erect, significant differences were observed between the intercepts calculated for the CCW and CW rotation directions. Furthermore, all subjects had intercept shifts in the same direction erect: subtracting the CCW from the CW intercepts yielded positive results. Three of the intercept differences were significant based on 95%

**a. Supine dome: linear fits of mean eye deviation vs. mean SPV**

| Subject | CCW rotation | | CW rotation | | intercept difference | p < ? | CCW and CW grouped | |
|---|---|---|---|---|---|---|---|---|
| | slope | intercept | slope | intercept | CW - CCW | | slope | intercept |
| M | -1.26 | 1.14 | -0.87 | -0.02 | -1.16 | ns | -1.20 | 1.23 |
| N | -0.37 | -1.06 | 0.74 | -1.65 | -0.59 | ns | 0.08 | 0.07 |
| O | -0.03 | -0.11 | -1.27 | 2.34 | 2.45 | ns | -0.16 | -0.13 |
| P | -1.20 | -0.17 | -0.54 | 0.63 | 0.80 | ns | -0.80 | 1.24 |
| Q | -2.21 | -1.45 | -1.63 | 2.36 | 3.81 | ns | -1.16 | 1.18 |
| R | -- | -- | -- | -- | -- | -- | -- | -- |
| S | -1.33 | -0.73 | -0.79 | 1.74 | 2.47 | ns | -0.78 | 1.64 |

**b. Erect dome: linear fits of mean eye deviation vs. mean SPV**

| Subject | CCW rotation | | CW rotation | | intercept difference | p < ? | CCW and CW grouped | |
|---|---|---|---|---|---|---|---|---|
| | slope | intercept | slope | intercept | CW - CCW | | slope | intercept |
| M | 0.45 | 2.75 | -2.08 | 3.10 | 0.35 | ns | -1.05 | 0.17 |
| N | -0.39 | -2.71 | -1.06 | 5.05 | 7.76 | ns | 0.30 | -0.40 |
| O | -1.39 | -3.03 | -0.98 | 3.93 | 6.06 | 0.05 | -- | -- |
| P | -1.51 | -4.30 | -1.06 | 3.02 | 7.32 | 0.10 | -- | -- |
| Q | -1.29 | -3.00 | -1.12 | 3.93 | 6.93 | 0.05 | -- | -- |
| R | -0.19 | 0.57 | -0.21 | 1.39 | 0.82 | ns | -0.11 | 1.00 |
| S | -1.35 | -3.07 | -0.88 | 2.53 | 5.60 | 0.05 | -- | -- |

Table 5.15. Least squares linear regression fits to plots of mean eye reset position vs. mean SPV. Separate fits were performed for CCW and CW rotations. When fits were not significantly different at 90% confidence levels, another fit was computed with both directions grouped. [a.] Supine dome. [b.] Erect dome.

confidence intervals (subjects O, Q, and S), while one reached significance only at the 90% level (subject P).

The differences in the y-intercepts erect demonstrated a consistent, direction-dependent shift of the regression line in the corresponding slow phase direction going from the supine to the erect orientation. The resulting discontinuity in the line relating reset position to SPV for the erect case is evident in the plots for subjects N, O, P, Q, and S. For the cases (both erect and supine) where the CCW and CW regression lines showed no significant differences in the y-intercepts at a 90% confidence level, collective linear regressions were performed using the combined results for both directions (Table 5.15).

**a. Subject M: erect dome**



y = -1.05x + 0.17

mean eye reset position (deg) vs. mean SPV (deg/sec)

**b. Subject M: supine dome**



y = -1.20x + 1.23

mean eye reset position (deg) vs. mean SPV (deg/sec)
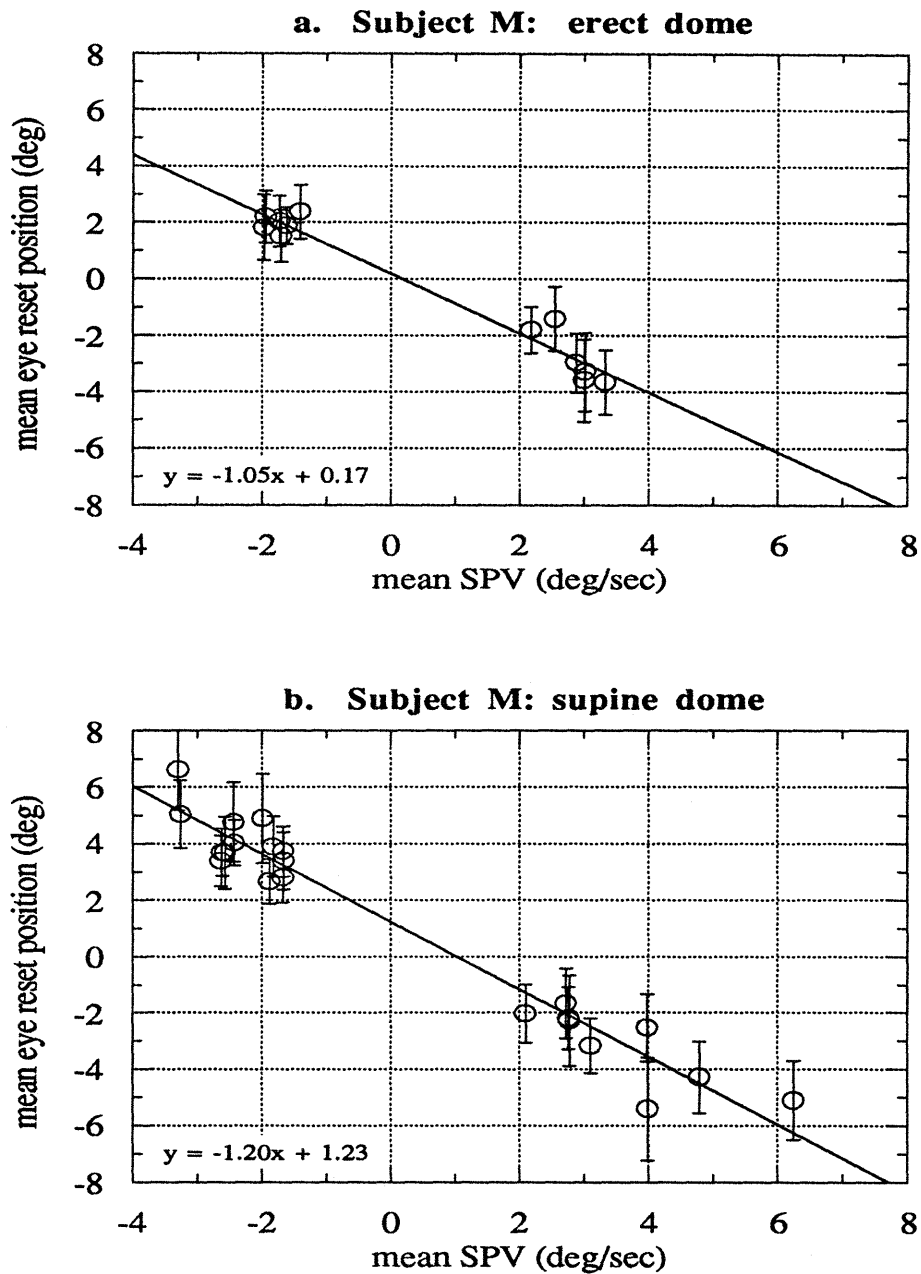
**Figure 5.23.** Subject M: Mean eye reset position vs. mean SPV. [a.] Erect dome. [b.] Supine dome. No significant differences between CCW and CW regression lines were observed for either orientation, so fits are shown for both directions combined.

148

## a. Subject N: erect dome



$y = -1.06x + 5.05$

$y = 0.30x - 0.40$

$y = -0.39x - 2.71$

## b. Subject N: supine dome



$y = 0.08x + 0.07$
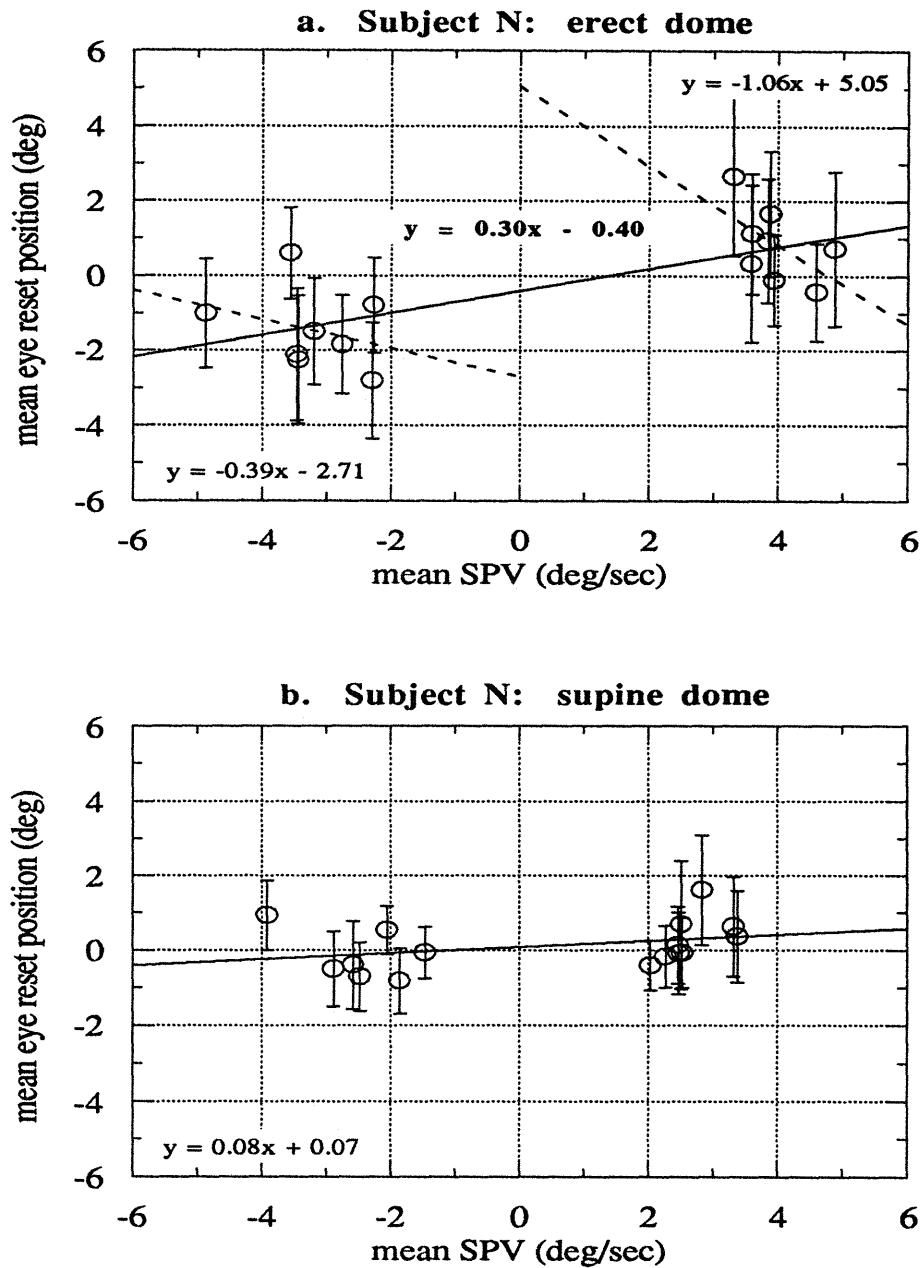
Figure 5.24. Subject N: Mean eye reset position vs. mean SPV. [a.] Erect dome. Dashed lines indicate separate linear fits for CCW and CW dome rotations. [b.] Supine dome. No significant differences between CCW and CW regression lines were observed for either orientation, so fits are shown for both directions combined (solid lines).

149

**a. Subject O: erect dome**

y = -0.98x + 3.93

p < 0.05

y = -1.39x - 3.03

mean eye reset position (deg)

mean SPV (deg/sec)



**b. Subject O: supine dome**

y = -0.16x - 0.13

mean eye reset position (deg)

mean SPV (deg/sec)
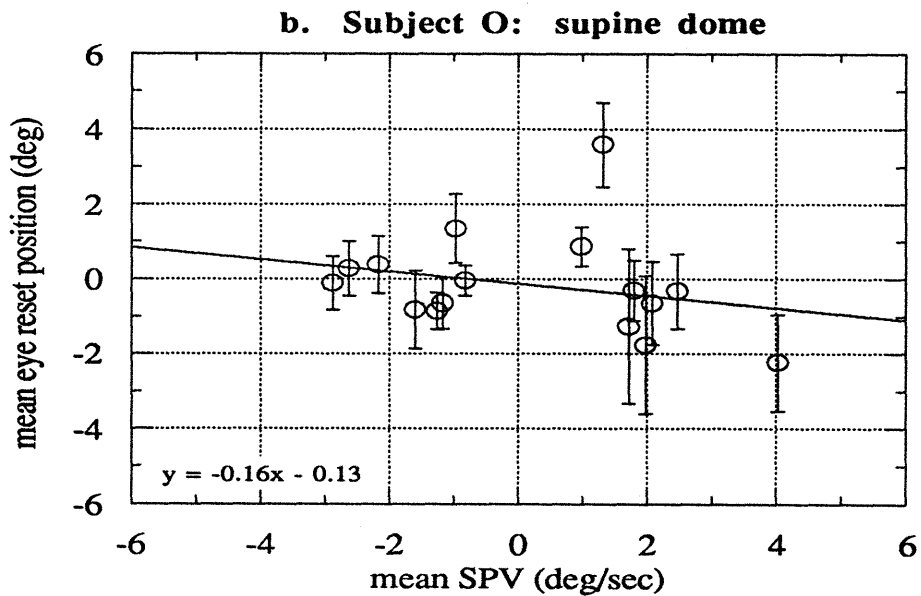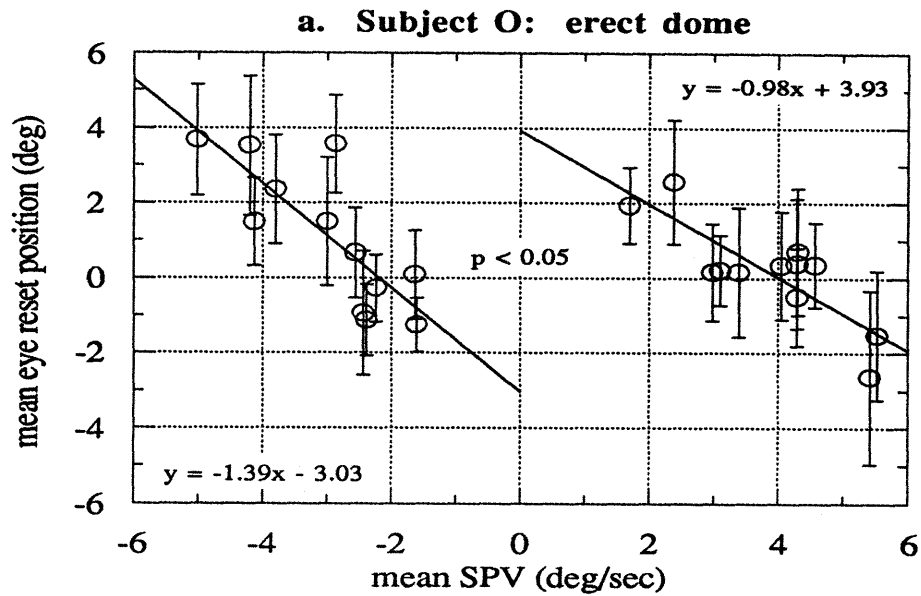
Figure 5.25. Subject O: Mean eye reset position vs. mean SPV. [a.] Erect dome. Y-intercept values for the CCW and CW fits were significantly different (p < 0.05). [b.] Supine dome. No significant differences between CCW and CW regression lines were observed, so a fit is shown for both directions combined.

150

## a. Subject P: erect dome



$y = -1.06x + 3.02$

$y = -1.51x - 4.30$

p < 0.1

## b. Subject P: supine dome



$y = -0.80x + 1.24$
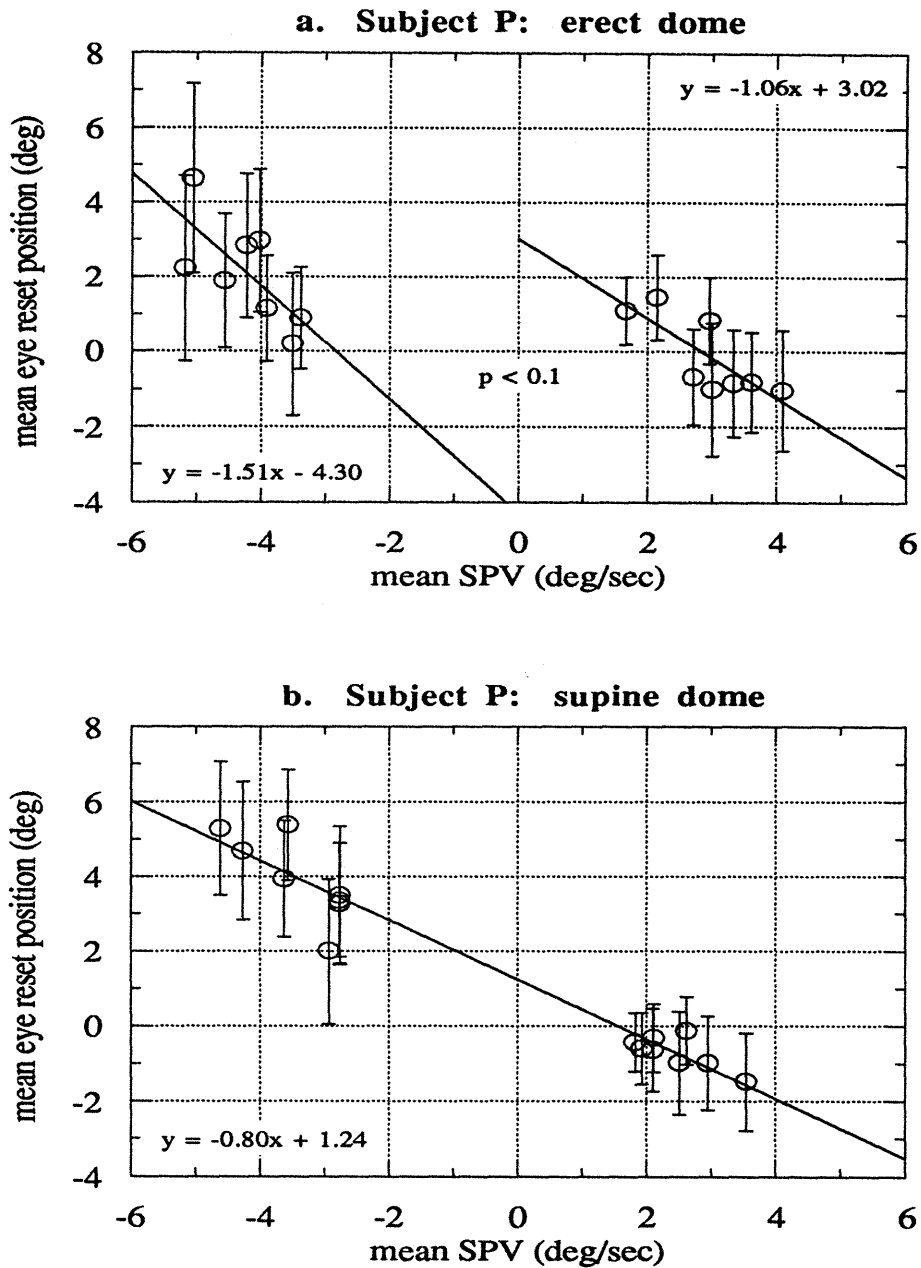
Figure 5.26.  Subject P:  Mean eye reset position vs. mean SPV. [a.]  Erect dome.  Y-intercept values for the CCW and CW fits were significantly different (p < 0.1).  [b.]  Supine dome.  No significant differences between CCW and CW regression lines were observed, so a fit is shown for both directions combined.

## a. Subject Q: erect dome

$y = -1.12x + 3.93$

$p < 0.05$

$y = -1.29x - 3.00$

mean eye reset position (deg)

mean SPV (deg/sec)

## b. Subject Q: supine dome

$y = -1.16x + 1.18$

mean eye reset position (deg)

mean SPV (deg/sec)
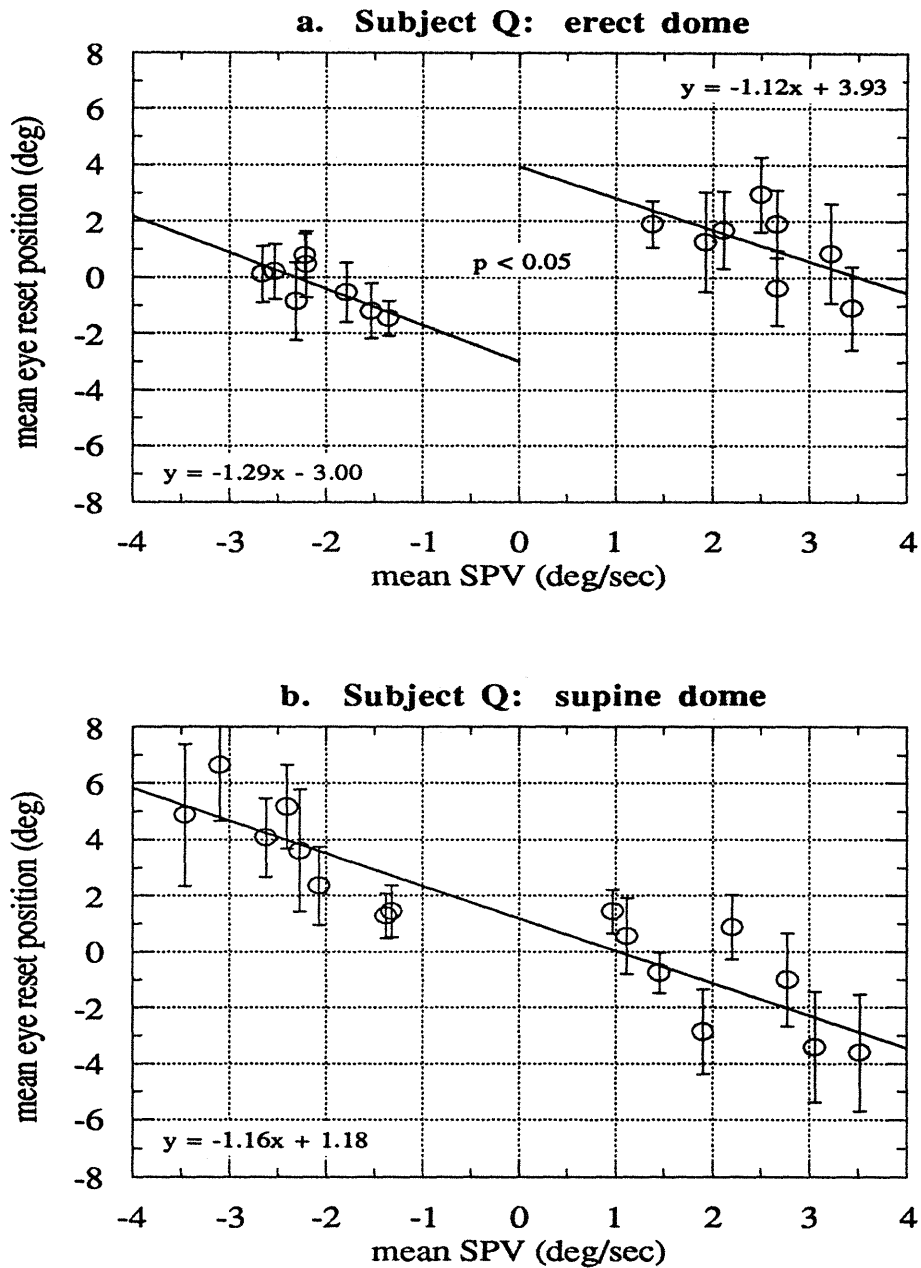
Figure 5.27. Subject Q: Mean eye reset position vs. mean SPV. [a.] Erect dome. Y-intercept values for the CCW and CW fits were significantly different ($p < 0.05$). [b.] Supine dome. No significant differences between CCW and CW regression lines were observed, so a fit is shown for both directions combined.

**Subject R: erect dome**
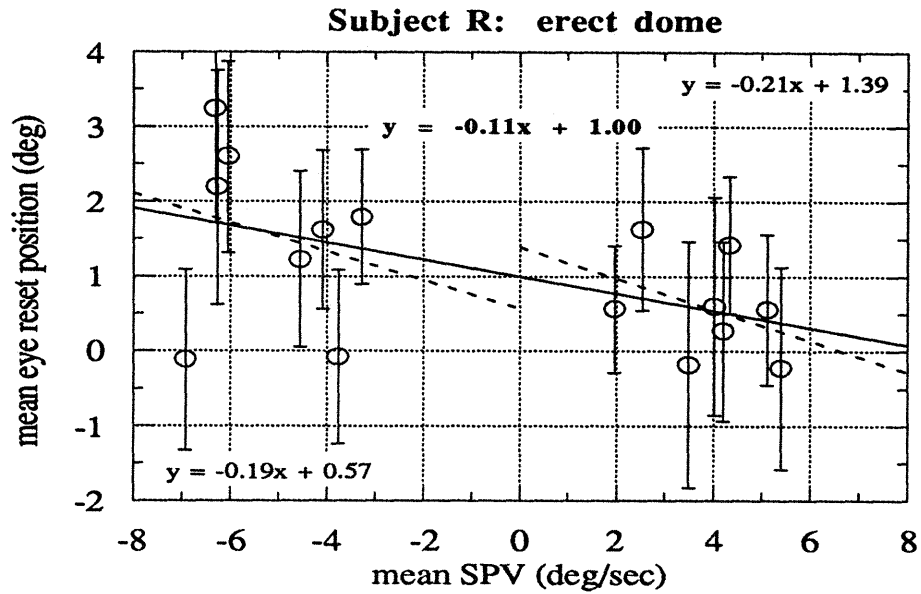
Figure 5.28. Subject R, erect dome: Mean eye reset position vs. mean SPV. Dashed lines indicate separate linear fits for CCW and CW dome rotations. No significant differences between CCW and CW regression lines were observed, so a fit is shown for both directions combined (solid line).

## a. Subject S: erect dome



$y = -0.88x + 2.53$

$p < 0.05$

$y = -1.35x - 3.07$

mean eye reset position (deg)

mean SPV (deg/sec)

## b. Subject S: supine dome



$y = -0.78x + 1.64$

mean eye reset position (deg)

mean SPV (deg/sec)
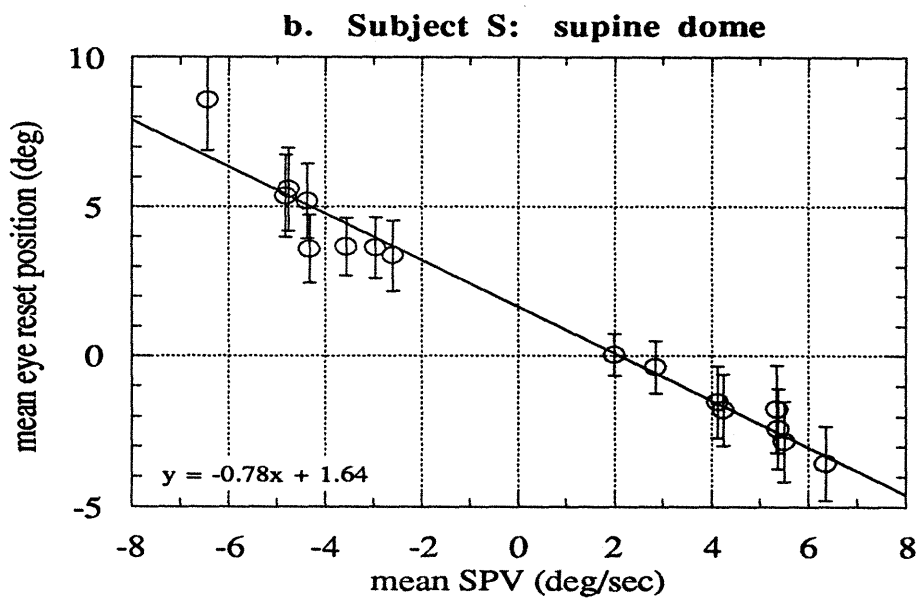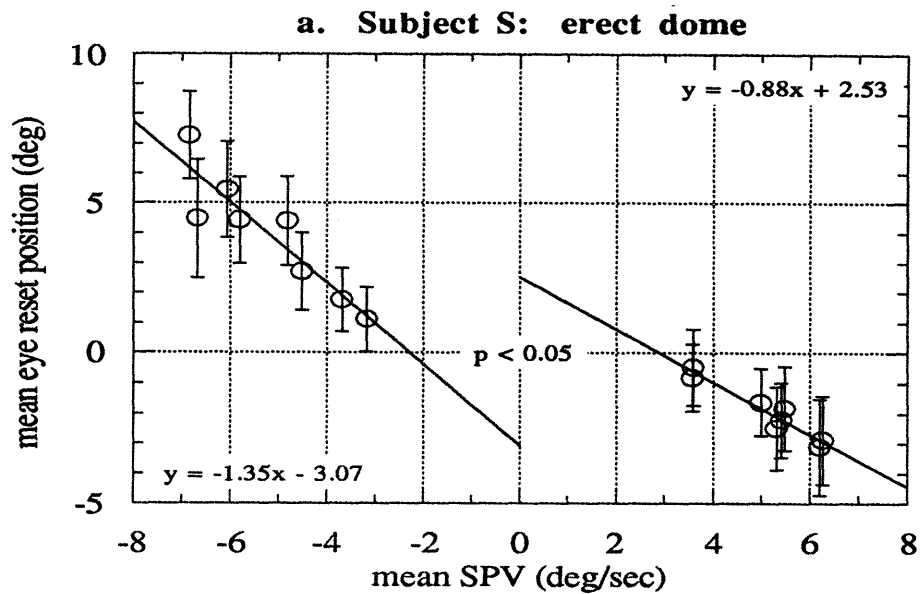
**Figure 5.29. Subject S: Mean eye reset position vs. mean SPV. [a.] Erect dome. Y-intercept values for the CCW and CW fits were significantly different ($p < 0.05$). [b.] Supine dome. No significant differences between CCW and CW regression lines were observed, so a fit is shown for both directions combined.**

154

### 5.5.1. Relationship of eye position at stimulus end to presence of slow SPV decay

Sixty-two of the 218 trials did not exhibit a "slow" decay in eye SPV following the end of visual field rotation. (The total of 62 included 51 trials for which $\tau_l < 0.7$ seconds, as well as the 11 trials for which reasonable exponential fits were not obtained. The latter 11 generally demonstrated an immediate reversal of SPV direction when the dome stopped.) Figure 5.30 shows the mean eye position at the end of dome rotation when the trials were grouped according to the presence or absence of a "slow" SPV decay. Negative eye position indicates deviation in the direction of the fast phase; positive positions correspond to deviations in the slow phase direction.

For all subjects, the trials showing only a sharp deceleration of the eye ($\tau_l < 0.7$) exhibited a greater mean torsional deviation in the slow phase direction (Table 5.16). The difference in mean eye deviation between the two groups proved significant at the 0.1 level or higher for subjects N, P, Q, R and S. The tendency toward deviation in the fast phase direction for trials with slow SPV decays was also significant ($p < 0.001$) when the results for all subjects were grouped.

### 5.5.2. Relationship between Tonic Eye Deviation and Vection State

Attempts at computing cross-correlations between the eye position and vection traces proved ineffective due to problems similar to those encountered with SPV correlations. Peaks in the cross-correlation functions were generally not sharp, and the times associated with the correlation peaks scattered widely in the range from -20 to +20 sec. For these reasons, the occurrence of vection state changes was used to investigate the possible relationship between vection and changes in mean eye position (after Finke and Held, 1978).

Perception of self-motion (roll vection) characterized State 1, while State 2 was defined by the absence of vection, accompanied by a perception of pure dome rotation. State 2 included the period prior to vection onset, as well as segments of vection dropout. For each trial, the mean eye position was calculated for the two states, and the difference in mean

155
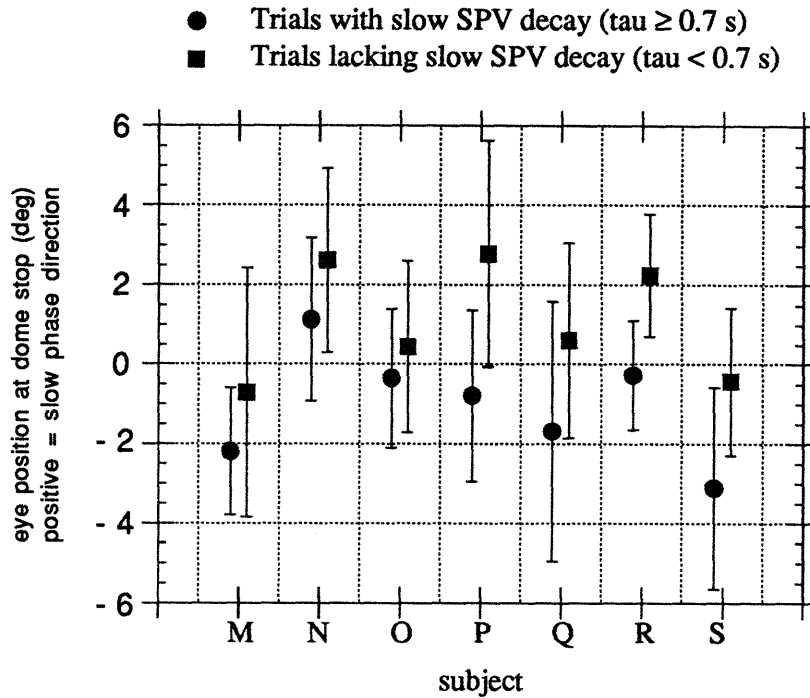
**Figure 5.30.** Mean eye deviation at end of visual field rotation, grouped according to presence or absence of a "slow" SPV decay (time constant longer than 0.7 seconds). Positive values indicate deviation in the slow phase direction.

| Subject | # trials | # trials $\tau_l < 0.7$ s. | slow SPV decay mean | slow SPV decay standard deviation | no slow decay mean | no slow decay standard deviation | mean diff. | p < ? (t test) |
|---------|----------|------------|------|--------------------|------|--------------------|-----------|----------------|
| M | 34 | 3 | -2.19 | 1.60 | -0.70 | 3.13 | -1.49 | ns |
| N | 32 | 16 | 1.14 | 2.05 | 2.62 | 2.30 | -1.49 | 0.10 |
| O | 40 | 19 | -0.35 | 1.75 | 0.46 | 2.17 | -0.80 | ns |
| P | 32 | 2 | -0.79 | 2.16 | 2.79 | 2.85 | -3.58 | 0.05 |
| Q | 32 | 11 | -1.68 | 3.27 | 0.61 | 2.46 | -2.29 | 0.10 |
| R | 16 | 5 | -0.27 | 1.39 | 2.25 | 1.53 | -2.52 | 0.01 |
| S | 32 | 6 | -3.11 | 2.54 | -0.42 | 1.87 | -2.69 | 0.05 |
| All subjects | 218 | 62 | -1.28 | 2.51 | 1.12 | 2.44 | -2.40 | 0.001 |

**Table 5.16.** Mean position of eye at time of dome stop, grouped by presence or absence of slow decay ($\tau \geq 0.7$ s) of OKAN SPV. Group lacking slow SPV decay includes trials for which no reasonable fit to SPV was obtained. Probability (p) denotes likelihood that two groups have same mean position at dome stop (p < 0.1 indicates significant difference).

156

position between State 1 and State 2 was computed. The difference was normalized by the peak-to-peak position range reached during OKN within each trial, because the magnitude of eye deviation depended on the SPV and by extension on dome speed.

Figure 5.31 displays the means of the normalized position differences (State 1 - State 2) for each subject. Negative values indicate greater average deviation in the OKN fast phase direction during episodes of vection (State 1). Six of the seven subjects exhibited a bias in mean eye position toward the direction of the fast phase during vection; in four of these six the difference between State 1 and State 2 proved significant at the 0.01 level or better ($p < 0.01$ for O and P; $p < 0.001$ for M and S). The difference was not significant for the one subject (N) who displayed greater deviation in the fast phase direction during State 2.
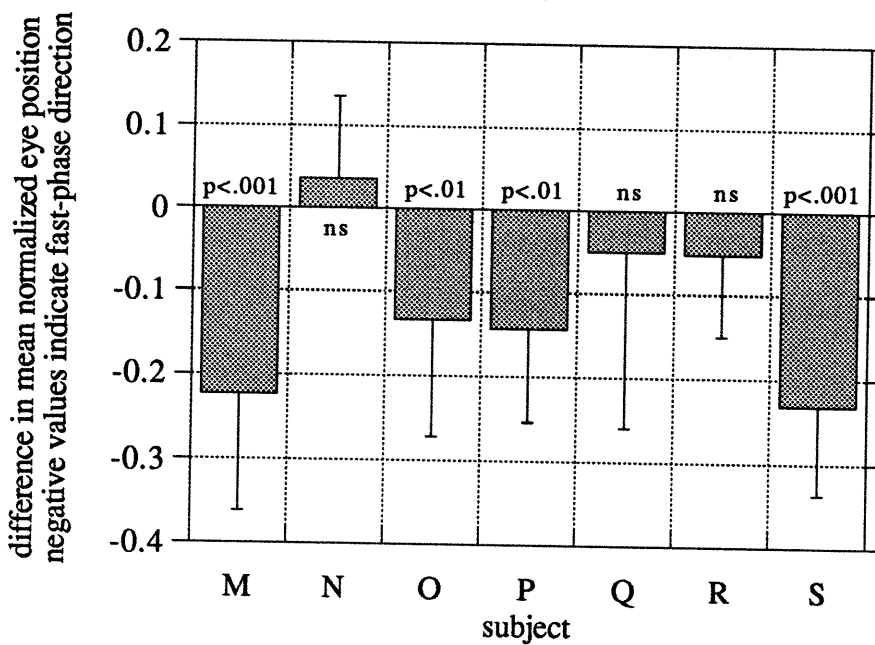


**Figure 5.31. Difference in mean normalized eye position between vection (State 1) and no vection (State 2) conditions. Negative values indicate greater deviation in the fast phase direction during vection.**

## 5.6. Discussion of Mean Eye Position during Torsional OKN

During vestibular nystagmus, the amplitude and velocity of the slow phases increase with increasing gaze eccentricity in the direction of the fast phase. Likewise, gaze in the slow phase direction results in decreased amplitude and velocity. This phenomenon, first described by Alexander in 1912, has become known as Alexander's Law (Doslak et. al., 1979). In addition, Young found that the following velocity of OKN could be increased by diverting gaze in the direction of the fast phase (in Henn et. al., 1980).

The nonlinear elastic properties of the oculomotor musculature and globe supporting tissues provide one possible explanation for these empirical observations. The elastic nature of the oculomotor plant may cause the eye to "spring" back at a higher velocity when a fast phase resets the eye away from the central rest position. Many torsional slow phases are concave in shape, with the highest velocity immediately following the fast phase and a gradual decline in velocity thereafter (Figure 5.1). This observation, combined with the torsional "leash" effect noted in forced cycloduction experiments (Simonsz et. al., 1984), provides some support for the hypothesized mechanical origin of Alexander's Law.

### 5.6.1. Relationship of Tonic Eye Deviation to SPV

While oculomotor plant mechanics may impose a gaze dependence on smooth eye velocity, such an effect seems unlikely to account for the results described in this thesis. Mean eye reset position varied approximately linearly with mean SPV. The direct dependence of mean torsional SPV on stimulus velocity implies that increased mean eye position deviations in the direction of the fast phase resulted from increased SPV, rather than the reverse.

For horizontal eye movements, it appears that mean eye position tends toward the direction of the fast phase of both vestibular and optokinetic nystagmus in a diverse array of species including pikes, rabbits, monkeys, and humans (reviewed by Yasui, 1974). Yasui found that the magnitude of the deviation in the fast phase direction increased linearly with

increasing SPV. During horizontal OKN, he observed that the mean eye reset position deviated between 0.5° and 0.75° in the fast phase direction for every degree per second of SPV.

A likely functional basis for the shift of eye position opposite the slow phase direction involves the acquisition of new visual information. The compensatory eye movement reflexes exist primary to stabilize visual images on the retina during head movements. During horizontal or vertical head rotations, it would be advantageous to acquire the incoming visual scene as quickly as possible, rather than tracking the part of the image leaving the field of view. Clearly, such an argument becomes irrelevant for torsional rotations about the visual axis. Nevertheless, considerable evidence demonstrates that the visual and vestibular systems rely on a coupled three dimensional internal representation. Since eye torsion exists as part of a three dimensional oculomotor mechanism rather than a separate entity, the tonic torsional deviation during OKN probably results from the carryover of a process with important implications in the other two axes.

Yasui (1974) proposed a model of nystagmus fast phase generation which produced the appropriate deviation in mean eye position. In this model (Figure 5.32), fast phases are generated on the basis of slow phase efferent information which leads the actual slow phase eye movements slightly in time. This slow phase efference copy originates either in visual or vestibular centers. Fast phases arise from an internal model which "simulates" nystagmus based on efferent motor information. The internally simulated model resets itself to zero with each fast phase. However, the transmission time delay to the eye causes a lag in the execution of the actual slow phase, and the fast phase generation effectively relies on "future" eye position. Thus, the true eye reset position deviates from the center toward the fast phase direction. The magnitude of the deviation is proportional to the slow phase velocity, with constant of proportionality equal to the proposed slow phase time lag.
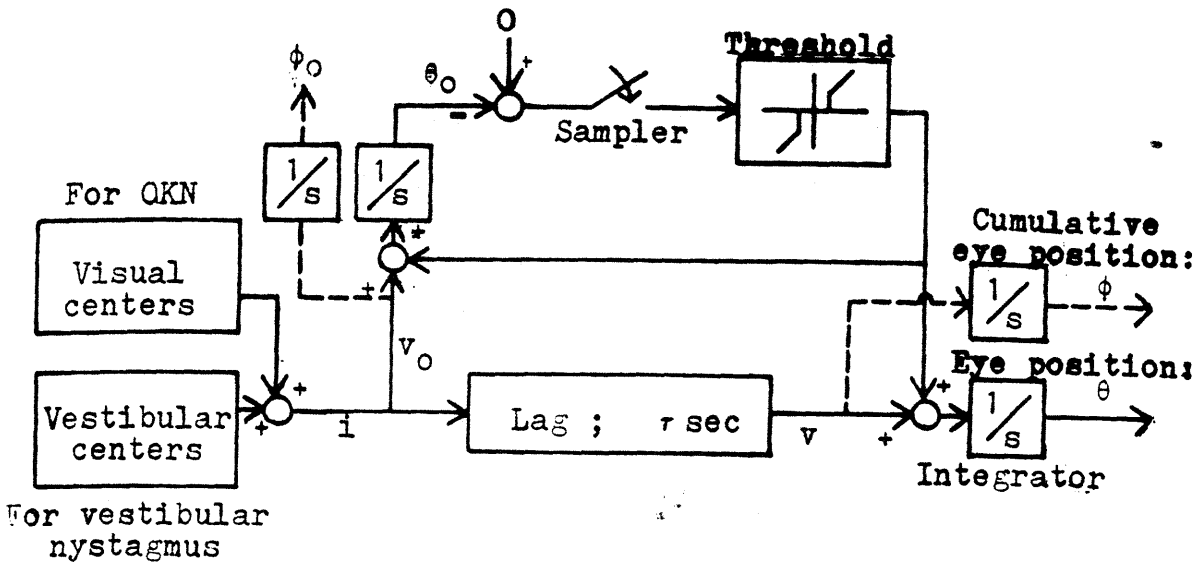
**Figure 5.32.** Model of fast phase generation which produces mean deviation in the direction of the fast phase (Yasui, 1974)

## 5.6.2. Consequences for Interpretation of Subjective Eye Torsion Measures

A number of experiments which incorporated a subjective afterimage method to measure ocular torsion during roll OKN found a consistent deviation of mean eye position in the slow phase direction for both erect and supine conditions (Finke and Held, 1978; Wolfe and Held, 1979; Merker and Held, 1980). These results are contrary to the average shift in the fast phase direction observed in most cases in the present experiment. The scleral coil measurements appear not only to invalidate the afterimage technique as a measure of eye torsion, but also to call into question the conclusions drawn by these authors regarding the relationship between perception and eye movements.

### 5.6.3. Effect of Subject Orientation on Tonic Eye Deviation

For the supine orientation, the line relating the eye reset position to SPV generally passed through the origin. In contrast, the entire line shifted in the slow phase direction for the erect runs. A possible explanation for this shift rests on the phenomenon of visually induced tilt. Based on the perceived shift of the vertical during visual roll stimulation, Dichgans et. al. (1972) hypothesized a central recalculation of the gravity vector based on visual information. Since otolith-mediated static ocular counterrolling with a gain near 0.1 occurs in response to real tilts with respect to gravity, a shift in the central representation of the gravity vector might induce counterrolling as well.

The perceived tilt during roll vection occurs in the direction opposite field rotation, so the projected counterroll would occur in the direction of field motion--the slow phase direction of OKN. Counterroll due to perceived tilt might then sum with the deviation in the fast phase direction, resulting in the shift toward the slow phase direction erect. The proposed tilt-counterroll mechanism would be rendered inactive in the supine position because the gravity vector coincides with the axis of field rotation.

Figure 5.33 depicts a block diagram formulation of the processes affecting the deviation of mean eye position during torsional OKN. In the supine position, switch S is open, and the nystagmus beating field shifts in the fast phase direction according to the Yasui's model. In the erect position, switch S closes, and visually induced tilt produces a static ocular counterroll of approximately one-tenth the perceived tilt. This counterroll--in the slow phase direction--adds to the original shift in the fast phase direction. Since the visually induced tilt curve (Dichgans et. al., 1972) is relatively flat over the range of stimulus velocities tested in this experiment, the
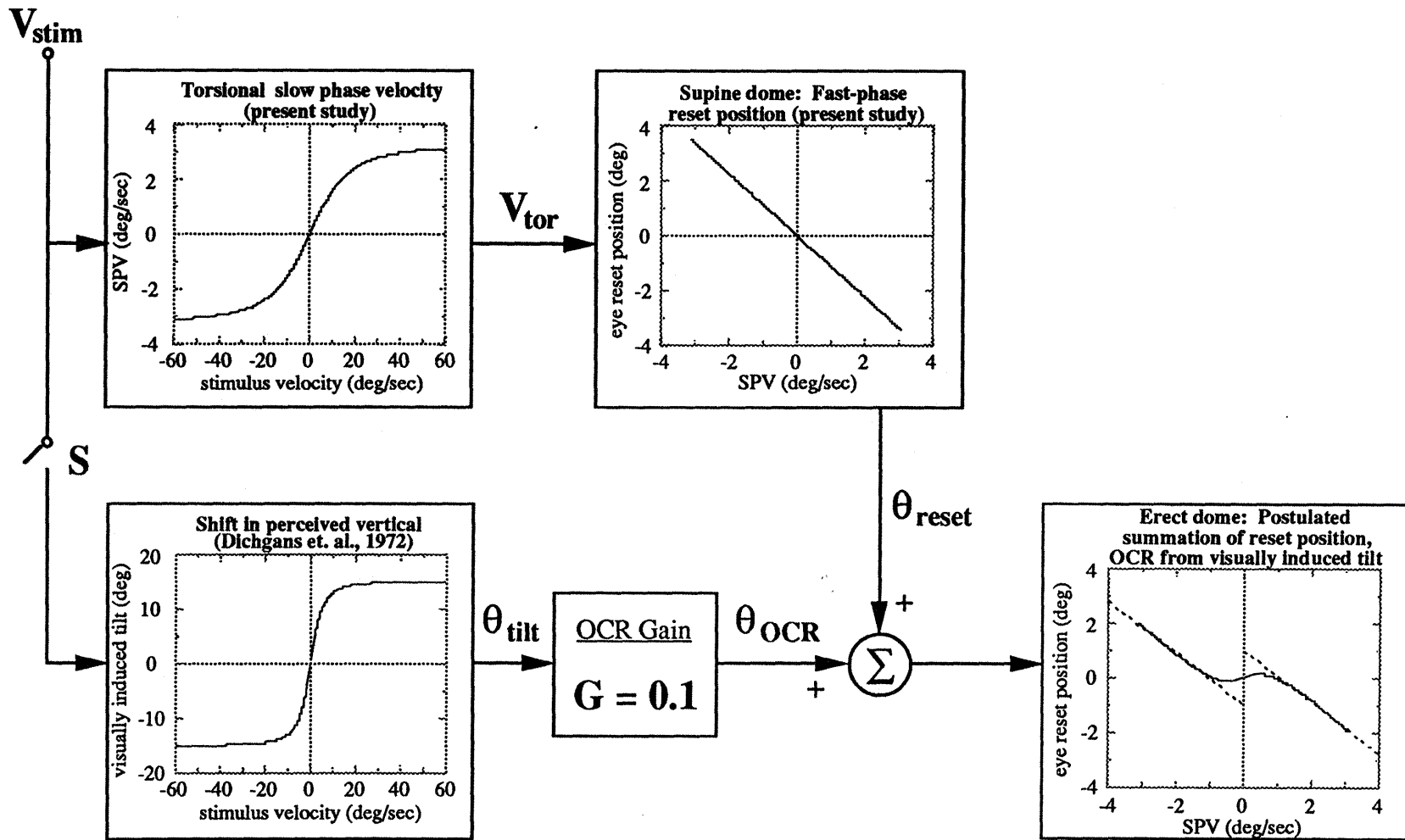
Figure 5.33. Block diagram describing proposed shift of mean eye deviation erect based on static ocular counterrolling resulting from a central recomputation of the gravity vector. In supine position, switch S is open. Stimulus velocity generates SPV, which in turn yields linear relation between mean deviation and SPV. In erect position, switch S closes. Visually induced tilt results from a central recalculation of the gravity vector; the shift in the perceived gravity reference causes static ocular counterrolling with an approximate gain of 0.1. The OCR effect adds to the prior mean eye deviation, resulting in the observed shift of the deviation line in the slow phase direction. •

combined eye deviation presents as an apparent shift of the entire deviation line in the direction of the slow phase.

Using an ocular counterrolling gain of 0.1 and a maximum visually induced tilt of 15° results in a shift of the line describing the SPV-deviation relation by only 1.5°. In contrast, changes in the intercept of up to 4° were observed when the present subjects reoriented from supine to erect. While the model as presented predicts smaller shifts, some investigators have found visually induced tilts in the range from 30°-60° (Young et. al., 1975; Howard and Cheung, 1988). Furthermore, Ferman et. al. (1987) recorded mean static ocular counterrolling gains as high as 0.23. Incorporating these higher parameter values would result in predicted shifts near the observed changes.

Interestingly, Clément and Lathan (1991) observed changes in the mean "center of interest" of pitch OKN when subjects went from erect to a 90° roll position. The authors defined the center of interest (CI) as the midpoint of the fast phase. In the erect position, they observed a mean CI of 12° down for upward stimuli, but only 0° - 3° up for downward field motion. In the 90° roll position, the mean CI for upward slow phases was reduced to 6° down, while the value jumped to 10° up for downward slow phases.

While these observations show that mean eye position shifts in the fast phase direction in all three axes, explaining the vertical OKN results in a manner similar to the torsional case requires an asymmetry between forward and backward visually induced pitch between. The greatly reduced deviation in the fast phase direction for downward slow phases erect suggests that backward visually induced tilt should be strong. Likewise, the absence of an increase in fast phase direction bias going from erect to supine for upward slow phases argues for relatively weak forward pitch.

Young et. al. (1975) found the opposite asymmetry in visually induced pitch: forward tilt proved stronger than backward tilt. However, Howard and Cheung (1988) did observe larger tilts backward than forward; the latter results are essential to the above interpretation. The fact that the deviation in the fast phase direction for upward stimuli actually declined in the

90° roll condition might be explained by the significantly lower OKN gains recorded in this orientation.

### 5.6.4. Possible Confounding of Tonic Eye Deviation with Head Rotation

The dental biteboards employed in this experiment were intended to keep the subjects' heads fixed in space, thereby preventing head movements which would be recorded as eye torsion. However, it is conceivable that small head tilts may have occurred if the subjects did not bite down firmly on the biteboard at all times. Since true head position was not recorded during the tests, no conclusive statements can be made about the actual degree of head stationarity during the experimental trials.

Pseudo-vestibulocollic righting reflexes would tend to produce head tilts in the same direction as field rotation. Thus, head movements cannot account for the observed deviation of the mean eye position in the fast phase direction (opposite dome rotation). However, the shifts in the lines relating deviation to SPV (seen for the erect runs) are in the correct direction to be explained by small, visually induced head tilts.

In an attempt to resolve this concern, the biteboard torque traces were examined in lieu of actual head position records. However, the biteboard output does not provide a satisfactory alternative for two reasons. First, the biteboard and holder are quite stiff, so even high torques should result in very small head movements if the subjects bites down properly. Also, the biteboard circuitry acts as a high-pass filter, so the biteboard signals provide at best a coarse approximation to higher frequency head rolls.

Unfortunately, this cursory investigation proved inconclusive. The biteboard torque did not appear to correlate well with eye position in the majority of cases, but a few trials showed a fairly close correspondence between the two signals (Figure 5.34). While the generally low correlation between neck torque and eye position argued against head tilt as an explanation for the mean eye deviations observed here, such an effect could not be ruled out completely.

**a. Eye position exhibits little correlation with biteboard torque**



**b. Apparent correlation between eye position and biteboard torque**
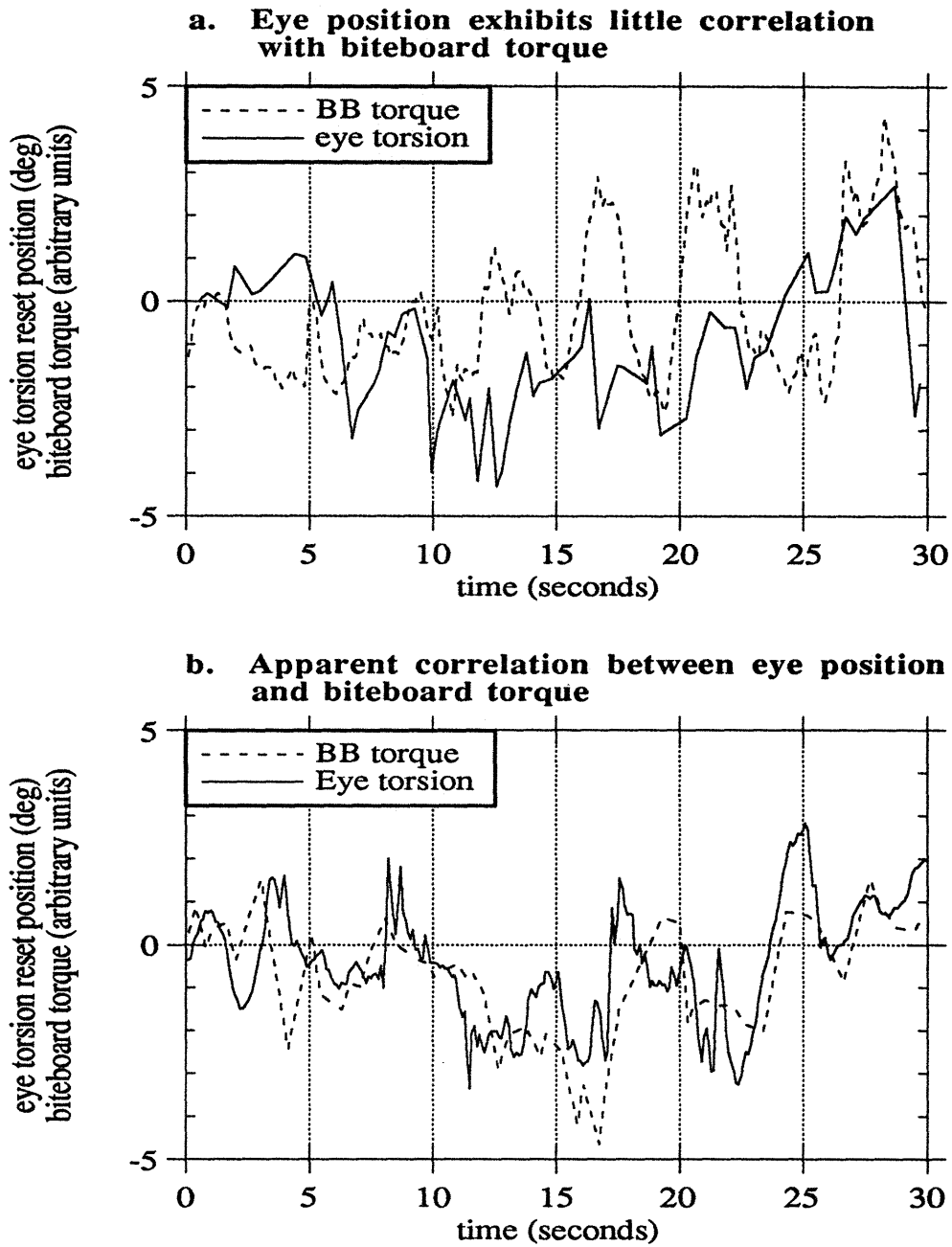


Figure 5.34. Eye reset position plotted together with biteboard torque (Subject P). [a.] Eye position exhibits little correlation with biteboard torque. [b.]. Apparent correlation between eye position and biteboard torque.

165

### 5.6.5. Mean Eye Position, Vection State, and Velocity Storage

Comparison of mean torsional eye position in periods with and without vection revealed that the eye deviated further in the fast phase direction during vection than during perception of pure surround motion. These results are consistent with the conclusion of Finke and Held (1978) that greater torsion in the direction of the slow phase occurred when subjects perceived no self-rotation.

Brandt et. al. (1974) observed a related phenomenon in extended duration horizontal OKN studies. When subjects were exposed to optokinetic yaw stimuli for several minutes, they experienced vection dropouts and even reversals in the direction of perceived self-rotation. These episodes occurred simultaneously with shifts of the nystagmus beating field (or *Schlagfeld*) from the direction of the fast phase toward the slow phase direction.

The apparent dependence of mean eye position on vection state during OKN may be traced back to the postulated evolutionary advantage of the normal shift in the *Schlagfeld* associated with optokinetic and vestibular nystagmus. During head movements, the organism presumably needs to see the oncoming visual scene as quickly as possible. Thus, during perceived self-motion--resulting either from head motion or vection--mean eye position should be biased toward the fast phase direction. If, on the other hand, the subject perceives surround motion, it may be more advantageous to track the moving images in the central visual field and even to the limits of the slow phase direction. On this basis, the mean eye position during OKN should not tend toward the fast phase direction in the absence of perceived self motion.

The contention that mean eye position during OKN depends on an internal reconstruction of self motion is supported by the OKAN data collected in the present experiment. When a slow decay in SPV occurred during OKAN, the eye position just prior to stimulus offset was shown to lie further in the fast phase direction than for cases when the SPV dropped rapidly to zero. This effect occurred uniformly across all subjects, and implied a

connection between the activation of velocity storage (responsible for OKAN) and the mean eye position during OKN.

Velocity storage is in essence a central reconstruction of head velocity based on integration of visual and vestibular inputs. Thus, the proposed dependence of mean eye position on the activation of velocity storage advances the notion that the shift of the *Schlagfeld* toward the fast phase direction of nystagmus evolved to assist the acquisition of new visual information during self motion. The observed correspondence between mean eye position and vection state indicates that both OKN and vection rely on some of the same basic mechanisms.

Nevertheless, these and prior experiments have demonstrated conclusively that important dissociations exist between compensatory eye movements and self-motion perception under many circumstances. Brandt et. al. (1973) demonstrated that stimuli moving in opposite directions could generate contrary OKN and vection responses. Likewise, the poor correspondence between vection and either eye position or SPV, shown by the failed attempts at cross-correlation in the present experiments, argues against a strong link between roll vection and torsional OKN.

# 6. CONCLUSIONS

A fairly large body of knowledge has been accumulated which describes the eye movements and psychophysical effects associated with visual field rotations about the yaw and pitch axes. Further experiments have yielded insight into the perceptual phenomena known as roll vection and visually induced tilt. Until now, however, virtually no studies have been undertaken to fully characterize the torsional eye movements associated with fields rotating about the visual axis. The experiments described in this thesis were made possible by the magnetic scleral search coil system at the MIT Man-Vehicle Laboratory, and provide a first step toward filling this gap in the biomedical literature.

The present study had three central aims: (1) Characterization of the slow phase velocity and tonic eye deviation properties during torsional OKN; (2) Investigation into the existence of torsional OKAN; and (3) Clarification of the possible relationship between torsional eye movements and roll vection. To meet these goals, 7 subjects were tested using a rotating dome which presented a full-field pattern rolling about the visual axis. Torsional eye movements and subjective vection were recorded in erect and supine orientations at four stimulus speeds for CCW and CW dome rotations. Eye movement aftereffects following torsional OKN were also measured under three visual field conditions: in the light with a stationary visual field, in the dark with a central fixation point, and in complete darkness.

The slow phase eye velocity gain during torsional OKN was defined as the mean SPV divided by the stimulus rate. Overall, the gain of torsional OKN was quite low compared to horizontal and vertical gains. Furthermore, torsional SPV gain dropped sharply with increasing stimulus velocity. Over the range tested, SPV gain averaged only 0.15 at a stimulus velocity of 15°/sec, and fell to 0.06 at 60°/sec. Interestingly, higher SPV gains were measured erect than supine for most subjects. Based on otolithic suppression of torsional OKN in the monkey, increased gains were expected supine; only one of the subjects exhibited this

predicted pattern. (Habituation to the optokinetic stimulus may have contributed to the depressed SPV gains observed supine in the majority of subjects.)

In most subjects, the mean eye position during OKN deviated in the direction of the fast phase. This finding is consistent with similar observations for horizontal and vertical optokinetic and vestibular nystagmus in a range of species. However, previous experiments using an unvalidated afterimage technique to measure ocular torsion reported uniform deviations in the slow phase direction. The present results, obtained using more advanced technology, may raise questions regarding the validity of the prior conclusions.

The magnitude of the torsional deviation in the fast phase direction increased with increasing SPV. In the supine position, the relationship between position bias and SPV was approximated by a single line through the origin. For the erect case, the slopes of the lines describing the deviation-SPV relationship remained the same--the deviation of the reset position in the direction of the fast phase still increased with increasing SPV. However, the entire lines were translated, moving the y-intercepts in the direction of the slow phase. A model was proposed which accounted for this effect using the phenomenon of visually induced tilt. Static ocular counterrolling resulting from an internal recomputation of the gravity vector during visual roll stimuli would produce eye torsion with the proper direction and magnitude to explain the observed results.

The presence of torsional OKAN was demonstrated following the cessation of optokinetic stimulation, although afternystagmus was quite variable and differed in quality from subject to subject. The time constant describing the decay of slow phase velocity during OKAN was quite short, averaging approximately 2.4 seconds. The short OKAN discharge time constant, combined with the low gain and variability of torsional OKN, indicates that velocity storage plays a relatively minor role about the roll axis. This contrasts with results obtained in the monkey, which probably relies almost completely on the velocity storage pathway in the generation of roll OKN.

169

Torsional OKAN was suppressed by both gravitational and visual cues. Time constants of SPV decay were somewhat shorter erect than supine. This observation is consistent with the strong conditioning effect of otolith inputs on velocity storage about off-vertical axes. Time constants were also shorter under stationary visual field conditions and even in the presence of a round 0.5° fixation point. Similar "dumping" of velocity storage has been reported for horizontal and vertical OKAN under conditions of fixation suppression.

Cross-correlations of roll vection with torsional eye position and SPV found no close relationship between the time course of OKN and vection. Comparisons of asymmetries in SPV gain with vection asymmetries also failed to establish a link between vection and SPV, as did evaluations of SPV gain during periods with and without vection. Overall, these results indicate that important dissociations exist between compensatory eye movements and perceptual processes. OKN does not cause vection, while vection does not produce OKN.

However, significantly greater deviation of the eye in the direction of the fast phase of OKN was observed during episodes of vection. This relationship of mean eye position to vection state supports the hypothesis that the deviation of the eye in the fast phase direction during OKN enables quick acquisition of the oncoming visual field during actual head rotations. A further correspondence was found between velocity storage activation and deviation in mean eye position. Together, these results indicate that both OKN and vection rely to a certain extent on a centrally stored reconstruction of head velocity. Although compensatory eye movements and self-motion perception appear to be mediated through largely distinct processes, some of the same low-level mechanisms probably subserve both phenomena.

## 6.1. Recommendations for further study

The scleral coil system makes possible a range of experiments on ocular torsion, while the tests described here suggest several avenues for future study. One goal might encompass a better description of the dynamic properties of torsional OKN. Only velocity step inputs were

tested in this work; sinusoidal stimuli could provide a measure of the frequency response of the torsional OKN system. Since voluntary ocular torsion has been demonstrated, it might be interesting to try to improve OKN gain through extended training.

The dependence of torsional OKN on various properties of the visual stimulus should be evaluated. Variables such as spatial frequency, contrast density, and stimulus area could be studied. Another important question regards the portion of the visual field best suited to producing torsional OKN. The central visual field has been shown to dominate horizontal and vertical OKN. However, linear retinal slip velocity increases in proportion to eccentricity for roll stimuli, so the periphery may be considerably more important in torsion. Along these lines, a setup presenting oppositely rotating stimuli in the central and peripheral fields could be adapted for torsion. It may be possible to induce opposing optokinetic and vection responses in roll as well as in yaw.

Cortical binocular processes are important in generating horizontal and vertical OKN in frontal eyed animals. The effects of binocular disparity, monocular viewing, or oppositely directed displays to each eye could be tested. Some studies have shown that asymmetries in ocular torsion between the two eyes may predict susceptibility to space motion sickness (Diamond and Markham, 1990). Pending the development of an appropriate calibration scheme, torsional disconjugacies could be investigated.

The intriguing conjecture that static ocular counterrolling may be caused solely by a visually induced recomputation of the gravity vector must be further examined. At least one subject should be retested using an additional coil taped to the forehead in order to eliminate the possibility that head movements contributed to the effects reported here. As an extension, the possible relationship between visually induced tilt and ocular torsion could be tested by having subjects indicate the perceived vertical rather than vection magnitude.

171

# APPENDIX A: ROTATING DOME CIRCUITRY

This section contains the circuit diagram for the motor controller used to drive the rotating dome. The circuit consisted of a times-three gain stage followed by a power booster. A switch controlled the direction of dome rotation. The MacAdios D/A board provided the input signal, while the output drove the DC dome motor.
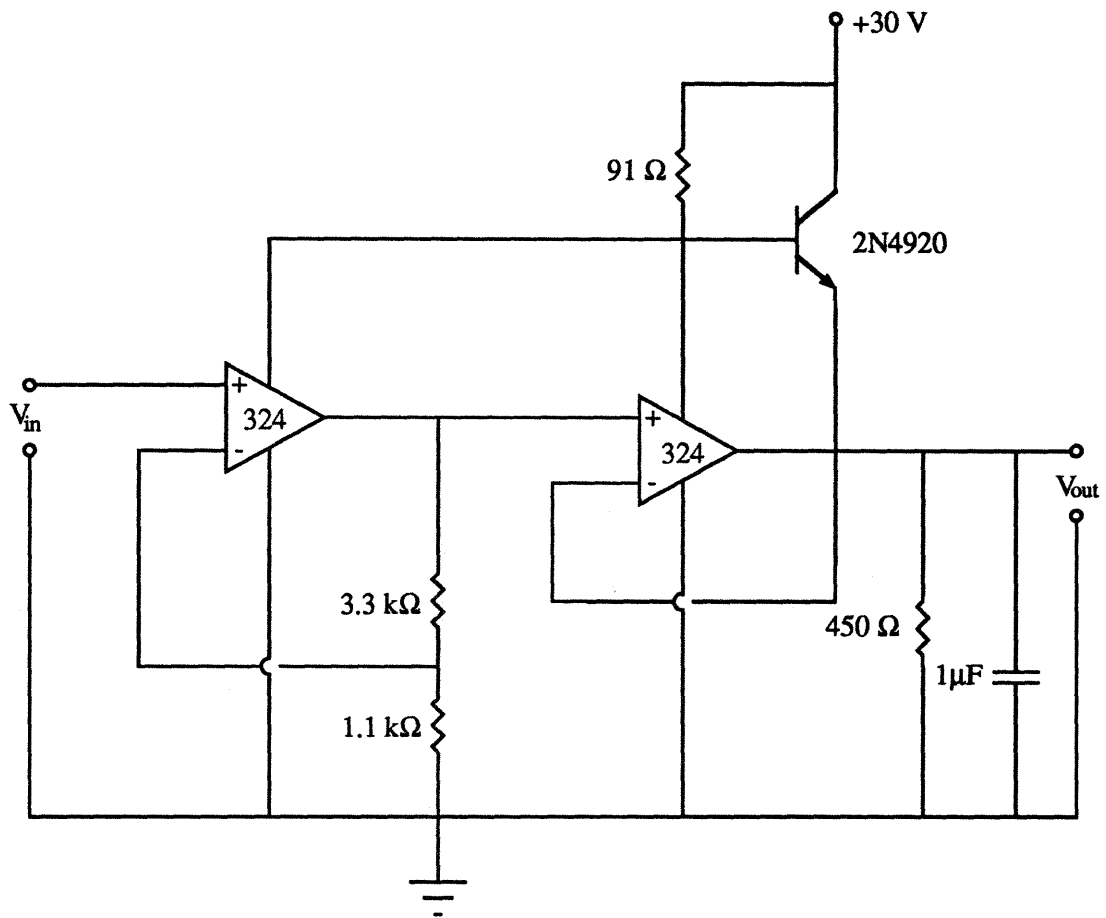
Figure A.1. Dome motor drive circuitry. Vin is output by the computer D/A board. Vout leads to a double pole-double throw switch which controls the rotation direction. The switched output voltage powers the drive motor.

# APPENDIX B: EXPERIMENTAL PROTOCOL

The protocol for an experimental rotating dome session is contained here. This protocol details subject preparation, coil system setup and calibration, scleral coil insertion, and the test procedure.

# ROTATING DOME/ SCLERAL SEARCH COIL PROTOCOL

## I. Rotating Dome Setup

A. Have subject sign informed consent statement
B. Biteboard
   1. Make subject biteboard from flight reject blank, 2 part dental compound
   2. Insert biteboard in holder
C. Dome Height: adjust dome height to center of coil
D. Subject Height
   1. Erect: using iron plates, step, etc., raise subject such that eye is level with calibration washer
   2. Supine: adjust height of coils relative to chair seat
E. Power
   1. Motor (power supply on, highest voltage--28 V, switch on amp to center position)
   2. Lights
   3. Biteboard/Joystick 15 V. brick power supply
   4. Computer, LaCie drive
   5. Stripchart recorder
F. Stripchart connections
   1. Coil torsion channel
   2. Coil horizontal channel
   3. Coil vertical channel
   4. Joystick
G. Signal Check (use LabView 'cread/cwrite demo', stripchart)
   1. Motor (both directions)
   2. Joystick
   3. Biteboard
      a. Zero biteboard no-torque signal
   4. Optical encoder

## II. Magnetic Coil System Setup

A. Interface connectors
   1. BNCs to horizontal/vertical and torsion boxes
   2. Female leads
      a. Tape wires down to prevent loops, crossing, movement
      b. Put leads under velcro
B. Insert calibration device
C. Torsion coil
   1. Check resistance between torsion leads, horizontal/vertical leads--should be ~27 ohms
   2. Plug in leads
      a. "T" leads to blue female; others to white female
      b. Replace velcro
   3. Tape coil to calibration device
D. Electronics warmup
   1. Turn coil system on
   2. Wait 1/2 hour
E. Calibration
   1. Adjust calibration device to zero (vertical, torsion)

2. Zero torsion channel
   a. Check torsion signal to Macintosh
   b. On 5V scale, use offset knob to zero
   c. If cannot zero, flip polarity switch, then try again
3. Adjust torsion gain
   a. Use 50V scale
   b. Turn calibration device ±10 deg, adjust gain for $2V = 10°$
4. Repeat (2, 3) for vertical channel
F. Sterilization
   1. Remove coil from calibration device
   2. Immerse coil completely in hydrogen peroxide
   3. Remove calibration device
   4. Allow coil to sit for 10 to 30 minutes
G. Reboot Macintosh, run LabView 'Keoki thesis'

## III. Scleral Coil Insertion

A. Wash hands
B. Rinse coil
   1. Remove from hydrogen peroxide
   2. Rinse coil, wire, fingers with saline from large bottle
   3. Place in saline solution
C. Anesthetize right eye
   1. Place one drop "Ophthetic" anaesthetic on eye
   2. Wait 1-2 minutes, insert a second drop
   3. Dab closed eye with tissue to dry
   4. Administer additional anesthetic as needed during experiment runs
D. Rinse coil
   1. Use saline solution from disposable sterile bottles
   2. Rinse coil, wire, fingers (hold coil in hand)
E. Insert coil
   1. Use fingers to hold lids open
   2. Place coil on eye
   3. Turn coil so that lead comes out horizontally
   4. Have subject close eye; press on lid to remove air bubbles trapped by coil
F. Start stopwatch (for checking against 1/2 hour limit on coil in eye)
G. Secure leads--tape to forehead, cheek, frame
H. Zero channels with subject on biteboard, looking at fixation point (do not adjust gain settings)

## IV. Dome Run (repeat steps for second run)

A. Turn off room lights
B. For post-rotation lights-out/LED run, plug in fixation LED battery
C. Dim computer screen
D. Select dome run subject code, run number
E. Give joystick to subject
F. Start stripchart (5 mm/s)
F. Run LabView 'Keoki Thesis'
G. Dome trial (repeat these steps for 8 trials total--2 directions, 4 speeds)
   1. Move dome light switch to 'on' position
   2. Select dome rotation direction (CW/CCW) with switch on amplifier box
   3. Instruct subject to fixate on center LED (about 5-10 sec before start of dome rotation)

4. 5 sec pre-rotation sampling
5. 30 sec dome rotation (for runs requiring darkness when rotation stops, move dome light switch to 'off' position)
6. 30 sec post-rotation sampling (fixating in darkness, with LED, or with lights on, depending on run condition)
7. Save trial, if data is good

## V.  Cleanup

A.  Turn on room lights
B.  Remove coil from subject's eye
C.  Clean coil gently with hydrogen peroxide; immerse in hydrogen peroxide
D.  Supply subject with eye drops (saline, sensitive eyes, etc.) if desired
E.  Back up data

# APPENDIX C: HUMAN USE DOCUMENTATION

This appendix contains the COUHES human use applications for the rotating dome experiment and the scleral coil system. A sample of the informed consent statement, signed by each subject prior to testing, is included.

**MASSACHUSETTS INSTITUTE OF TECHNOLOGY**
**Committee on the Use of Humans as Experimental Subjects**


**APPLICATION FOR APPROVAL TO USE HUMANS AS EXPERIMENTAL SUBJECTS**

(This application form shall be used for submission to the Clinical Research Center Policy Committee, if it is desired to use the facilities of the Clinical Research Center.)

**TITLE OF STUDY:**

    Rotating dome experiments

**PRINCIPAL INVESTIGATOR:**　　　　　　　　　　Dept.　A&A
　　　　　　　　　　　　　　　　　　　　　　　Room　　37-207
    L.R. Young　　　　　　　　　　　　　　Telephone　3-7759


**ASSOCIATED INVESTIGATORS:**

    M. Shelhamer

**FINANCIAL SUPPORT:** (Research grant title, agency and award number, if any. If none, please give a brief statement of how proposal will be financed.)

    NASA Contract NASW-3651, Vestibular Experiments in the German Spacelab

**PURPOSE OF STUDY:** (A concise statement of the background, nature and reasons for the proposed study. Possible benefits to the subject and to society must be considered by the committee in relation to the possible risks to the subject.)

The purpose of this study is to explore the effect of visual stimulation on the perception of orientation. A rotating dome has been designed to provide such instrumentation and to measure both subjective perception of orientation and torque applied to a biteboard. Additionally, emg recordings of neck muscle are taken to measure neck torque.

A randomized dot pattern which fills the subject's field of view and rotates or translates uniformly will induce a sensation of self-motion after a certain period of time. This motion may be either continuous rotation (circularvection) or linear translation (linearvection). The literature on these phenomena was reviewed in the following papers (Benson, A.J., (1975) Handbook of Sensory Physiology Vol. VI, Vestibular System, H.H. Kornhuber, Ed. Springer Verlag, Berlin; Berthoz, A., Pavard, B., and Young, L.R., (1975) "Perception of linear horizontal self-motion induced by peripheral vision (linearvection). Basic characteristics of visual-vestibular interactions", Exp. Brain Res. 23, 471-489; Brandt, Th., Wist, E., and Dichgans, J., (1971) "Optisch induzierte pseudocoriolis effecte and circularvektion",

Arch Psychiat Nervenkr 214:365-385; Dichgans, Held, R., Young, L.R. and Brandt, Th., and Young, L.R., (1972) "Moving visual scenes influence the apparent direction of gravity", Science 178:1217-1219). If circularvection occurs about an axis other than one aligned with the gravitoinertial vertical, a sensation of visually induced tilt is also found. The sensation is a paradoxical one of continuous rotation accompanied by a steady state angle of tilt. It is likely that the magnitude of the tilt and angular motion sensation is limited by conflict between otolith and available tactile/proprioceptive cues which do not confirm the visually indicated continuous angular motion. This theory is supported by tests by Dichgans et al. (Dichgans, J., Diener, H., and Brandt, Th. (1974) "Optokinetic graviceptive interaction in different head positions", Acta Otolaryng. 78:391-398) and by Young et al. (Young, L.R., Oman, C.M., and Dichgans, J.(1975) "Influence of head orientation on visually induced pitch and roll sensation", Aviat Space & Environ Med 46:264-268) which show that the magnitude of visually induced tilt is increased when the head is tilted to the side or inverted. Tests involving rotations about the roll axis conducted with subjects lying supine produce a steady state sensation of continuous roll veclocity with no limitation on accumulation of roll angle, consistent with the notion that inhibitory effects of the otoliths are eliminated. Tests on the KC-135 (Young, L.R., Lichtenberg, B., Arrott, A., Crites, T., Oman, C. and Edelman, E.R., "Ocular torsion on earth and in weightlessness", Annals of the New York Academy of Sciences 374:80-92, 1981) confirm that continuous unlimited roll appears in weightlessness, and indicates that -- at least on very brief exposure to zero-g -- tactile cues increase the latency of onset of rotation sensation. Preliminary results from Spacelab-1 indicate that, as predicted, onset to vection is decreased, sensations of continuous roll more easily attained, and that the use of tactile cues is more inhibitory early in flight than late. There are no benefits directly to the subject. Care has been taken to ensure that there are no hazards to the subject. Possible benefits to society include a better understanding of the nature of perception and possible insight into the causes of space motion sickness.


**EXPERIMENTAL PROTOCOL:** (An outline of the actual experiments to be performed, including statements as to exact doses of drugs and chemicals to be used, total quantity of blood samples to be drawn, nature of any special diets, physical or emotional stress, protective measures, and so forth. The procedure of social studies and psychological experiments also should be explained in detail. If a questionnaire is involved, a copy should be attached to each application copy. If oral or informal questions are to be asked of subjects, an outline of the questions should be attached similarly. Please attach an additional sheet if necessary. If a protocol incorporating all of these points has already been prepared, it may be attached in lieu of this statement.)

The rotating dome is essentially a shallow cylinder closed on one end, the interior of which is covered with a random pattern of 3/4" colored dots. The dome is designed to fill the positioned subject's field of view. An opening at the center of the closed end is used for the video recording of eye movements. The subject's head is kept positioned within the dome by a biteboard firmly attached to the stationary frame of the dome. The subject is instructed to indicate his perception of self-rotation by means of a joystick mounted on the dome frame. Data is recorded by a dedicated microcomputer

system and video recorder. Three different rates of dome rotation are used (30, 45, and 60 deg/sec), as well as clockwise and counterclockwise directions. A test session consists of two dome runs, each of which is six minutes in length and contains all six stimulus conditions (3 speeds, 2 directions) and lasts approximately 45 minutes. Test sessions are done twice - once for the upright dome and once for the supine dome protocols. During the upright dome protocol, the subject stands erect before the dome, which has been adjusted to match the height of the subject. During the supine tests, the subject lies on his back beneath the dome, which is supported by a sturdy frame.

Contact lenses (COUHES Application #621) will be used only with subjects who will have been especially fitted and trained in their use by an optometrist or ophthalmologist. These lenses will be marked with a star-burst/dot pattern (presently thought to be the most useful pattern for analysis) by the method developed by Dr. Leroy Meshel of the Narcissus Medical Foundation using an FDA approved dye. The Foundation marked the lenses that were flown on Spacelab-1 and used by the SL-1 crew pre, post, and during flight. Similarly marked lenses have been used by over 5000 patients over the last six years. The results from these patients shows that these lenses are as safe as lenses that are unmarked. The markings on the lenses are primarily on the iris and limbus areas and thus do not interfere significantly with vision. Two sets of six lenses per crew member are needed for flight. Two lenses for each eye are needed for the pre and postflight testing. Preparation of these lenses involves only a brief measurement of curvature of the surface of the eye, taking about five minutes. Once the lenses have been fabricated, it is anticipated that about one to two hours per crewman will be sufficient for training in their use.

Dome Protocol:

1. The subject is electroded. Four standard EMG electrodes are placed on the subject's neck (two on each side on the sternocleidomastoideus muscle) and a ground electrode is placed over the collarbone, after cleaning with an alcohol swab (no scratches). (If contact lenses are being used, the subject places the lens in his eye and irrigates the eye with distilled water to ensure lens adherence.)

2. The subject is positioned in the dome, using a specially prepared biteboard which fits into an intrumented holder. The camera is focussed, electrode leads attached, and the subject is reminded of the instructions concerning the joystick.

3. Six one-minute runs at various combinations of the three dome speeds (30, 45, and 60 deg) and the two directions (clockwise and counterclockwise) are then performed under microprocessor control. A test conductor is present at all times. The subject may egress the upright dome at any time. The test conductor is available to assist subject egress from the supine dome, if for any reason the subject wishes to discontinue the experiment.

4. The subject is given a few minutes to rest.

5. Step three is repeated using a different order of presentation.

6. The subject's electrodes are removed and the skin is again wiped with an alcohol swab to prevent any chance of irritation. (Subject removes contact lens, if used.)


**SPECIFIC QUESTIONS TO BE ANSWERED**: Please answer all questions and indicate NA where not applicable. Explain all positive answers.

How will subjects be obtained?  Volunteers from the MIT community, Spacelab crew members.

Will there be any remuneration? No

Number of subjects?  Approximately 30

Expected duration of study for each subject? One hour

Where will study be performed? Building 37

Will drugs be used? No

Any Investigational New Drugs (IND)? No

Electrical stimulation? No

Radiation or radioactive materials? No

Special diets? No

Sleep deprivation? No

Humiliation, deception or invasion of privacy? No

Physical pain? No

Unusual physical or psychological stress? No

Will subject's anonymity be preserved? If so, how?
  Yes. Subjects will be referred to only by codes.

**SUMMARIZE THE RISKS TO THE INDIVIDUAL SUBJECT AND POTENTIAL BENEFITS TO THE INDIVIDUAL SUBJECT:** (Please provide reprints for explanation of all effects from use of a drug, chemical, or material not already approved by the Food and Drug Administration for general use. Provide all necessary documentation if this application will include a request to use an Investigational New Drug. Describe also any possible risk of invasion of privacy, embarrassment or exposure of confidential data, and how the investigators propose to deal with these risks.)

The following are seen as potential hazards:

Lenses may cause a slight mechanical irritation of the cornea and conjunctiva associated with the lens insertion until the subjects are sufficiently practiced in the technique. Lenses will be fit under the direction of an ophthalmologist and the subjects will be instructed and aided in learning the techniques associated with lens insertion. To avoid any contamination of the pre and post flight lenses, which are reused, these lenses are thoroughly cleansed and disinfected prior to each test session.The biteboard, strain gauge bridge, and dome structure are electrically connected (metal-to-metal joints). Thus, in the remote possibility that a strain gauge connection fails and the 12 volt supply line comes into contact with the biteboard, there will be no potential difference between the biteboard and any other metal in contact with the subject. See hazard analysis, attached. EMG measurements use standard electrodes (surface electrodes, without needles) appropriately shielded.


**DETECTION AND REPORTING OF HARMFUL EFFECTS:** If applicable here, please describe what follow up efforts will be made to detect harm to subjects, and how this committee will be kept informed.

Although no after effects are anticipated, subjects will be requested to report any unusual effects to the experimenter. The committee will be informed if this should occur.

183

**INFORMED CONSENT MECHANISMS:** The committee is mandated by the DHEW and Institute regulations to require documentation of informed consent. Under certain circumstances, the committee may waive documentation. The elements of such informed consent are:

1. A fair explanation of the procedures to be followed and their purposes, including identification of any procedures which are experimental.

2. A description of any attendant discomforts and risks reasonably to be expected.

3. A description of any benefits reasonably to be expected.

4. A disclosure of any appropriate alternative procedures that might be advantageous for the subject.

5. An offer to answer any inquiries concerning the procedures.

6. An instruction that the person is free to withdraw his consent and to discontinue participation in the project or activity at any time without prejudice to the subject.

7. There shall be no exculpatory language making the subject seem to waive any rights.

These elements should be clearly stated in a document to be signed by the subject or a legally authorized representative in the case of minors or incompetent individuals. The material presented in such as document must be in clear English, easily understandable to the least educated of subjects. Diagrams or pictures may make such an exposition simpler to comprehend. The committee may request, in special circumstances, that the subject be given a copy of such as document for future reference. Similarly, the committee may request in special circumstances a statement that the COUHES is accessible to aggrieved subjects for the purpose of documenting adverse reactions or grievances which may arise. In that case, the informed consent documents should state the address and telephone number of this committee. If such a formal written document is unreasonable, then the committee may accept oral explanation to the subjects. This explanation must be validated by a document stating that such a presentation has been made to the subject; this document shall be signed by the subject or a legally authorized representative, by a responsible person making the explanation, and by an auditor-witness not immediately associated with the experiment. In addition, the committee must approve a summary of what is to be told to each subject; the summary statement must also be signed at the time of oral explanation by the person obtaining the informed consent, and by the auditor-witness who thus agrees that these elments of explanation were indeed stated to the subjects. The DHEW requires that copies of the proposed validation document and the summary document be submitted to this commitee with the original application; and that signed copies for each subject be kept in the permanent files of the investigation (please see sample documents attached to the Informational Memorandum).The DHEW requires that copies of all such documents signed by individuals referred to above be kept in the permanent files of the investigation. This will include the standard informed consent document referred to in Paragraph I above, as well as the

184

oral validation document and the summary document referred to in paragraph II. For further information regarding such documents, please see sample documents attached to the Informational Memorandum.

In some situations, informed consent documentation will be unnecessary (use of discarded blood or tissue samples, for instance); or self-defeating (certain psychological studies involving intentional deception); or impossible (record searchs, use of stored data). In a case of any deception, debriefing mechanisms must be acceptable before the aproval of an application may be completed. The committee expects that the investigators will notify the committee if any hazards develop in excess of those anticipated.
Informed consent document attached.

     Principal Investigator_____Date_____

     Department Head_____Date_____

Approved COUHES_____Date_____

For projects to be conducted under the auspices of the Clinical Research Center
Clinical Research Center Policy Committee_____Date_____

INFORMED CONSENT STATEMENT

Experiment description:

1. The subject is electroded. Four standard EMG electrodes are placed on the subject's neck (two on each side on the sternocleidomastoideus muscle) and a ground electrode is placed over the collarbone, after cleaning with an alcohol swab. (If contact lenses are being used, the subject places the lens in his eye and irrigates the eye with distilled water to ensure lens adherence.)

2. The subject is positioned in the dome, using a specially prepared bite-board which fits into an intrumented holder. The camera is focussed, electrode leads attached, and the subject is reminded of the instructions concerning the joystick.

3. Six one-minute runs at various combinations of the three dome speeds (30, 45, and 60 deg) and the two directions (clockwise and counterclockwise) are then performed under microprocessor control. A test conductor is present at all times. The subject may egress the upright dome at any time. The test conductor is available to assist subject egress from the supine dome, if for any reason the subject wishes to discontinue the experiment.

4. The subject is given a few minutes to rest.

5. Step three is repeated using a different order of presentation.

6. The subject's electrodes are removed and the skin is again wiped with an alcohol swab to prevent any chance of irritation. (Subject removes contact lens, if used.)

Possible hazards: Lenses may cause a slight mechanical irritation of the cornea and conjunctiva associated with the lens insertion until the subjects are sufficiently practiced in the technique. Lenses will be fit under the direction of an ophthalmologist and the subjects will be instructed and aided in learning the techniques associated with lens insertion. To avoid any contamination of the pre and post flight lenses, which are reused, these lenses are thoroughly cleansed and disinfected prior to each test session. Consent: I understand that I will take part in an experiment to measure the effects of visual stimulation on my perception of self-motion. During this experiment, EMG electrodes will be placed on my neck and shoulder and I will bite on a specially prepared biteboard while viewing a rotating visual display. I understand that I will view the display while standing upright and/or while lying on my back. I understand that I will be asked to indicate my perception of self-rotation or tilt by means of a potentiometer knob. I understand that I may become a bit disoriented by viewing the display.

I understand that I am free to ask questions at any time during the experiment and that I am free to withdraw from participation at any time.

In the unlikely event of physical injury resulting from participation in this research, I understand that medical treatment will be available  from the MIT Medical Department, including first aid, emergency treatment and follow-up care as needed, and that my insurance carrier may be billed for the cost of such treatment.  However, no compensation can be provided for medical care apart from the foregoing.  I further understand that making such medical treatment available, or providing it, does not imply that such injury is the investigator's fault.  I also understand that by my participation in this study I am not waiving any of my legal rights.*

I understand that I may also contact the Chairman of the Committee on the Use of Humans as Experimental Subjects, Dr. George Wolf (MIT 56-213, 253-6781), if I feel I have been treated unfairly as a subject."

I agree to participate in this experiment.

        Signed:_____

        Date:_____

Witness:_____


*Further information may be obtained by calling the Institute's Insurance and Legal Affairs Office at 253-2822.

MASSACHUSETTS INSTITUTE OF TECHNOLOGY
Committee on the Use of Humans as Experimental Subjects

APPLICATION FOR APPROVAL TO USE HUMANS AS EXPERIMENTAL SUBJECTS

PART I.

TITLE OF STUDY:    Visual Vestibular Interaction

PRINCIPAL INVESTIGATOR:    C.M. Oman, L.R. Young        Dept.    A&A
                                                        Room    37-211
                                                        Telephone  3-7508


ASSOCIATED INVESTIGATORS:  Conrad Wall, Ph.D., Mass Eye and Ear Infirmary

Collaborating Institution(s), if applicable:  Mass Eye and Ear Institute
(Please attach copies of approval documents or correspondence from
collaborating institution(s) where applicable.)

FINANCIAL SUPPORT: (Research grant title, agency and award number, if any.

If not applicable, please indicate how project will be financed.)

NASA Ames Research Center NAG2-445

PURPOSE OF STUDY:  (Please provide a  concise statement of the background,
nature and reasons for the proposed study.)

Human visual-vestibular interaction will be investigated by studying eye
movements and perception of self-motion.  The experiments will emphasize
vertical eye movements and ocular torsion in conjunction with vertical
linearvection.  Motions which stimulate the utricular or saccular otolith
organs will be combined with corresponding wide field motion displays
capable of producing optokinetic nystagmus and self-motion illusions.  The
experiments utilize our linear acceleration sled.

This research concerns human visual vestibular interaction with emphasis
on stimulation in the vertical and longitudinal axes.  The measurements
will be psychophysical estimates of vection and objective measurements of .
ocular torsion and vertical eye movements.  We will utilize our linear
"sled" to produce horizontal longitudinal linear acceleration for
comparison with horizontal lateral acceleration.  Measurements of vertical

eye movements for z-axis acceleration, in comparison with lateral eye movements for y-axis acceleration, with and without confirming and conflicting visual wide field stimuli, will be made in conjunction with subjective estimations of self-motion. This set of experiments will permit us to delineate between linear acceleration effects on eye movements and affects on motion perception when the stimulus is primarily along the presumed axis of sensitivity of the saccular otolith organ.


Part II.

EXPERIMENTAL PROTOCOL: Please provide an outline of the actual experiments to be performed, including, where applicable, detailed information as to exact dosages of drugs and chemicals to be used, total quantity of blood samples to be drawn, nature of any special diets, physical or emotional stress, and the appropriate protective measures you are planning to take.

For applications in the social sciences, please provide a detailed description of your proposed study, and include a copy of any questionnaire you plan to incorporate into your project. If your study involves interviews, please submit an outline indicating the types of questions you will include.

If convenient, you may attach photocopies of material from previously-submitted proposals, etc.; however, please try to avoid submitting extraneous material, such as grant applications in their entirety.

The ultimate goals of these experiments are to quantitatively describe the transfer functions of both the utricular and saccular otolithic and optokinetic torsion systems and to understand their interactions when suppressive and conflicting visual/motion conditions are produced.

Torsion eye movements will be measured using the magnetic search coil method described below. The coils used to generate the external magnetic field will be mounted on the sled. He will wear either a commercial Skalar lenses or the coil lenses described below. The subject will be secured in the sled by shoulder and lap seatbelts and his head will be held in position by a bite-bar and wood/foam head restraint. Sinusoidal and step profiles will be the motion stimuli.

The proposed experiments on linear visual-vestibular interaction emphasize the differences between Z-axis optokinetic and vestibular responses and the corresponding Y-axis responses. For all of the experiments in the series two kinds of measurements are taken: eye movements along the axis of stimulation and subjective magnitude estimation of body velocity. The experiments will begin with simple tests of pure optokinetic and pure inertial stimuli, in Z and Y axes, followed by interactive experiments with confirming and conflicting visual and vestibular stimuli.

189

The principal motion stimulus will be provided by the MIT Sled, a rail mounted linear acceleration cart designed by Lichtenberg (1979) and modified by Loo (1980) and by Arrott (1982). In the most closely related work, using measurements of motion perception and of eye movements, it was employed for the normative studies supporting our Spacelab-1 pre and post flight vestibular assessments, and in the lateral visual-vestibular interaction perception experiments (Huang, 1983). The seat can be positioned to allow X, Y or Z axis motion of the subject along the horizontal rails. The cart is controlled by a pre-tensioned cable wound around a pulley at one end and a winch at the other. Power is supplied through a 3.5 hp DC permanent magnet torque motor controlled by a pulse-width modulated velocity control. Sled motion as well as data logging is under the control of a PDP 11/34 microcomputer and Lab Peripheral System. An interactive FORTRAN program provides real time control of cart motion profiles and provides supervisory control and one level of safety devices (Arrott, 1985). A dedicated microcomputer (PC type) will be programmed to take over this function. This should further increase the reliability of the system. Current motion profiles provide for single sinusoids, sum of sines, constant accelerations, subthreshold positioning, frequency sweep, and subject control of cart velocity. The envelope of sled motion is determined by its length (4.7 m), maximum acceleration (0.8 g) and bandwidth (7 Hz.).

Visual stimulus for our visual-vestibular interaction experiments has, in the past, been provided through a point-light source, moving film strip system which reflected from a long mirror to a rear projection screen attached to the sled cart (Huang, 1983). In order to provide a flexible moving field linear display which could be mounted to the cart for z-axis (subject supine) as well as y-axis acceleration, we recently developed a new mechanical stimulator. This "window shade" device (Vargas, 1985) provides computer controlled linear acceleration of a 47.5 x 47.5 cm screen placed 47.5 cm from the subject, and will be our primary source for optokinetic and linear VVI experiments in conjunction with the sled. A drawing of the windowshade attachment is enclosed.

Eye movements will be measured both by means of the coil system and standard electro-oculography, using our own dc-coupled, high input impedance amplifiers and pregelled infant EOG electrodes. We record EOG binocularly for horizontal eye movements and have determined that, for normal subjects, vergence eye movements and lack of conjugate gaze is not a problem. By using pre-experiment time for dark adaptation and electrode stabilization, we can achieve stable recordings requiring only pre and post-test calibration. Three distinct types of lateral or vertical eye movements are encountered during linear body acceleration in the dark, as opposed to the simple OKN seen for field motion. The eye movement pattern may be nystagmoid, a smooth pendular response, or highly irregular. In all cases the EOG records are inspected and then "desaccaded" by computer (Massoumnia, 1983) to produce the cumulative slow phase eye position and slow phase velocity (SPV).

190

The scleral search coil method of measuring eye movements uses two sets of coils. One or more pairs of transmitter coils surrounds the subject's head and transmit an electromagnetic field that is designed to be uniform in the area of the subject's eye. Another set of receiving coils is temporarily attached to the subject's eye via a silastic rubber annulus and move with the eye. Eye movements are detected and measured by electrically comparing the received signals to the transmitted signals. Properly selected combinations of coils allow for measurement of horizontal, vertical, and torsional eye movement components. The scleral search coil method will be the primary means to measure ocular torsion and will also be useful in assessing vertical eye movements. The C&C search coil system will be specifically designed for use with our sled. Phase detector sensors will be provided to measure horizontal, vertical and torsional eye movements simultaneously. The Skalar medical torsion coil annulus may be used. The procedures recommended by Skalar Medical for safe use and installation of the coil annulus will be followed. Care will be taken to limit the time that the annulus is worn by the subject to a maximum of 30 minutes. Since the coils are relatively expensive and can be re-used, they will be disinfected and stored in accordance with the Skalar Medical procedure. This procedure has been approved by the National Institutes of Health and the Center for Disease Control. Subject calibration for this system will be provided by a calibration fixture which comes with the C&C search coil system.

The sequence of visual-vestibular interaction experiments begins with pure visual (optokinetic) stimuli, comparing vertical eye movements and linear-vection to lateral (horizontal) responses for subjects supine and erect. The next step will be pure vestibular experiments on the sled, in darkness, comparing z-axis to y-axis horizontal acceleration conditions. Finally, visual and vestibular conditions will be combined by putting the linear "window shade" on the sled.

For each condition there will be three basic stimulus profiles: steps of constant velocity, sines of constant peak velocity covering the range of frequencies, and pseudorandom sums of 25 sinusoids. Both the eye movement and the subjective velocity measurements will be analyzed using linear systems analysis techniques to extract the gain and phase of the response velocity relative to the stimulus velocity. For the case of vertical motions, particular attention will be paid to up-down asymmetries, which will necessitate separate consideration of upward and downward phases of eye and self-motion velocity indications. For the sines and pseudo-random signals, we use FFT analysis of self velocity and cumulative slow phase velocity to calculate the frequency response, harmonics, and remnant.

For these linear visual-vestibular interaction experiments, we plan to use the same four combinations of stimuli which have proven effective in the development of models for VVI about the angular axes. The first is the countermotion (CON) condition, in which the visual field moves opposite to the sled, at the same speed, so that it represents the fixed laboratory environment and the optokinetic and vestibular drives are consistent. The second condition is the fixed (FIX) visual field, which provides for

visual suppression of vestibular nystagmus and inhibition of vection, but which also promotes the oculogravic illusion. The third condition is constant velocity (CV) field motion, independent of the sled motion. The last condition is the dual random input stimulus in which independent pseudorandom inputs of different frequency content are presented to the sled motion drive and to the visual velocity drive to enable calculation of the subject's dual input describing function (DIDF). This technique has proven very valuable when used with closed loop velocity nulling by the subject in yaw (Zacharias and Young, 1981, Huang and Young 1985a), but has been difficult to implement for linear acceleration studies (Hiltner, 1983, Huang, 1983.)

For the static visual stimulation experiments, the subject's head will be fixed by the helmet we also use in the sled experiments or the subject will be provided with a personal biteboard. Following calibration with fixed 15 degree targets the subject will be instructed to stare ahead to generate "stare nystagmus" as opposed to tracking nystagmus. The vertical EOG calibration problem will be dealt with by a separate investigation of each subject in which voluntary fixation and vertical saccades will be monitored by EOG and the coil system and the extent of the correction noted. Pattern movements for constant velocity steps are anticipated to be of 20 second durations at five speeds in each direction, logarithmically spaced between 1 cm/sec and 1 m/sec. Sines will also be logarithmically spaced between 0.02 Hz and 2.0 Hz, with a peak velocity of 50 cm/sec. The pseudorandom signal will consist of 25 sines between 0.02 Hz and 1.25 Hz. The pure vestibular linear acceleration tests on the sled will follow a similar pattern, limited only by the performance envelope of the device. The sled has been safety rated up to 1.0 g's for subject erect (y-axis) and subject supine (z-axis). The combined visual and vestibular stimuli are conducted on the sled with the moving visual field device attached.

The total number of subjects to be used in each test series depends, of course, on the stability of the measurements and the inter-subject variability. Based upon our experience over the course of many years, we estimate that at least six subjects will be required for each of the subjective estimation tests, but that 10-15 subjects will be required to obtain reliable patterns of linear acceleration induced eye movements. Since so many of the tests involve comparison between conditions, subjects will be selected from within the Laboratory's population of students and staff, who will be willing to commit to a long duration study with numerous retests over the course of several years. Order effects will be taken into account in the experimental design for each comparison, such as y-axis vs. z-axis.

PART III.    Please answer all questions and indicate NA where not applicable.  Positive answers should be briefly explained, with detailed information included in Part II.

1.    How will subjects be obtained?  Word-of-mouth
Number of subjects needed?          20
Age(s) of subjects?               > 18

2.    Will subjects receive any payment or other compensation for participation?  Yes

3.    Will your subjects be studied outside MIT premises?  No.
If so, please indicate location.                              .

4.    Will the facilities of the Clinical Research Center be used?  No.
If so, the approval of the CRC Policy Committee is also required.

For proposed investigations in social sciences, management, and other non-biomedical areas, please continue with question 9.

5.    Will drugs be used?   No.
Any Investigational New Drugs (IND)?

6.    Will radiation or radioactive materials be employed?   No.
If so, your study must also be approved by the Committee on Radiation Exposure to Human Subjects.  Application forms are available from Mr. Francis X. Masse, Radiation Protection Office, 20B-238, x3-2180 or 18-3212.

7.    Will special diets be used?  If so, please state proposed duration(s).
No.

8.    Will subjects experience physical pain or stress?   No.

9.    Will a questionnaire be used?  No.
If so, please attach a copy.

10.    Are personal interviews involved?   No.
If so, include an explanation in Part II and attach an outline.

11.    Will subjects experience psychological stress?   No.

12.    Does this study involve planned deception of subjects?       No.

13.    Can information acquired through this investigation adversely affect a subject's relationship with other individuals (e.g. employee-supervisor, patient-physician, student-teacher, co-worker, family relationships)?       No.

14.    Please explain how subject's anonymity will be protected and/or confidentiality of data will be preserved.

Subjects will be referred to only by codes.

PART IV.

A.   Please summarize the risks to the individual subject, and the
     benefits, if any; include any possible risk of invasion of
     privacy, embarrassment or exposure of sensitive or confidential
     data, and explain how you propose to deal with these risks.

     Risks associated with the use of the Skalar search coil system:  The
     subject wears a very small coil that is completely imbedded in a
     silicon rubber annulus and which is shaped to adhere to the limbus of the
     eye.  There is a 12.5 mm central hole in the annulus so that  vision is
     not occluded.  The manufacturer of the annulus has developed procedures
     for the safe insertion of the coil and also for cleaning, disinfecting
     and storing the coils.  These procedures will be adhered to in the
     measurement protocol.  Personnel who insert the  coil will be approved in
     writing by a collaborating ophthalmologist  or doctor of optometry.  A 30
     minute guideline for maximum          wearing of the search coil will be
     adhered to as mentioned in the   manufacturer's procedures.

     Prior to insertion of the annulus, the eye will be briefly anes-
     thetized by 1 or 2 drops of a topical ophthalmic anesthesia such as
     Novosine (oxybuprocane 0.4%).  The annulus will be removed from the
     subject's eye in accordance with the recommended procedures.  After
     use, the annulus will be cleaned by thorough rising in a stream of
     lukewarm water and subsequently disinfected by immersion in fresh 3%
     hydrogen peroxide for 10 minutes.  This procedure is in agreement
     with a recent guideline based on studies at the National Institutes
     of Health and the Center for Disease Control.  After the immersion,
     there will be a second thorough rinsing with water and the device
     will be air dried on tissue paper.

B.   Detection and reporting of harmful effects: If applicable here,
     please describe what follow up efforts will be made to detect
     harm to subjects, and how this committee will be kept informed.

     The probability of even a minor irritation to the eye is very low.
     Investigators at other institutions (National Eye Institute, Johns
     Hopkins University, UCLA) have found it to be less than one percent.
     All subjects will be examined by an optometrist prior to participa-
     ting in any experiments involoving lenses or annular rings.
     In case of irritation, the subject's eye will be patched and treated
     with an ophthalmologic topical antibiotic and then re-examined the
     next day.  The Committee will be informed in the event of any such
     occurrences.  These procedures have been carried out on 50-60
     insertions of the lenses with subjects from Dr. Wall's laboratory
     with only one case of minor irritation (see attached protocol from
     MEEI).

194

PART V.

INFORMED CONSENT MECHANISMS:  The committee is mandated by the DHHS and
Institute regulations to require documentation of informed consent.  Under
certain circumstances, the committee may waive documentation. The elements
of such informed consent are:

1.      An instruction that the person is free to withdraw his/her
        consent and to discontinue participation in the project or
        activity at any time without prejudice to the subject.

2.      A fair explanation of the procedures to be followed and their
        purposes, including identification of any procedures which are
        experimental.

3.         A description of any attendant discomforts and risks
        reasonably to be expected.

4.      A description of any benefits reasonably to be expected.

5.      A disclosure of any appropriate alternative procedures that
        might be advantageous for the subject.

6.      An offer on the part of the investigator to answer any inqui-
        ries concerning the procedures.

7.      There shall be no exculpatory language making the subject seem
        to waive any rights.

8.      The following statement shall appear on all informed consent
        documents, except that in certain cases of experiments in the
        social sciences, management, or other non-biomedical discip-
        lines, where it is clearly not applicable, it may be omitted.
        COUHES, however, reserves the right to request that this para-
        graph be included.

"In the unlikely event of physical injury resulting from participation in
this research, I understand that medical treatment will be available  from
the MIT Medical Department, including first aid, emergency treatment and
follow-up care as needed, and that my insurance carrier may be billed for
the cost of such treatment.  However, no compensation can be provided for
medical care apart from the foregoing.  I further understand that making
such medical treatment available, or providing it, does not imply that such
injury is the investigator's fault.  I also understand that by my participation
in this study I am not waiving any of my legal rights.

I understand that I may also contact the Chairman of the Committee on the
Use of Humans as Experimental Subjects (MIT, 253-6787), if I feel I have
been treated unfairly as a subject."

Consent forms in cooperating institutions must assure that the rights of
the subjects are protected at least to the same degree.

These elements should be clearly stated in a document to be signed by the
subject or a legally authorized representative in the case of minors or

incompetent individuals. The material presented in such as document must be in clear English, easily understandable to the least educated of subjects. Diagrams or pictures may make such an exposition simpler to comprehend. Where minors are involved as subjects, due consideration should be given to their capability to give consent. The Informed Consent document should be signed by both the subject and parent and guardian wherever possible.

In the case of Questionnaires or Interviews, the Committee may decide that a consent form is not required if the intent is merely to obtain the requested information. However, it must be clear to the subject that:

- Participation is voluntary.

- The subject may decline to answer any questions.

- The subject may decline further participation at any time without prejudice.

- Confidentiality and/or anonymity are assured.

In addition:

- No coercion to participate will be involved. For example, handing out or collecting questionnaires personally may be so interpreted.

- The date collected will be reported in such a way that the identity of individuals is protected.

- Proper measures will be taken to safeguard the data.

Other examples of situations in which informed consent documentation is not required include use of discarded blood, certain psychological studies involving intentional deception or use of stored data. In a case of any deception, debriefing mechanisms must be acceptable before the approval of an application may be completed. The committee expects that the investigators will notify the committee if any hazards develop in excess of those anticipated.


Principal Investigator_____Date_____

Department Head_____Date_____

Please return this application with 3 photocopies to COUHES Chairman, E23-389, 253-6787

INFORMED CONSENT STATEMENT

You have been asked to participate in an experiment aimed at better understanding the visual, vestibular, and postural control systems. Your participation is purely voluntary and you are free to withdraw at any time. In the experiment, your entire visual field will be filled by a rotating dome covered with dots. The experiment will be performed in either the erect or supine position; your head will be fixed in place by a dental biteboard. You will be asked to look at a moving visual display and to indicate your perception of movement. At the end of the experiment, you will be asked to discuss how you perceived various stages of the experiment.

Please feel free to ask any questions you care to about the experiment. While the dome is rotating, you may have the investigator stop it at any time. If at any time you experience any discomfort or have any misgivings about continuing the experiment, we ask that you tell us--we will stop the test at any time you like.

Your eye movements will be measured using soft contact lens search coils, the most accurate method available today. The cornea will be anesthetized using eye drops. The anaesthetic used is proparacaine HCl. If you have any allergies to this anaesthetic, you should withdraw from participation in this experiment. The lens, in which a tiny search coil is embedded, will be applied to your eye. This will be worn for no longer than thirty minutes. Before application and after removal, your eyes will be examined by an optometrist to rule out any possible corneal abrasion. There is a less than one percent chance that the wearing of the soft contact lens may cause a slight corneal abrasion. If this does occur, a prophylactic antibiotic and covering will be applied overnight. Finally, we may also record your eye movements using a small video camera with a low level light source.

"In the unlikely event of injury resulting from participation in this research, I understand that medical treatment will be available from the MIT Medical Department, including first aid, emergency treatment and follow-up care as needed, and that my insurance carrier may be billed for the cost of such treatment. However, no compensation can be provided for medical care apart from the foregoing. I further understand that making such medical treatment available, or providing it, does not imply that such injury is the investigator's fault. I also understand that by my participation in this study I am not waiving any of my legal rights (for more information, call the Institute's Insurance and Legal Affairs Office at 253-2822). I understand that I may also contact the Chairman of the Committee on the Use of Humans as Experimental Subjects, Dr. H. Walter Jones (MIT E23-389, 253-6787), if I feel I have been treated unfairly as a subject."

I have been informed as to the procedures and purpose of this experiment and agree to participate.

Signed: _____

Date: _____

Witness: _____

# APPENDIX D: DATA PARAMETERS

The data parameters for each experimental trial are summarized in 7 tables:

1. Individual trial information

2. OKN SPV data

3. OKN SPV data: vection vs. no vection

4. Eye position data

5. Eye position data: vection vs. no vection

6. OKAN SPV: double exponential fits

7. Vection parameters

A plot of a typical vection response is included for each subject.

**Table D.1.  Individual trial information.  Trial presentation order for each experimental run.**

This table contains the following:

1. Subject:  subject code letter (M - S)

2. Run #:  run in order performed

3. Orientation:  subject orientation (erect or supine)

4. Post-rotation condition:  visual field presented following dome rotation
   •LED--fixation point in darkness (designated as LED #1 and LED #2 if two such runs were performed)
   •dark--complete darkness
   •light--lighted dome provided a stationary visual field

5. Trial #:  trial order with a single run

6. Dome direction:  CW or CCW from subject's point of vies

8. Dome speed:  negative values indicate CCW rotation

# Dome run information

| Subject | Run # | Orientation | Post-rotation condition | Trial # | Dome direction | Dome speed deg/sec |
|---|---|---|---|---|---|---|
| M | 1 | erect | LED | 1 | CW | 30.0 |
| M | 1 | erect | LED | 2 | CCW | -45.0 |
| M | 1 | erect | LED | 3 | CCW | -60.0 |
| M | 1 | erect | LED | 4 | CW | 45.0 |
| M | 1 | erect | LED | 5 | CCW | -30.0 |
| M | 1 | erect | LED | 6 | CW | 60.0 |
| M | 2 | erect | light | 1 | CW | 30.0 |
| M | 2 | erect | light | 2 | CCW | -45.0 |
| M | 2 | erect | light | 3 | CCW | -60.0 |
| M | 2 | erect | light | 4 | CW | 45.0 |
| M | 2 | erect | light | 5 | CCW | -30.0 |
| M | 2 | erect | light | 6 | CW | 60.0 |
| M | 3 | supine | LED #1 | 1 | CCW | -56.2 |
| M | 3 | supine | LED #1 | 2 | CCW | -56.2 |
| M | 3 | supine | LED #1 | 3 | CCW | -56.2 |
| M | 3 | supine | LED #1 | 4 | CCW | -21.2 |
| M | 3 | supine | LED #1 | 5 | CW | 41.5 |
| M | 3 | supine | LED #1 | 6 | CCW | -41.5 |
| M | 4 | supine | LED #2 | 1 | CW | 20.5 |
| M | 4 | supine | LED #2 | 2 | CCW | -21.2 |
| M | 4 | supine | LED #2 | 3 | CCW | -41.5 |
| M | 4 | supine | LED #2 | 4 | CW | 41.2 |
| M | 4 | supine | LED #2 | 5 | CW | 72.3 |
| M | 4 | supine | LED #2 | 6 | CW | 56.0 |
| M | 4 | supine | LED #2 | 7 | CCW | -72.7 |
| M | 4 | supine | LED #2 | 8 | CCW | -56.4 |
| M | 5 | supine | light | 1 | CW | 21.4 |
| M | 5 | supine | light | 2 | CCW | -21.7 |
| M | 5 | supine | light | 3 | CCW | -42.0 |
| M | 5 | supine | light | 4 | CW | 41.5 |
| M | 5 | supine | light | 5 | CCW | -72.0 |
| M | 5 | supine | light | 6 | CW | 55.7 |
| M | 5 | supine | light | 7 | CW | 72.6 |
| M | 5 | supine | light | 8 | CCW | -56.8 |

| Subject | Run # | Orientation | Post-rotation condition | Trial # | Dome direction | Dome speed deg/sec |
|---|---|---|---|---|---|---|
| Subject | Run # | Orientation | Post-rotation condition | Trial # | Dome direction | Dome speed deg/sec |
| N | 1 | erect | LED #1 | 1 | CCW | -14.5 |
| N | 1 | erect | LED #1 | 2 | CW | 13.9 |
| N | 1 | erect | LED #1 | 3 | CCW | -29.6 |
| N | 1 | erect | LED #1 | 4 | CW | 29.5 |
| N | 2 | erect | LED #2 | 1 | CCW | -14.4 |
| N | 2 | erect | LED #2 | 2 | CW | 14.4 |
| N | 2 | erect | LED #2 | 3 | CCW | -29.7 |
| N | 2 | erect | LED #2 | 4 | CW | 29.5 |
| N | 2 | erect | LED #2 | 5 | CCW | -59.5 |
| N | 2 | erect | light | 6 | CW | 44.6 |
| N | 2 | erect | LED #2 | 7 | CW | 59.5 |
| N | 2 | erect | LED #2 | 8 | CCW | -45.2 |
| N | 3 | erect | dark | 1 | CW | 29.8 |
| N | 3 | erect | dark | 2 | CCW | -59.8 |
| N | 3 | erect | dark | 3 | CCW | -14.8 |
| N | 3 | erect | dark | 4 | CW | 44.8 |
| N | 4 | supine | LED | 1 | CW | 30.1 |
| N | 4 | supine | LED | 2 | CCW | -60.0 |
| N | 4 | supine | LED | 3 | CCW | -15.5 |
| N | 4 | supine | LED | 4 | CW | 45.4 |
| N | 4 | supine | LED | 5 | CW | 15.4 |
| N | 4 | supine | LED | 6 | CCW | -30.8 |
| N | 4 | supine | light | 7 | CW | 60.2 |
| N | 4 | supine | LED | 8 | CW | 45.8 |
| N | 5 | supine | dark | 1 | CCW | -15.9 |
| N | 5 | supine | dark | 2 | CW | 15.4 |
| N | 5 | supine | light | 3 | CCW | -30.9 |
| N | 5 | supine | dark | 4 | CW | 30.5 |
| N | 5 | supine | dark | 5 | CCW | -60.2 |
| N | 5 | supine | dark | 6 | CW | 45.7 |
| N | 5 | supine | light | 7 | CW | 60.3 |
| N | 5 | supine | dark | 8 | CCW | -46.1 |

# Dome run information

| Subject | Run # | Orientation | Post-rotation condition | Trial # | Dome direction | Dome speed deg/sec |
|---------|-------|-------------|-------------------------|---------|----------------|--------------------|
| O | 1 | erect | LED | 1 | CW | 29.8 |
| O | 1 | erect | LED | 2 | CCW | -59.6 |
| O | 1 | erect | LED | 3 | CCW | -14.7 |
| O | 1 | erect | LED | 4 | CW | 44.8 |
| O | 1 | erect | LED | 5 | CW | 14.9 |
| O | 1 | erect | LED | 6 | CCW | -30.0 |
| O | 1 | erect | LED | 7 | CW | 59.8 |
| O | 1 | erect | LED | 8 | CCW | -45.4 |
| O | 2 | erect | dark | 1 | CCW | -29.3 |
| O | 2 | erect | dark | 2 | CW | 59.2 |
| O | 2 | erect | dark | 3 | CCW | -14.5 |
| O | 2 | erect | dark | 4 | CW | 44.8 |
| O | 2 | erect | dark | 5 | CW | 14.6 |
| O | 2 | erect | dark | 6 | CW | 30.0 |
| O | 2 | erect | dark | 7 | CCW | -59.8 |
| O | 2 | erect | dark | 8 | CCW | -45.3 |
| O | 3 | erect | light | 1 | CCW | -14.5 |
| O | 3 | erect | light | 2 | CW | 14.2 |
| O | 3 | erect | light | 3 | CCW | -29.8 |
| O | 3 | erect | light | 4 | CW | 29.8 |
| O | 3 | erect | light | 5 | CCW | -59.8 |
| O | 3 | erect | light | 6 | CW | 44.8 |
| O | 3 | erect | light | 7 | CW | 59.7 |
| O | 3 | erect | light | 8 | CCW | -45.4 |
| O | 4 | supine | LED | 1 | CCW | -15.3 |
| O | 4 | supine | LED | 2 | CW | 15.3 |
| O | 4 | supine | LED | 3 | CCW | -30.3 |
| O | 4 | supine | LED | 4 | CW | 29.9 |
| O | 4 | supine | LED | 5 | CW | 29.7 |
| O | 4 | supine | LED | 6 | CCW | -59.8 |
| O | 4 | supine | LED | 7 | CCW | -15.2 |
| O | 4 | supine | LED | 8 | CW | 45.3 |
| O | 5 | supine | dark | 1 | CW | 15.5 |
| O | 5 | supine | dark | 2 | CCW | -30.5 |
| O | 5 | supine | dark | 3 | CW | 60.0 |
| O | 5 | supine | dark | 4 | CCW | -45.9 |
| O | 5 | supine | dark | 5 | CW | 30.8 |
| O | 5 | supine | dark | 6 | CCW | -60.4 |
| O | 5 | supine | dark | 7 | CCW | -15.6 |
| O | 5 | supine | dark | 8 | CW | 45.7 |

| Subject | Run # | Orientation | Post-rotation condition | Trial # | Dome direction | Dome speed deg/sec |
|---------|-------|-------------|-------------------------|---------|----------------|---------------------|
| Subject | Run # | Orientation | Post-rotation condition | Trial # | Dome direction | Dome speed deg/sec |
| P | 1 | erect | LED | 1 | CW | 29.5 |
| P | 1 | erect | LED | 2 | CCW | -59.6 |
| P | 1 | erect | LED | 3 | CCW | -14.6 |
| P | 1 | erect | LED | 4 | CW | 44.8 |
| P | 1 | erect | LED | 5 | CW | 14.8 |
| P | 1 | erect | LED | 6 | CCW | -30.1 |
| P | 1 | erect | LED | 7 | CW | 59.8 |
| P | 1 | erect | LED | 8 | CCW | -45.4 |
| P | 2 | erect | dark | 1 | CCW | -14.8 |
| P | 2 | erect | dark | 2 | CW | 14.7 |
| P | 2 | erect | dark | 3 | CCW | -30.2 |
| P | 2 | erect | dark | 4 | CW | 30.0 |
| P | 2 | erect | dark | 5 | CCW | -60.0 |
| P | 2 | erect | dark | 6 | CW | 45.2 |
| P | 2 | erect | dark | 7 | CW | 60.1 |
| P | 2 | erect | dark | 8 | CCW | -45.5 |
| P | 3 | supine | LED | 1 | CCW | -14.8 |
| P | 3 | supine | LED | 2 | CW | 14.2 |
| P | 3 | supine | LED | 3 | CW | 29.0 |
| P | 3 | supine | light | 4 | CCW | -58.9 |
| P | 3 | supine | LED | 5 | CCW | -14.8 |
| P | 3 | supine | LED | 6 | CW | 44.2 |
| P | 3 | supine | LED | 7 | CW | 14.7 |
| P | 3 | supine | LED | 8 | CCW | -29.9 |
| P | 4 | supine | dark | 1 | CW | 59.2 |
| P | 4 | supine | dark | 2 | CCW | -45.1 |
| P | 4 | supine | dark | 3 | CW | 29.8 |
| P | 4 | supine | dark | 4 | CCW | -59.5 |
| P | 4 | supine | dark | 5 | CCW | -15.1 |
| P | 4 | supine | dark | 6 | CW | 44.8 |
| P | 4 | supine | dark | 7 | CW | 15.2 |
| P | 4 | supine | dark | 8 | CCW | -30.4 |

# Dome run information

| Subject | Run # | Orientation | Post-rotation condition | Trial # | Dome direction | Dome speed deg/sec |
|---------|-------|-------------|-------------------------|---------|----------------|--------------------|
| Q | 1 | erect | LED | 1 | CCW | -14.5 |
| Q | 1 | erect | LED | 2 | CW | 14.1 |
| Q | 1 | erect | LED | 3 | CCW | -29.7 |
| Q | 1 | erect | LED | 4 | CW | 29.6 |
| Q | 1 | erect | LED | 5 | CCW | -59.8 |
| Q | 1 | erect | LED | 6 | CW | 44.9 |
| Q | 1 | erect | LED | 7 | CW | 59.9 |
| Q | 1 | erect | LED | 8 | CCW | -45.4 |
| Q | 2 | erect | dark | 1 | CW | 30.0 |
| Q | 2 | erect | dark | 2 | CCW | -60.1 |
| Q | 2 | erect | dark | 3 | CCW | -14.9 |
| Q | 2 | erect | dark | 4 | CW | 44.9 |
| Q | 2 | erect | dark | 5 | CW | 14.9 |
| Q | 2 | erect | dark | 6 | CCW | -30.1 |
| Q | 2 | erect | dark | 7 | CW | 60.0 |
| Q | 2 | erect | dark | 8 | CCW | -45.7 |
| Q | 3 | supine | LED | 1 | CW | 29.5 |
| Q | 3 | supine | LED | 2 | CCW | -59.4 |
| Q | 3 | supine | LED | 3 | CCW | -14.8 |
| Q | 3 | supine | LED | 4 | CW | 44.6 |
| Q | 3 | supine | LED | 5 | CW | 14.8 |
| Q | 3 | supine | LED | 6 | CCW | -30.3 |
| Q | 3 | supine | LED | 7 | CW | 59.7 |
| Q | 3 | supine | LED | 8 | CCW | -45.5 |
| Q | 4 | supine | dark | 1 | CCW | -15.3 |
| Q | 4 | supine | dark | 2 | CW | 15.1 |
| Q | 4 | supine | dark | 3 | CCW | -30.4 |
| Q | 4 | supine | dark | 4 | CW | 29.7 |
| Q | 4 | supine | dark | 5 | CCW | -59.9 |
| Q | 4 | supine | dark | 6 | CW | 44.9 |
| Q | 4 | supine | dark | 7 | CW | 60.0 |
| Q | 4 | supine | dark | 8 | CCW | -45.8 |

| Subject | Run # | Orientation | Post-rotation condition | Trial # | Dome direction | Dome speed deg/sec |
|---|---|---|---|---|---|---|
| Subject | Run # | Orientation | Post-rotation condition | Trial # | Dome direction | Dome speed deg/sec |
| R | 1 | erect | LED | 1 | CW | 29.4 |
| R | 1 | erect | LED | 2 | CCW | -59.7 |
| R | 1 | erect | LED | 3 | CCW | -14.4 |
| R | 1 | erect | LED | 4 | CW | 44.6 |
| R | 1 | erect | LED | 5 | CW | 14.6 |
| R | 1 | erect | LED | 6 | CCW | -30.2 |
| R | 1 | erect | LED | 7 | CW | 59.7 |
| R | 1 | erect | LED | 8 | CCW | -45.6 |
| R | 2 | erect | dark | 1 | CCW | -14.9 |
| R | 2 | erect | dark | 2 | CW | 14.5 |
| R | 2 | erect | dark | 3 | CCW | -30.3 |
| R | 2 | erect | dark | 4 | CW | 29.7 |
| R | 2 | erect | dark | 5 | CCW | -60.1 |
| R | 2 | erect | light | 6 | CW | 44.9 |
| R | 2 | erect | dark | 7 | CW | 60.1 |
| R | 2 | erect | dark | 8 | CCW | -45.6 |

# Dome run information

| Subject | Run # | Orientation | Post-rotation condition | Trial # | Dome direction | Dome speed deg/sec |
|---|---|---|---|---|---|---|
| S | 1 | erect | LED | 1 | CCW | -14.8 |
| S | 1 | erect | LED | 2 | CW | 14.2 |
| S | 1 | erect | LED | 3 | CCW | -29.9 |
| S | 1 | erect | LED | 4 | CW | 29.4 |
| S | 1 | erect | LED | 5 | CCW | -59.8 |
| S | 1 | erect | LED | 6 | CW | 44.9 |
| S | 1 | erect | LED | 7 | CW | 59.9 |
| S | 1 | erect | LED | 8 | CCW | -45.6 |
| S | 2 | erect | dark | 1 | CW | 30.0 |
| S | 2 | erect | dark | 2 | CCW | -60.3 |
| S | 2 | erect | dark | 3 | CCW | -15.1 |
| S | 2 | erect | dark | 4 | CW | 45.2 |
| S | 2 | erect | dark | 5 | CW | 15.0 |
| S | 2 | erect | dark | 6 | CCW | -30.5 |
| S | 2 | erect | dark | 7 | CW | 59.9 |
| S | 2 | erect | dark | 8 | CCW | -45.8 |
| S | 3 | supine | LED | 1 | CW | 29.7 |
| S | 3 | supine | LED | 2 | CCW | -59.7 |
| S | 3 | supine | LED | 3 | CCW | -15.2 |
| S | 3 | supine | LED | 4 | CW | 45.0 |
| S | 3 | supine | LED | 5 | CW | 15.3 |
| S | 3 | supine | LED | 6 | CCW | -30.5 |
| S | 3 | supine | LED | 7 | CW | 60.0 |
| S | 3 | supine | LED | 8 | CCW | -45.7 |
| S | 4 | supine | dark | 1 | CCW | -15.6 |
| S | 4 | supine | dark | 2 | CW | 15.3 |
| S | 4 | supine | dark | 3 | CCW | -30.6 |
| S | 4 | supine | dark | 4 | CW | 30.1 |
| S | 4 | supine | dark | 5 | CCW | -60.2 |
| S | 4 | supine | dark | 6 | CW | 45.3 |
| S | 4 | supine | dark | 7 | CW | 60.2 |
| S | 4 | supine | dark | 8 | CCW | -46.0 |

**Table D.2.  OKN SPV data.  SPV and SPV gain parameters for each trial.**

1. Max SPV:  maximum SPV during dome rotation calculated using the mean SPV for each individual slow phase.

2. Mean SPV:  mean SPV calculated over entire period of dome rotation

3. St. dev. SPV:  standard deviation of the SPV over period of dome rotation

4. Mean SPV gain:  mean SPV gain calculated by dividing mean SPV by dome speed.

5. St. dev. SPV gain:  standard deviation of SPV gain

| subject | Run # | trial | max. SPV deg/sec | max. SPV gain | mean SPV deg/sec | st. dev. SPV deg/sec | mean SPV gain | st. dev. SPV gain |
|---|---|---|---|---|---|---|---|---|
| M | 1 | 1 | 7.49 | 0.249 | 2.55 | 1.65 | 0.085 | 0.055 |
| M | 1 | 2 | -4.88 | 0.109 | -1.70 | 1.08 | 0.038 | 0.024 |
| M | 1 | 3 | -4.88 | 0.082 | -1.94 | 1.39 | 0.032 | 0.023 |
| M | 1 | 4 | 7.63 | 0.170 | 3.34 | 1.72 | 0.074 | 0.038 |
| M | 1 | 5 | -4.87 | 0.162 | -1.73 | 1.05 | 0.058 | 0.035 |
| M | 1 | 6 | 8.31 | 0.138 | 2.89 | 1.69 | 0.048 | 0.028 |
| M | 2 | 1 | 5.50 | 0.183 | 2.18 | 1.13 | 0.073 | 0.038 |
| M | 2 | 2 | -4.02 | 0.089 | -1.41 | 1.04 | 0.031 | 0.023 |
| M | 2 | 3 | -6.29 | 0.105 | -1.97 | 1.47 | 0.033 | 0.025 |
| M | 2 | 4 | 8.87 | 0.197 | 3.02 | 1.80 | 0.067 | 0.040 |
| M | 2 | 5 | -3.29 | 0.110 | -1.62 | 0.88 | 0.054 | 0.029 |
| M | 2 | 6 | 13.64 | 0.228 | 3.01 | 1.97 | 0.050 | 0.033 |
| M | 3 | 1 | -3.93 | 0.070 | -1.67 | 1.21 | 0.030 | 0.021 |
| M | 3 | 2 | -6.91 | 0.123 | -1.99 | 1.59 | 0.035 | 0.028 |
| M | 3 | 3 | -6.89 | 0.123 | -2.44 | 1.67 | 0.043 | 0.030 |
| M | 3 | 4 | -4.55 | 0.214 | -1.66 | 1.32 | 0.078 | 0.062 |
| M | 3 | 5 | 10.81 | 0.260 | 4.00 | 1.98 | 0.096 | 0.048 |
| M | 3 | 6 | -4.88 | 0.118 | -1.82 | 1.39 | 0.044 | 0.034 |
| M | 4 | 1 | 7.13 | 0.345 | 2.10 | 1.40 | 0.103 | 0.068 |
| M | 4 | 2 | -5.48 | 0.260 | -1.67 | 1.41 | 0.079 | 0.066 |
| M | 4 | 3 | -6.50 | 0.158 | -2.57 | 1.71 | 0.062 | 0.041 |
| M | 4 | 4 | 12.08 | 0.293 | 4.80 | 2.11 | 0.117 | 0.051 |
| M | 4 | 5 | 13.50 | 0.196 | 6.25 | 2.60 | 0.086 | 0.036 |
| M | 4 | 6 | 11.99 | 0.214 | 3.99 | 2.17 | 0.071 | 0.039 |
| M | 4 | 7 | -9.66 | 0.140 | -3.30 | 1.96 | 0.045 | 0.027 |
| M | 4 | 8 | -8.14 | 0.144 | -3.26 | 1.84 | 0.058 | 0.033 |
| M | 5 | 1 | 7.28 | 0.339 | 3.11 | 1.57 | 0.146 | 0.073 |
| M | 5 | 2 | -5.16 | 0.239 | -1.88 | 1.31 | 0.086 | 0.060 |
| M | 5 | 3 | -8.08 | 0.192 | -2.43 | 1.50 | 0.058 | 0.036 |
| M | 5 | 4 | 7.89 | 0.189 | 2.77 | 1.60 | 0.067 | 0.039 |
| M | 5 | 5 | -7.40 | 0.099 | -2.63 | 1.61 | 0.037 | 0.022 |
| M | 5 | 6 | 8.56 | 0.159 | 2.73 | 1.81 | 0.049 | 0.032 |
| M | 5 | 7 | 11.13 | 0.162 | 2.78 | 2.30 | 0.038 | 0.032 |
| M | 5 | 8 | -5.86 | 0.102 | -2.61 | 1.37 | 0.046 | 0.024 |

| subject | Run # | trial | max. SPV deg/sec | max. SPV gain | mean SPV deg/sec | st. dev. SPV deg/sec | mean SPV gain | st. dev. SPV gain |
|---------|-------|-------|------------------|---------------|------------------|----------------------|---------------|-------------------|
| N | 1 | 1 | -5.68 | 0.389 | -2.29 | 1.39 | 0.158 | 0.095 |
| N | 1 | 2 | 6.88 | 0.532 | 3.60 | 1.36 | 0.259 | 0.098 |
| N | 1 | 3 | -6.17 | 0.208 | -3.56 | 1.52 | 0.120 | 0.051 |
| N | 1 | 4 | 6.92 | 0.236 | 4.59 | 1.45 | 0.156 | 0.049 |
| N | 2 | 1 | -6.26 | 0.428 | -2.76 | 1.53 | 0.192 | 0.106 |
| N | 2 | 2 | 6.96 | 0.505 | 3.94 | 1.48 | 0.274 | 0.103 |
| N | 2 | 3 | -8.33 | 0.281 | -3.44 | 1.90 | 0.116 | 0.064 |
| N | 2 | 4 | 7.25 | 0.248 | 3.84 | 1.64 | 0.130 | 0.056 |
| N | 2 | 5 | -8.53 | 0.153 | -4.87 | 1.74 | 0.082 | 0.029 |
| N | 2 | 6 | 7.95 | 0.180 | 4.88 | 1.99 | 0.109 | 0.045 |
| N | 2 | 7 | 8.48 | 0.153 | 3.88 | 1.79 | 0.065 | 0.030 |
| N | 2 | 8 | -6.16 | 0.136 | -3.19 | 1.85 | 0.071 | 0.041 |
| N | 3 | 1 | 6.53 | 0.220 | 3.31 | 1.48 | 0.111 | 0.050 |
| N | 3 | 2 | -9.14 | 0.164 | -3.46 | 1.93 | 0.058 | 0.032 |
| N | 3 | 3 | -4.56 | 0.311 | -2.27 | 1.36 | 0.153 | 0.092 |
| N | 3 | 4 | 10.86 | 0.243 | 3.59 | 1.65 | 0.080 | 0.037 |
| N | 4 | 1 | 5.58 | 0.185 | 3.32 | 1.17 | 0.111 | 0.039 |
| N | 4 | 2 | -8.74 | 0.157 | -3.91 | 1.55 | 0.065 | 0.026 |
| N | 4 | 3 | -4.88 | 0.315 | -2.05 | 0.99 | 0.133 | 0.064 |
| N | 4 | 4 | 5.16 | 0.113 | 3.38 | 1.11 | 0.075 | 0.024 |
| N | 4 | 5 | 3.21 | 0.207 | 2.27 | 1.25 | 0.147 | 0.081 |
| N | 4 | 6 | -6.38 | 0.206 | -2.88 | 1.54 | 0.094 | 0.050 |
| N | 4 | 7 | 4.34 | 0.073 | 2.84 | 1.26 | 0.047 | 0.021 |
| N | 4 | 8 | 6.62 | 0.145 | 2.48 | 1.44 | 0.054 | 0.031 |
| N | 5 | 1 | -4.46 | 0.280 | -2.47 | 1.19 | 0.156 | 0.075 |
| N | 5 | 2 | 3.32 | 0.214 | 2.04 | 0.83 | 0.132 | 0.054 |
| N | 5 | 3 | -3.34 | 0.107 | -1.86 | 1.29 | 0.060 | 0.042 |
| N | 5 | 4 | 3.98 | 0.131 | 2.47 | 1.63 | 0.081 | 0.054 |
| N | 5 | 5 | -5.25 | 0.087 | -2.58 | 1.27 | 0.043 | 0.021 |
| N | 5 | 6 | 5.53 | 0.120 | 2.53 | 1.35 | 0.055 | 0.030 |
| N | 5 | 7 | 5.00 | 0.084 | 2.52 | 0.99 | 0.042 | 0.016 |
| N | 5 | 8 | -3.46 | 0.074 | -1.46 | 1.59 | 0.032 | 0.035 |

# OKN SPV data

| subject | Run # | trial | max. SPV deg/sec | max. SPV gain | mean SPV deg/sec | st. dev. SPV deg/sec | mean SPV gain | st. dev. SPV gain |
|---|---|---|---|---|---|---|---|---|
| O | 1 | 1 | 8.57 | 0.284 | 4.30 | 1.95 | 0.144 | 0.065 |
| O | 1 | 2 | -8.26 | 0.138 | -5.01 | 2.20 | 0.084 | 0.037 |
| O | 1 | 3 | -4.06 | 0.278 | -3.00 | 1.74 | 0.205 | 0.118 |
| O | 1 | 4 | 14.17 | 0.314 | 5.53 | 2.51 | 0.123 | 0.056 |
| O | 1 | 5 | 6.86 | 0.497 | 2.99 | 1.98 | 0.201 | 0.133 |
| O | 1 | 6 | -4.13 | 0.139 | -2.56 | 1.65 | 0.085 | 0.055 |
| O | 1 | 7 | 10.11 | 0.169 | 5.41 | 2.74 | 0.091 | 0.046 |
| O | 1 | 8 | -9.41 | 0.208 | -2.87 | 1.99 | 0.063 | 0.044 |
| O | 2 | 1 | -5.29 | 0.179 | -4.13 | 1.20 | 0.141 | 0.041 |
| O | 2 | 2 | 7.55 | 0.140 | 4.29 | 1.52 | 0.072 | 0.026 |
| O | 2 | 3 | -3.56 | 0.244 | -2.38 | 1.09 | 0.164 | 0.075 |
| O | 2 | 4 | 7.01 | 0.167 | 4.29 | 1.53 | 0.096 | 0.034 |
| O | 2 | 5 | 4.31 | 0.323 | 2.39 | 1.41 | 0.163 | 0.097 |
| O | 2 | 6 | 9.16 | 0.308 | 3.39 | 1.60 | 0.113 | 0.053 |
| O | 2 | 7 | -5.43 | 0.090 | -3.80 | 1.10 | 0.064 | 0.018 |
| O | 2 | 8 | -6.53 | 0.143 | -4.20 | 1.49 | 0.093 | 0.033 |
| O | 3 | 1 | -2.82 | 0.193 | -1.60 | 2.41 | 0.110 | 0.166 |
| O | 3 | 2 | 5.79 | 0.408 | 1.71 | 1.79 | 0.120 | 0.126 |
| O | 3 | 3 | -3.83 | 0.130 | -1.63 | 2.87 | 0.055 | 0.096 |
| O | 3 | 4 | 12.89 | 0.441 | 3.11 | 3.32 | 0.104 | 0.111 |
| O | 3 | 5 | -5.18 | 0.087 | -2.43 | 3.48 | 0.041 | 0.058 |
| O | 3 | 6 | 9.53 | 0.211 | 4.05 | 3.59 | 0.090 | 0.080 |
| O | 3 | 7 | 15.78 | 0.263 | 4.57 | 3.62 | 0.077 | 0.061 |
| O | 3 | 8 | -5.77 | 0.127 | -2.24 | 3.31 | 0.049 | 0.073 |
| O | 4 | 1 | -4.59 | 0.323 | -2.87 | 0.91 | 0.187 | 0.059 |
| O | 4 | 2 | 2.98 | 0.198 | 1.32 | 0.98 | 0.087 | 0.064 |
| O | 4 | 3 | -3.67 | 0.120 | -2.63 | 0.80 | 0.087 | 0.026 |
| O | 4 | 4 | 5.17 | 0.180 | 2.47 | 1.21 | 0.083 | 0.040 |
| O | 4 | 5 | 5.42 | 0.188 | 2.09 | 1.38 | 0.070 | 0.047 |
| O | 4 | 6 | -3.42 | 0.058 | -2.17 | 0.94 | 0.036 | 0.016 |
| O | 4 | 7 | -3.45 | 0.222 | -1.26 | 0.71 | 0.083 | 0.047 |
| O | 4 | 8 | 9.41 | 0.206 | 1.72 | 1.95 | 0.038 | 0.043 |
| O | 5 | 1 | 2.24 | 0.153 | 0.99 | 0.91 | 0.064 | 0.059 |
| O | 5 | 2 | -2.14 | 0.069 | -0.82 | 0.78 | 0.027 | 0.025 |
| O | 5 | 3 | 7.11 | 0.118 | 1.99 | 1.44 | 0.033 | 0.024 |
| O | 5 | 4 | -3.33 | 0.073 | -0.97 | 1.13 | 0.021 | 0.025 |
| O | 5 | 5 | 4.62 | 0.151 | 1.80 | 1.15 | 0.059 | 0.037 |
| O | 5 | 6 | -3.23 | 0.054 | -1.60 | 0.93 | 0.026 | 0.015 |
| O | 5 | 7 | -2.33 | 0.150 | -1.17 | 0.71 | 0.075 | 0.046 |
| O | 5 | 8 | 6.97 | 0.152 | 4.03 | 1.43 | 0.088 | 0.031 |

| subject | Run # | trial | max. SPV deg/sec | max. SPV gain | mean SPV deg/sec | st. dev. SPV deg/sec | mean SPV gain | st. dev. SPV gain |
|---|---|---|---|---|---|---|---|---|
| P | 1 | 1 | 7.11 | 0.236 | 2.97 | 1.32 | 0.100 | 0.045 |
| P | 1 | 2 | -9.00 | 0.150 | -4.56 | 2.02 | 0.077 | 0.034 |
| P | 1 | 3 | -7.87 | 0.538 | -3.51 | 1.55 | 0.240 | 0.106 |
| P | 1 | 4 | 8.59 | 0.192 | 3.34 | 1.42 | 0.075 | 0.032 |
| P | 1 | 5 | 5.03 | 0.344 | 2.16 | 1.11 | 0.146 | 0.075 |
| P | 1 | 6 | -9.71 | 0.327 | -3.91 | 1.61 | 0.130 | 0.054 |
| P | 1 | 7 | 8.49 | 0.142 | 4.10 | 1.85 | 0.069 | 0.031 |
| P | 1 | 8 | -11.91 | 0.263 | -5.17 | 2.95 | 0.114 | 0.065 |
| P | 2 | 1 | -8.00 | 0.546 | -3.38 | 1.36 | 0.228 | 0.092 |
| P | 2 | 2 | 3.78 | 0.258 | 1.67 | 1.03 | 0.114 | 0.070 |
| P | 2 | 3 | -11.41 | 0.379 | -4.22 | 1.81 | 0.140 | 0.060 |
| P | 2 | 4 | 5.56 | 0.187 | 2.72 | 1.64 | 0.091 | 0.055 |
| P | 2 | 5 | -12.20 | 0.202 | -5.05 | 2.59 | 0.084 | 0.043 |
| P | 2 | 6 | 10.51 | 0.233 | 3.01 | 1.73 | 0.067 | 0.038 |
| P | 2 | 7 | 7.59 | 0.126 | 3.62 | 1.92 | 0.060 | 0.032 |
| P | 2 | 8 | -9.66 | 0.213 | -4.02 | 2.92 | 0.088 | 0.064 |
| P | 3 | 1 | -8.52 | 0.566 | -2.93 | 1.51 | 0.197 | 0.102 |
| P | 3 | 2 | 6.73 | 0.489 | 1.93 | 1.26 | 0.136 | 0.088 |
| P | 3 | 3 | 5.44 | 0.186 | 2.52 | 1.38 | 0.087 | 0.048 |
| P | 3 | 4 | -9.29 | 0.157 | -4.62 | 2.01 | 0.078 | 0.034 |
| P | 3 | 5 | -7.74 | 0.529 | -2.76 | 1.71 | 0.187 | 0.116 |
| P | 3 | 6 | 13.02 | 0.294 | 2.95 | 1.61 | 0.067 | 0.036 |
| P | 3 | 7 | 3.93 | 0.305 | 1.83 | 1.10 | 0.124 | 0.075 |
| P | 3 | 8 | -8.14 | 0.270 | -3.62 | 1.69 | 0.121 | 0.056 |
| P | 4 | 1 | 8.38 | 0.143 | 3.55 | 1.64 | 0.060 | 0.028 |
| P | 4 | 2 | -8.69 | 0.193 | -3.57 | 2.16 | 0.079 | 0.048 |
| P | 4 | 3 | 5.38 | 0.182 | 2.10 | 1.37 | 0.071 | 0.046 |
| P | 4 | 4 | -10.44 | 0.176 | -4.27 | 1.79 | 0.072 | 0.030 |
| P | 4 | 5 | -8.11 | 0.538 | -2.77 | 1.51 | 0.184 | 0.100 |
| P | 4 | 6 | 5.44 | 0.130 | 2.63 | 1.38 | 0.059 | 0.031 |
| P | 4 | 7 | 5.36 | 0.346 | 2.12 | 1.59 | 0.139 | 0.105 |
| P | 4 | 8 | -5.60 | 0.188 | -2.76 | 1.66 | 0.091 | 0.055 |

| subject | Run # | trial | max. SPV deg/sec | max. SPV gain | mean SPV deg/sec | st. dev. SPV deg/sec | mean SPV gain | st. dev. SPV gain |
|---|---|---|---|---|---|---|---|---|
| Q | 1 | 1 | -2.41 | 0.164 | -1.35 | 1.28 | 0.093 | 0.088 |
| Q | 1 | 2 | 3.79 | 0.267 | 1.93 | 1.87 | 0.137 | 0.132 |
| Q | 1 | 3 | -3.76 | 0.126 | -2.20 | 1.61 | 0.074 | 0.054 |
| Q | 1 | 4 | 4.72 | 0.157 | 2.50 | 1.31 | 0.084 | 0.044 |
| Q | 1 | 5 | -7.96 | 0.133 | -2.53 | 1.47 | 0.042 | 0.025 |
| Q | 1 | 6 | 5.64 | 0.133 | 2.66 | 1.50 | 0.059 | 0.033 |
| Q | 1 | 7 | 6.79 | 0.113 | 3.22 | 2.11 | 0.054 | 0.035 |
| Q | 1 | 8 | -4.21 | 0.093 | -2.31 | 1.59 | 0.051 | 0.035 |
| Q | 2 | 1 | 6.35 | 0.213 | 2.12 | 2.85 | 0.070 | 0.095 |
| Q | 2 | 2 | -4.93 | 0.082 | -2.66 | 2.44 | 0.044 | 0.041 |
| Q | 2 | 3 | -2.84 | 0.194 | -1.53 | 2.71 | 0.103 | 0.182 |
| Q | 2 | 4 | 4.94 | 0.110 | 2.67 | 1.66 | 0.059 | 0.037 |
| Q | 2 | 5 | 2.90 | 0.198 | 1.38 | 0.95 | 0.093 | 0.064 |
| Q | 2 | 6 | -2.86 | 0.094 | -1.79 | 1.33 | 0.059 | 0.044 |
| Q | 2 | 7 | 5.39 | 0.090 | 3.44 | 1.81 | 0.057 | 0.030 |
| Q | 2 | 8 | -4.77 | 0.106 | -2.22 | 2.31 | 0.049 | 0.051 |
| Q | 3 | 1 | 4.83 | 0.168 | 2.20 | 0.96 | 0.075 | 0.033 |
| Q | 3 | 2 | -5.68 | 0.096 | -3.46 | 1.11 | 0.058 | 0.019 |
| Q | 3 | 3 | -2.61 | 0.174 | -1.37 | 0.72 | 0.093 | 0.048 |
| Q | 3 | 4 | 4.94 | 0.110 | 2.77 | 1.00 | 0.062 | 0.022 |
| Q | 3 | 5 | 3.43 | 0.242 | 0.97 | 0.75 | 0.066 | 0.051 |
| Q | 3 | 6 | -4.62 | 0.153 | -2.27 | 1.00 | 0.075 | 0.033 |
| Q | 3 | 7 | 6.87 | 0.115 | 3.52 | 1.28 | 0.059 | 0.021 |
| Q | 3 | 8 | -4.53 | 0.099 | -2.62 | 0.90 | 0.058 | 0.020 |
| Q | 4 | 1 | -3.95 | 0.255 | -1.32 | 0.66 | 0.086 | 0.043 |
| Q | 4 | 2 | 2.88 | 0.192 | 1.12 | 0.81 | 0.074 | 0.054 |
| Q | 4 | 3 | -4.18 | 0.137 | -2.07 | 0.83 | 0.068 | 0.027 |
| Q | 4 | 4 | 2.10 | 0.073 | 1.46 | 0.70 | 0.049 | 0.023 |
| Q | 4 | 5 | -5.15 | 0.086 | -3.10 | 1.02 | 0.052 | 0.017 |
| Q | 4 | 6 | 3.27 | 0.074 | 1.91 | 0.90 | 0.042 | 0.020 |
| Q | 4 | 7 | 5.78 | 0.096 | 3.06 | 1.09 | 0.051 | 0.018 |
| Q | 4 | 8 | -4.03 | 0.088 | -2.40 | 0.91 | 0.052 | 0.020 |

# OKN SPV data

| subject | Run # | trial | max. SPV deg/sec | max. SPV gain | mean SPV deg/sec | st. dev. SPV deg/sec | mean SPV gain | st. dev. SPV gain |
|---|---|---|---|---|---|---|---|---|
| R | 1 | 1 | 7.94 | 0.271 | 4.34 | 1.29 | 0.147 | 0.044 |
| R | 1 | 2 | -11.93 | 0.199 | -6.92 | 2.27 | 0.116 | 0.038 |
| R | 1 | 3 | -7.49 | 0.528 | -3.76 | 1.52 | 0.261 | 0.105 |
| R | 1 | 4 | 8.58 | 0.194 | 5.12 | 1.49 | 0.115 | 0.033 |
| R | 1 | 5 | 5.48 | 0.374 | 2.54 | 1.15 | 0.174 | 0.079 |
| R | 1 | 6 | -10.97 | 0.365 | -6.27 | 1.87 | 0.208 | 0.062 |
| R | 1 | 7 | 11.62 | 0.194 | 5.40 | 2.11 | 0.090 | 0.035 |
| R | 1 | 8 | -11.10 | 0.244 | -6.04 | 2.27 | 0.133 | 0.050 |
| R | 2 | 1 | -7.28 | 0.497 | -3.28 | 1.55 | 0.220 | 0.104 |
| R | 2 | 2 | 3.81 | 0.260 | 1.96 | 1.10 | 0.135 | 0.076 |
| R | 2 | 3 | -7.20 | 0.235 | -4.08 | 2.34 | 0.135 | 0.077 |
| R | 2 | 4 | 7.97 | 0.269 | 3.49 | 1.98 | 0.118 | 0.067 |
| R | 2 | 5 | -9.70 | 0.162 | -6.31 | 2.74 | 0.105 | 0.046 |
| R | 2 | 6 | 7.16 | 0.160 | 4.20 | 2.71 | 0.094 | 0.060 |
| R | 2 | 7 | 7.53 | 0.125 | 4.03 | 2.51 | 0.067 | 0.042 |
| R | 2 | 8 | -7.72 | 0.171 | -4.55 | 2.68 | 0.100 | 0.059 |

# OKN SPV data

| subject | Run # | trial | max. SPV deg/sec | max. SPV gain | mean SPV deg/sec | st. dev. SPV deg/sec | mean SPV gain | st. dev. SPV gain |
|---|---|---|---|---|---|---|---|---|
| S | 1 | 1 | -6.44 | 0.428 | -3.68 | 2.87 | 0.249 | 0.194 |
| S | 1 | 2 | 7.49 | 0.527 | 3.58 | 2.71 | 0.251 | 0.190 |
| S | 1 | 3 | -12.14 | 0.409 | -6.06 | 3.76 | 0.202 | 0.126 |
| S | 1 | 4 | 9.76 | 0.333 | 5.41 | 3.53 | 0.184 | 0.120 |
| S | 1 | 5 | -11.07 | 0.185 | -6.84 | 3.33 | 0.114 | 0.056 |
| S | 1 | 6 | 9.96 | 0.220 | 5.48 | 3.47 | 0.122 | 0.077 |
| S | 1 | 7 | 13.15 | 0.219 | 6.26 | 3.54 | 0.104 | 0.059 |
| S | 1 | 8 | -8.83 | 0.195 | -4.51 | 3.49 | 0.099 | 0.077 |
| S | 2 | 1 | 9.79 | 0.324 | 4.99 | 1.64 | 0.166 | 0.055 |
| S | 2 | 2 | -12.86 | 0.213 | -6.67 | 2.16 | 0.111 | 0.036 |
| S | 2 | 3 | -5.91 | 0.382 | -3.17 | 1.83 | 0.210 | 0.121 |
| S | 2 | 4 | 20.66 | 0.457 | 5.31 | 3.72 | 0.117 | 0.082 |
| S | 2 | 5 | 6.91 | 0.446 | 3.60 | 3.31 | 0.239 | 0.220 |
| S | 2 | 6 | -9.49 | 0.307 | -4.81 | 3.63 | 0.158 | 0.119 |
| S | 2 | 7 | 14.16 | 0.237 | 6.20 | 3.03 | 0.103 | 0.051 |
| S | 2 | 8 | -20.78 | 0.455 | -5.80 | 3.37 | 0.127 | 0.074 |
| S | 3 | 1 | 10.24 | 0.345 | 5.50 | 1.72 | 0.185 | 0.058 |
| S | 3 | 2 | -11.67 | 0.195 | -6.44 | 2.03 | 0.108 | 0.034 |
| S | 3 | 3 | -5.31 | 0.343 | -2.95 | 1.00 | 0.194 | 0.066 |
| S | 3 | 4 | 14.15 | 0.314 | 6.35 | 1.75 | 0.141 | 0.039 |
| S | 3 | 5 | 7.46 | 0.495 | 2.85 | 1.31 | 0.187 | 0.085 |
| S | 3 | 6 | -10.15 | 0.336 | -4.37 | 1.59 | 0.143 | 0.052 |
| S | 3 | 7 | 10.55 | 0.175 | 5.37 | 2.02 | 0.090 | 0.034 |
| S | 3 | 8 | -9.56 | 0.209 | -4.82 | 1.83 | 0.105 | 0.040 |
| S | 4 | 1 | -4.46 | 0.288 | -2.59 | 0.95 | 0.167 | 0.061 |
| S | 4 | 2 | 7.79 | 0.503 | 2.00 | 1.16 | 0.131 | 0.076 |
| S | 4 | 3 | -7.15 | 0.231 | -3.56 | 1.62 | 0.116 | 0.053 |
| S | 4 | 4 | 10.99 | 0.360 | 4.12 | 1.72 | 0.137 | 0.057 |
| S | 4 | 5 | -8.55 | 0.142 | -4.76 | 1.71 | 0.079 | 0.028 |
| S | 4 | 6 | 10.06 | 0.221 | 4.25 | 1.98 | 0.094 | 0.044 |
| S | 4 | 7 | 13.83 | 0.230 | 5.35 | 2.29 | 0.089 | 0.038 |
| S | 4 | 8 | -10.27 | 0.225 | -4.32 | 1.64 | 0.094 | 0.036 |

**Table D.3.** **SPV data: vection vs. no vection**

1. Mean SPV; state 1: mean SPV during total period of vection for each trial

2. St. dev. SPV; state 1: standard deviation of SPV during vection period

3. Mean SPV; state 2: mean SPV during total period without vection for each trial

4. St. dev. SPV; state 2: standard deviation of SPV during no-vection periods.

5. SPV ratio; st 1 / st 2: Ratio of mean SPV in state 1 (vection) to mean SPV in state 2 (no vection)

# SPV data:  vection vs. no vection

| Subject | Run # | Trial # | mean SPV state 1 (deg/s) | st. dev. SPV state 1 (deg/s) | mean SPV state 2 (deg/s) | st. dev. SPV state 2 (deg/s) | SPV ratio st 1 / st 2 |
|---|---|---|---|---|---|---|---|
| M | 1 | 1 | -- | -- | -- | -- | -- |
| M | 1 | 2 | -1.82 | 1.06 | -1.08 | 0.92 | 1.69 |
| M | 1 | 3 | -2.19 | 1.13 | -1.28 | 1.76 | 1.71 |
| M | 1 | 4 | 3.53 | 1.62 | 1.07 | 0.95 | 3.30 |
| M | 1 | 5 | -1.82 | 1.02 | -0.63 | 0.76 | 2.91 |
| M | 1 | 6 | 2.96 | 1.69 | 2.35 | 1.66 | 1.26 |
| M | 2 | 1 | 2.34 | 1.04 | 0.61 | 0.67 | 3.83 |
| M | 2 | 2 | -1.48 | 1.02 | -0.31 | 0.67 | 4.78 |
| M | 2 | 3 | -2.09 | 1.44 | -0.43 | 1.02 | 4.83 |
| M | 2 | 4 | 3.08 | 1.85 | 2.49 | 1.17 | 1.24 |
| M | 2 | 5 | -1.65 | 0.85 | -1.36 | 1.05 | 1.22 |
| M | 2 | 6 | 3.08 | 1.99 | 2.33 | 1.65 | 1.32 |
| M | 3 | 1 | -1.78 | 1.13 | -0.76 | 1.43 | 2.35 |
| M | 3 | 2 | -2.17 | 1.60 | -1.06 | 1.21 | 2.05 |
| M | 3 | 3 | -2.64 | 1.55 | -1.63 | 1.84 | 1.62 |
| M | 3 | 4 | -1.87 | 1.18 | -1.32 | 1.46 | 1.41 |
| M | 3 | 5 | 4.37 | 1.84 | 1.77 | 1.08 | 2.47 |
| M | 3 | 6 | -2.06 | 1.39 | -1.03 | 1.08 | 2.00 |
| M | 4 | 1 | 2.19 | 1.38 | 1.50 | 1.32 | 1.45 |
| M | 4 | 2 | -1.91 | 1.34 | -0.35 | 0.99 | 5.47 |
| M | 4 | 3 | -2.85 | 1.60 | -0.74 | 1.20 | 3.86 |
| M | 4 | 4 | 5.06 | 2.01 | 2.89 | 1.86 | 1.75 |
| M | 4 | 5 | 6.46 | 2.36 | 4.91 | 3.43 | 1.32 |
| M | 4 | 6 | 4.01 | 2.15 | 3.88 | 2.26 | 1.03 |
| M | 4 | 7 | -3.46 | 1.82 | -2.43 | 2.41 | 1.42 |
| M | 4 | 8 | -3.30 | 1.75 | -3.03 | 2.26 | 1.09 |
| M | 5 | 1 | 3.29 | 1.50 | 1.52 | 1.18 | 2.16 |
| M | 5 | 2 | -1.99 | 1.30 | -0.87 | 0.98 | 2.28 |
| M | 5 | 3 | -2.38 | 1.45 | -2.58 | 1.67 | 0.92 |
| M | 5 | 4 | 2.74 | 1.55 | 2.84 | 1.74 | 0.97 |
| M | 5 | 5 | -2.61 | 1.59 | -2.75 | 1.73 | 0.95 |
| M | 5 | 6 | 2.58 | 1.64 | 3.76 | 2.49 | 0.69 |
| M | 5 | 7 | 2.64 | 2.14 | 3.45 | 2.87 | 0.77 |
| M | 5 | 8 | -2.83 | 1.23 | -1.48 | 1.49 | 1.91 |

SPV data: vection vs. no vection

| Subject | Run # | Trial # | mean SPV state 1 (deg/s) | st. dev. SPV state 1 (deg/s) | mean SPV state 2 (deg/s) | st. dev. SPV state 2 (deg/s) | SPV ratio st 1 / st 2 |
|---|---|---|---|---|---|---|---|
| N | 1 | 1 | -1.95 | 1.39 | -2.46 | 1.35 | 0.79 |
| N | 1 | 2 | 3.57 | 1.21 | 3.72 | 1.78 | 0.96 |
| N | 1 | 3 | -3.61 | 1.42 | -3.47 | 1.67 | 1.04 |
| N | 1 | 4 | 4.66 | 1.43 | 4.33 | 1.48 | 1.08 |
| N | 2 | 1 | -2.70 | 1.52 | -2.85 | 1.53 | 0.95 |
| N | 2 | 2 | 4.10 | 1.33 | 3.60 | 1.72 | 1.14 |
| N | 2 | 3 | -3.37 | 1.94 | -3.62 | 1.76 | 0.93 |
| N | 2 | 4 | 3.39 | 1.52 | 4.73 | 1.49 | 0.72 |
| N | 2 | 5 | -4.83 | 1.70 | -5.02 | 1.88 | 0.96 |
| N | 2 | 6 | 4.69 | 1.98 | 5.70 | 1.83 | 0.82 |
| N | 2 | 7 | 3.62 | 1.75 | 4.74 | 1.66 | 0.76 |
| N | 2 | 8 | -2.92 | 1.84 | -3.64 | 1.79 | 0.80 |
| N | 3 | 1 | 3.02 | 1.36 | 3.99 | 1.54 | 0.76 |
| N | 3 | 2 | -3.39 | 1.81 | -3.62 | 2.16 | 0.94 |
| N | 3 | 3 | -2.27 | 1.20 | -2.27 | 1.42 | 1.00 |
| N | 3 | 4 | 3.53 | 1.70 | 3.85 | 1.41 | 0.92 |
| N | 4 | 1 | 3.32 | 1.18 | 3.33 | 1.13 | 1.00 |
| N | 4 | 2 | -3.79 | 1.50 | -4.25 | 1.65 | 0.89 |
| N | 4 | 3 | -- | -- | -- | -- | -- |
| N | 4 | 4 | 3.26 | 1.04 | 3.66 | 1.21 | 0.89 |
| N | 4 | 5 | 2.38 | 1.42 | 2.24 | 1.19 | 1.06 |
| N | 4 | 6 | -2.57 | 1.48 | -3.21 | 1.53 | 0.80 |
| N | 4 | 7 | 2.87 | 1.17 | 2.80 | 1.34 | 1.02 |
| N | 4 | 8 | 2.33 | 1.35 | 2.84 | 1.59 | 0.82 |
| N | 5 | 1 | -- | -- | -- | -- | -- |
| N | 5 | 2 | 1.90 | 0.71 | 2.09 | 0.86 | 0.91 |
| N | 5 | 3 | -1.36 | 1.17 | -1.98 | 1.29 | 0.69 |
| N | 5 | 4 | 2.54 | 1.46 | 2.35 | 1.88 | 1.08 |
| N | 5 | 5 | -2.31 | 1.15 | -2.87 | 1.32 | 0.81 |
| N | 5 | 6 | -- | -- | -- | -- | -- |
| N | 5 | 7 | -- | -- | -- | -- | -- |
| N | 5 | 8 | -0.88 | 2.12 | -1.67 | 1.30 | 0.53 |

# SPV data:  vection vs. no vection

| Subject | Run # | Trial # | mean SPV state 1 (deg/s) | st. dev. SPV state 1 | mean SPV state 2 (deg/s) | st. dev. SPV state 2 | SPV ratio st 1 / st 2 |
|---|---|---|---|---|---|---|---|
| O | 1 | 1 | 4.54 | 1.85 | 2.94 | 1.92 | 1.55 |
| O | 1 | 2 | -5.09 | 2.19 | -4.25 | 2.11 | 1.20 |
| O | 1 | 3 | -3.08 | 1.67 | -2.67 | 1.94 | 1.16 |
| O | 1 | 4 | 5.46 | 2.48 | 5.77 | 2.61 | 0.95 |
| O | 1 | 5 | 2.94 | 2.00 | 3.10 | 1.95 | 0.95 |
| O | 1 | 6 | -2.56 | 1.55 | -2.53 | 2.01 | 1.01 |
| O | 1 | 7 | 5.06 | 2.62 | 7.60 | 2.45 | 0.67 |
| O | 1 | 8 | -2.83 | 2.05 | -3.32 | 1.22 | 0.85 |
| O | 2 | 1 | -4.17 | 1.10 | -3.41 | 2.25 | 1.22 |
| O | 2 | 2 | 4.14 | 1.36 | 5.04 | 2.01 | 0.82 |
| O | 2 | 3 | -2.42 | 1.02 | -2.31 | 1.22 | 1.05 |
| O | 2 | 4 | 4.25 | 1.40 | 4.47 | 2.04 | 0.95 |
| O | 2 | 5 | 2.31 | 1.32 | 3.17 | 1.98 | 0.73 |
| O | 2 | 6 | 3.37 | 1.57 | 3.56 | 1.78 | 0.95 |
| O | 2 | 7 | -3.83 | 1.05 | -3.32 | 1.72 | 1.15 |
| O | 2 | 8 | -4.16 | 1.41 | -4.58 | 2.06 | 0.91 |
| O | 3 | 1 | -1.59 | 2.46 | -1.69 | 1.98 | 0.94 |
| O | 3 | 2 | 1.68 | 1.78 | 1.78 | 1.81 | 0.94 |
| O | 3 | 3 | -1.74 | 2.87 | -1.11 | 2.82 | 1.56 |
| O | 3 | 4 | 3.07 | 3.31 | 3.73 | 3.35 | 0.82 |
| O | 3 | 5 | -2.99 | 3.39 | -1.49 | 3.43 | 2.01 |
| O | 3 | 6 | 3.93 | 3.53 | 5.04 | 3.87 | 0.78 |
| O | 3 | 7 | 4.52 | 3.60 | 5.66 | 3.94 | 0.80 |
| O | 3 | 8 | -2.34 | 3.32 | -1.87 | 3.25 | 1.25 |
| O | 4 | 1 | -2.87 | 0.85 | -2.88 | 1.16 | 1.00 |
| O | 4 | 2 | 1.25 | 0.78 | 1.61 | 1.48 | 0.78 |
| O | 4 | 3 | -2.59 | 0.74 | -2.85 | 1.05 | 0.91 |
| O | 4 | 4 | 2.37 | 1.17 | 3.61 | 1.01 | 0.66 |
| O | 4 | 5 | 2.04 | 1.33 | 2.84 | 1.90 | 0.72 |
| O | 4 | 6 | -2.17 | 0.91 | -2.16 | 1.33 | 1.00 |
| O | 4 | 7 | -1.15 | 0.68 | -1.47 | 0.73 | 0.78 |
| O | 4 | 8 | 1.64 | 1.91 | 3.77 | 1.64 | 0.43 |
| O | 5 | 1 | 0.92 | 0.86 | 1.93 | 1.03 | 0.47 |
| O | 5 | 2 | -0.75 | 0.75 | -1.47 | 0.71 | 0.51 |
| O | 5 | 3 | 1.95 | 1.40 | 3.11 | 1.98 | 0.63 |
| O | 5 | 4 | -0.95 | 1.16 | -1.10 | 0.75 | 0.87 |
| O | 5 | 5 | 1.78 | 1.06 | 2.02 | 1.66 | 0.88 |
| O | 5 | 6 | -1.53 | 0.93 | -1.98 | 0.83 | 0.78 |
| O | 5 | 7 | -1.17 | 0.68 | -1.17 | 0.73 | 1.00 |
| O | 5 | 8 | 4.55 | 1.61 | 3.90 | 1.35 | 1.17 |

# SPV data: vection vs. no vection

| Subject | Run # | Trial # | mean SPV state 1 (deg/s) | st. dev. SPV state 1 (deg/s) | mean SPV state 2 (deg/s) | st. dev. SPV state 2 (deg/s) | SPV ratio st 1 / st 2 |
|---------|-------|---------|------|------|------|------|------|
| P | 1 | 1 | 2.94 | 1.25 | 3.11 | 1.62 | 0.95 |
| P | 1 | 2 | -4.87 | 2.04 | -3.85 | 1.77 | 1.27 |
| P | 1 | 3 | -3.66 | 0.82 | -3.49 | 1.60 | 1.05 |
| P | 1 | 4 | 3.36 | 1.37 | 3.23 | 1.64 | 1.04 |
| P | 1 | 5 | 2.36 | 1.13 | 1.71 | 0.89 | 1.38 |
| P | 1 | 6 | -4.20 | 1.71 | -3.33 | 1.20 | 1.26 |
| P | 1 | 7 | 4.29 | 1.85 | 3.31 | 1.61 | 1.29 |
| P | 1 | 8 | -5.30 | 2.51 | -5.04 | 3.35 | 1.05 |
| P | 2 | 1 | -3.66 | 1.33 | -3.19 | 1.35 | 1.15 |
| P | 2 | 2 | 1.80 | 1.02 | 1.09 | 0.87 | 1.66 |
| P | 2 | 3 | -4.48 | 1.88 | -3.49 | 1.31 | 1.28 |
| P | 2 | 4 | 2.92 | 1.67 | 1.94 | 1.27 | 1.50 |
| P | 2 | 5 | -5.32 | 2.55 | -3.77 | 2.39 | 1.41 |
| P | 2 | 6 | 3.02 | 1.71 | 2.94 | 1.90 | 1.03 |
| P | 2 | 7 | 3.62 | 1.95 | 3.56 | 1.54 | 1.02 |
| P | 2 | 8 | -4.17 | 2.93 | -3.74 | 2.88 | 1.12 |
| P | 3 | 1 | -3.15 | 1.51 | -2.31 | 1.32 | 1.37 |
| P | 3 | 2 | 2.04 | 1.26 | 1.43 | 1.09 | 1.43 |
| P | 3 | 3 | 2.59 | 1.39 | 1.75 | 1.10 | 1.48 |
| P | 3 | 4 | -4.73 | 2.00 | -3.02 | 1.19 | 1.57 |
| P | 3 | 5 | -3.30 | 1.65 | -2.26 | 1.61 | 1.46 |
| P | 3 | 6 | 2.96 | 1.65 | 2.86 | 1.09 | 1.04 |
| P | 3 | 7 | 1.88 | 1.04 | 1.65 | 1.28 | 1.13 |
| P | 3 | 8 | -3.76 | 1.66 | -2.58 | 1.51 | 1.45 |
| P | 4 | 1 | 3.57 | 1.63 | 2.72 | 1.84 | 1.31 |
| P | 4 | 2 | -3.59 | 2.18 | -3.37 | 2.00 | 1.07 |
| P | 4 | 3 | 2.25 | 1.32 | 1.15 | 1.27 | 1.96 |
| P | 4 | 4 | -4.36 | 1.79 | -3.19 | 1.41 | 1.37 |
| P | 4 | 5 | -2.87 | 1.57 | -2.62 | 1.40 | 1.10 |
| P | 4 | 6 | 2.64 | 1.36 | 2.52 | 1.63 | 1.05 |
| P | 4 | 7 | 2.16 | 1.55 | 1.79 | 1.95 | 1.20 |
| P | 4 | 8 | -2.86 | 1.66 | -2.21 | 1.57 | 1.30 |

SPV data: vection vs. no vection

| Subject | Run # | Trial # | mean SPV state 1 (deg/s) | st. dev. SPV state 1 (deg/s) | mean SPV state 2 (deg/s) | st. dev. SPV state 2 (deg/s) | SPV ratio st 1 / st 2 |
|---|---|---|---|---|---|---|---|
| Q | 1 | 1 | -1.37 | 1.28 | -1.30 | 1.27 | 1.06 |
| Q | 1 | 2 | 1.91 | 1.83 | 2.10 | 2.10 | 0.91 |
| Q | 1 | 3 | -2.21 | 1.60 | -2.03 | 1.79 | 1.09 |
| Q | 1 | 4 | 2.47 | 1.26 | 2.72 | 1.66 | 0.91 |
| Q | 1 | 5 | -2.51 | 1.42 | -3.06 | 2.28 | 0.82 |
| Q | 1 | 6 | 2.61 | 1.45 | 3.13 | 1.80 | 0.84 |
| Q | 1 | 7 | 3.17 | 2.07 | 3.73 | 2.49 | 0.85 |
| Q | 1 | 8 | -2.32 | 1.61 | -2.22 | 1.46 | 1.05 |
| Q | 2 | 1 | 2.05 | 2.81 | 2.30 | 2.94 | 0.89 |
| Q | 2 | 2 | -2.56 | 2.36 | -3.86 | 3.00 | 0.66 |
| Q | 2 | 3 | -1.52 | 2.61 | -1.56 | 2.91 | 0.97 |
| Q | 2 | 4 | 2.65 | 1.63 | 2.94 | 2.16 | 0.90 |
| Q | 2 | 5 | 1.36 | 0.85 | 1.47 | 1.37 | 0.93 |
| Q | 2 | 6 | -1.74 | 1.33 | -2.28 | 1.28 | 0.76 |
| Q | 2 | 7 | 3.39 | 1.74 | 3.79 | 2.21 | 0.89 |
| Q | 2 | 8 | -2.18 | 2.26 | -2.58 | 2.74 | 0.84 |
| Q | 3 | 1 | 2.13 | 0.80 | 2.30 | 1.14 | 0.93 |
| Q | 3 | 2 | -3.85 | 0.98 | -2.79 | 0.99 | 1.38 |
| Q | 3 | 3 | -1.71 | 0.66 | -1.34 | 0.71 | 1.27 |
| Q | 3 | 4 | 2.81 | 0.93 | 2.52 | 1.36 | 1.12 |
| Q | 3 | 5 | 0.84 | 0.61 | 1.05 | 0.81 | 0.80 |
| Q | 3 | 6 | -2.39 | 0.97 | -1.34 | 0.71 | 1.78 |
| Q | 3 | 7 | 3.58 | 1.27 | 2.93 | 1.24 | 1.22 |
| Q | 3 | 8 | -2.70 | 0.95 | -2.50 | 0.80 | 1.08 |
| Q | 4 | 1 | -1.47 | 0.70 | -1.26 | 0.64 | 1.16 |
| Q | 4 | 2 | 1.38 | 0.67 | 1.02 | 0.84 | 1.35 |
| Q | 4 | 3 | -2.31 | 0.87 | -1.85 | 0.74 | 1.25 |
| Q | 4 | 4 | 1.46 | 0.68 | 1.43 | 0.77 | 1.02 |
| Q | 4 | 5 | -3.16 | 0.99 | -2.53 | 1.11 | 1.25 |
| Q | 4 | 6 | 1.94 | 0.89 | 1.72 | 0.93 | 1.13 |
| Q | 4 | 7 | 3.13 | 1.09 | 2.55 | 0.99 | 1.23 |
| Q | 4 | 8 | -2.44 | 0.88 | -2.25 | 1.03 | 1.08 |

# SPV data: vection vs. no vection

| Subject | Run # | Trial # | mean SPV state 1 (deg/s) | st. dev. SPV state 1 (deg/s) | mean SPV state 2 (deg/s) | st. dev. SPV state 2 (deg/s) | SPV ratio st 1 / st 2 |
|---|---|---|---|---|---|---|---|
| R | 1 | 1 | -- | -- | -- | -- | -- |
| R | 1 | 2 | -7.34 | 2.25 | -6.20 | 2.13 | 1.19 |
| R | 1 | 3 | -3.99 | 1.46 | -3.12 | 1.52 | 1.28 |
| R | 1 | 4 | 6.40 | 1.52 | 4.97 | 1.42 | 1.29 |
| R | 1 | 5 | 2.62 | 1.13 | 2.49 | 1.16 | 1.05 |
| R | 1 | 6 | -6.56 | 1.65 | -5.91 | 2.06 | 1.11 |
| R | 1 | 7 | 5.97 | 2.44 | 5.05 | 1.80 | 1.18 |
| R | 1 | 8 | -5.49 | 2.11 | -6.12 | 2.28 | 0.90 |
| R | 2 | 1 | -- | -- | -- | -- | -- |
| R | 2 | 2 | -- | -- | -- | -- | -- |
| R | 2 | 3 | -- | -- | -- | -- | -- |
| R | 2 | 4 | 3.42 | 2.10 | 3.50 | 1.96 | 0.98 |
| R | 2 | 5 | -- | -- | -- | -- | -- |
| R | 2 | 6 | -- | -- | -- | -- | -- |
| R | 2 | 7 | -- | -- | -- | -- | -- |
| R | 2 | 8 | -- | -- | -- | -- | -- |

# SPV data: vection vs. no vection

| Subject | Run # | Trial # | mean SPV state 1 (deg/s) | st. dev. SPV state 1 (deg/s) | mean SPV state 2 (deg/s) | st. dev. SPV state 2 (deg/s) | SPV ratio st 1 / st 2 |
|---|---|---|---|---|---|---|---|
| S | 1 | 1 | -3.80 | 2.88 | -2.83 | 2.62 | 1.34 |
| S | 1 | 2 | 3.63 | 2.67 | 2.57 | 3.18 | 1.41 |
| S | 1 | 3 | -6.31 | 3.68 | -3.75 | 3.65 | 1.68 |
| S | 1 | 4 | 5.55 | 3.49 | 3.77 | 3.58 | 1.47 |
| S | 1 | 5 | -6.92 | 3.29 | -5.98 | 3.71 | 1.16 |
| S | 1 | 6 | 5.60 | 3.42 | 3.69 | 3.57 | 1.52 |
| S | 1 | 7 | 6.30 | 3.54 | 5.44 | 3.54 | 1.16 |
| S | 1 | 8 | -4.64 | 3.47 | -3.72 | 3.50 | 1.25 |
| S | 2 | 1 | 5.04 | 1.61 | 4.35 | 1.82 | 1.16 |
| S | 2 | 2 | -6.74 | 2.16 | -6.02 | 2.07 | 1.12 |
| S | 2 | 3 | -3.19 | 1.83 | -2.95 | 1.83 | 1.08 |
| S | 2 | 4 | 5.33 | 3.68 | 4.89 | 4.34 | 1.09 |
| S | 2 | 5 | 3.61 | 3.30 | 3.31 | 3.46 | 1.09 |
| S | 2 | 6 | -4.81 | 3.61 | -4.88 | 3.90 | 0.99 |
| S | 2 | 7 | 6.18 | 2.97 | 6.75 | 4.21 | 0.91 |
| S | 2 | 8 | -5.80 | 3.33 | -5.78 | 3.89 | 1.00 |
| S | 3 | 1 | 5.66 | 1.66 | 3.29 | 0.78 | 1.72 |
| S | 3 | 2 | -6.47 | 1.92 | -5.71 | 3.62 | 1.13 |
| S | 3 | 3 | -3.00 | 0.95 | -2.27 | 1.35 | 1.32 |
| S | 3 | 4 | 6.39 | 1.75 | 5.93 | 1.78 | 1.08 |
| S | 3 | 5 | 2.88 | 1.29 | 2.39 | 1.45 | 1.21 |
| S | 3 | 6 | -4.44 | 1.56 | -2.86 | 1.66 | 1.55 |
| S | 3 | 7 | 5.21 | 1.92 | 6.89 | 2.33 | 0.76 |
| S | 3 | 8 | -4.89 | 1.78 | -3.42 | 2.17 | 1.43 |
| S | 4 | 1 | -2.63 | 0.93 | -2.20 | 1.02 | 1.20 |
| S | 4 | 2 | 2.02 | 1.16 | 1.64 | 1.02 | 1.23 |
| S | 4 | 3 | -3.59 | 1.61 | -2.99 | 1.75 | 1.20 |
| S | 4 | 4 | 4.21 | 1.71 | 2.90 | 1.34 | 1.45 |
| S | 4 | 5 | -4.78 | 1.65 | -4.50 | 2.37 | 1.06 |
| S | 4 | 6 | 4.32 | 1.97 | 2.51 | 1.02 | 1.72 |
| S | 4 | 7 | 5.21 | 2.17 | 6.86 | 2.83 | 0.76 |
| S | 4 | 8 | -4.37 | 1.61 | -3.31 | 1.73 | 1.32 |

**Table D.4. Eye position data. Values for mean eye position and mean reset position during OKN.**

1. mean position: mean eye position during OKN

2. st. dev. position: standard deviation of eye position during OKN.

3. mean reset position: mean of eye positions at end of each fast phase during OKN.

4. st. dev. reset position: standard deviation of fast phase reset positions during OKN

5. deviation range: peak-to-peak eye position range during OKN

6. position at dome stop: eye position immediately prior to the stop of the dome

# Eye position data

| Subject | Run # | Trial # | mean position (deg) | st. dev. position (deg) | mean reset position (deg) | st. dev. reset position (deg) | deviation range (deg) | position at dome stop (deg) |
|---|---|---|---|---|---|---|---|---|
| M | 1 | 1 | -0.65 | 1.03 | -1.41 | 1.13 | 4.77 | -1.65 |
| M | 1 | 2 | 0.79 | 0.94 | 1.52 | 0.93 | 5.76 | -0.78 |
| M | 1 | 3 | 1.61 | 0.85 | 2.20 | 0.92 | 6.18 | -0.26 |
| M | 1 | 4 | -2.92 | 1.20 | -3.67 | 1.15 | 6.88 | -2.53 |
| M | 1 | 5 | 1.54 | 0.78 | 2.04 | 0.91 | 4.59 | -0.99 |
| M | 1 | 6 | -2.18 | 1.07 | -2.98 | 1.04 | 7.50 | 0.37 |
| M | 2 | 1 | -1.18 | 0.89 | -1.81 | 0.82 | 5.76 | -1.07 |
| M | 2 | 2 | 1.66 | 0.96 | 2.38 | 0.97 | 4.37 | -0.77 |
| M | 2 | 3 | 1.02 | 1.10 | 1.82 | 1.17 | 5.83 | -1.61 |
| M | 2 | 4 | -2.63 | 1.27 | -3.30 | 1.39 | 7.81 | -1.69 |
| M | 2 | 5 | 1.46 | 0.62 | 1.88 | 0.65 | 3.76 | -5.05 |
| M | 2 | 6 | -2.85 | 1.30 | -3.59 | 1.46 | 8.81 | 1.31 |
| M | 3 | 1 | 2.77 | 1.09 | 3.73 | 0.89 | 5.83 | -2.79 |
| M | 3 | 2 | 3.75 | 1.66 | 4.89 | 1.58 | 8.57 | -3.99 |
| M | 3 | 3 | 3.79 | 1.50 | 4.77 | 1.41 | 7.03 | -2.58 |
| M | 3 | 4 | 2.71 | 1.07 | 3.39 | 1.03 | 5.54 | -3.12 |
| M | 3 | 5 | -4.47 | 1.88 | -5.41 | 1.82 | 10.47 | -5.00 |
| M | 3 | 6 | 3.25 | 1.28 | 3.90 | 1.08 | 5.66 | -4.42 |
| M | 4 | 1 | -1.17 | 1.01 | -2.03 | 1.04 | 5.05 | -0.06 |
| M | 4 | 2 | 2.10 | 0.92 | 2.79 | 0.87 | 5.42 | -1.28 |
| M | 4 | 3 | 2.78 | 1.35 | 3.68 | 1.28 | 7.84 | -2.34 |
| M | 4 | 4 | -3.42 | 1.45 | -4.28 | 1.27 | 8.47 | -5.45 |
| M | 4 | 5 | -4.25 | 1.47 | -5.11 | 1.39 | 8.57 | -3.31 |
| M | 4 | 6 | -1.70 | 1.18 | -2.53 | 1.21 | 7.45 | -1.02 |
| M | 4 | 7 | 5.66 | 1.52 | 6.61 | 1.42 | 8.84 | -4.10 |
| M | 4 | 8 | 4.30 | 1.25 | 5.03 | 1.20 | 7.84 | -3.34 |
| M | 5 | 1 | -2.55 | 1.02 | -3.17 | 0.97 | 6.54 | -1.88 |
| M | 5 | 2 | 2.24 | 0.86 | 2.66 | 0.80 | 5.20 | -1.54 |
| M | 5 | 3 | 3.60 | 0.93 | 4.04 | 0.81 | 6.91 | -2.86 |
| M | 5 | 4 | -1.57 | 1.26 | -2.19 | 1.11 | 7.10 | -1.98 |
| M | 5 | 5 | 2.86 | 0.84 | 3.40 | 0.90 | 6.25 | -2.99 |
| M | 5 | 6 | -1.28 | 1.19 | -1.65 | 1.25 | 6.45 | -0.41 |
| M | 5 | 7 | -1.15 | 1.63 | -2.28 | 1.61 | 8.94 | 2.06 |
| M | 5 | 8 | 2.99 | 1.04 | 3.69 | 0.85 | 5.64 | -2.95 |

# Eye position data

| Subject | Run # | Trial # | mean position (deg) | st. dev. position (deg) | mean reset position (deg) | st. dev. reset position (deg) | deviation range (deg) | position at dome stop (deg) |
|---|---|---|---|---|---|---|---|---|
| N | 1 | 1 | -4.45 | 1.67 | -2.81 | 1.55 | 8.35 | 5.59 |
| N | 1 | 2 | 2.22 | 1.73 | 1.13 | 1.61 | 9.50 | 1.02 |
| N | 1 | 3 | -0.91 | 1.68 | 0.60 | 1.22 | 9.06 | 0.82 |
| N | 1 | 4 | 0.82 | 1.51 | -0.43 | 1.31 | 8.57 | 1.68 |
| N | 2 | 1 | -3.12 | 1.47 | -1.84 | 1.33 | 8.42 | 0.55 |
| N | 2 | 2 | 0.91 | 1.32 | -0.12 | 1.21 | 6.88 | 1.52 |
| N | 2 | 3 | -3.69 | 1.78 | -2.25 | 1.72 | 8.40 | 5.94 |
| N | 2 | 4 | 2.06 | 1.79 | 0.95 | 1.65 | 9.13 | 1.46 |
| N | 2 | 5 | -2.50 | 1.64 | -1.01 | 1.46 | 9.74 | 3.30 |
| N | 2 | 6 | 2.11 | 2.12 | 0.73 | 2.07 | 10.35 | -1.93 |
| N | 2 | 7 | 2.96 | 1.95 | 1.67 | 1.67 | 10.60 | 2.01 |
| N | 2 | 8 | -2.89 | 1.63 | -1.49 | 1.43 | 7.57 | 1.75 |
| N | 3 | 1 | 3.59 | 2.09 | 2.67 | 2.12 | 10.06 | 3.94 |
| N | 3 | 2 | -3.56 | 1.83 | -2.11 | 1.77 | 12.33 | 2.69 |
| N | 3 | 3 | -2.04 | 1.50 | -0.79 | 1.27 | 7.10 | -3.75 |
| N | 3 | 4 | 1.43 | 2.06 | 0.33 | 2.10 | 13.06 | 1.79 |
| N | 4 | 1 | 1.42 | 1.34 | 0.63 | 1.34 | 7.30 | 0.44 |
| N | 4 | 2 | -0.36 | 1.30 | 0.93 | 0.93 | 6.81 | 1.68 |
| N | 4 | 3 | -0.15 | 0.83 | 0.54 | 0.64 | 4.43 | -0.50 |
| N | 4 | 4 | 1.04 | 1.20 | 0.36 | 1.23 | 6.49 | 1.57 |
| N | 4 | 5 | 0.25 | 0.82 | -0.17 | 0.82 | 4.71 | 0.27 |
| N | 4 | 6 | -1.23 | 1.11 | -0.50 | 0.99 | 6.49 | 3.64 |
| N | 4 | 7 | 2.50 | 1.54 | 1.62 | 1.47 | 6.62 | 2.40 |
| N | 4 | 8 | 0.61 | 1.17 | -0.07 | 1.09 | 7.30 | 3.53 |
| N | 5 | 1 | -1.36 | 0.95 | -0.70 | 0.90 | 5.88 | -0.03 |
| N | 5 | 2 | 0.05 | 0.79 | -0.40 | 0.66 | 5.00 | 0.87 |
| N | 5 | 3 | -1.29 | 0.88 | -0.82 | 0.87 | 5.18 | 0.50 |
| N | 5 | 4 | 0.73 | 1.06 | 0.14 | 1.03 | 6.20 | -0.04 |
| N | 5 | 5 | -1.24 | 1.25 | -0.39 | 1.17 | 7.08 | 1.92 |
| N | 5 | 6 | 0.57 | 1.04 | -0.06 | 0.93 | 4.90 | 7.99 |
| N | 5 | 7 | 1.57 | 1.86 | 0.69 | 1.72 | 9.54 | 2.94 |
| N | 5 | 8 | -0.51 | 0.69 | -0.07 | 0.69 | 4.17 | 4.61 |

# Eye position data

| Subject | Run # | Trial # | mean position (deg) | st. dev. position (deg) | mean reset pos. (deg) | st. dev. reset pos. (deg) | deviation range (deg) | position at dome top (deg) |
|---|---|---|---|---|---|---|---|---|
| O | 1 | 1 | 1.64 | 1.79 | 0.71 | 1.69 | 11.21 | 0.72 |
| O | 1 | 2 | 2.82 | 1.55 | 3.67 | 1.48 | 8.98 | 0.31 |
| O | 1 | 3 | 0.66 | 1.91 | 1.49 | 1.70 | 9.40 | -1.02 |
| O | 1 | 4 | -0.55 | 1.87 | -1.52 | 1.72 | 11.47 | 2.00 |
| O | 1 | 5 | 0.57 | 1.34 | 0.16 | 1.30 | 7.25 | 2.18 |
| O | 1 | 6 | -0.13 | 1.47 | 0.66 | 1.20 | 8.47 | 4.10 |
| O | 1 | 7 | -1.74 | 2.30 | -2.64 | 2.32 | 12.06 | 0.35 |
| O | 1 | 8 | 3.00 | 1.28 | 3.57 | 1.30 | 7.59 | -1.92 |
| O | 2 | 1 | 0.50 | 1.45 | 1.49 | 1.16 | 7.89 | 0.97 |
| O | 2 | 2 | 0.05 | 1.44 | -0.50 | 1.30 | 9.99 | 0.38 |
| O | 2 | 3 | -1.76 | 1.17 | -1.12 | 0.95 | 6.54 | 0.19 |
| O | 2 | 4 | 1.00 | 1.73 | 0.39 | 1.74 | 9.28 | 0.42 |
| O | 2 | 5 | 2.95 | 1.65 | 2.57 | 1.66 | 10.30 | -2.73 |
| O | 2 | 6 | 0.62 | 1.66 | 0.16 | 1.73 | 12.18 | 1.24 |
| O | 2 | 7 | 1.82 | 1.42 | 2.36 | 1.45 | 7.18 | -5.39 |
| O | 2 | 8 | 2.77 | 1.77 | 3.52 | 1.85 | 10.40 | 1.90 |
| O | 3 | 1 | -1.56 | 0.79 | -1.25 | 0.72 | 4.88 | 2.33 |
| O | 3 | 2 | 2.22 | 0.99 | 1.93 | 1.01 | 5.30 | -0.54 |
| O | 3 | 3 | -0.33 | 1.25 | 0.09 | 1.18 | 5.76 | 2.44 |
| O | 3 | 4 | 0.68 | 0.92 | 0.21 | 0.94 | 5.98 | 0.17 |
| O | 3 | 5 | -1.64 | 1.70 | -0.94 | 1.66 | 6.49 | -0.11 |
| O | 3 | 6 | 1.08 | 1.48 | 0.34 | 1.44 | 8.72 | 1.84 |
| O | 3 | 7 | 1.21 | 1.30 | 0.36 | 1.13 | 7.67 | 1.00 |
| O | 3 | 8 | -0.68 | 1.03 | -0.27 | 0.90 | 5.64 | 2.45 |
| O | 4 | 1 | -0.59 | 0.84 | -0.12 | 0.71 | 4.66 | 0.18 |
| O | 4 | 2 | 3.99 | 1.22 | 3.59 | 1.11 | 6.52 | 1.67 |
| O | 4 | 3 | -0.11 | 0.75 | 0.28 | 0.72 | 4.15 | -1.11 |
| O | 4 | 4 | 0.13 | 1.09 | -0.32 | 1.00 | 6.37 | -1.75 |
| O | 4 | 5 | -0.31 | 1.13 | -0.65 | 1.11 | 7.64 | 0.22 |
| O | 4 | 6 | -0.01 | 0.76 | 0.38 | 0.76 | 4.37 | -0.15 |
| O | 4 | 7 | -1.12 | 0.56 | -0.85 | 0.49 | 2.76 | 0.10 |
| O | 4 | 8 | -0.73 | 2.02 | -1.26 | 2.06 | 9.45 | -4.03 |
| O | 5 | 1 | 1.06 | 0.62 | 0.87 | 0.53 | 4.20 | -0.57 |
| O | 5 | 2 | -0.33 | 0.63 | -0.05 | 0.40 | 4.15 | 0.48 |
| O | 5 | 3 | -1.35 | 1.99 | -1.76 | 1.84 | 9.62 | -1.03 |
| O | 5 | 4 | 1.26 | 0.95 | 1.35 | 0.92 | 3.83 | -1.04 |
| O | 5 | 5 | 0.27 | 1.11 | -0.30 | 0.80 | 6.84 | -1.43 |
| O | 5 | 6 | -1.24 | 1.05 | -0.82 | 1.04 | 5.37 | 1.94 |
| O | 5 | 7 | -0.90 | 0.71 | -0.64 | 0.68 | 4.20 | -0.45 |
| O | 5 | 8 | -1.31 | 1.53 | -2.23 | 1.29 | 9.13 | -4.92 |

# Eye position data

| Subject | Run # | Trial # | mean position (deg) | st. dev. position (deg) | mean reset position (deg) | st. dev. reset position (deg) | deviation range (deg) | position at dome stop (deg) |
|---|---|---|---|---|---|---|---|---|
| P | 1 | 1 | 1.77 | 1.34 | 0.85 | 1.16 | 6.47 | 4.81 |
| P | 1 | 2 | 0.53 | 2.04 | 1.89 | 1.80 | 10.69 | -3.16 |
| P | 1 | 3 | -0.84 | 1.96 | 0.20 | 1.91 | 9.94 | -0.33 |
| P | 1 | 4 | 0.22 | 1.40 | -0.84 | 1.43 | 8.28 | 1.28 |
| P | 1 | 5 | 1.96 | 0.93 | 1.46 | 1.14 | 5.79 | 2.02 |
| P | 1 | 6 | 0.17 | 1.50 | 1.15 | 1.42 | 10.11 | -1.39 |
| P | 1 | 7 | 0.01 | 1.67 | -1.03 | 1.60 | 8.94 | -0.60 |
| P | 1 | 8 | 1.14 | 2.24 | 2.22 | 2.49 | 12.50 | -0.72 |
| P | 2 | 1 | 0.03 | 1.43 | 0.90 | 1.36 | 9.59 | 0.41 |
| P | 2 | 2 | 1.77 | 0.94 | 1.10 | 0.90 | 6.62 | 2.91 |
| P | 2 | 3 | 1.79 | 1.88 | 2.84 | 1.93 | 11.96 | -0.98 |
| P | 2 | 4 | 0.31 | 1.37 | -0.67 | 1.27 | 6.88 | 1.43 |
| P | 2 | 5 | 3.46 | 2.51 | 4.64 | 2.53 | 14.48 | -0.46 |
| P | 2 | 6 | -0.03 | 1.57 | -1.00 | 1.78 | 10.64 | 1.47 |
| P | 2 | 7 | 0.08 | 1.33 | -0.81 | 1.33 | 8.96 | -1.60 |
| P | 2 | 8 | 2.00 | 1.83 | 2.97 | 1.91 | 9.99 | 0.20 |
| P | 3 | 1 | 1.45 | 1.66 | 2.00 | 1.95 | 9.38 | -1.56 |
| P | 3 | 2 | 0.14 | 1.01 | -0.61 | 0.95 | 5.40 | 1.18 |
| P | 3 | 3 | -0.14 | 1.22 | -0.99 | 1.37 | 6.84 | 0.88 |
| P | 3 | 4 | 4.43 | 1.82 | 5.29 | 1.78 | 11.74 | -5.86 |
| P | 3 | 5 | 3.02 | 1.77 | 3.50 | 1.84 | 9.69 | -1.86 |
| P | 3 | 6 | -0.44 | 1.14 | -0.99 | 1.26 | 7.10 | -1.81 |
| P | 3 | 7 | -0.04 | 0.72 | -0.44 | 0.78 | 4.00 | 0.20 |
| P | 3 | 8 | 3.15 | 1.50 | 3.94 | 1.56 | 9.20 | -2.22 |
| P | 4 | 1 | -0.97 | 1.24 | -1.49 | 1.30 | 6.59 | 1.10 |
| P | 4 | 2 | 4.76 | 1.59 | 5.38 | 1.48 | 9.33 | -4.66 |
| P | 4 | 3 | -0.10 | 1.02 | -0.63 | 1.11 | 5.05 | 0.32 |
| P | 4 | 4 | 4.07 | 1.72 | 4.68 | 1.85 | 10.42 | -0.83 |
| P | 4 | 5 | 2.63 | 1.48 | 3.36 | 1.52 | 9.03 | -4.61 |
| P | 4 | 6 | 0.17 | 0.92 | -0.12 | 0.90 | 4.64 | 0.39 |
| P | 4 | 7 | 0.06 | 0.95 | -0.31 | 0.91 | 5.98 | 0.77 |
| P | 4 | 8 | 2.78 | 1.53 | 3.27 | 1.64 | 9.18 | -4.81 |

# Eye position data

| Subject | Run # | Trial # | mean position (deg) | st. dev. position (deg) | mean reset position (deg) | st. dev. reset position (deg) | deviation range (deg) | position at dome stop (deg) |
|---------|-------|---------|---------------------|-------------------------|---------------------------|-------------------------------|-----------------------|-----------------------------|
| Q | 1 | 1 | -1.77 | 0.73 | -1.46 | 0.62 | 3.76 | 2.45 |
| Q | 1 | 2 | 1.88 | 1.78 | 1.26 | 1.77 | 8.18 | 0.57 |
| Q | 1 | 3 | -0.07 | 1.14 | 0.47 | 1.19 | 5.79 | 0.13 |
| Q | 1 | 4 | 3.52 | 1.29 | 2.95 | 1.34 | 6.84 | 1.31 |
| Q | 1 | 5 | -0.38 | 0.99 | 0.20 | 0.99 | 5.69 | 0.22 |
| Q | 1 | 6 | 2.32 | 1.26 | 1.90 | 1.20 | 9.81 | 2.55 |
| Q | 1 | 7 | 1.59 | 1.77 | 0.85 | 1.78 | 7.37 | 3.11 |
| Q | 1 | 8 | -1.40 | 1.29 | -0.87 | 1.38 | 7.93 | -0.26 |
| Q | 2 | 1 | 2.16 | 1.45 | 1.69 | 1.37 | 8.11 | 4.54 |
| Q | 2 | 2 | -0.53 | 1.02 | 0.12 | 1.00 | 5.57 | -0.86 |
| Q | 2 | 3 | -1.51 | 0.95 | -1.20 | 0.98 | 4.49 | 1.88 |
| Q | 2 | 4 | 0.17 | 1.22 | -0.38 | 1.34 | 5.98 | -0.76 |
| Q | 2 | 5 | 2.16 | 0.87 | 1.89 | 0.83 | 4.91 | 2.54 |
| Q | 2 | 6 | -0.83 | 1.00 | -0.55 | 1.07 | 5.40 | 1.29 |
| Q | 2 | 7 | -0.63 | 1.44 | -1.10 | 1.49 | 7.40 | 0.66 |
| Q | 2 | 8 | 0.35 | 0.81 | 0.78 | 0.77 | 4.66 | 0.41 |
| Q | 3 | 1 | 1.39 | 1.02 | 0.88 | 1.17 | 7.79 | -4.04 |
| Q | 3 | 2 | 4.62 | 2.35 | 4.87 | 2.51 | 10.03 | -7.80 |
| Q | 3 | 3 | 1.01 | 0.84 | 1.28 | 0.81 | 5.32 | -0.22 |
| Q | 3 | 4 | -0.56 | 1.70 | -1.01 | 1.68 | 8.35 | -3.66 |
| Q | 3 | 5 | 1.65 | 0.73 | 1.44 | 0.78 | 3.32 | 2.37 |
| Q | 3 | 6 | 3.14 | 2.18 | 3.61 | 2.18 | 10.08 | -7.60 |
| Q | 3 | 7 | -3.21 | 2.01 | -3.62 | 2.08 | 9.99 | -2.49 |
| Q | 3 | 8 | 3.64 | 1.28 | 4.07 | 1.40 | 8.47 | -3.27 |
| Q | 4 | 1 | 1.23 | 0.89 | 1.45 | 0.93 | 4.81 | -3.58 |
| Q | 4 | 2 | 0.87 | 1.30 | 0.56 | 1.35 | 5.49 | -0.47 |
| Q | 4 | 3 | 1.89 | 1.29 | 2.36 | 1.39 | 6.71 | -1.38 |
| Q | 4 | 4 | -0.52 | 0.72 | -0.76 | 0.73 | 3.54 | -0.24 |
| Q | 4 | 5 | 6.26 | 1.95 | 6.64 | 1.97 | 12.18 | -6.12 |
| Q | 4 | 6 | -2.58 | 1.51 | -2.86 | 1.52 | 6.93 | -4.44 |
| Q | 4 | 7 | -2.96 | 1.90 | -3.41 | 1.97 | 8.96 | 0.49 |
| Q | 4 | 8 | 4.80 | 1.42 | 5.17 | 1.48 | 8.50 | -5.96 |

228

# Eye position data

| Subject | Run # | Trial # | mean position (deg) | st. dev. position (deg) | mean reset position (deg) | st. dev. reset position (deg) | deviation range (deg) | position at dome stop (deg) |
|---|---|---|---|---|---|---|---|---|
| R | 1 | 1 | 1.99 | 0.95 | 1.42 | 0.92 | 5.68 | 2.42 |
| R | 1 | 2 | -1.14 | 1.40 | -0.11 | 1.21 | 8.86 | 1.02 |
| R | 1 | 3 | -0.87 | 1.23 | -0.08 | 1.16 | 8.03 | 1.03 |
| R | 1 | 4 | 1.41 | 1.17 | 0.55 | 1.01 | 6.76 | 1.07 |
| R | 1 | 5 | 2.21 | 1.14 | 1.63 | 1.09 | 7.15 | 1.01 |
| R | 1 | 6 | 1.36 | 1.58 | 2.19 | 1.56 | 8.98 | -2.87 |
| R | 1 | 7 | 0.69 | 1.36 | -0.23 | 1.35 | 9.11 | 1.04 |
| R | 1 | 8 | 1.72 | 1.38 | 2.60 | 1.28 | 8.45 | -0.33 |
| R | 2 | 1 | 1.15 | 0.98 | 1.79 | 0.89 | 6.43 | -0.81 |
| R | 2 | 2 | 1.02 | 0.85 | 0.56 | 0.85 | 5.17 | 0.25 |
| R | 2 | 3 | 0.99 | 1.04 | 1.62 | 1.06 | 5.54 | -1.58 |
| R | 2 | 4 | 0.45 | 1.47 | -0.18 | 1.65 | 8.45 | 0.54 |
| R | 2 | 5 | 2.17 | 1.76 | 3.24 | 1.52 | 10.31 | 0.88 |
| R | 2 | 6 | 0.89 | 1.11 | 0.27 | 1.20 | 5.41 | 1.99 |
| R | 2 | 7 | 1.81 | 1.76 | 0.60 | 1.46 | 9.37 | 4.78 |
| R | 2 | 8 | 0.64 | 1.17 | 1.23 | 1.17 | 5.48 | -2.11 |

# Eye position data

| Subject | Run # | Trial # | mean position (deg) | st. dev. position (deg) | mean reset position (deg) | st. dev. reset position (deg) | deviation range (deg) | position at dome stop (deg) |
|---------|-------|---------|------|------|------|------|------|------|
| S | 1 | 1 | 1.28 | 1.05 | 1.76 | 1.07 | 6.13 | -3.81 |
| S | 1 | 2 | -0.07 | 1.09 | -0.82 | 1.10 | 5.83 | 0.21 |
| S | 1 | 3 | 4.24 | 1.69 | 5.45 | 1.61 | 10.23 | -6.97 |
| S | 1 | 4 | -1.42 | 1.30 | -2.22 | 1.24 | 7.96 | 0.28 |
| S | 1 | 5 | 6.20 | 1.65 | 7.27 | 1.46 | 10.52 | -4.90 |
| S | 1 | 6 | -1.20 | 1.33 | -1.84 | 1.40 | 7.54 | -0.50 |
| S | 1 | 7 | -2.04 | 1.49 | -2.88 | 1.48 | 8.94 | -3.00 |
| S | 1 | 8 | 2.13 | 1.23 | 2.70 | 1.30 | 7.47 | -3.05 |
| S | 2 | 1 | -0.86 | 1.24 | -1.63 | 1.11 | 8.42 | -0.34 |
| S | 2 | 2 | 3.54 | 1.87 | 4.48 | 1.98 | 10.99 | -4.31 |
| S | 2 | 3 | 0.42 | 1.08 | 1.10 | 1.07 | 5.83 | -1.49 |
| S | 2 | 4 | -1.69 | 1.39 | -2.49 | 1.38 | 9.96 | -2.50 |
| S | 2 | 5 | 0.06 | 1.20 | -0.47 | 1.26 | 6.84 | 0.25 |
| S | 2 | 6 | 3.61 | 1.46 | 4.40 | 1.50 | 10.08 | -5.41 |
| S | 2 | 7 | -2.45 | 1.46 | -3.12 | 1.61 | 9.59 | 0.55 |
| S | 2 | 8 | 3.52 | 1.46 | 4.42 | 1.45 | 8.74 | -6.62 |
| S | 3 | 1 | -2.03 | 1.38 | -2.84 | 1.33 | 9.11 | 0.86 |
| S | 3 | 2 | 7.51 | 1.96 | 8.57 | 1.68 | 14.09 | -8.42 |
| S | 3 | 3 | 3.01 | 1.12 | 3.62 | 1.02 | 7.54 | -2.18 |
| S | 3 | 4 | -2.56 | 1.40 | -3.56 | 1.23 | 9.01 | -2.03 |
| S | 3 | 5 | 0.14 | 0.85 | -0.37 | 0.87 | 5.47 | -0.75 |
| S | 3 | 6 | 4.43 | 1.28 | 5.19 | 1.25 | 9.20 | -6.57 |
| S | 3 | 7 | -1.56 | 1.43 | -2.42 | 1.33 | 8.37 | -1.56 |
| S | 3 | 8 | 4.44 | 1.49 | 5.35 | 1.38 | 10.57 | -6.27 |
| S | 4 | 1 | 2.93 | 1.08 | 3.36 | 1.18 | 6.05 | -2.01 |
| S | 4 | 2 | 0.40 | 0.69 | 0.03 | 0.70 | 4.20 | 1.09 |
| S | 4 | 3 | 2.99 | 1.03 | 3.65 | 0.97 | 7.01 | -4.35 |
| S | 4 | 4 | -0.84 | 1.22 | -1.52 | 1.19 | 7.52 | -1.45 |
| S | 4 | 5 | 4.75 | 1.50 | 5.59 | 1.39 | 10.01 | -3.50 |
| S | 4 | 6 | -0.96 | 1.21 | -1.79 | 1.18 | 7.03 | -3.18 |
| S | 4 | 7 | -0.76 | 1.68 | -1.76 | 1.44 | 11.52 | 1.36 |
| S | 4 | 8 | 2.73 | 1.16 | 3.58 | 1.14 | 7.45 | -2.78 |

**Table D.5. Eye position data: vection vs. no vection. Eye position parameters by vection state**

1. mean position; state 1: mean eye position during total period of vection for each trial

2. st. dev. position; state 1: standard deviation of eye position during vection period

3. mean position; state 2: mean eye position during total period without vection

4. st. dev. position; state 2: standard deviation of eye position during no-vection period

5. position difference; st 1 - st 2: difference in mean eye position between state 1 (vection) and state 2 (no vection)

# Eye position data: vection vs. no vection

| Subject | Run # | Trial # | mean position state 1 (deg) | st. dev. position state 1 (deg) | mean position state 2 (deg) | st. dev. position state 2 (deg) | position difference st 1 - st 2 (deg) |
|---|---|---|---|---|---|---|---|
| M | 1 | 1 | -- | -- | -- | -- | -- |
| M | 1 | 2 | -0.92 | 0.93 | -0.08 | 0.57 | -0.83 |
| M | 1 | 3 | -1.77 | 0.80 | -1.18 | 0.81 | -0.60 |
| M | 1 | 4 | -3.09 | 1.08 | -0.95 | 0.74 | -2.14 |
| M | 1 | 5 | -1.58 | 0.79 | -1.03 | 0.36 | -0.56 |
| M | 1 | 6 | -2.32 | 0.95 | -1.09 | 1.31 | -1.23 |
| M | 2 | 1 | -1.37 | 0.68 | 0.72 | 0.33 | -2.08 |
| M | 2 | 2 | -1.77 | 0.90 | -0.11 | 0.11 | -1.66 |
| M | 2 | 3 | -1.14 | 1.04 | 0.49 | 0.55 | -1.63 |
| M | 2 | 4 | -2.71 | 1.28 | -1.93 | 0.94 | -0.78 |
| M | 2 | 5 | -1.56 | 0.55 | -0.73 | 0.63 | -0.82 |
| M | 2 | 6 | -2.89 | 1.31 | -2.41 | 1.13 | -0.48 |
| M | 3 | 1 | -3.02 | 0.73 | -0.71 | 1.30 | -2.30 |
| M | 3 | 2 | -4.14 | 1.49 | -1.80 | 0.93 | -2.34 |
| M | 3 | 3 | -4.32 | 0.93 | -1.72 | 1.53 | -2.60 |
| M | 3 | 4 | -3.01 | 0.84 | -2.21 | 1.22 | -0.80 |
| M | 3 | 5 | -4.95 | 1.56 | -1.63 | 0.87 | -3.32 |
| M | 3 | 6 | -3.82 | 0.72 | -1.36 | 0.84 | -2.46 |
| M | 4 | 1 | -1.29 | 0.97 | -0.31 | 0.83 | -0.99 |
| M | 4 | 2 | -2.39 | 0.65 | -0.51 | 0.39 | -1.89 |
| M | 4 | 3 | -3.11 | 1.11 | -0.63 | 0.50 | -2.48 |
| M | 4 | 4 | -3.72 | 1.23 | -1.30 | 1.09 | -2.42 |
| M | 4 | 5 | -4.43 | 1.25 | -3.20 | 2.13 | -1.22 |
| M | 4 | 6 | -1.87 | 1.10 | -0.87 | 1.22 | -1.00 |
| M | 4 | 7 | -6.11 | 0.96 | -3.26 | 1.73 | -2.85 |
| M | 4 | 8 | -4.67 | 0.81 | -2.41 | 1.44 | -2.25 |
| M | 5 | 1 | -2.74 | 0.84 | -0.76 | 0.65 | -1.98 |
| M | 5 | 2 | -2.42 | 0.69 | -0.55 | 0.44 | -1.86 |
| M | 5 | 3 | -3.91 | 0.56 | -2.52 | 1.13 | -1.39 |
| M | 5 | 4 | -1.63 | 1.23 | -1.38 | 1.31 | -0.25 |
| M | 5 | 5 | -2.99 | 0.71 | -2.13 | 1.14 | -0.86 |
| M | 5 | 6 | -1.18 | 1.16 | -2.01 | 1.11 | 0.83 |
| M | 5 | 7 | -1.00 | 1.61 | -1.86 | 1.54 | 0.86 |
| M | 5 | 8 | -3.31 | 0.73 | -1.31 | 0.78 | -2.00 |

# Eye position data: vection vs. no vection

| Subject | Run # | Trial # | mean position state 1 (deg) | st. dev. position state 1 (deg) | mean position state 2 (deg) | st. dev. position state 2 (deg) | position difference st 1 - st 2 (deg) |
|---|---|---|---|---|---|---|---|
| N | 1 | 1 | 4.80 | 1.56 | 4.28 | 1.69 | 0.53 |
| N | 1 | 2 | 2.02 | 1.79 | 2.91 | 1.29 | -0.89 |
| N | 1 | 3 | 0.57 | 1.48 | 1.57 | 1.85 | -1.01 |
| N | 1 | 4 | 0.63 | 1.51 | 1.49 | 1.30 | -0.86 |
| N | 2 | 1 | 3.16 | 1.57 | 3.04 | 1.30 | 0.12 |
| N | 2 | 2 | 0.68 | 1.32 | 1.42 | 1.15 | -0.75 |
| N | 2 | 3 | 3.60 | 1.78 | 3.95 | 1.76 | -0.35 |
| N | 2 | 4 | 2.42 | 1.90 | 1.36 | 1.31 | 1.06 |
| N | 2 | 5 | 2.48 | 1.73 | 2.61 | 1.22 | -0.13 |
| N | 2 | 6 | 2.50 | 2.09 | 0.39 | 1.16 | 2.11 |
| N | 2 | 7 | 3.42 | 1.88 | 1.42 | 1.32 | 2.00 |
| N | 2 | 8 | 2.93 | 1.53 | 2.82 | 1.79 | 0.10 |
| N | 3 | 1 | 4.22 | 2.02 | 2.09 | 1.39 | 2.12 |
| N | 3 | 2 | 3.58 | 1.89 | 3.50 | 1.69 | 0.08 |
| N | 3 | 3 | 1.60 | 1.38 | 2.22 | 1.51 | -0.62 |
| N | 3 | 4 | 1.54 | 2.20 | 0.93 | 1.16 | 0.61 |
| N | 4 | 1 | 1.56 | 1.43 | 0.95 | 0.84 | 0.60 |
| N | 4 | 2 | 0.33 | 1.30 | 0.46 | 1.27 | -0.14 |
| N | 4 | 3 | -- | -- | -- | -- | -- |
| N | 4 | 4 | 1.12 | 1.28 | 0.88 | 0.97 | 0.24 |
| N | 4 | 5 | 0.68 | 0.52 | 0.11 | 0.85 | 0.57 |
| N | 4 | 6 | 1.67 | 1.00 | 0.77 | 1.03 | 0.90 |
| N | 4 | 7 | 2.50 | 1.26 | 2.51 | 1.76 | -0.01 |
| N | 4 | 8 | 0.92 | 1.11 | -0.19 | 0.93 | 1.12 |
| N | 5 | 1 | -- | -- | -- | -- | -- |
| N | 5 | 2 | -0.14 | 0.78 | 0.12 | 0.78 | -0.26 |
| N | 5 | 3 | 1.84 | 0.43 | 1.16 | 0.91 | 0.68 |
| N | 5 | 4 | 0.77 | 1.15 | 0.67 | 0.87 | 0.11 |
| N | 5 | 5 | 1.12 | 0.96 | 1.37 | 1.50 | -0.25 |
| N | 5 | 6 | -- | -- | -- | -- | -- |
| N | 5 | 7 | -- | -- | -- | -- | -- |
| N | 5 | 8 | 0.93 | 0.60 | 0.37 | 0.65 | 0.57 |

# Eye position data: vection vs. no vection

| Subject | Run # | Trial # | mean pos. state 1 (deg) | st. dev. position state 1 | mean pos. state 2 (deg) | st. dev. position state 2 | position difference st 1 - st 2 |
|---|---|---|---|---|---|---|---|
| O | 1 | 1 | 1.46 | 1.79 | 2.68 | 1.38 | -1.23 |
| O | 1 | 2 | -3.04 | 1.39 | -0.55 | 1.19 | -2.49 |
| O | 1 | 3 | -1.25 | 1.56 | 1.79 | 1.12 | -3.04 |
| O | 1 | 4 | -0.78 | 1.83 | 0.31 | 1.75 | -1.10 |
| O | 1 | 5 | 0.43 | 1.39 | 0.88 | 1.16 | -0.46 |
| O | 1 | 6 | -0.09 | 1.31 | 1.04 | 1.71 | -1.12 |
| O | 1 | 7 | -1.62 | 2.12 | -2.46 | 3.14 | 0.84 |
| O | 1 | 8 | -3.12 | 1.26 | -1.69 | 0.57 | -1.43 |
| O | 2 | 1 | -0.56 | 1.43 | 0.66 | 1.49 | -1.22 |
| O | 2 | 2 | -0.21 | 1.32 | 1.34 | 1.31 | -1.55 |
| O | 2 | 3 | 1.99 | 1.21 | 1.28 | 0.93 | 0.71 |
| O | 2 | 4 | 0.75 | 1.68 | 2.19 | 1.43 | -1.44 |
| O | 2 | 5 | 3.05 | 1.67 | 2.03 | 1.00 | 1.02 |
| O | 2 | 6 | 0.43 | 1.68 | 1.80 | 0.80 | -1.37 |
| O | 2 | 7 | -1.95 | 1.34 | 0.47 | 0.65 | -2.42 |
| O | 2 | 8 | -2.92 | 1.69 | -1.45 | 1.87 | -1.47 |
| O | 3 | 1 | 1.61 | 0.78 | 1.09 | 0.73 | 0.52 |
| O | 3 | 2 | 2.07 | 1.01 | 2.61 | 0.81 | -0.55 |
| O | 3 | 3 | 0.00 | 0.96 | 1.86 | 1.30 | -1.86 |
| O | 3 | 4 | 0.66 | 0.92 | 1.10 | 0.66 | -0.44 |
| O | 3 | 5 | 0.63 | 0.94 | 3.32 | 1.30 | -2.70 |
| O | 3 | 6 | 1.09 | 1.52 | 1.07 | 1.15 | 0.02 |
| O | 3 | 7 | 1.18 | 1.28 | 2.02 | 1.36 | -0.85 |
| O | 3 | 8 | 0.46 | 0.76 | 1.44 | 1.43 | -0.98 |
| O | 4 | 1 | 0.39 | 0.70 | 1.61 | 0.76 | -1.23 |
| O | 4 | 2 | 4.00 | 0.99 | 3.95 | 1.86 | 0.06 |
| O | 4 | 3 | 0.11 | 0.77 | 0.09 | 0.53 | 0.02 |
| O | 4 | 4 | 0.03 | 1.04 | 1.12 | 1.11 | -1.08 |
| O | 4 | 5 | -0.39 | 1.11 | 0.92 | 0.73 | -1.30 |
| O | 4 | 6 | -0.05 | 0.74 | 1.02 | 0.36 | -1.07 |
| O | 4 | 7 | 0.90 | 0.43 | 1.55 | 0.54 | -0.65 |
| O | 4 | 8 | -0.77 | 2.05 | 0.05 | 1.09 | -0.82 |
| O | 5 | 1 | 1.07 | 0.62 | 1.05 | 0.58 | 0.01 |
| O | 5 | 2 | 0.25 | 0.47 | 1.16 | 1.21 | -0.91 |
| O | 5 | 3 | -1.42 | 1.99 | 0.51 | 0.56 | -1.93 |
| O | 5 | 4 | -1.38 | 0.90 | 0.05 | 0.16 | -1.43 |
| O | 5 | 5 | 0.05 | 0.91 | 1.96 | 1.07 | -1.90 |
| O | 5 | 6 | 1.34 | 1.08 | 0.67 | 0.58 | 0.66 |
| O | 5 | 7 | 0.41 | 0.46 | 1.18 | 0.68 | -0.77 |
| O | 5 | 8 | -1.06 | 1.38 | -1.37 | 1.56 | 0.31 |

# Eye position data: vection vs. no vection

| Subject | Run # | Trial # | mean position state 1 (deg) | st. dev. position state 1 (deg) | mean position state 2 (deg) | st. dev. position state 2 (deg) | position difference st 1 - st 2 (deg) |
|---|---|---|---|---|---|---|---|
| P | 1 | 1 | 1.87 | 1.41 | 1.23 | 0.63 | 0.64 |
| P | 1 | 2 | -1.12 | 2.01 | 0.82 | 1.36 | -1.94 |
| P | 1 | 3 | -0.24 | 0.86 | 0.95 | 2.00 | -1.18 |
| P | 1 | 4 | 0.05 | 1.38 | 1.02 | 1.20 | -0.98 |
| P | 1 | 5 | 1.91 | 0.90 | 2.07 | 1.00 | -0.17 |
| P | 1 | 6 | -0.60 | 1.56 | 0.70 | 0.85 | -1.30 |
| P | 1 | 7 | -0.28 | 1.70 | 1.16 | 0.82 | -1.43 |
| P | 1 | 8 | -1.08 | 1.70 | -1.19 | 2.69 | 0.11 |
| P | 2 | 1 | -0.79 | 1.23 | 0.50 | 1.31 | -1.29 |
| P | 2 | 2 | 1.79 | 0.99 | 1.66 | 0.66 | 0.14 |
| P | 2 | 3 | -2.37 | 1.68 | -0.16 | 1.37 | -2.21 |
| P | 2 | 4 | 0.16 | 1.40 | 0.89 | 1.04 | -0.73 |
| P | 2 | 5 | -4.26 | 1.78 | 0.36 | 1.93 | -4.62 |
| P | 2 | 6 | -0.15 | 1.57 | 0.78 | 1.29 | -0.93 |
| P | 2 | 7 | 0.01 | 1.36 | 0.86 | 0.62 | -0.85 |
| P | 2 | 8 | -2.46 | 1.67 | -1.12 | 1.81 | -1.33 |
| P | 3 | 1 | -1.95 | 1.54 | -0.05 | 1.11 | -1.90 |
| P | 3 | 2 | 0.00 | 1.02 | 0.76 | 0.63 | -0.76 |
| P | 3 | 3 | -0.24 | 1.22 | 0.91 | 0.57 | -1.15 |
| P | 3 | 4 | -4.71 | 1.52 | -0.49 | 0.85 | -4.23 |
| P | 3 | 5 | -4.08 | 1.51 | -2.03 | 1.38 | -2.05 |
| P | 3 | 6 | -0.48 | 1.17 | 0.02 | 0.70 | -0.51 |
| P | 3 | 7 | -0.03 | 0.72 | -0.08 | 0.73 | 0.05 |
| P | 3 | 8 | -3.45 | 1.27 | -0.89 | 1.20 | -2.56 |
| P | 4 | 1 | -1.02 | 1.22 | 0.63 | 0.51 | -1.66 |
| P | 4 | 2 | -5.09 | 1.23 | -2.36 | 1.86 | -2.73 |
| P | 4 | 3 | -0.26 | 0.96 | 0.88 | 0.75 | -1.14 |
| P | 4 | 4 | -4.31 | 1.50 | -1.09 | 1.36 | -3.22 |
| P | 4 | 5 | -3.09 | 1.41 | -2.01 | 1.34 | -1.08 |
| P | 4 | 6 | 0.15 | 0.90 | 0.45 | 1.08 | -0.30 |
| P | 4 | 7 | 0.08 | 0.98 | -0.10 | 0.60 | 0.17 |
| P | 4 | 8 | -3.13 | 1.34 | -0.99 | 1.17 | -2.14 |

# Eye position data: vection vs. no vection

| Subject | Run # | Trial # | mean position state 1 (deg) | st. dev. position state 1 (deg) | mean position state 2 (deg) | st. dev. position state 2 (deg) | position difference st 1 - st 2 (deg) |
|---|---|---|---|---|---|---|---|
| Q | 1 | 1 | 1.92 | 0.72 | 1.45 | 0.65 | 0.47 |
| Q | 1 | 2 | 2.14 | 1.68 | -0.12 | 1.09 | 2.25 |
| Q | 1 | 3 | 0.11 | 1.15 | -0.50 | 0.94 | 0.61 |
| Q | 1 | 4 | 3.57 | 1.33 | 3.10 | 0.78 | 0.47 |
| Q | 1 | 5 | 0.40 | 1.00 | -0.09 | 0.64 | 0.49 |
| Q | 1 | 6 | 2.40 | 1.28 | 1.59 | 0.71 | 0.81 |
| Q | 1 | 7 | 1.63 | 1.83 | 1.12 | 0.81 | 0.51 |
| Q | 1 | 8 | 1.55 | 1.27 | 0.52 | 1.01 | 1.04 |
| Q | 2 | 1 | 2.60 | 1.19 | 0.92 | 1.41 | 1.67 |
| Q | 2 | 2 | 0.60 | 1.01 | -0.38 | 0.66 | 0.98 |
| Q | 2 | 3 | 1.82 | 0.94 | 0.88 | 0.58 | 0.94 |
| Q | 2 | 4 | 0.17 | 1.25 | 0.17 | 0.60 | 0.00 |
| Q | 2 | 5 | 2.09 | 0.74 | 2.50 | 1.30 | -0.41 |
| Q | 2 | 6 | 0.98 | 0.90 | -0.80 | 0.51 | 1.79 |
| Q | 2 | 7 | -0.87 | 1.31 | 1.33 | 0.83 | -2.20 |
| Q | 2 | 8 | -0.34 | 0.84 | -0.46 | 0.37 | 0.11 |
| Q | 3 | 1 | 1.08 | 0.89 | 1.85 | 1.03 | -0.77 |
| Q | 3 | 2 | -6.13 | 1.30 | -2.02 | 1.19 | -4.11 |
| Q | 3 | 3 | -0.69 | 0.54 | -1.03 | 0.86 | 0.34 |
| Q | 3 | 4 | -0.65 | 1.76 | 0.14 | 0.89 | -0.79 |
| Q | 3 | 5 | 1.97 | 0.71 | 1.47 | 0.69 | 0.50 |
| Q | 3 | 6 | -3.45 | 2.14 | -0.94 | 0.57 | -2.50 |
| Q | 3 | 7 | -3.54 | 1.81 | -0.02 | 0.50 | -3.52 |
| Q | 3 | 8 | -4.13 | 1.07 | -2.88 | 1.21 | -1.25 |
| Q | 4 | 1 | -2.05 | 1.14 | -0.94 | 0.54 | -1.11 |
| Q | 4 | 2 | -0.46 | 0.84 | 1.37 | 1.06 | -1.84 |
| Q | 4 | 3 | -2.89 | 1.05 | -0.98 | 0.64 | -1.91 |
| Q | 4 | 4 | -0.51 | 0.73 | -0.56 | 0.70 | 0.04 |
| Q | 4 | 5 | -6.67 | 1.53 | -2.50 | 1.34 | -4.17 |
| Q | 4 | 6 | -2.84 | 1.45 | -1.15 | 0.94 | -1.70 |
| Q | 4 | 7 | -3.27 | 1.76 | -0.86 | 1.38 | -2.41 |
| Q | 4 | 8 | -5.19 | 1.05 | -3.01 | 1.49 | -2.18 |

# Eye position data: vection vs. no vection

| Subject | Run # | Trial # | mean position state 1 (deg) | st. dev. position state 1 (deg) | mean position state 2 (deg) | st. dev. position state 2 (deg) | position difference st 1 - st 2 (deg) |
|---|---|---|---|---|---|---|---|
| R | 1 | 1 | -- | -- | -- | -- | -- |
| R | 1 | 2 | 1.04 | 1.46 | 1.31 | 1.26 | -0.28 |
| R | 1 | 3 | 0.50 | 1.09 | 1.94 | 0.93 | -1.44 |
| R | 1 | 4 | 1.40 | 1.31 | 1.41 | 1.15 | -0.02 |
| R | 1 | 5 | 2.53 | 1.21 | 2.05 | 1.07 | 0.48 |
| R | 1 | 6 | -2.18 | 1.23 | -0.34 | 1.37 | -1.83 |
| R | 1 | 7 | 0.17 | 1.53 | 1.02 | 1.14 | -0.85 |
| R | 1 | 8 | -1.75 | 0.85 | -1.71 | 1.43 | -0.04 |
| R | 2 | 1 | -- | -- | -- | -- | -- |
| R | 2 | 2 | -- | -- | -- | -- | -- |
| R | 2 | 3 | -- | -- | -- | -- | -- |
| R | 2 | 4 | 0.68 | 1.08 | 0.42 | 1.51 | 0.27 |
| R | 2 | 5 | -- | -- | -- | -- | -- |
| R | 2 | 6 | -- | -- | -- | -- | -- |
| R | 2 | 7 | -- | -- | -- | -- | -- |
| R | 2 | 8 | -- | -- | -- | -- | -- |

# Eye position data: vection vs. no vection

| Subject | Run # | Trial # | mean position state 1 (deg) | st. dev. position state 1 (deg) | mean position state 2 (deg) | st. dev. position state 2 (deg) | position difference st 1 - st 2 (deg) |
|---|---|---|---|---|---|---|---|
| S | 1 | 1 | -1.47 | 0.87 | 0.13 | 1.15 | -1.60 |
| S | 1 | 2 | -0.12 | 1.08 | 0.86 | 0.82 | -0.98 |
| S | 1 | 3 | -4.52 | 1.48 | -1.69 | 1.33 | -2.84 |
| S | 1 | 4 | -1.58 | 1.19 | 0.37 | 1.07 | -1.95 |
| S | 1 | 5 | -6.39 | 1.49 | -3.94 | 1.76 | -2.45 |
| S | 1 | 6 | -1.35 | 1.23 | 0.98 | 0.51 | -2.33 |
| S | 1 | 7 | -2.13 | 1.47 | -0.46 | 0.96 | -1.67 |
| S | 1 | 8 | -2.33 | 1.13 | -0.94 | 1.12 | -1.38 |
| S | 2 | 1 | -0.88 | 1.26 | -0.51 | 0.99 | -0.37 |
| S | 2 | 2 | -3.81 | 1.72 | -1.07 | 1.27 | -2.74 |
| S | 2 | 3 | -0.46 | 1.10 | 0.12 | 0.44 | -0.58 |
| S | 2 | 4 | -1.83 | 1.25 | 1.26 | 0.82 | -3.09 |
| S | 2 | 5 | 0.01 | 1.21 | 0.93 | 0.55 | -0.92 |
| S | 2 | 6 | -3.78 | 1.29 | -0.86 | 1.40 | -2.92 |
| S | 2 | 7 | -2.55 | 1.38 | 0.02 | 1.19 | -2.57 |
| S | 2 | 8 | -3.73 | 1.22 | -0.91 | 1.65 | -2.82 |
| S | 3 | 1 | -2.20 | 1.28 | 0.22 | 0.62 | -2.41 |
| S | 3 | 2 | -7.75 | 1.58 | -2.54 | 2.67 | -5.20 |
| S | 3 | 3 | -3.14 | 0.99 | -1.13 | 1.26 | -2.00 |
| S | 3 | 4 | -2.74 | 1.30 | -0.59 | 0.95 | -2.15 |
| S | 3 | 5 | 0.10 | 0.86 | 0.80 | 0.43 | -0.70 |
| S | 3 | 6 | -4.58 | 1.04 | -1.05 | 1.50 | -3.53 |
| S | 3 | 7 | -1.65 | 1.40 | -0.80 | 1.50 | -0.85 |
| S | 3 | 8 | -4.62 | 1.24 | -0.96 | 1.76 | -3.66 |
| S | 4 | 1 | -3.14 | 0.86 | -0.82 | 0.87 | -2.32 |
| S | 4 | 2 | 0.40 | 0.71 | 0.30 | 0.28 | 0.10 |
| S | 4 | 3 | -3.08 | 0.91 | -1.05 | 1.40 | -2.03 |
| S | 4 | 4 | -0.97 | 1.15 | 0.98 | 0.61 | -1.95 |
| S | 4 | 5 | -4.98 | 1.18 | -1.43 | 1.57 | -3.56 |
| S | 4 | 6 | -1.01 | 1.20 | 0.40 | 0.50 | -1.41 |
| S | 4 | 7 | -0.77 | 1.74 | -0.66 | 0.87 | -0.11 |
| S | 4 | 8 | -2.82 | 1.09 | -0.98 | 1.09 | -1.84 |

**Table D.6. OKAN SPV: double exponential fits. A double exponential function of the following form was fit to the SPV decay during OKAN:**

SPV = v_long*exp(tau_long) + v_short*exp(tau_short) + v_bias

1. v_long: magnitude of slow decay of OKAN SPV

2. tau_long: time constant of slow decay of OKAN SPV

3. v_short: magnitude of fast decay of OKAN SPV

4. tau_short: time constant of fast decay of OKAN SPV

5. v_bias: bias or "drift" velocity seen regardless of stimulation. Generally quite close to zero.

# OKAN SPV: double exponential fits

| Subject | Run # | Trial # | v_long (deg/sec) | tau_long (sec) | v_short (deg/sec) | tau_short (sec) | v_bias (deg/sec) |
|---------|-------|---------|--------|----------|---------|-----------|--------|
| M | 1 | 1 | 3.37 | 1.34 | 1.93 | 0.27 | 0.08 |
| M | 1 | 2 | -0.53 | 2.33 | -1.74 | 0.39 | 0.14 |
| M | 1 | 3 | -0.12 | 1.81 | -1.20 | 0.42 | 0.14 |
| M | 1 | 4 | 0.36 | 7.28 | 3.50 | 0.95 | 0.03 |
| M | 1 | 5 | -0.54 | 1.85 | -0.76 | 1.85 | 0.13 |
| M | 1 | 6 | 0.63 | 8.98 | 1.53 | 0.61 | -0.04 |
| M | 2 | 1 | 0.74 | 1.31 | 0.66 | 1.31 | 0.25 |
| M | 2 | 2 | -1.62 | 1.33 | -0.74 | 0.13 | 0.04 |
| M | 2 | 3 | -0.53 | 0.83 | -0.76 | 0.83 | 0.09 |
| M | 2 | 4 | 2.27 | 1.13 | 0.96 | 0.10 | 0.03 |
| M | 2 | 5 | -0.53 | 2.48 | -3.53 | 0.40 | 0.04 |
| M | 2 | 6 | 0.73 | 1.47 | 0.36 | 1.46 | 0.06 |
| M | 3 | 1 | -2.09 | 1.31 | -0.76 | 0.22 | 0.08 |
| M | 3 | 2 | -2.38 | 1.40 | -1.77 | 0.22 | 0.12 |
| M | 3 | 3 | -1.58 | 1.31 | -0.13 | 1.31 | 0.08 |
| M | 3 | 4 | -1.27 | 1.43 | -1.10 | 1.43 | 0.15 |
| M | 3 | 5 | 1.91 | 1.07 | 2.48 | 1.07 | 0.12 |
| M | 3 | 6 | -2.24 | 1.61 | -2.30 | 0.39 | 0.13 |
| M | 4 | 1 | 1.00 | 0.64 | 0.42 | 0.64 | 0.15 |
| M | 4 | 2 | -0.87 | 1.16 | -0.93 | 1.16 | 0.19 |
| M | 4 | 3 | -1.23 | 1.10 | -1.24 | 1.10 | 0.17 |
| M | 4 | 4 | 2.28 | 1.47 | 2.58 | 1.47 | 0.01 |
| M | 4 | 5 | 2.09 | 2.34 | 2.72 | 0.31 | 0.03 |
| M | 4 | 6 | 0.73 | 2.18 | 0.80 | 2.18 | 0.08 |
| M | 4 | 7 | -- | -- | -- | -- | -- |
| M | 4 | 8 | -1.16 | 1.51 | -1.12 | 1.51 | 0.09 |
| M | 5 | 1 | 0.41 | 8.20 | 2.15 | 0.82 | -0.09 |
| M | 5 | 2 | -0.29 | 1.80 | -2.15 | 0.63 | 0.02 |
| M | 5 | 3 | -0.74 | 1.85 | -0.99 | 1.84 | 0.35 |
| M | 5 | 4 | 2.55 | 1.14 | 1.09 | 0.23 | 0.07 |
| M | 5 | 5 | -1.25 | 1.34 | -2.30 | 0.43 | 0.06 |
| M | 5 | 6 | 0.44 | 4.32 | 1.57 | 0.25 | -0.03 |
| M | 5 | 7 | -- | -- | -- | -- | -- |
| M | 5 | 8 | -1.01 | 0.90 | -0.99 | 0.90 | 0.10 |

# OKAN SPV: double exponential fits

| Subject | Run # | Trial # | v_long (deg/sec) | tau_long (sec) | v_short (deg/sec) | tau_short (sec) | v_bias (deg/sec) |
|---------|-------|---------|--------|---------|---------|-----------|--------|
| N | 1 | 1 | -1.59 | 0.63 | -1.57 | 0.63 | 0.06 |
| N | 1 | 2 | 1.37 | 0.83 | 1.48 | 0.83 | 0.21 |
| N | 1 | 3 | -2.03 | 0.69 | -1.80 | 0.69 | 0.07 |
| N | 1 | 4 | 2.72 | 0.24 | 2.19 | 0.24 | 0.39 |
| N | 2 | 1 | -2.43 | 0.66 | -2.23 | 0.66 | -0.04 |
| N | 2 | 2 | 0.79 | 2.05 | 0.63 | 2.05 | 0.26 |
| N | 2 | 3 | -- | -- | -- | -- | -- |
| N | 2 | 4 | 2.22 | 0.40 | 0.69 | 0.40 | 0.33 |
| N | 2 | 5 | -3.53 | 0.26 | -3.43 | 0.26 | 0.21 |
| N | 2 | 6 | 2.92 | 1.19 | 2.81 | 1.19 | 0.19 |
| N | 2 | 7 | 2.26 | 0.29 | 2.33 | 0.29 | 0.17 |
| N | 2 | 8 | -2.94 | 0.35 | -3.75 | 0.35 | 0.45 |
| N | 3 | 1 | 1.83 | 1.25 | 1.92 | 1.25 | 0.19 |
| N | 3 | 2 | -2.29 | 0.27 | -1.72 | 0.27 | 0.29 |
| N | 3 | 3 | -0.35 | 1.86 | -3.46 | 0.40 | 0.16 |
| N | 3 | 4 | 1.39 | 1.88 | 2.55 | 0.16 | 0.40 |
| N | 4 | 1 | 1.68 | 0.84 | 1.66 | 0.82 | 0.04 |
| N | 4 | 2 | -2.48 | 0.38 | -2.52 | 0.38 | 0.17 |
| N | 4 | 3 | -1.67 | 0.59 | -1.68 | 0.59 | 0.11 |
| N | 4 | 4 | 0.14 | 4.83 | 3.70 | 0.33 | 0.11 |
| N | 4 | 5 | 0.54 | 6.92 | 1.09 | 0.22 | 0.09 |
| N | 4 | 6 | -0.36 | 11.27 | -0.82 | 0.36 | 0.17 |
| N | 4 | 7 | 1.54 | 1.15 | 0.64 | 0.21 | 0.20 |
| N | 4 | 8 | 0.35 | 13.83 | 1.45 | 0.08 | 0.05 |
| N | 5 | 1 | -0.65 | 3.45 | -2.28 | 0.18 | 0.52 |
| N | 5 | 2 | 1.45 | 2.31 | 1.83 | 0.21 | 0.30 |
| N | 5 | 3 | -1.93 | 0.35 | -1.89 | 0.35 | 0.09 |
| N | 5 | 4 | 0.78 | 4.17 | 0.17 | 4.16 | 0.30 |
| N | 5 | 5 | -- | -- | -- | -- | -- |
| N | 5 | 6 | -- | -- | -- | -- | -- |
| N | 5 | 7 | 1.23 | 1.46 | 2.33 | 0.29 | 0.16 |
| N | 5 | 8 | -0.45 | 0.53 | -0.47 | 0.53 | 0.03 |

## OKAN SPV: double exponential fits

| Subject | Run # | Trial # | v_long (deg/sec) | tau_long (sec) | v_short (deg/sec) | tau_short (sec) | v_bias (deg/sec) |
|---------|-------|---------|------------------|----------------|-------------------|-----------------|------------------|
| O | 1 | 1 | 1.39 | 1.34 | 3.31 | 0.13 | 0.29 |
| O | 1 | 2 | -2.75 | 0.20 | -0.21 | 0.20 | 0.09 |
| O | 1 | 3 | -0.82 | 3.60 | -2.40 | 0.15 | 0.05 |
| O | 1 | 4 | 0.54 | 9.41 | 4.39 | 0.31 | 0.05 |
| O | 1 | 5 | 0.13 | 5.16 | 4.40 | 0.16 | 0.10 |
| O | 1 | 6 | -- | -- | -- | -- | -- |
| O | 1 | 7 | 0.49 | 3.02 | 0.65 | 0.07 | 0.16 |
| O | 1 | 8 | -- | -- | -- | -- | -- |
| O | 2 | 1 | -0.51 | 10.09 | -2.83 | 0.19 | -0.14 |
| O | 2 | 2 | 0.44 | 0.19 | 2.34 | 0.19 | 0.15 |
| O | 2 | 3 | -0.83 | 3.35 | -1.31 | 0.41 | -0.24 |
| O | 2 | 4 | 0.39 | 0.22 | 2.36 | 0.22 | 0.23 |
| O | 2 | 5 | 2.66 | 0.30 | 1.89 | 0.30 | 0.25 |
| O | 2 | 6 | 0.42 | 0.18 | 3.43 | 0.18 | 0.08 |
| O | 2 | 7 | -2.05 | 1.01 | -1.32 | 1.00 | -0.63 |
| O | 2 | 8 | -- | -- | -- | -- | -- |
| O | 3 | 1 | -1.66 | 0.28 | -1.93 | 0.28 | 0.43 |
| O | 3 | 2 | 1.46 | 0.94 | 1.41 | 0.94 | 0.12 |
| O | 3 | 3 | -- | -- | -- | -- | -- |
| O | 3 | 4 | 1.01 | 1.89 | 2.80 | 0.11 | 0.14 |
| O | 3 | 5 | -1.59 | 1.49 | -4.08 | 0.20 | 0.34 |
| O | 3 | 6 | 0.91 | 0.17 | 1.57 | 0.17 | 0.34 |
| O | 3 | 7 | 1.19 | 3.50 | 2.13 | 0.78 | 0.17 |
| O | 3 | 8 | -- | -- | -- | -- | -- |
| O | 4 | 1 | -0.99 | 6.02 | -3.32 | 0.14 | -0.40 |
| O | 4 | 2 | 1.53 | 0.33 | 0.48 | 0.33 | -0.24 |
| O | 4 | 3 | -1.23 | 3.98 | -1.78 | 0.20 | 0.13 |
| O | 4 | 4 | 0.91 | 1.66 | 0.83 | 1.66 | -0.06 |
| O | 4 | 5 | 1.25 | 0.28 | 1.05 | 0.28 | -0.04 |
| O | 4 | 6 | -0.37 | 7.41 | -0.62 | 0.19 | 0.04 |
| O | 4 | 7 | -0.40 | 6.74 | -0.13 | 0.17 | 0.04 |
| O | 4 | 8 | 1.17 | 2.11 | 2.22 | 0.26 | 0.12 |
| O | 5 | 1 | 0.27 | 0.28 | 0.53 | 0.28 | 0.31 |
| O | 5 | 2 | -0.94 | 3.04 | -0.62 | 3.04 | 0.61 |
| O | 5 | 3 | 2.16 | 0.35 | 0.78 | 0.35 | 0.00 |
| O | 5 | 4 | -0.80 | 1.91 | -0.93 | 1.91 | -0.12 |
| O | 5 | 5 | -- | -- | -- | -- | -- |
| O | 5 | 6 | -0.98 | 0.62 | -0.63 | 0.62 | 0.39 |
| O | 5 | 7 | -0.52 | 1.47 | -0.47 | 1.47 | 0.20 |
| O | 5 | 8 | 3.24 | 0.56 | 3.43 | 0.56 | 0.15 |

# OKAN SPV: double exponential fits

| Subject | Run # | Trial # | v_long (deg/sec) | tau_long (sec) | v_short (deg/sec) | tau_short (sec) | v_bias (deg/sec) |
|---|---|---|---|---|---|---|---|
| P | 1 | 1 | 1.76 | 0.15 | 0.80 | 0.15 | -0.14 |
| P | 1 | 2 | -3.71 | 1.65 | -1.91 | 0.35 | -0.17 |
| P | 1 | 3 | -2.47 | 5.04 | -1.85 | 0.19 | -0.07 |
| P | 1 | 4 | 1.25 | 2.63 | 2.16 | 0.21 | -0.21 |
| P | 1 | 5 | 0.64 | 8.58 | 1.42 | 0.44 | -0.32 |
| P | 1 | 6 | -2.22 | 3.00 | -3.05 | 0.41 | 0.02 |
| P | 1 | 7 | 2.74 | 1.44 | 3.11 | 0.20 | -0.14 |
| P | 1 | 8 | -1.38 | 1.70 | -2.07 | 1.70 | -0.53 |
| P | 2 | 1 | -1.79 | 4.46 | -0.91 | 4.46 | -0.25 |
| P | 2 | 2 | 0.34 | 3.17 | 2.43 | 0.00 | -0.24 |
| P | 2 | 3 | -2.04 | 10.31 | -2.14 | 0.30 | 0.31 |
| P | 2 | 4 | 0.66 | 4.31 | 2.37 | 0.18 | -0.11 |
| P | 2 | 5 | -2.72 | 4.88 | -1.18 | 0.08 | -0.07 |
| P | 2 | 6 | 0.45 | 6.58 | 1.29 | 0.61 | -0.12 |
| P | 2 | 7 | 1.52 | 2.60 | 3.20 | 0.12 | 0.37 |
| P | 2 | 8 | -1.67 | 3.07 | -1.84 | 3.07 | 0.05 |
| P | 3 | 1 | -1.56 | 1.56 | -2.64 | 0.56 | 0.00 |
| P | 3 | 2 | 0.62 | 1.15 | 0.41 | 1.06 | -0.11 |
| P | 3 | 3 | 0.68 | 0.94 | 0.49 | 0.94 | 0.05 |
| P | 3 | 4 | -2.42 | 3.27 | -5.02 | 0.43 | -0.11 |
| P | 3 | 5 | -1.56 | 2.58 | -1.89 | 0.34 | 0.10 |
| P | 3 | 6 | 1.02 | 2.29 | 1.25 | 2.29 | -0.03 |
| P | 3 | 7 | 0.96 | 2.27 | 1.47 | 0.62 | 0.17 |
| P | 3 | 8 | -2.94 | 1.23 | -3.53 | 1.23 | 0.02 |
| P | 4 | 1 | 1.16 | 1.41 | 1.15 | 1.41 | 0.10 |
| P | 4 | 2 | -1.91 | 6.45 | -2.57 | 0.31 | 0.41 |
| P | 4 | 3 | 0.95 | 3.44 | 2.91 | 0.31 | 0.19 |
| P | 4 | 4 | -1.01 | 4.60 | -1.70 | 0.85 | 0.27 |
| P | 4 | 5 | -2.64 | 2.84 | -1.83 | 0.35 | 0.05 |
| P | 4 | 6 | 1.01 | 1.58 | 1.25 | 0.21 | 0.31 |
| P | 4 | 7 | 0.29 | 0.36 | 1.20 | 0.36 | 0.41 |
| P | 4 | 8 | -1.83 | 4.93 | -4.33 | 0.32 | 0.49 |

# OKAN SPV: double exponential fits

| Subject | Run # | Trial # | v_long (deg/sec) | tau_long (sec) | v_short (deg/sec) | tau_short (sec) | v_bias (deg/sec) |
|---------|-------|---------|------------------|----------------|-------------------|-----------------|------------------|
| Q | 1 | 1 | -0.64 | 1.19 | -0.70 | 1.19 | -0.01 |
| Q | 1 | 2 | 1.24 | 0.77 | 1.34 | 0.77 | -0.01 |
| Q | 1 | 3 | -1.23 | 1.91 | -1.24 | 0.63 | 0.05 |
| Q | 1 | 4 | 1.68 | 0.43 | 1.73 | 0.43 | 0.04 |
| Q | 1 | 5 | -1.44 | 0.30 | -1.02 | 0.30 | -0.02 |
| Q | 1 | 6 | 0.92 | 0.31 | 2.09 | 0.31 | -0.04 |
| Q | 1 | 7 | 2.40 | 0.20 | 0.63 | 0.20 | -0.14 |
| Q | 1 | 8 | -1.50 | 0.54 | -1.53 | 0.54 | -0.08 |
| Q | 2 | 1 | 0.07 | 5.12 | 0.06 | 4.97 | 0.22 |
| Q | 2 | 2 | -0.56 | 2.12 | -1.19 | 2.12 | -0.32 |
| Q | 2 | 3 | -0.20 | 0.27 | -0.11 | 0.27 | -0.50 |
| Q | 2 | 4 | 1.22 | 2.41 | 1.16 | 0.59 | 0.11 |
| Q | 2 | 5 | 0.32 | 2.03 | 2.09 | 0.19 | -0.01 |
| Q | 2 | 6 | -0.41 | 0.14 | -1.25 | 0.14 | -0.49 |
| Q | 2 | 7 | 1.52 | 1.22 | 1.18 | 0.00 | 0.02 |
| Q | 2 | 8 | -1.58 | 0.22 | -0.18 | 0.22 | -0.44 |
| Q | 3 | 1 | 3.34 | 1.01 | 2.61 | 1.01 | -0.07 |
| Q | 3 | 2 | -1.47 | 1.96 | -2.54 | 1.96 | -0.07 |
| Q | 3 | 3 | -0.62 | 0.61 | -0.59 | 0.61 | -0.13 |
| Q | 3 | 4 | 2.16 | 1.03 | 1.79 | 1.02 | 0.04 |
| Q | 3 | 5 | 0.65 | 0.48 | 0.57 | 0.48 | -0.21 |
| Q | 3 | 6 | -1.89 | 1.88 | -1.98 | 1.88 | -0.19 |
| Q | 3 | 7 | 1.17 | 1.45 | 1.61 | 1.45 | -0.02 |
| Q | 3 | 8 | -0.92 | 2.11 | -1.79 | 0.53 | -0.21 |
| Q | 4 | 1 | -0.76 | 2.13 | -0.94 | 2.13 | -0.39 |
| Q | 4 | 2 | 1.68 | 2.11 | 0.38 | 2.11 | -0.15 |
| Q | 4 | 3 | -0.36 | 2.61 | -0.60 | 2.15 | -0.28 |
| Q | 4 | 4 | 1.42 | 4.10 | 0.72 | 0.20 | -0.35 |
| Q | 4 | 5 | -1.72 | 2.93 | -2.11 | 0.40 | -0.29 |
| Q | 4 | 6 | 1.36 | 1.82 | 1.52 | 1.42 | -0.16 |
| Q | 4 | 7 | 0.90 | 3.05 | 4.14 | 0.23 | -0.17 |
| Q | 4 | 8 | -2.08 | 0.70 | -1.98 | 0.70 | -0.32 |

# OKAN SPV: double exponential fits

| Subject | Run # | Trial # | v_long (deg/sec) | tau_long (sec) | v_short (deg/sec) | tau_short (sec) | v_bias (deg/sec) |
|---|---|---|---|---|---|---|---|
| R | 1 | 1 | 1.85 | 0.65 | 2.41 | 0.65 | -0.28 |
| R | 1 | 2 | -2.97 | 0.46 | -2.94 | 0.46 | -0.18 |
| R | 1 | 3 | -1.23 | 4.76 | -2.77 | 0.22 | 0.02 |
| R | 1 | 4 | 1.85 | 0.36 | 2.22 | 0.36 | -0.04 |
| R | 1 | 5 | 0.43 | 6.97 | 4.36 | 0.37 | -0.09 |
| R | 1 | 6 | -4.67 | 1.04 | -1.89 | 0.15 | -0.27 |
| R | 1 | 7 | 1.70 | 1.46 | 3.03 | 0.42 | -0.12 |
| R | 1 | 8 | -2.10 | 1.38 | -1.78 | 1.38 | 0.06 |
| R | 2 | 1 | -0.96 | 14.64 | -1.13 | 14.63 | -0.03 |
| R | 2 | 2 | 1.31 | 2.00 | 0.89 | 2.00 | -0.35 |
| R | 2 | 3 | -2.15 | 9.60 | -4.51 | 0.04 | 0.18 |
| R | 2 | 4 | 1.28 | 1.44 | 1.69 | 0.20 | -0.04 |
| R | 2 | 5 | -1.50 | 10.02 | -3.20 | 0.28 | -0.10 |
| R | 2 | 6 | 1.42 | 0.37 | 1.75 | 0.37 | -0.17 |
| R | 2 | 7 | 0.16 | 0.29 | 0.13 | 0.07 | -0.20 |
| R | 2 | 8 | -2.19 | 4.97 | -2.43 | 0.11 | -0.28 |

# OKAN SPV: double exponential fits

| Subject | Run # | Trial # | v_long (deg/sec) | tau_long (sec) | v_short (deg/sec) | tau_short (sec) | v_bias (deg/sec) |
|---|---|---|---|---|---|---|---|
| S | 1 | 1 | -3.02 | 1.23 | -2.80 | 1.23 | 0.21 |
| S | 1 | 2 | 1.08 | 1.08 | 0.77 | 1.08 | 0.31 |
| S | 1 | 3 | -3.93 | 0.95 | -4.78 | 0.95 | 0.11 |
| S | 1 | 4 | 0.90 | 2.85 | 3.69 | 0.14 | -0.06 |
| S | 1 | 5 | -3.95 | 1.27 | -3.76 | 0.26 | 0.21 |
| S | 1 | 6 | 2.54 | 1.06 | 2.25 | 1.06 | 0.01 |
| S | 1 | 7 | 1.07 | 1.66 | 7.61 | 0.28 | -0.09 |
| S | 1 | 8 | -3.15 | 0.33 | -3.09 | 0.33 | 0.13 |
| S | 2 | 1 | 2.28 | 1.31 | 3.86 | 0.18 | -0.19 |
| S | 2 | 2 | -2.18 | 1.13 | -2.16 | 1.13 | -0.13 |
| S | 2 | 3 | -0.50 | 11.89 | -0.93 | 11.87 | 0.20 |
| S | 2 | 4 | 3.17 | 0.23 | 2.99 | 0.23 | -0.07 |
| S | 2 | 5 | 0.77 | 0.05 | 0.72 | 0.05 | 0.08 |
| S | 2 | 6 | -2.68 | 7.35 | -2.00 | 0.44 | 0.30 |
| S | 2 | 7 | 4.98 | 0.19 | 2.64 | 0.19 | 0.05 |
| S | 2 | 8 | -1.60 | 4.34 | -7.97 | 0.37 | -0.05 |
| S | 3 | 1 | 2.13 | 0.64 | 1.70 | 0.64 | -0.09 |
| S | 3 | 2 | -5.05 | 1.31 | -3.37 | 0.24 | 0.06 |
| S | 3 | 3 | -0.94 | 3.97 | -1.88 | 0.24 | 0.12 |
| S | 3 | 4 | 1.33 | 3.34 | 7.53 | 0.55 | -0.05 |
| S | 3 | 5 | 2.46 | 1.83 | 2.62 | 0.11 | -0.01 |
| S | 3 | 6 | -2.45 | 2.40 | -6.85 | 0.24 | 0.05 |
| S | 3 | 7 | 2.01 | 1.11 | 6.99 | 0.28 | 0.00 |
| S | 3 | 8 | -4.17 | 1.95 | -2.05 | 0.49 | 0.08 |
| S | 4 | 1 | -0.96 | 1.58 | -1.12 | 1.58 | -0.16 |
| S | 4 | 2 | 0.56 | 12.32 | 1.39 | 0.08 | -0.20 |
| S | 4 | 3 | -2.52 | 1.70 | -3.35 | 0.33 | -0.02 |
| S | 4 | 4 | 1.68 | 2.04 | 1.46 | 0.13 | 0.01 |
| S | 4 | 5 | -0.57 | 13.43 | -4.47 | 0.69 | 0.40 |
| S | 4 | 6 | 1.78 | 1.74 | 2.27 | 0.24 | 0.07 |
| S | 4 | 7 | 2.41 | 0.61 | 2.44 | 0.61 | 0.06 |
| S | 4 | 8 | -1.77 | 1.75 | -1.76 | 1.75 | 0.05 |

## Table D.7.  Vection parameters

1. time with vection:  percent of dome rotation period during which vection was perceived

2. onset time:  time before a threshold vection level of 4% was achieved and maintained for at least 0.5 second

3. max vection:  maximum vection score recorded during each trial

4. ave vection:  mean vection over entire period of dome rotation

# Vection parameters

| Subject | Run # | Trial # | time with vection (%) | onset time (sec) | ax vection (%) | ve vection (%) |
|---|---|---|---|---|---|---|
| M | 1 | 1 | 0.0 | . | . | . |
| M | 1 | 2 | 84.5 | 3.5 | 99.0 | 56.6 |
| M | 1 | 3 | 72.3 | 6.3 | 97.2 | 30.7 |
| M | 1 | 4 | 91.9 | 3.7 | 99.9 | 76.5 |
| M | 1 | 5 | 92.4 | 3.4 | 58.3 | 36.3 |
| M | 1 | 6 | 88.1 | 5.4 | 100.5 | 62.2 |
| M | 2 | 1 | 90.8 | 4.1 | 100.5 | 68.5 |
| M | 2 | 2 | 93.7 | 2.9 | 99.0 | 80.5 |
| M | 2 | 3 | 92.6 | 3.3 | 96.8 | 53.4 |
| M | 2 | 4 | 90.1 | 4.5 | 100.7 | 75.0 |
| M | 2 | 5 | 88.5 | 5.2 | 96.0 | 69.1 |
| M | 2 | 6 | 90.9 | 4.1 | 73.2 | 39.5 |
| M | 3 | 1 | 89.1 | 3.3 | 89.4 | 46.8 |
| M | 3 | 2 | 83.6 | 4.9 | 53.1 | 26.4 |
| M | 3 | 3 | 79.7 | 6.1 | 73.6 | 36.6 |
| M | 3 | 4 | 61.9 | 6.0 | 24.1 | 12.0 |
| M | 3 | 5 | 85.6 | 4.3 | 53.5 | 34.0 |
| M | 3 | 6 | 76.8 | 7.0 | 42.1 | 20.3 |
| M | 4 | 1 | 87.3 | 3.8 | 73.7 | 51.5 |
| M | 4 | 2 | 84.5 | 4.7 | 56.5 | 36.3 |
| M | 4 | 3 | 86.7 | 4.0 | 99.8 | 53.7 |
| M | 4 | 4 | 87.7 | 3.7 | 101.7 | 68.8 |
| M | 4 | 5 | 85.9 | 4.2 | 87.2 | 58.4 |
| M | 4 | 6 | 82.7 | 5.2 | 81.1 | 42.3 |
| M | 4 | 7 | 84.4 | 4.7 | 77.0 | 39.5 |
| M | 4 | 8 | 84.0 | 4.8 | 71.2 | 36.0 |
| M | 5 | 1 | 90.0 | 3.0 | 101.1 | 70.6 |
| M | 5 | 2 | 90.5 | 2.9 | 61.6 | 47.6 |
| M | 5 | 3 | 77.9 | 6.7 | 52.6 | 27.6 |
| M | 5 | 4 | 74.1 | 4.6 | 58.5 | 31.6 |
| M | 5 | 5 | 85.6 | 4.3 | 45.0 | 27.1 |
| M | 5 | 6 | 87.3 | 3.8 | 63.3 | 37.8 |
| M | 5 | 7 | 83.0 | 5.1 | 62.6 | 36.9 |
| M | 5 | 8 | 84.0 | 4.8 | 67.0 | 35.9 |

Vection parameters

| Subject | Run # | Trial # | time with vection (%) | onset time (sec) | ax vection (%) | ve vection (%) |
|---|---|---|---|---|---|---|
| N | 1 | 1 | 33.4 | 20.0 | 10.9 | 2.0 |
| N | 1 | 2 | 77.9 | 6.7 | 34.5 | 16.6 |
| N | 1 | 3 | 65.8 | 10.3 | 24.8 | 11.8 |
| N | 1 | 4 | 78.3 | 6.5 | 46.3 | 30.1 |
| N | 2 | 1 | 62.4 | 11.3 | 19.9 | 10.1 |
| N | 2 | 2 | 68.3 | 9.5 | 25.6 | 16.4 |
| N | 2 | 3 | 74.3 | 7.7 | 19.1 | 12.8 |
| N | 2 | 4 | 65.9 | 10.2 | 19.8 | 13.2 |
| N | 2 | 5 | 78.8 | 6.4 | 25.3 | 15.5 |
| N | 2 | 6 | 81.8 | 5.5 | 38.4 | 23.3 |
| N | 2 | 7 | 77.1 | 6.9 | 27.6 | 18.9 |
| N | 2 | 8 | 62.3 | 10.8 | 6.5 | 2.8 |
| N | 3 | 1 | 70.4 | 8.9 | 22.4 | 15.6 |
| N | 3 | 2 | 69.4 | 9.2 | 18.9 | 12.8 |
| N | 3 | 3 | 29.0 | 17.4 | 6.7 | 1.6 |
| N | 3 | 4 | 81.1 | 5.7 | 27.0 | 18.9 |
| N | 4 | 1 | 77.0 | 6.9 | 30.7 | 22.1 |
| N | 4 | 2 | 74.2 | 7.8 | 25.9 | 15.7 |
| N | 4 | 3 | 0.0 | . | 5.9 | 1.9 |
| N | 4 | 4 | 69.6 | 9.1 | 24.4 | 18.4 |
| N | 4 | 5 | 23.9 | 22.8 | 13.9 | 8.4 |
| N | 4 | 6 | 51.6 | 14.5 | 27.1 | 12.2 |
| N | 4 | 7 | 48.4 | 10.7 | 21.9 | 11.7 |
| N | 4 | 8 | 71.9 | 8.4 | 18.9 | 13.0 |
| N | 5 | 1 | 0.0 | . | 6.9 | 2.0 |
| N | 5 | 2 | 25.5 | 13.1 | 14.4 | 8.4 |
| N | 5 | 3 | 19.6 | 23.4 | 13.5 | 2.9 |
| N | 5 | 4 | 62.5 | 8.2 | 16.6 | 10.9 |
| N | 5 | 5 | 52.1 | 7.1 | 19.3 | 7.1 |
| N | 5 | 6 | 0.0 | . | 9.5 | 7.9 |
| N | 5 | 7 | 0.0 | . | 9.5 | 8.2 |
| N | 5 | 8 | 26.0 | 21.7 | 12.1 | 2.8 |

## Vection parameters

| Subject | Run # | Trial # | time with vection (%) | onset time (sec) | ax vection (%) | ve vection (%) |
|---------|-------|---------|------------------------|------------------|----------------|----------------|
| O | 1 | 1 | 85.1 | 4.5 | 101.1 | 61.9 |
| O | 1 | 2 | 91.2 | 2.7 | 99.6 | 49.1 |
| O | 1 | 3 | 80.6 | 5.8 | 99.3 | 66.5 |
| O | 1 | 4 | 79.2 | 6.3 | 51.9 | 38.2 |
| O | 1 | 5 | 68.1 | 9.6 | 99.8 | 50.3 |
| O | 1 | 6 | 80.4 | 5.1 | 54.2 | 37.2 |
| O | 1 | 7 | 86.1 | 4.2 | 66.7 | 51.9 |
| O | 1 | 8 | 91.6 | 2.5 | 68.3 | 45.5 |
| O | 2 | 1 | 95.0 | 1.5 | 54.4 | 40.3 |
| O | 2 | 2 | 83.5 | 5.0 | 43.3 | 33.1 |
| O | 2 | 3 | 67.2 | 9.9 | 99.2 | 50.7 |
| O | 2 | 4 | 83.0 | 5.1 | 38.8 | 26.1 |
| O | 2 | 5 | 90.9 | 2.8 | 100.3 | 58.6 |
| O | 2 | 6 | 86.1 | 4.2 | 37.0 | 25.3 |
| O | 2 | 7 | 94.5 | 1.7 | 99.6 | 86.3 |
| O | 2 | 8 | 89.8 | 2.4 | 26.3 | 19.9 |
| O | 3 | 1 | 90.1 | 3.0 | 65.1 | 48.6 |
| O | 3 | 2 | 72.8 | 8.2 | 101.4 | 53.1 |
| O | 3 | 3 | 82.2 | 1.9 | 70.3 | 42.1 |
| O | 3 | 4 | 94.9 | 1.5 | 40.8 | 33.5 |
| O | 3 | 5 | 62.5 | 1.1 | 76.4 | 23.9 |
| O | 3 | 6 | 89.1 | 3.3 | 56.7 | 33.4 |
| O | 3 | 7 | 95.8 | 1.3 | 57.5 | 39.8 |
| O | 3 | 8 | 78.2 | 4.0 | 70.7 | 32.5 |
| O | 4 | 1 | 83.9 | 4.8 | 88.1 | 58.5 |
| O | 4 | 2 | 79.1 | 6.3 | 102.3 | 69.1 |
| O | 4 | 3 | 86.6 | 4.0 | 69.3 | 45.6 |
| O | 4 | 4 | 91.3 | 2.6 | 57.5 | 33.3 |
| O | 4 | 5 | 93.8 | 1.9 | 89.2 | 52.5 |
| O | 4 | 6 | 94.6 | 1.6 | 60.8 | 48.0 |
| O | 4 | 7 | 66.0 | 10.2 | 46.9 | 17.6 |
| O | 4 | 8 | 96.1 | 1.2 | 84.9 | 55.5 |
| O | 5 | 1 | 93.1 | 2.1 | 58.2 | 28.8 |
| O | 5 | 2 | 90.9 | 1.8 | 30.5 | 23.2 |
| O | 5 | 3 | 96.6 | 1.0 | 88.9 | 48.1 |
| O | 5 | 4 | 91.9 | 2.4 | 66.0 | 33.5 |
| O | 5 | 5 | 88.5 | 3.5 | 38.5 | 22.4 |
| O | 5 | 6 | 85.8 | 4.3 | 28.1 | 19.6 |
| O | 5 | 7 | 36.3 | 19.1 | 18.3 | 6.5 |
| O | 5 | 8 | 19.6 | 4.3 | 27.4 | 6.0 |

# Vection parameters

| Subject | Run # | Trial # | time with vection (%) | onset time (sec) | ax vection (%) | ve vection (%) |
|---------|-------|---------|-----------------------|------------------|----------------|----------------|
| P | 1 | 1 | 83.9 | 4.9 | 41.7 | 30.4 |
| P | 1 | 2 | 69.7 | 9.1 | 28.5 | 14.6 |
| P | 1 | 3 | 8.8 | 16.6 | 8.2 | 0.9 |
| P | 1 | 4 | 82.3 | 5.3 | 54.5 | 32.9 |
| P | 1 | 5 | 69.2 | 8.3 | 20.2 | 12.8 |
| P | 1 | 6 | 66.8 | 7.8 | 19.5 | 9.7 |
| P | 1 | 7 | 80.1 | 6.0 | 56.4 | 33.8 |
| P | 1 | 8 | 51.6 | 5.9 | 18.1 | 5.5 |
| P | 2 | 1 | 41.0 | 10.4 | 16.7 | 4.6 |
| P | 2 | 2 | 81.6 | 5.5 | 26.8 | 18.8 |
| P | 2 | 3 | 73.9 | 7.3 | 21.1 | 12.4 |
| P | 2 | 4 | 79.4 | 6.2 | 46.4 | 28.2 |
| P | 2 | 5 | 82.8 | 5.2 | 53.5 | 24.4 |
| P | 2 | 6 | 87.9 | 3.7 | 55.5 | 39.9 |
| P | 2 | 7 | 91.0 | 2.7 | 71.7 | 51.1 |
| P | 2 | 8 | 65.5 | 4.6 | 18.9 | 9.0 |
| P | 3 | 1 | 73.6 | 7.9 | 27.5 | 13.3 |
| P | 3 | 2 | 82.2 | 5.4 | 33.5 | 19.9 |
| P | 3 | 3 | 91.4 | 2.6 | 51.7 | 40.7 |
| P | 3 | 4 | 93.2 | 2.1 | 55.6 | 39.0 |
| P | 3 | 5 | 48.0 | 13.5 | 17.2 | 6.7 |
| P | 3 | 6 | 91.2 | 2.6 | 56.6 | 41.5 |
| P | 3 | 7 | 79.8 | 6.1 | 40.5 | 24.2 |
| P | 3 | 8 | 88.4 | 3.5 | 50.0 | 27.8 |
| P | 4 | 1 | 96.8 | 1.0 | 68.9 | 47.1 |
| P | 4 | 2 | 88.0 | 3.6 | 51.5 | 29.8 |
| P | 4 | 3 | 86.6 | 3.5 | 30.6 | 20.2 |
| P | 4 | 4 | 92.3 | 2.3 | 48.8 | 29.7 |
| P | 4 | 5 | 58.2 | 6.3 | 16.9 | 7.4 |
| P | 4 | 6 | 92.6 | 2.2 | 51.5 | 38.1 |
| P | 4 | 7 | 90.1 | 3.0 | 36.7 | 25.1 |
| P | 4 | 8 | 83.9 | 4.9 | 47.8 | 21.1 |

# Vection parameters

| Subject | Run # | Trial # | time with vection (%) | onset time (sec) | ax vection (%) | ve vection (%) |
|---------|-------|---------|-----------------------|------------------|----------------|----------------|
| Q | 1 | 1 | 69.2 | 9.3 | 27.3 | 11.6 |
| Q | 1 | 2 | 88.7 | 3.4 | 100.7 | 50.3 |
| Q | 1 | 3 | 93.5 | 2.0 | 47.2 | 32.7 |
| Q | 1 | 4 | 89.5 | 3.2 | 54.0 | 33.9 |
| Q | 1 | 5 | 95.9 | 1.2 | 72.1 | 46.3 |
| Q | 1 | 6 | 90.5 | 2.9 | 63.1 | 44.2 |
| Q | 1 | 7 | 91.8 | 2.5 | 73.4 | 49.4 |
| Q | 1 | 8 | 84.8 | 3.8 | 47.8 | 20.7 |
| Q | 2 | 1 | 74.2 | 4.9 | 35.2 | 19.4 |
| Q | 2 | 2 | 92.6 | 2.2 | 86.9 | 61.9 |
| Q | 2 | 3 | 67.5 | 9.8 | 93.3 | 36.8 |
| Q | 2 | 4 | 94.4 | 1.7 | 54.3 | 41.3 |
| Q | 2 | 5 | 83.8 | 4.9 | 100.9 | 57.8 |
| Q | 2 | 6 | 91.5 | 2.6 | 61.4 | 40.1 |
| Q | 2 | 7 | 88.9 | 3.4 | 101.3 | 59.7 |
| Q | 2 | 8 | 90.3 | 2.9 | 87.5 | 63.7 |
| Q | 3 | 1 | 59.2 | 10.8 | 102.2 | 35.5 |
| Q | 3 | 2 | 63.2 | 11.1 | 95.6 | 36.1 |
| Q | 3 | 3 | 8.4 | 27.5 | 9.6 | 4.7 |
| Q | 3 | 4 | 87.8 | 3.7 | 86.6 | 49.4 |
| Q | 3 | 5 | 34.7 | 17.3 | 31.6 | 12.7 |
| Q | 3 | 6 | 87.9 | 3.6 | 90.1 | 42.6 |
| Q | 3 | 7 | 90.6 | 2.8 | 87.8 | 62.0 |
| Q | 3 | 8 | 61.1 | 11.7 | 49.4 | 22.7 |
| Q | 4 | 1 | 26.2 | 22.2 | 41.7 | 4.8 |
| Q | 4 | 2 | 27.6 | 21.7 | 66.5 | 18.0 |
| Q | 4 | 3 | 47.7 | 15.7 | 61.4 | 23.1 |
| Q | 4 | 4 | 81.3 | 5.6 | 54.7 | 35.0 |
| Q | 4 | 5 | 90.2 | 3.0 | 62.2 | 47.3 |
| Q | 4 | 6 | 84.8 | 4.6 | 95.8 | 59.5 |
| Q | 4 | 7 | 87.3 | 3.8 | 102.1 | 72.3 |
| Q | 4 | 8 | 81.7 | 5.5 | 47.0 | 23.4 |

Vection parameters

| Subject | Run # | Trial # | time with vection (%) | onset time (sec) | ax vection (%) | ve vection (%) |
|---------|-------|---------|-----------|-----------|-----------|-----------|
| R | 1 | 1 | 0.0 | . | 8.3 | 5.9 |
| R | 1 | 2 | 62.9 | 5.0 | 24.8 | 14.4 |
| R | 1 | 3 | 74.3 | 7.7 | 40.2 | 26.4 |
| R | 1 | 4 | 10.2 | 18.8 | 20.3 | 8.6 |
| R | 1 | 5 | 33.5 | 6.7 | 20.1 | 9.2 |
| R | 1 | 6 | 55.3 | 13.4 | 34.1 | 13.5 |
| R | 1 | 7 | 38.2 | 13.5 | 22.1 | 11.3 |
| R | 1 | 8 | 11.9 | 25.9 | 7.2 | 0.2 |
| R | 2 | 1 | 0.0 | . | 7.9 | 0.0 |
| R | 2 | 2 | 0.0 | . | 16.2 | 8.0 |
| R | 2 | 3 | 0.0 | . | 2.9 | 2.3 |
| R | 2 | 4 | 12.1 | 26.4 | 12.6 | 8.4 |
| R | 2 | 5 | 0.0 | . | 8.7 | 4.1 |
| R | 2 | 6 | 0.0 | . | 8.9 | 4.3 |
| R | 2 | 7 | 0.0 | . | 9.3 | 6.3 |
| R | 2 | 8 | 0.0 | . | 6.6 | 0.9 |

# Vection parameters

| Subject | Run # | Trial # | time with vection (%) | onset time (sec) | ax vection (%) | ve vection (%) |
|---------|-------|---------|-----------------------|------------------|----------------|----------------|
| S | 1 | 1 | 87.8 | 3.7 | 99.2 | 67.6 |
| S | 1 | 2 | 95.2 | 1.5 | 102.1 | 82.5 |
| S | 1 | 3 | 90.2 | 3.0 | 67.9 | 52.9 |
| S | 1 | 4 | 92.0 | 2.4 | 101.1 | 76.2 |
| S | 1 | 5 | 92.0 | 2.4 | 27.5 | 18.6 |
| S | 1 | 6 | 93.5 | 2.0 | 63.2 | 50.3 |
| S | 1 | 7 | 94.7 | 1.6 | 57.7 | 44.1 |
| S | 1 | 8 | 85.9 | 4.2 | 49.1 | 22.0 |
| S | 2 | 1 | 93.3 | 2.0 | 86.4 | 67.5 |
| S | 2 | 2 | 90.2 | 3.0 | 95.2 | 73.4 |
| S | 2 | 3 | 93.6 | 1.9 | 99.3 | 77.7 |
| S | 2 | 4 | 95.4 | 1.4 | 75.0 | 63.8 |
| S | 2 | 5 | 95.3 | 1.4 | 101.5 | 86.6 |
| S | 2 | 6 | 94.3 | 1.7 | 53.0 | 41.4 |
| S | 2 | 7 | 96.1 | 1.2 | 50.1 | 40.0 |
| S | 2 | 8 | 92.5 | 2.3 | 69.9 | 44.6 |
| S | 3 | 1 | 93.3 | 2.0 | 67.7 | 55.4 |
| S | 3 | 2 | 95.6 | 1.3 | 50.0 | 43.5 |
| S | 3 | 3 | 93.5 | 2.0 | 99.6 | 85.4 |
| S | 3 | 4 | 91.6 | 2.5 | 52.8 | 42.9 |
| S | 3 | 5 | 94.5 | 1.7 | 102.8 | 89.8 |
| S | 3 | 6 | 95.6 | 1.3 | 56.8 | 48.3 |
| S | 3 | 7 | 90.4 | 0.8 | 60.5 | 48.9 |
| S | 3 | 8 | 95.1 | 1.5 | 56.4 | 47.4 |
| S | 4 | 1 | 91.2 | 2.7 | 99.2 | 70.9 |
| S | 4 | 2 | 94.8 | 1.6 | 80.3 | 64.4 |
| S | 4 | 3 | 95.4 | 1.4 | 39.0 | 28.4 |
| S | 4 | 4 | 93.3 | 2.0 | 85.8 | 62.8 |
| S | 4 | 5 | 93.4 | 2.0 | 55.3 | 35.5 |
| S | 4 | 6 | 95.8 | 1.3 | 50.2 | 47.0 |
| S | 4 | 7 | 91.3 | 2.6 | 81.4 | 72.4 |
| S | 4 | 8 | 95.1 | 1.5 | 61.6 | 48.7 |

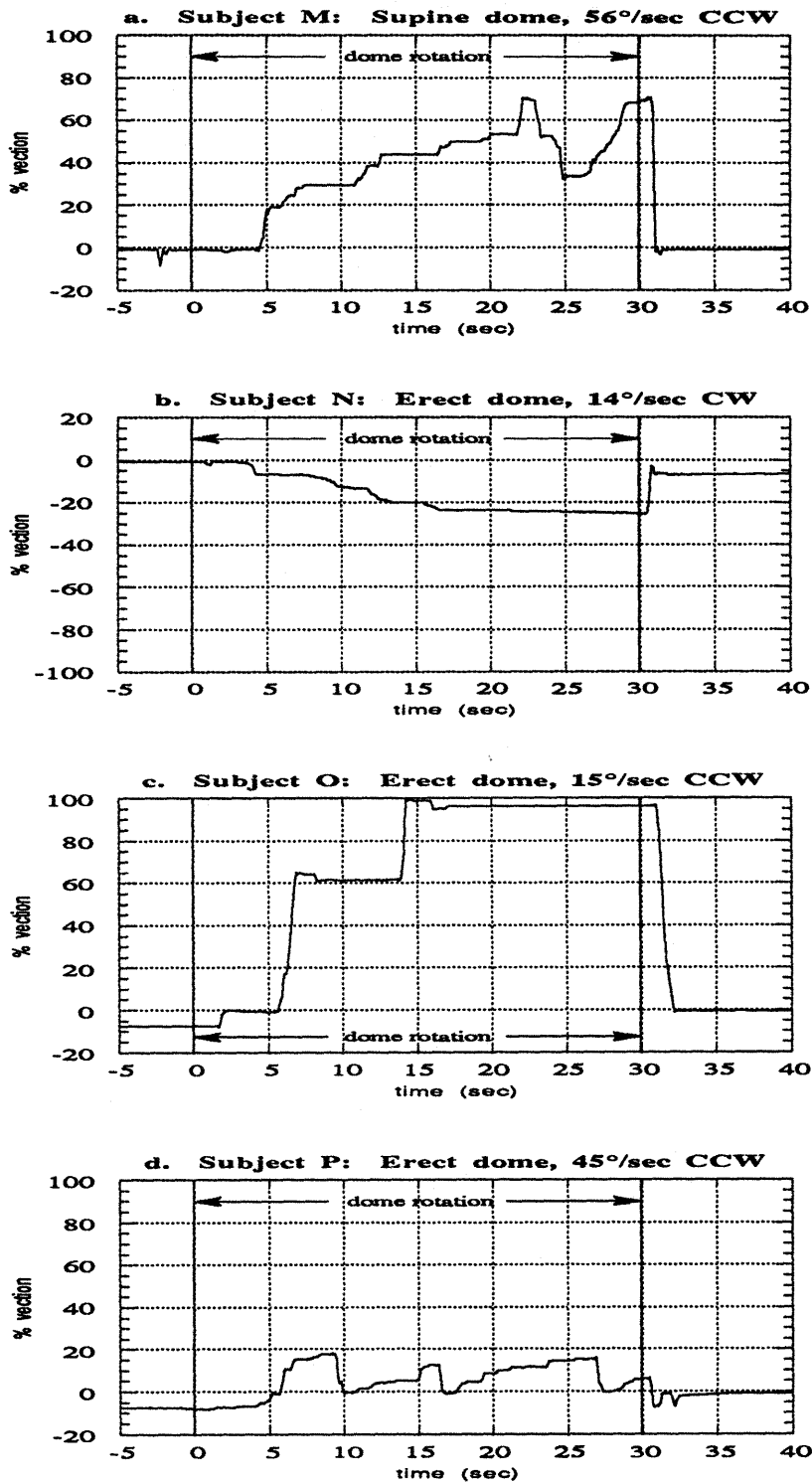**Figure D.1.** Typical vection responses for individual subjects. [a.] Subject M. [b.] Subject N. [c.] Subject O. [d.] Subject P.

255

e. **Subject Q: Erect dome, 30°/sec CW**

f. **Subject R: Erect dome, 60°/sec CW**
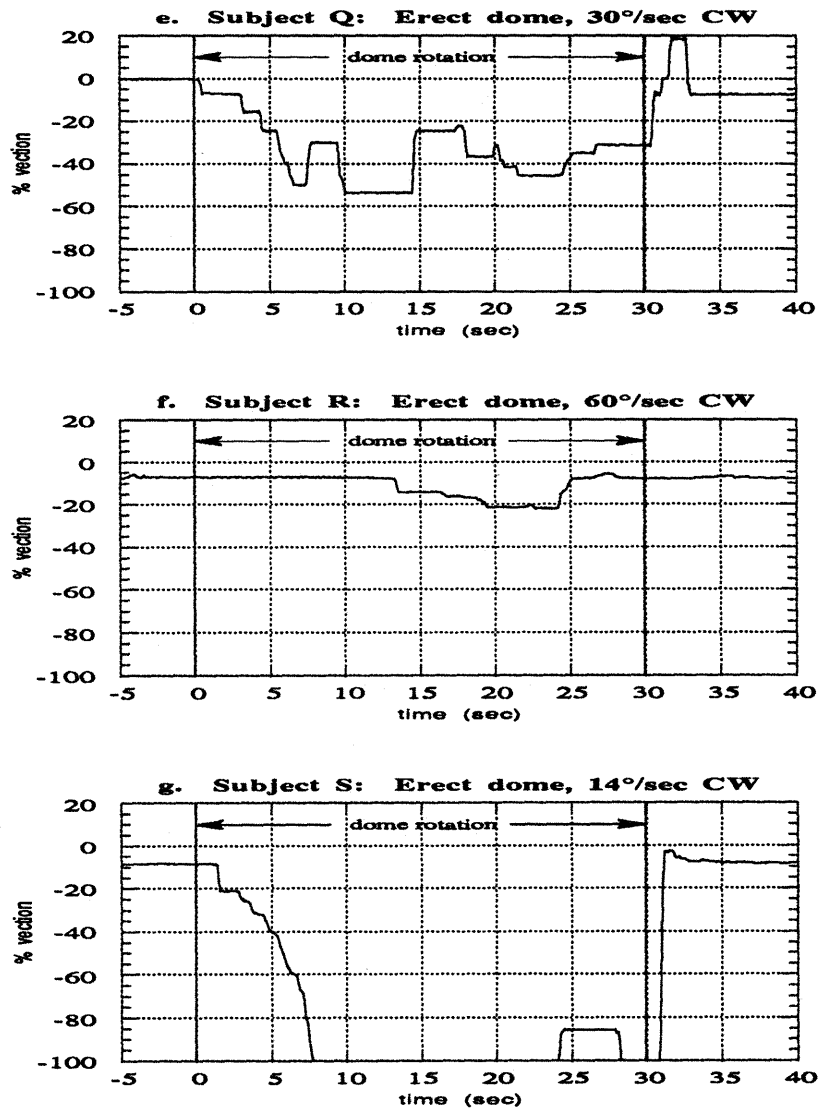
g. **Subject S: Erect dome, 14°/sec CW**

Figure D.1. Typical vection responses (continued from previous page). [e.] Subject Q. [f.] Subject R. [g.] Subject S

256

# APPENDIX E: SUBJECT COMMENTS

Following each test session, the subjects were asked to describe various aspects of their perceptions during the rotating dome experiment. This section paraphrases the notes taken during these subject debriefs.

## E.1.  Subject N Comments

### E.1.1.  Erect Session

•CW trials produced stronger vection and greater perception of tile

•Vection was not saturated
        -maximum vection achieved was approximately 70% for some CW trials

•Maximum perceived tilt was near 15°

•No vection aftereffects were perceived following the end of dome rotation

•Visual aftereffects were limited to vague afterimages consisting of concentric rings

•Vection decreased during lapses of fixation on the central LED

•Some dropouts may have occurred following blinks

•No motion sickness symptoms were observed other than slight headache

•Subject was conscious of tilt through pressure on biteboard

### E.1.2.  Supine Session

•Vection much weaker supine

•Same afterimages--concentric circles expanding outward

•For trials with lights on immediately following dome rotation, center of dome perceived to rotate slowly in direction counter to previous rotation. Visual sensation lasted only about 2 sec.; no vection reversal perceived upon dome stop

## E.2. Subject O Comments

### E.2.1. Erect Sessions

• During first run, motion sickness began about halfway through run. Reached symptom level of 7 where 10 is vomiting.
  - symptoms included nausea, excessive warmth, pallor

• Did get saturated vection on some of the slower trials; however, no "head over heels" rotation

• Higher speeds were not "believable" in terms of vection illusion

• Afterimage perceived to continue rotating in direction of prior dome rotation; effect mostly visual, since vection cuts out as soon as dome stops

• Fixation point perceived to drift around after about 20 sec. in darkness

• Dropouts occurred when "staring"

• Individual dots perceived as spinning during dome rotation

• Maximum tilt perceived was approximately 30°.

### E.2.2. Supine Session

• Surprised at how little vection was felt

• Never perceived saturated vection

• Slow trials produced slightly more vection

• More vection for CCW dome rotations

• LED perceived as drifting up after about 10 sec. in darkness; moved about 15° total

259

## E.3.  Subject P Comments

### E.3.1.  Erect Session

•Felt strong vection at same time as strong neck torque against biteboard

•Faster trials produced stronger vection

•At maximum, felt approximately 50% vection and 10° tilt

•Observed no afterimages or vection aftereffects

•Felt that CW runs might have caused slightly stronger vection

### E.3.2.  Supine Session

•Felt much less of a biteboard cue

•Sometimes saw circular afterimage moving in the same direction as prior dome rotation

•Felt more vection and faster onset for CCW dome rotation

•Did not feel full 360° continuous rotation

•Thought vection erect was stronger

## E.4. Subject Q Comments

### E.4.1. Erect Session

•Had balance problem during later trials for segments in complete darkness

•On one trial, felt outlasting vection in both directions

•Afterimages perceived to rotate about once around

•Saturated vection perceived for CW dome rotation only; once on very slow trial

•Felt faster self-rotation for faster trials

•Felt some pitch forward (approximately 15°)

•Spots appear to dots during stimulus rotation

### E.4.2. Supine Session

•Felt that vection was more intense, as if being rotated on a turntable

•Only felt saturated vection on one trial

•Perceived swing outward of approximately 45°

•More vection for CW dome rotations

•When lights go out, afterimage streaks appear to move opposite prior dome rotation.

•On 5 or 6 trials, perceived short period of self rotation after dome stop in direction opposite to prior vection (about 1 revolution only)

•Felt combination of roll right and pitch back for two CCW trials.

## E.5. Subject S Comments

### E.5.1. Erect Session

- Vection started almost immediately with dome rotation; stopped when lights went out

- Slight pulse of opposite vection when lights went out; stronger without LED fixation point

- Vection generally constant except at high stimulus speeds

- Sometimes felt as though laying on back and rotating through a full 360°. Vection reached approximately 50%.

- No strong sensation of constant roll angle

- Felt greater postural instability in the dark

- Higher speeds were "almost nauseogenic"

- Stronger vection perceived for CW dome rotations

### E.5.2. Supine Session

- Still perceived full 360° rotation

- No directional asymmetries noted

- Vection approximately 50% regardless of dome speed

- Saturation occurred only on one slow trial

- Occasional dropouts during fast trials

- No aftereffects

- Much harder to fixate in dark; perceived strong upward drift of LED in dark

- Vection began immediately upon start of dome rotation

# APPENDIX F: DATA ANALYSIS PROGRAMS

This appendix contains the major programs used in the data reduction and analysis. With one exception (**dome_convert**--a C program) the programs are all written in MatLab. A short description of each program is given:

**dome_convert:**     This C program loads binary data files saved by LabView and convertes them into MatLab variable format.

**enc_speed:**     MatLab script which calculates dome rotation rate from optical encoder output

**sac_em:**     From edited SPV and raw velocity traces, determines saccade and slow phase parameters, including end points, magnitudes, peak velocities, and frequencies. Also generates cumulative slow phase eye position traces

**spv_gain:**     From edited SPV and sac_em output, calculates mean and maximum SPV and SPV gain values for each trial

**tor_pos:**     From raw eye position and sac_em output, calculates mean, minimum, and maximum eye positions for each trial.

**fit_gains:**     Fits mean SPV gains to function relating gain to stimulus velocity. Actual function is of the form:

$$\text{Gain}_{SPV} = \left| \frac{G_0}{\dfrac{jV_{corner}}{V_{dome}} + 1} \right|$$

**pole_fun:**     Implements function to be fit in fit_gains. In essence, generates norm of error vector between actual data points and model predictions generated by current best fit values

**show_okan:**     Fits OKAN SPV decay to double exponential model with constant bias term. Model function is of the form

$$\text{SPV}_{OKAN} = V_{short}e^{-t/\tau_s} + V_{long}e^{-t/\tau_l} + V_{bias}$$

**okanfun:**     Implements function to be fit in show_okan. Generates norm of error vector between true SPV series and model predictions generated by current best fit values

**get_vect:**     For each trial calculates onset and dropout times, as well as maximum and average vection parameters

**plot_corr:**      For every trial, computes cross-correlation function between vection and SPV and between vection and eye position. Plots all time series and results of cross-correlations. Stores times of peaks in cross-correlation functions

**state_spv:**      Makes comparisons of SPV magnitude and mean eye position based on vection state. For SPVs, calculates ratio of mean SPV during vection segments to mean SPV during periods without vection. For eye position, calculates difference between mean positions during times with and without vection, then scales difference by total torsional range during trial

**T_1mean:**      Compares population mean with null hypothesis using double sided t-test. Returns probability that null hypothesis is correct.

**T_2means:**      Compares the means of two populations using a double sided t-test. Returns probability that the two populations have the same mean.

**T_line_conf:**      Given a set of (x,y) coordinates, performs a linear regression fit and generates a 90% or 95% confidence interval about the slope and the y-intercept.

```
/*********************************************************************

dome_convert.c
This program was written by M. Dave Balkwill
Modified slightly for rotating dome use by Keoki Jackson

This program can convert binary data files saved by LabView into MatLab variable
files

*********************************************************************/




#include <stdio.h>
#include <stdlib.h>
#include <fcntl.h>
#include <unix.h>

#define FALSE 0
#define TRUE  1

#define MAX_LINE_LENGTH 81

#define BLOCK_SIZE 16384

#define MATLAB_NAME "info"

#define BAD_TYPE    0
#define DOUBLE_TYPE 1
#define FLOAT_TYPE  2
#define LONG_TYPE   3
#define SHORT_TYPE  4

#define MATLAB_DOUBLE 1000
#define MATLAB_FLOAT  1010
#define MATLAB_LONG   1020
#define MATLAB_SHORT  1030

#define TORSIONAL_VAR    "tor"  /* channel 1 */
#define HORIZONTAL_VAR   "hor"  /* channel 2 */
#define VERTICAL_VAR     "ver"  /* channel 3 */
#define ACCELERATION_VAR "acc"  /* channel 4 */

char *matvar_names[] = {
  TORSIONAL_VAR, HORIZONTAL_VAR, VERTICAL_VAR, ACCELERATION_VAR
  };

char run_code[MAX_LINE_LENGTH];

char in_filename[MAX_LINE_LENGTH];
int in_fnamelen;
int in_handle;
FILE *in_fptr;
```

```c
char *in_buffer;
int in_bytes;

char out_filename[MAX_LINE_LENGTH];
int out_handle;
FILE *out_fptr;
char *out_buffer;
int out_bytes;

char inter_filename[MAX_LINE_LENGTH];
int inter_handle;
FILE *inter_fptr;

typedef struct {
    long type;
    long mrows;
    long ncols;
    long imagf;
    long namlen;
    } Fmatrix;

Fmatrix F_out;
long mrows = 0L;
long ncols = 0L;

int sample_size[5] = { 0, 10, 4, 4, 2 };
int in_size, out_size;
int in_type, out_type;
int num_channels;
long total_bytes;

int save_intermediate = FALSE;

#define ALLOCATE_BUFFER(BUF) \
{\
(BUF) = malloc(BLOCK_SIZE);\
if (!(BUF)) {\
printf("Out of memory on buffer allocation.\n");\
goto done;\
}\
}

#define READ_BUFFER() \
in_bytes = read(in_handle,in_buffer,BLOCK_SIZE);

#define WRITE_BUFFER(NUM) \
write(out_handle,out_buffer,NUM);

#define WRITE_INTER(NUM) \
write(inter_handle,out_buffer,NUM);

char in_line[MAX_LINE_LENGTH];
char matlab_name[MAX_LINE_LENGTH];
```

```
main()
{
    int open_input_file(), create_output_file(), create_inter_file(), get_file_parameters();
    int specify_run();
    long calculate_num_samples();
    void write_matlab_header(), transfer_data();
    int i;

    ALLOCATE_BUFFER(in_buffer)
    ALLOCATE_BUFFER(out_buffer)

    while (specify_run()) {

        for (i = 1; i <= 6; i++) {

            in_filename[in_fnamelen] = '0' + i;

            if (open_input_file()) {

                if (create_output_file()) {

                    if (get_file_parameters(i)) {

/*
                        printf("input file = %s\n",in_filename);
                        printf("output file = %s\n",out_filename);
                        printf("input type = %d\n",in_type);
                        printf("ouput type = %d\n",out_type);
                        printf("number of channels = %d\n",ncols);
                        printf("matlab name = %s\n",matlab_name);
*/
/*
                        if (save_intermediate) {
                            if (create_inter_file()) {
                                mrows = calculate_num_samples();
                                write_matlab_header();
                                transfer_data();
                            }
                        }
                        else {
*/

                        mrows = calculate_num_samples();
                        write_matlab_header();
                        transfer_data();
/*

                        }
*/
                    }

                }

            save_intermediate = FALSE;
        }
```

267

```c
        }
    }

done:
    close(in_handle);
    close(out_handle);
    close(inter_handle);
}


int specify_run()
{
    int i,l;
    int retval = TRUE;

    printf("Enter input file name:");
    gets(run_code);
    l = strlen(run_code);
    in_fnamelen = l;
    /* while (l != 6) { */

        if (l == 0) {
            retval = FALSE;
        /*   break; */
            }


        /*
        printf("\nInvalid file name -- enter only first six characters.\n");
        printf("Enter input file name (6 character run code):");
        gets(run_code);
        l = strlen(run_code);

        } */

    strcpy(in_filename,run_code);
    for (i = 0; i < (in_fnamelen); i++) {
        if ((in_filename[i] >= 'a') && (in_filename[i] <= 'z'))
            in_filename[i] += 'A' - 'a';
        }
    /*strcat(in_filename,"C1.DAT"); */

    return(retval);
}

int open_input_file()
{
    int l;
    int retval = TRUE;

    in_handle = open(in_filename,O_BINARY|O_RDONLY);
    if (in_handle <= 0) {
        printf("Input file %s is missing.\n",in_filename);
        retval = FALSE;
        }
```

```c
        return(retval);
}


int create_output_file()
{
    int l;
    int retval = TRUE;

    l = strlen(in_filename);
    strcpy( (char *)out_filename, (char *)in_filename );
    /*if (strncmp(".DAT",(char *)(&out_filename[l-4]),4))*/
        strcat(out_filename,".matlab");
    /*else
        out_filename[l-3] = 'M';*/
    out_fptr = fopen(out_filename,"rt");
    if (out_fptr) {
        printf("Output file %s already exists.  Overwrite (y/n) ?", out_filename);
        gets(in_line);
        if ((in_line[0] == 'y') || (in_line[0] == 'Y')) {
            printf("Overwriting %s.\n",out_filename);
            fclose(out_fptr);
            out_fptr = fopen(out_filename,"wt");
            }
        else {
            printf("Aborting for this file.\n");
            fclose(out_fptr);
            retval = FALSE;
            }
        }
    else {
        printf("Creating new output file %s.\n",out_filename);
        out_fptr = fopen(out_filename,"wt");
        }
    return(retval);
}

int create_inter_file()
{
    int l;
    int retval = TRUE;

    l = strlen(in_filename);
    strcpy( (char *)inter_filename, (char *)in_filename );
    if (strncmp(".DAT",(char *)(&inter_filename[l-4]),4))
        strcat(inter_filename,".nysa");
    else {
        inter_filename[l-3] = 'N';
        inter_filename[l-2] = 'Y';
        inter_filename[l-1] = 'S';
        }
    inter_fptr = fopen(inter_filename,"rt");
    if (inter_fptr) {
        printf("NysA file %s already exists.  Overwrite (y/n) ?", inter_filename);
```

269

```
                gets(in_line);
                if ((in_line[0] == 'y') || (in_line[0] == 'Y')) {
                    printf("Overwriting %s.\n",inter_filename);
                    fclose(inter_fptr);
                    inter_handle = open(inter_filename,O_BINARY|O_RDWR);
                    }
                else {
                    printf("Aborting for this file.\n");
                    fclose(inter_fptr);
                    retval = FALSE;
                    }
                }
            else {
                printf("Creating new NysA file %s.\n",inter_filename);
                inter_handle = open(inter_filename,O_BINARY|O_RDWR|O_CREAT);
                }
            return(retval);
        }

    int get_file_parameters(index)
    int index;
    {
        int get_buffer_type();
        int retval = TRUE;
        int i, j;

        in_type = get_buffer_type("input");
        in_type = 2;
        if (in_type == BAD_TYPE) {
            retval = FALSE;
            }
        else {
            in_size = sample_size[in_type];
            out_type = get_buffer_type("output");
            out_type = 4;
            if (out_type == BAD_TYPE) {
                retval = FALSE;
                }
            else {
                out_size = sample_size[out_type];

/* modified for Jock's special use -- assumes only one column of data per file */
/*
                printf("Enter number of data channels:");
                gets(in_line);
                sscanf(in_line,"%d",&num_channels);
*/
                num_channels = 1;
                if (num_channels <= 0)
                    retval = FALSE;
                else {
                    ncols = num_channels;
                strcpy(matlab_name,in_filename);
                for (i=0; i<in_fnamelen; i++) {
```

```c
                matlab_name[i] += 'a' - 'A';
            }
/*
            save_intermediate = (index > 2);
                printf("Enter MatLab variable name:");
                gets(in_line);
                if (strlen(in_line) == 0)
                    retval = FALSE;
                else {
                    for (i = 0; in_line[i] <= ' '; i++);
                    for (j = i; in_line[j] > ' '; j++)
                        matlab_name[j-i] = in_line[j];
                    matlab_name[j-i] = '\0';
                    if (strcmp(matlab_name,HEOG_VAR) == 0)
                        save_intermediate = TRUE;
                    else if (strcmp(matlab_name,VEOG_VAR) == 0)
                        save_intermediate = TRUE;
                }
*/


                }
            }
        }
    return(retval);
}

int get_buffer_type(io)
char *io;
{
    int type;

/*
    printf("Enter %s file type.\n",io);
    printf("    1: double\n");
    printf("    2: float\n");
    printf("    3: long\n");
    printf("    4: short\n");
    gets(in_line);
    sscanf(in_line,"%d",&type);
    if ((type < 1) || (type > 4)) {
        type = BAD_TYPE;
        printf("Invalid %s file type.  Aborting this file.\n",io);
    }
*/
/* modified for Jock's special use -- assumes I/O types are short two-byte integer */
    type = 2;

    return(type);
}

long calculate_num_samples()
{
    long num = 0L;
```

```c
      do {
        READ_BUFFER()
        num += in_bytes;
        }
      while (in_bytes == BLOCK_SIZE);
      total_bytes = num;
      num /= (ncols * in_size);
      close(in_handle);
      printf("Converting %ld samples.\n",num);
      return(num);
}

void write_matlab_header()
{
    switch (out_type) {
      case DOUBLE_TYPE:
        F_out.type = MATLAB_DOUBLE;
        break;
      case FLOAT_TYPE:
        F_out.type = MATLAB_FLOAT;
        break;
      case LONG_TYPE:
        F_out.type = MATLAB_LONG;
        break;
      case SHORT_TYPE:
        F_out.type = MATLAB_SHORT;
        break;
      }
    F_out.mrows = mrows;
    F_out.ncols = ncols;
    F_out.imagf = FALSE;
/*  F_out.namlen = strlen(MATLAB_NAME) + 1;*/
/* allow user-specified matlab variable name */
    F_out.namlen = strlen(matlab_name) + 1;
    fwrite( &F_out, sizeof(Fmatrix), 1, out_fptr );
/*  fwrite( MATLAB_NAME, sizeof(char), (int)F_out.namlen, out_fptr);*/
/* allow user-specified matlab variable name */
    fwrite( matlab_name, sizeof(char), (int)F_out.namlen, out_fptr);
    fclose(out_fptr);
}


void transfer_data()
{
    void double_to_float(), double_to_long(), double_to_short();
    void float_to_double(), float_to_long(), float_to_short();
    void long_to_double(), long_to_float(), long_to_short();
    void short_to_double(), short_to_float(), short_to_long();
    void short_reverse(), long_reverse();

    in_handle = open(in_filename,O_BINARY|O_RDONLY);
    out_handle = open(out_filename,O_BINARY|O_RDWR|O_APPEND);
    if (in_type == out_type) {
      do {
```

```
        READ_BUFFER()
/* reverse order of bytes in a word for data ported from VAX -- mod. for JC */
        if (in_type == SHORT_TYPE)
            short_reverse();
        else if (in_type == LONG_TYPE)
            long_reverse();
        WRITE_BUFFER(in_bytes)
        if (save_intermediate)
            WRITE_INTER(in_bytes)
        }
    while (in_bytes == BLOCK_SIZE);
    }
else {
    switch (in_type) {
    case DOUBLE_TYPE:
      switch (out_type) {
      case FLOAT_TYPE:
          double_to_float();
          break;
      case LONG_TYPE:
          double_to_long();
          break;
      case SHORT_TYPE:
          double_to_short();
          break;
      }
    case FLOAT_TYPE:
      switch (out_type) {
      case DOUBLE_TYPE:
          float_to_double();
          break;
      case LONG_TYPE:
          float_to_long();
          break;
      case SHORT_TYPE:
          float_to_short();
          break;
      }
    case LONG_TYPE:
      switch (out_type) {
      case DOUBLE_TYPE:
          long_to_double();
          break;
      case FLOAT_TYPE:
          long_to_float();
          break;
      case SHORT_TYPE:
          long_to_short();
          break;
      }
    case SHORT_TYPE:
      switch (out_type) {
      case DOUBLE_TYPE:
          short_to_double();
```

```
              break;
          case FLOAT_TYPE:
              short_to_float();
              break;
          case LONG_TYPE:
              short_to_long();
              break;
          }
       }
     }
   close(in_handle);
   close(out_handle);
}


void short_reverse()
{
   int i;

   for (i = 0; i < in_bytes; i += 2) {
     out_buffer[i] = in_buffer[i+1];
     out_buffer[i+1] = in_buffer[i];
       }
}


void long_reverse()
{
   int i;

   for (i = 0; i < in_bytes; i += 4) {
     out_buffer[i]   = in_buffer[i+3];
     out_buffer[i+1] = in_buffer[i+2];
     out_buffer[i+2] = in_buffer[i+1];
     out_buffer[i+3] = in_buffer[i];
       }
 }


void double_to_float()
{
   int i,j,k;
   int ratio;
   double *in;
   float *out;
   int in_samples, out_samples;
   long remaining;

   in = (double *)in_buffer;
   out = (float *)out_buffer;
   ratio = in_size / out_size;
   in_samples = BLOCK_SIZE / in_size;
   out_samples = BLOCK_SIZE / out_size;
   remaining = mrows * ncols;
```

```
    READ_BUFFER()
    j = 0;
    k = 0;
    while (remaining) {
        out[k] = in[j];
        j++;
        k++;
        remaining--;
        if (j == in_samples) {
            READ_BUFFER()
            j = 0;
        }
        if (k == out_samples) {
            WRITE_BUFFER(BLOCK_SIZE)
            k = 0;
        }
    }
    if (k > 0)
        WRITE_BUFFER(k * out_size)

}

void double_to_long()
{
    int i,j,k;
    int ratio;
    double *in;
    long *out;
    int in_samples, out_samples;
    long remaining;

    in = (double *)in_buffer;
    out = (long *)out_buffer;
    ratio = in_size / out_size;
    in_samples = BLOCK_SIZE / in_size;
    out_samples = BLOCK_SIZE / out_size;
    remaining = mrows * ncols;
    READ_BUFFER()
    j = 0;
    k = 0;
    while (remaining) {
        out[k] = in[j];
        j++;
        k++;
        remaining--;
        if (j == in_samples) {
            READ_BUFFER()
            j = 0;
        }
        if (k == out_samples) {
            WRITE_BUFFER(BLOCK_SIZE)
            k = 0;
        }
    }
```

```
    if (k > 0)
      WRITE_BUFFER(k * out_size)

}

void double_to_short()
{
    int i,j,k;
    int ratio;
    double *in;
    short *out;
    int in_samples, out_samples;
    long remaining;

    in = (double *)in_buffer;
    out = (short *)out_buffer;
    ratio = in_size / out_size;
    in_samples = BLOCK_SIZE / in_size;
    out_samples = BLOCK_SIZE / out_size;
    remaining = mrows * ncols;
    READ_BUFFER()
    j = 0;
    k = 0;
    while (remaining) {
      out[k] = in[j];
      j++;
      k++;
      remaining--;
      if (j == in_samples) {
        READ_BUFFER()
        j = 0;
        }
      if (k == out_samples) {
        WRITE_BUFFER(BLOCK_SIZE)
        k = 0;
        }
      }
   if (k > 0)
      WRITE_BUFFER(k * out_size)

}

void float_to_long()
{
    int i,j,k;
    int ratio;
    float *in;
    long *out;
    int in_samples, out_samples;
    long remaining;

    in = (float *)in_buffer;
    out = (long *)out_buffer;
    ratio = in_size / out_size;
```

```
   in_samples = BLOCK_SIZE / in_size;
   out_samples = BLOCK_SIZE / out_size;
   remaining = mrows * ncols;
   READ_BUFFER()
   j = 0;
   k = 0;
   while (remaining) {
      out[k] = in[j];
      j++;
      k++;
      remaining--;
      if (j == in_samples) {
         READ_BUFFER()
         j = 0;
         }
      if (k == out_samples) {
         WRITE_BUFFER(BLOCK_SIZE)
         k = 0;
         }
      }
   if (k > 0)
      WRITE_BUFFER(k * out_size)

}

void float_to_short()
{
   int i,j,k;
   int ratio;
   float *in;
   short *out;
   int in_samples, out_samples;
   long remaining;

   in = (float *)in_buffer;
   out = (short *)out_buffer;
   ratio = in_size / out_size;
   in_samples = BLOCK_SIZE / in_size;
   out_samples = BLOCK_SIZE / out_size;
   remaining = mrows * ncols;
   READ_BUFFER()
   j = 0;
   k = 0;
   while (remaining) {
      out[k] = in[j];
      j++;
      k++;
      remaining--;
      if (j == in_samples) {
         READ_BUFFER()
         j = 0;
         }
      if (k == out_samples) {
         WRITE_BUFFER(BLOCK_SIZE)
```

```
        k = 0;
        }
    }
  if (k > 0)
    WRITE_BUFFER(k * out_size)

}

void long_to_short()
{
    int i,j,k;
    int ratio;
    long *in;
    short *out;
    int in_samples, out_samples;
    long remaining;

    in = (long *)in_buffer;
    out = (short *)out_buffer;
    ratio = in_size / out_size;
    in_samples = BLOCK_SIZE / in_size;
    out_samples = BLOCK_SIZE / out_size;
    remaining = mrows * ncols;
    READ_BUFFER()
    j = 0;
    k = 0;
    while (remaining) {
        out[k] = in[j];
        j++;
        k++;
        remaining--;
        if (j == in_samples) {
            READ_BUFFER()
            j = 0;
        }
        if (k == out_samples) {
            WRITE_BUFFER(BLOCK_SIZE)
            k = 0;
        }
    }
  if (k > 0)
    WRITE_BUFFER(k * out_size)
}


void float_to_double()
{
    int i,j,k;
    int ratio;
    float *in;
    double *out;
    int in_samples, out_samples;
    long remaining;
```

```
   in = (float *)in_buffer;
   out = (double *)out_buffer;
   ratio = out_size / in_size;
   in_samples = BLOCK_SIZE / in_size;
   out_samples = BLOCK_SIZE / out_size;
   remaining = mrows * ncols;
READ_BUFFER()
j = 0;
k = 0;
while (remaining) {
   out[k] = in[j];
   j++;
   k++;
   remaining--;
   if (j == in_samples) {
      READ_BUFFER()
      j = 0;
      }
   if (k == out_samples) {
      WRITE_BUFFER(BLOCK_SIZE)
      k = 0;
      }
   }
if (k > 0)
   WRITE_BUFFER(k * out_size)

}

void long_to_double()
{
   int i,j,k;
   int ratio;
   long *in;
   double *out;
   int in_samples, out_samples;
   long remaining;

   in = (long *)in_buffer;
   out = (double *)out_buffer;
   ratio = out_size / in_size;
   in_samples = BLOCK_SIZE / in_size;
   out_samples = BLOCK_SIZE / out_size;
   remaining = mrows * ncols;
READ_BUFFER()
j = 0;
k = 0;
while (remaining) {
   out[k] = in[j];
   j++;
   k++;
   remaining--;
   if (j == in_samples) {
      READ_BUFFER()
      j = 0;
```

```c
          }
      if (k == out_samples) {
          WRITE_BUFFER(BLOCK_SIZE)
          k = 0;
          }
      }
  if (k > 0)
    WRITE_BUFFER(k * out_size)

}

void long_to_float()
{
    int i,j,k;
    int ratio;
    long *in;
    float *out;
    int in_samples, out_samples;
    long remaining;

    in = (long *)in_buffer;
    out = (float *)out_buffer;
    ratio = out_size / in_size;
    in_samples = BLOCK_SIZE / in_size;
    out_samples = BLOCK_SIZE / out_size;
    remaining = mrows * ncols;
    READ_BUFFER()
    j = 0;
    k = 0;
    while (remaining) {
        out[k] = in[j];
        j++;
        k++;
        remaining--;
        if (j == in_samples) {
            READ_BUFFER()
            j = 0;
            }
        if (k == out_samples) {
            WRITE_BUFFER(BLOCK_SIZE)
            k = 0;
            }
        }
    if (k > 0)
      WRITE_BUFFER(k * out_size)


}

void short_to_double()
{
    int i,j,k;
    int ratio;
    short *in;
```

```
    double *out;
    int in_samples, out_samples;
    long remaining;

    in = (short *)in_buffer;
    out = (double *)out_buffer;
    ratio = out_size / in_size;
    in_samples = BLOCK_SIZE / in_size;
    out_samples = BLOCK_SIZE / out_size;
    remaining = mrows * ncols;
    READ_BUFFER()
    j = 0;
    k = 0;
    while (remaining) {
        out[k] = in[j];
        j++;
        k++;
        remaining--;
        if (j == in_samples) {
            READ_BUFFER()
            j = 0;
        }
        if (k == out_samples) {
            WRITE_BUFFER(BLOCK_SIZE)
            k = 0;
        }
    }
    if (k > 0)
        WRITE_BUFFER(k * out_size)

}

void short_to_float()
{
    int i,j,k;
    int ratio;
    short *in;
    float *out;
    int in_samples, out_samples;
    long remaining;

    in = (short *)in_buffer;
    out = (float *)out_buffer;
    ratio = out_size / in_size;
    in_samples = BLOCK_SIZE / in_size;
    out_samples = BLOCK_SIZE / out_size;
    remaining = mrows * ncols;
    READ_BUFFER()
    j = 0;
    k = 0;
    while (remaining) {
        out[k] = in[j];
        j++;
        k++;
```

```
            remaining--;
            if (j == in_samples) {
               READ_BUFFER()
               j = 0;
            }
            if (k == out_samples) {
               WRITE_BUFFER(BLOCK_SIZE)
               k = 0;
            }
         }
      if (k > 0)
         WRITE_BUFFER(k * out_size)


}

void short_to_long()
{
   int i,j,k;
   int ratio;
   short *in;
   long *out;
   int in_samples, out_samples;
   long remaining;

   in = (short *)in_buffer;
   out = (long *)out_buffer;
   ratio = out_size / in_size;
   in_samples = BLOCK_SIZE / in_size;
   out_samples = BLOCK_SIZE / out_size;
   remaining = mrows * ncols;
   READ_BUFFER()
   j = 0;
   k = 0;
   while (remaining) {
      out[k] = in[j];
      j++;
      k++;
      remaining--;
      if (j == in_samples) {
         READ_BUFFER()
         j = 0;
      }
      if (k == out_samples) {
         WRITE_BUFFER(BLOCK_SIZE)
         k = 0;
      }
   }
   if (k > 0)
      WRITE_BUFFER(k * out_size)

}
```

```
%************************************************************
%
%enc_speed
%
%counts edges of time encoder square wave output, then calculates dome speed by
%determining number of edges per time window

%************************************************************



in_path = 'DKJ_Thesis1:Thesis:P.SUPINE:P.supine_dark+nofix:';
numtrials = input('Enter number of trials: ');
for trl = 1:numtrials
run_code = int2str(trl);
%run_code = input('Enter trial number: ','s');
fname = ['RIGHT', run_code, '.matlab'];
eval (['load ', in_path, fname]);
eval (['sig = right', run_code, ';']);
eval (['clear right', run_code]);

l = length(sig);
up = 0*ones(l,1);
down = up;
samp = 200;
bin = 200;
ls = ceil(l/bin);
if (trl==1)
    speed_up = 0*ones(ls,numtrials);
    speed_down = speed_up;
end  %if
on = (sig(1) > 600);

for i = 2:l
    bin_num = floor((i-1)/bin) + 1;
    if (on & (sig(i) < 200))
        down(i) = 1;
        on = 0;
        speed_down(bin_num,trl) = speed_down(bin_num,trl) + 1;
    elseif ((~(on)) & (sig(i) > 600))
        up(i) = 1;
        on = 1;
        speed_up(bin_num,trl) = speed_up(bin_num,trl) + 1;
    end
end
end  %for trl

mystery_fact = .945;
edge_deg = (360/256)*(1.935/1.487)*(32/72)/(bin/samp)/mystery_fact;
speed_up = speed_up*edge_deg;
speed_down = speed_down*edge_deg;
speed = (speed_up + speed_down)/2;
```

```
eval(['save ', in_path, 'speeds speed_up speed_down speed']);
```

```
%***********************************************************
% sac_em
% find saccade frequency, size, max velocity
% also find saccade beginning and end points, slow phase magnitudes, mean velocites
%    of individual slow phases
% generate cumulative slow phase eye position record
% uses diff_list to find location of events
% should probably use edit_spv to deselect non-saccade events
%    and separate multiple saccades

%***********************************************************




%file_specs;
%data_path = 'DungBeetleMan!:Thesis:P.ERECT:P.erect_dark+fix:';
t=.005;
bin_size = 4;
%run_code = input('Enter run code: ','s');
%num_trials = input('Enter number of trials: ');
eval (['load ', nys_path, 'gains'])
num_trials = length(dome);
clear dome gain spv
cal = .0244;
%ans = input('Enter position file calibration: [def = .0224] ');
%if (isempty(ans) == 0)
%    cal = ans;
%end

for trial = 1:num_trials
run_code = int2str(trial);
disp (['Trial #', run_code]);
in_file = file_name(Pos1_File, run_code);
pos_var = file_name(Pos1_Var, run_code);
eval (['load ', in_path, in_file]);
eval (['pos = ', pos_var, ';']);
%if sum (Pos1_Var ~= 'pos')
eval (['clear ', pos_var]);
clear pos_var
%end
cal = .0244;
%if ((subject == 'M') & (cond == 1) & (trial == 6))
%    cal = .02441406;
%end %if
pos = pos*cal;
pos = condition (pos);

x = pos;
filtzero
vel = x;
clear x
```

285

```
%in_file = file_name(Vel1_File, run_code);
%eval (['load ', nys_path, in_file]);
%eval (['vel = ', Vel1_Var, ';']);
%if sum (Vel1_Var ~= 'vel')
%     eval (['clear ', Vel1_Var]);
%end

in_file = file_name(Edited1_File, run_code);
eval (['load ', nys_path, in_file]);
eval (['spv = ', Edited1_Var, ';']);
if (length(Edited1_Var) ~= 3)
    eval (['clear ', Edited1_Var]);
elseif sum (Edited1_Var ~= 'spv')
    eval (['clear ', Edited1_Var]);
end

l = length(pos);
time = [0:t:t*(l-1)]';
sac_mag = 0*ones(l,1);
sac_vel = 0*ones(l,1);
sac_dur = 0*ones(l,1);
sac_intl = 0*ones(l,1);
sac_fnl = 0*ones(l,1);
ind_sp = 0*ones(l,1);
ave_spv = 0*ones(l,1);
sp_mag = 0*ones(l,1);
l_fr = ceil(l*t/bin_size);
sac_freq = 0*ones(l_fr,1);
time_fr = [bin_size:bin_size:l_fr*bin_size]';
cum = pos;

events = diff_list(vel,spv);
n = size(events);
n = n(1,1);

for i=1:n
    x = events(i,1);
    if (x == 0)
        x = 1;
    end   %if x
    y = events(i,2);
    if ((y-x)>1)
        cum((x+1):(y-1)) = cum(x)*ones((y-x-1),1);
    end
    if (y<l)
        cum(y:l) = cum(y:l) - (pos(y) - pos(x));
    end
    samp_ev = round((x+y)/2);
    sac_mag(samp_ev) = pos(y) - pos(x);
    sac_intl(samp_ev) = pos(x);
    sac_fnl(samp_ev) = pos(y);
    sac_dur(samp_ev) = (y-x)*t;
    peak_v = max(vel(x:y));
    if (abs(min(vel(x:y))) > abs(peak_v))
```

```
            peak_v = min(vel(x:y));
        end
        sac_vel(samp_ev) = peak_v;
        time_ev = time(samp_ev);
        bin_ev = floor(time_ev/bin_size) + 1;
        sac_freq(bin_ev) = sac_freq(bin_ev) + 1;
        end_sp = x;
        if (i>1)
            beg_sp = events((i-1),2);
            samp_sp = round((beg_sp + end_sp)/2);
            sp_mag(samp_sp) = pos(end_sp)-pos(beg_sp);
            ave_spv(samp_sp) = sp_mag(samp_sp)/(time(end_sp)-time(beg_sp));
            ind_sp(samp_sp) = 1;
        elseif (end_sp > 1)
            beg_sp = 1;
            samp_sp = round((beg_sp + end_sp)/2);
            sp_mag(samp_sp) = pos(end_sp)-pos(beg_sp);
            ave_spv(samp_sp) = sp_mag(samp_sp)/(time(end_sp)-time(beg_sp));
            ind_sp(samp_sp) = 1;
        end
    end
    if (y<l)
        samp_sp = round((y+l)/2);
        ave_spv(samp_sp) = (pos(l) - pos(y))/(time(l) - time(y));
        ind_sp(samp_sp) = 1;
    end


    ev_index = find(sac_dur);
    sac_mag = sac_mag(ev_index);
    sac_dur = sac_dur(ev_index);
    sac_vel = sac_vel(ev_index);
    sac_intl = sac_intl(ev_index);
    sac_fnl = sac_fnl(ev_index);
    time_sac = time(ev_index);
    ind_sp = find(ind_sp);
    time_sp = time(ind_sp);
    ave_spv = ave_spv(ind_sp);
    sp_mag = sp_mag(ind_sp);
    ind_sp = find(ave_spv ~= NaN);
    time_sp = time_sp(ind_sp);
    ave_spv = ave_spv(ind_sp);
    sp_mag = sp_mag(ind_sp);
    cum = decimate(cum,8);

    out_path = [in_path, 'new_nysa:'];
    eval(['save ', out_path, 'saccade', run_code, '.dat time_sac time_fr', ...
            ' sac_mag sac_dur sac_vel sac_freq sac_intl sac_fnl time_sp', ...
            ' ave_spv sp_mag']);
    eval(['save ', out_path, 'tor', run_code, '.cum cum;']);
    clear pos vel spv bin_ev time_ev peak_v samp_ev x y events ev_index
    clear in_file run_code ans l l_fr n i
    clear ind_sp beg_sp end_sp samp_sp time out_path
    %break
end   %for trial
```

```
%clear_specs
clear cal t bin_size
end
```

```
%*****************************************************************

%spv_gain
%calculates mean and max SPV values from edited SPV and 'sac_em' values
%also determines mean and max SPV gain values
%variables:  dome = abs(dome speed)
%            spv = (1) mean SPV during rotation
%                  (2) max SPV from sac_em (ave_spv)
%                  (3) max SPV from filtered edited SPV
%            gain = spv/dome

%*****************************************************************


file_specs
%data_path = 'DungBeetleMan!:Thesis:P.ERECT:P.erect_dark+fix:';
%speed_path = 'DungBeetleMan!:Thesis:N.ERECT:N.erect_dark+fix2:';
speed_path = data_path;
%num_trials = input('Enter number of trials: ');
num_trials = 8;
spv = 0*ones(num_trials,3);
gain = spv;
[b a] = cheby1(2,.5,.005);

for trial = 1:num_trials
    run_code = int2str(trial);
    disp (['Trial #', run_code])
    in_file = file_name(Edited1_File,run_code);
    eval (['load ', data_path, in_file])
    eval (['vel = ', Edited1_Var, ';'])
    eval (['clear ', Edited1_Var])
    in_file = ['saccade', run_code, '.dat'];
    eval (['load ', data_path, in_file])
    eval (['load ', speed_path, 'speeds'])

    dome = mean(speed(7:35,:))';
  spv(trial,1) = mean(vel(1001:7000));
    gain(trial,1) = spv(trial,1)/dome(trial);
disp ('     done 1')
    ind = find(time_sp < 35);
    ind = find(time_sp(ind) > 5);
    if (sign(spv(trial,1)) == 1)
        max_spv = max(ave_spv(ind));
    else
        max_spv = min(ave_spv(ind));
    end   %if
    ind = find(ave_spv == max_spv);
    t_max = time_sp(ind(1));
    if ((t_max < 5) | (t_max > 35))
        disp ('Flag:  time out of range')
    end   %if
    spv(trial,2) = max_spv;
    gain(trial,2) = max_spv/speed(ceil(t_max),trial);
```

```
disp ('      done 2')
    filt_vel = filtfilt(b,a,vel);
    ind = [1001:7000]';
    if (sign(spv(trial,1)) == 1)
        max_spv = max(filt_vel(ind));
    else
        max_spv = min(filt_vel(ind));
    end   %if
    ind = find(filt_vel == max_spv);
    t_max = ind(1)*.005;
    if ((t_max < 5) | (t_max > 35))
        disp ('Flag:  time out of range')
    end   %if
  spv(trial,3) = max_spv;
    gain(trial,3) = max_spv/speed(ceil(t_max),trial);
disp ('      done 3')
    clear sac_freq sac_intl sac_fnl time_sac time_sp time_fr ave_spv
    clear sac_mag sac_dur sac_vel speed speed_up speed_down max_spv
  clear t_max filt_vel vel
end   %for trial

eval (['save ', data_path, 'gains dome spv gain'])
clear_specs
clear data_path in_file run_code a b ind num_trials speed_path trial
```

```
%*******************************************************************

%tor_pos
%calculates eye position parameters from raw eye position (LEFT#)
%   as well as from saccade data (saccade#)
%
%the variables are:
%  ppp--contains mean eye position pre (1), per (2), post (3) dome
%       rotation
%  intl--eye position at beginning of saccade; contains mean (1),
%       min (2), max (3)
%fnl--eye position at end of saccade; contains mean (1), min (2),
%       max (3)


%*******************************************************************




file_specs
cal = 50/2048;

%data_path = 'DungBeetleMan!:Thesis:P.ERECT:P.erect_dark+fix:';
%speed_path = 'DungBeetleMan!:Thesis:N.ERECT:N.erect_dark+fix2:';
%speed_path = data_path;
%num_trials = input('Enter number of trials: ');
%num_trials = 8;
%gain = spv;
%[b a] = cheby1(2,.5,.005);

eval (['load ', n_path, 'gains'])
num_trials = length(dome);
dome = dome.*sign(spv(:,1));
ppp = 0*ones(num_trials,3);
intl = 0*ones(num_trials,3);
fnl = intl;
clear spv gain
pre = pre*200;
per = pre + per*200;
%post = per + post*200;

for trial = 1:num_trials
    run_code = int2str(trial);
    disp (['Trial #', run_code])
    in_file = file_name(Pos1_File,run_code);
    eval (['load ', data_path, in_file])
    in_var = file_name(Pos1_Var,run_code);
    eval (['tor = ', in_var, ';'])
    tor = tor*cal;
    post = length(tor);
disp (['   post = ', int2str(post)])
    eval (['clear ', in_var])
    in_file = ['saccade', run_code, '.dat'];
```

```
        eval (['load ', n_path, in_file])

 ppp(trial,1) = mean(tor(1:pre));
    ppp(trial,2) = mean(tor((pre+1):per));
    ppp(trial,3) = mean(tor((per+600+1):post));
    ind = find(time_sac <= (per/200));
    ind = find(time_sac(ind) > (pre/200));
    intl(trial,1) = mean(sac_intl(ind));
    intl(trial,2) = min(sac_intl(ind));
    intl(trial,3) = max(sac_intl(ind));
    fnl(trial,1) = mean(sac_fnl(ind));
    fnl(trial,2) = min(sac_fnl(ind));
    fnl(trial,3) = max(sac_fnl(ind));
    clear sac_freq sac_intl sac_fnl time_sac time_sp time_fr ave_spv
    clear sac_mag sac_dur sac_vel speed speed_up speed_down max_spv
  clear t_max filt_vel vel
end   %for trial

eval (['save ', n_path, 'pos dome ppp intl fnl'])
clear_specs
clear data_path n_path in_file run_code ind num_trials trial in_var
clear pre per post cal tor
```

```
%*****************************************************************

%fit_gains
%fits mean SPV gain values extracted for each trial to a "first order lag" relating SPV gain
%   to stimulus velocity
%the function to be fit is contained in the separate function module 'polefun'

%*****************************************************************




global Data;
df = 1;
df1 = 2;
df2 = 3;
dnf = 4;
lt = 5;

sub_list = ['MNOPQRS'];
num_subs = length(sub_list);
for sub = 1:num_subs
%      hold off
%      clg
     subject = sub_list(sub);

     pstr = 'ERECT';
     cum_cond = [];
     cum_dome = [];
     cum_gain = [];
     cond_list = [];
     all_pole = [];
     CW_pole = [];
     CCW_pole = [];
     all_exp = [];
     CW_exp = [];
     CCW_exp = [];
     for cond = df:lt
          path_specs
          if (exist([nys_path, 'gains']) == 2)
               eval (['load ', nys_path, 'gains'])
               dome = dome.*sign(spv(:,1));
               gain = abs(gain(:,1));
               cum_dome = [cum_dome; dome];
               cum_gain = [cum_gain; gain];
               cum_cond = [cum_cond; cond*ones(length(dome),1)];
               neg_ind = find(dome < 0);
               pos_ind = find(dome > 0);
               x = abs(dome);
               Data = [x gain];
               k = [4 20];
               k = fmins('polefun',k,.0001);
               A = k(1) ./sqrt(k(2)^2 + x.^2);
```

293

```
f = norm(A - Data(:,2))/length(A);
all_pole = [all_pole; [k(1)/k(2) k(2) f]];
x = abs(dome(pos_ind));
Data = [x gain(pos_ind)];
k = [4 20];
k = fmins('polefun',k,.0001);
A = k(1) ./sqrt(k(2)^2 + x.^2);
f = norm(A - Data(:,2))/length(A);
CW_pole = [CW_pole; [k(1)/k(2) k(2) f]];
x = abs(dome(neg_ind));
Data = [x gain(neg_ind)];
k = [4 20];
k = fmins('polefun',k,.0001);
A = k(1) ./sqrt(k(2)^2 + x.^2);
f = norm(A - Data(:,2))/length(A);
CCW_pole = [CCW_pole; [k(1)/k(2) k(2) f]];

x = abs(dome);
y = log(gain);
k = polyfit(x,y,1);
z = exp(polyval(k,x));
y = exp(y);
f = norm(z - y)/length(z);
all_exp = [all_exp; [k(1) exp(k(2)) f]];
x = abs(dome(pos_ind));
y = log(gain(pos_ind));
k = polyfit(x,y,1);
z = exp(polyval(k,x));
y = exp(y);
f = norm(z - y)/length(z);
CW_exp = [CW_exp; [k(1) exp(k(2)) f]];
x = abs(dome(neg_ind));
y = log(gain(neg_ind));
k = polyfit(x,y,1);
z = exp(polyval(k,x));
y = exp(y);
f = norm(z - y)/length(z);
CCW_exp = [CCW_exp; [k(1) exp(k(2)) f]];

    cond_list = [cond_list; cond];
  end  %if exist
end  %for cond

neg_ind = find(cum_dome < 0);
pos_ind = find(cum_dome > 0);
Data = [abs(cum_dome) cum_gain];
x = Data(:,1);
k = [4 20];
k = fmins('polefun',k,.0001);
A = k(1) ./sqrt(k(2)^2 + x.^2);
f = norm(A - Data(:,2))/length(A);
er_all_pole = [k(1)/k(2) k(2) f];
Data = [abs(cum_dome(pos_ind)) cum_gain(pos_ind)];
x = Data(:,1);
```

```
k = [4 20];
k = fmins('polefun',k,.0001);
A = k(1) ./sqrt(k(2)^2 + x.^2);
f = norm(A - Data(:,2))/length(A);
er_CW_pole = [k(1)/k(2) k(2) f];
Data = [abs(cum_dome(neg_ind)) cum_gain(neg_ind)];
x = Data(:,1);
k = [4 20];
k = fmins('polefun',k,.0001);
A = k(1) ./sqrt(k(2)^2 + x.^2);
f = norm(A - Data(:,2))/length(A);
er_CCW_pole = [k(1)/k(2) k(2) f];

x = abs(cum_dome);
y = log(cum_gain);
k = polyfit(x,y,1);
z = exp(polyval(k,x));
y = exp(y);
f = norm(z - y)/length(z);
er_all_exp = [k(1) exp(k(2)) f];
x = abs(cum_dome(pos_ind));
y = log(cum_gain(pos_ind));
k = polyfit(x,y,1);
z = exp(polyval(k,x));
y = exp(y);
f = norm(z - y)/length(z);
er_CW_exp = [k(1) exp(k(2)) f];
x = abs(cum_dome(neg_ind));
y = log(cum_gain(neg_ind));
k = polyfit(x,y,1);
z = exp(polyval(k,x));
y = exp(y);
f = norm(z - y)/length(z);
er_CCW_exp = [k(1) exp(k(2)) f];
er_dome = cum_dome;
er_gain = cum_gain;


%      eval (['save ', pre_path, 'gain_fit er_all_pole er_CW_pole er_CCW_pole ', ...
%                  'er_all_exp er_CW_exp er_CCW_exp cond_list all_pole CW_pole ', ...
%                  'CCW_pole all_exp CW_exp CCW_exp'])

num_conds = length(cond_list);
plot_sym = ['*'; '+'; 'o'; 'x'];
dit = setstr(39);  %" ' "
command1 = ['plot ('];
command2 = command1;
command3 = command1;
speed = [15:.5:60]';
if (subject == 'M')
    speed = [30:.5:60]';
end  %if
for i = 1:num_conds
    cond = cond_list(i);
    ind = find(cum_cond == cond);
```

295

```
        dome = cum_dome(ind);
        gain = cum_gain(ind);
        i_str = int2str(i);
        eval (['dome', i_str, ' = dome;'])
        eval (['gain', i_str, ' = gain;'])
        command1 = [command1, 'dome', i_str, ', gain', i_str, ', ', ...
                        dit, plot_sym(i), dit];
        k = CW_pole(i,:);
        y = k(1) ./sqrt(1 + (speed/k(2)).^2);
%          k = CW_exp(i,:);
%          y = k(2)*exp(k(1)*speed);
        eval (['y', i_str, ' = y;'])
        command2 = [command2, 'speed', ', y', i_str];
        k = CCW_pole(i,:);
        z = k(1) ./sqrt(1 + (speed/k(2)).^2);
%        k = CCW_exp(i,:);
%          z = k(2)*exp(k(1)*speed);
        eval (['z', i_str, ' = z;'])
        command3 = [command3, '-speed', ', z', i_str];
        if (i ~= num_conds)
            command1= [command1, ','];
            command2 = [command2, ','];
            command3 = [command3, ','];
        end  %if (i)
    end  %for i
    command1 = [command1, ')'];
    command2 = [command2, ')'];
    command3 = [command3, ')'];
%    subplot(222)
%    eval(command1)
%    axis;
%    subplot(222)
%    eval(command2)
%    subplot(222)
%    eval(command3)
%    axis;
%    grid
%    title (['Erect fits (runs: [*]=1 [+]=2 [o]=3)'])
%    xlabel ('dome speed (deg/s)')
%    ylabel ('mean SPV gain')

pstr = 'SUPINE';
cum_cond = [];
cum_dome = [];
cum_gain = [];
cond_list = [];
all_pole = [];
CW_pole = [];
CCW_pole = [];
all_exp = [];
CW_exp = [];
CCW_exp = [];
for cond = df:lt
    path_specs
```

296

```
if (exist([nys_path, 'gains']) == 2)
    eval (['load ', nys_path, 'gains'])
    dome = dome.*sign(spv(:,1));
    gain = abs(gain(:,1));
    cum_dome = [cum_dome; dome];
    cum_gain = [cum_gain; gain];
    cum_cond = [cum_cond; cond*ones(length(dome),1)];
    neg_ind = find(dome < 0);
    pos_ind = find(dome > 0);
    x = abs(dome);
    Data = [x gain];
    k = [1 1];
    k = fmins('polefun',k,.0001);
    A = k(1) ./sqrt(k(2)^2 + x.^2);
    f = norm(A - Data(:,2))/length(A);
    all_pole = [all_pole; [k(1)/k(2) k(2) f]];
    x = abs(dome(pos_ind));
    Data = [x gain(pos_ind)];
    k = [4 20];
    k = fmins('polefun',k,.0001);
    A = k(1) ./sqrt(k(2)^2 + x.^2);
    f = norm(A - Data(:,2))/length(A);
    CW_pole = [CW_pole; [k(1)/k(2) k(2) f]];
    x = abs(dome(neg_ind));
    Data = [x gain(neg_ind)];
    k = [1 1];
    k = fmins('polefun',k,.0001);
    A = k(1) ./sqrt(k(2)^2 + x.^2);
    f = norm(A - Data(:,2))/length(A);
    CCW_pole = [CCW_pole; [k(1)/k(2) k(2) f]];

    x = abs(dome);
    y = log(gain);
    k = polyfit(x,y,1);
    z = exp(polyval(k,x));
    y = exp(y);
    f = norm(z - y)/length(z);
    all_exp = [all_exp; [k(1) exp(k(2)) f]];
    x = abs(dome(pos_ind));
    y = log(gain(pos_ind));
    k = polyfit(x,y,1);
    z = exp(polyval(k,x));
    y = exp(y);
    f = norm(z - y)/length(z);
    CW_exp = [CW_exp; [k(1) exp(k(2)) f]];
    x = abs(dome(neg_ind));
    y = log(gain(neg_ind));
    k = polyfit(x,y,1);
    z = exp(polyval(k,x));
    y = exp(y);
    f = norm(z - y)/length(z);
    CCW_exp = [CCW_exp; [k(1) exp(k(2)) f]];

    cond_list = [cond_list; cond];
```

297

```
    end  %if exist
end  %for cond

neg_ind = find(cum_dome < 0);
pos_ind = find(cum_dome > 0);
Data = [abs(cum_dome) cum_gain];
x = Data(:,1);
k = [1 1];
k = fmins('polefun',k,.0001);
A = k(1) ./sqrt(k(2)^2 + x.^2);
f = norm(A - Data(:,2))/length(A);
sup_all_pole = [k(1)/k(2) k(2) f];
Data = [abs(cum_dome(pos_ind)) cum_gain(pos_ind)];
x = Data(:,1);
k = [1 1];
k = fmins('polefun',k,.0001);
A = k(1) ./sqrt(k(2)^2 + x.^2);
f = norm(A - Data(:,2))/length(A);
sup_CW_pole = [k(1)/k(2) k(2) f];
Data = [abs(cum_dome(neg_ind)) cum_gain(neg_ind)];
x = Data(:,1);
k = [5 5];
k = fmins('polefun',k,.0001);
A = k(1) ./sqrt(k(2)^2 + x.^2);
f = norm(A - Data(:,2))/length(A);
sup_CCW_pole = [k(1)/k(2) k(2) f];

x = abs(cum_dome);
y = log(cum_gain);
k = polyfit(x,y,1);
z = exp(polyval(k,x));
y = exp(y);
f = norm(z - y)/length(z);
sup_all_exp = [k(1) exp(k(2)) f];
x = abs(cum_dome(pos_ind));
y = log(cum_gain(pos_ind));
k = polyfit(x,y,1);
z = exp(polyval(k,x));
y = exp(y);
f = norm(z - y)/length(z);
sup_CW_exp = [k(1) exp(k(2)) f];
x = abs(cum_dome(neg_ind));
y = log(cum_gain(neg_ind));
k = polyfit(x,y,1);
z = exp(polyval(k,x));
y = exp(y);
f = norm(z - y)/length(z);
sup_CCW_exp = [k(1) exp(k(2)) f];
sup_dome = cum_dome;
sup_gain = cum_gain;

%    eval (['save ', pre_path, 'gain_fit sup_all_pole sup_CW_pole ', ...
%                'sup_CCW_pole sup_all_exp sup_CW_exp sup_CCW_exp cond_list ', ...
%                'all_pole CW_pole CCW_pole all_exp CW_exp CCW_exp'])
```

298

```
num_conds = length(cond_list);
plot_sym = ['*'; '+'; 'o'; 'x'];
dit = setstr(39);  %" ' "
command1 = ['plot ('];
command2 = command1;
command3 = command1;
speed = [15:.5:60]';
if (subject == 'M')
    speed = [10:.5:80]';
end  %if
for i = 1:num_conds
    cond = cond_list(i);
    ind = find(cum_cond == cond);
    dome = cum_dome(ind);
    gain = cum_gain(ind);
    i_str = int2str(i);
  eval (['dome', i_str, ' = dome;'])
    eval (['gain', i_str, ' = gain;'])
    command1 = [command1, 'dome', i_str, ', gain', i_str, ', ', ...
                        dit, plot_sym(i), dit];
    k = CW_pole(i,:);
    y = k(1) ./sqrt(1 + (speed/k(2)).^2);
%       k = CW_exp(i,:);
%       y = k(2)*exp(k(1)*speed);
    eval (['y', i_str, ' = y;'])
    command2 = [command2, 'speed', ', y', i_str];
    k = CCW_pole(i,:);
    z = k(1) ./sqrt(1 + (speed/k(2)).^2);
%       k = CCW_exp(i,:);
%       z = k(2)*exp(k(1)*speed);
    eval (['z', i_str, ' = z;'])
    command3 = [command3, '-speed', ', z', i_str];
    if (i ~= num_conds)
        command1= [command1, ','];
        command2 = [command2, ','];
        command3 = [command3, ','];
    end  %if (i)
end  %for i
command1 = [command1, ')'];
command2 = [command2, ')'];
command3 = [command3, ')'];
%   subplot(224)
%   eval(command1)
%   axis;
%   subplot(224)
%   eval(command2)
%   subplot(224)
%   eval(command3)
%   axis;
%   grid
%   title (['Supine fits (runs: [*]=1 [+]=2 [o]=3)'])
%   xlabel ('dome speed (deg/s)')
%   ylabel ('mean SPV gain')
```

```
speed = [15:.5:60]';
if (subject == 'M')
    speed = [20:.5:80]';
end  %if
subplot(121)
plot(er_dome,er_gain,'*',sup_dome,sup_gain,'+')
axis;
k = er_CW_pole;
z = k(1) ./sqrt(1 + (speed/k(2)).^2);
subplot(121)
plot(speed,z)
k = er_CCW_pole;
z = k(1) ./sqrt(1 + (speed/k(2)).^2);
subplot(121)
plot(-speed,z)
k = sup_CW_pole;
z = k(1) ./sqrt(1 + (speed/k(2)).^2);
subplot(121)
plot(speed,z,'--g')
k = sup_CCW_pole;
z = k(1) ./sqrt(1 + (speed/k(2)).^2);
subplot (121)
plot(-speed,z,'--g')
axis;
grid
title (['Subject ', subject, ': Erect and supine SPV gains'])
xlabel ('dome speed (deg/s)')
ylabel ('mean SPV gain    [*, -]=erect [+, - -]=supine')

%    prtsc
%break
end  %for sub
```

```matlab
function f = polefun(k);

%**********************************************************************

%polefun
%Data array contains stimulus velocity in column 1 (x) and mean SPV gain in column 2 (y)
%For parameters in k vector, generates a norm representative of the error between the model
%   prediction and the actual data points
%Called by fit_gains

%**********************************************************************


x = Data(:,1);
y = Data(:,2);

A = k(1) ./sqrt(k(2)^2 + x.^2);

f = norm(A - y)/length(x);
```

```
%***********************************************************

%show_okan
%generates plot of after-nystagmus;  both position and velocity
%fits double exponential (plus constant bias) to OKAN SPV time series
%calls function okan_fun, which implements double exponential

%***********************************************************



global Data steps break_flag
df = 1;
df1 = 2;
df2 = 3;
dnf = 4;
lt = 5;

sub_list = 'O';
posture = ['ERECT '; 'SUPINE'];
cond = df;
for sub = 1:length(sub_list)
subject = sub_list(sub);
for post_num = 1:1
pstr = posture(post_num,:);

path_specs
if (exist([nys_path, 'pos']) == 2)
eval (['load ', nys_path, 'pos'])
num_trials = length(dome);
clear ppp intl fnl

cal = .0244;
post = 30;
extra = 5;
show = 30;
fit_t = 20;
if ((subject == 'M') & ((post_num == 2) & ((cond == lt)|(cond == df2))))
    post = 13.75;
    show = 13.75;
    fit_t = 13.7;
end  %if weird
delay = 0.0;
%start = 1;  %input('Start with trial #:  ');
%end_tr = num_trials
start = input('Which trial number? ');
end_tr = start;
for tr = start:end_tr
    trial = int2str(tr);
    eval (['load ', in_path, 'LEFT', trial, '.matlab']);
    eval (['pos = left', trial, ';'])
    eval (['clear left', trial])
```

302

```
eval (['load ', nys_path, 'tor', trial, '.edited']);
vel = edited;
clear edited
eval (['load ', nys_path, 'tor', trial, '.cum']);

l = length(pos);
p_ind = [(l - (post + extra)*200 + 1):l]';
fit_vel = decimate(vel(p_ind), 20);
vel = decimate(vel(p_ind), 8);

td = [.04:.04:(post + extra)]' - extra;
t = [.005:.005:(post + extra)]' - extra;
tf = [.1:.1:(fit_t + extra + delay)]' - extra;
fit_ind = find (tf >= delay);
Data = [(tf(fit_ind) - delay) fit_vel(fit_ind)];
%      k = [sign(dome(tr)) -1 sign(dome(tr)) -1 0];
k = input ('Start iteration with? ');
k = [k(1) 1/k(2) k(3) 1/k(4) k(5)];
    steps = 0;
    break_flag = 0;
    [k, count] = fmins('okanfun', k)
    x = tf(fit_ind) - delay;
    fit_result = k(5) + k(1)*exp(k(2)*x) + k(3)*exp(k(4)*x);
    pos = pos(p_ind)*cal;
    l = length(cum);
    d_ind = [(l - (post + extra)*25 + 1):l]';
    cum = cum(d_ind);
    cum = cum - cum(find(td == 0));
    p_show = [1:(show + extra)*200]';
    d_show = [1:(show + extra)*25]';
    high = max(abs(vel(d_show)));
    p_scl = high/max(abs(pos(p_show)));
    c_scl = high/max(abs(cum(d_show)));
    hold off
    clg
    plot(t(p_show),pos(p_show)*p_scl,td(d_show),cum(d_show)*c_scl, ...
            td(d_show),vel(d_show),tf(fit_ind),fit_result,'-r')
    grid
    ax = axis;
    hold
    plot ([0 0], ax([3 4]), '--r')
    xt = ax(1) + (ax(2)-ax(1))/3;
    y_range = ax(4)-ax(3);
    yt = ax(3) + 4*y_range/5;
    text(xt,(yt+ .05*y_range),['k = [',num2str(k(1)),' ',num2str(1/k(2)), ' ', ...
            num2str(k(3)), ' ', num2str(1/k(4)), ' ', num2str(k(5)), ']'])
    text (xt, yt, ['count = ', num2str(count), '      break = ', ...
            int2str(break_flag)]);
    axis;
    hold off
    title (['Subject ', subject, ': ', pstr, ' ', ...
            cond_name(cond,[1:cond_len(cond)]), '      Trial #', trial, ...
        '   speed = ', int2str(round(dome(tr))), ' deg/s'])
xlabel ('time (sec)')
```

```
ylabel ('SPV  (deg/s)')

if (exist([nys_path, 'vel_okan_fit']) ~= 2)
    tr_list = tr;
    brk_list = break_flag;
    vel_k = [k(1) 1/k(2) k(3) 1/k(4) k(5)];
else
    eval (['load ', nys_path, 'vel_okan_fit'])
    ind = find(tr_list ~= tr);
    tr_list = [tr_list(ind); tr];
    brk_list = [brk_list(ind); break_flag];
    vel_k = [vel_k(ind,:); [k(1) 1/k(2) k(3) 1/k(4) k(5)]];
    [tr_list, ind] = sort(tr_list);
    brk_list = brk_list(ind);
    vel_k = vel_k(ind,:);
end  %if exist
eval (['save ', nys_path, 'vel_okan_fit tr_list brk_list vel_k'])

%  prtsc

%  pause
end  %for   tr
end  %if exist
end  %for  post_num
end  %for sub
```

```
function f = okanfun(k);

%*********************************************************************
%
%okanfun
%implements double exponential (plus bias term) for OKAN SPV model fit
%called by show_okan
%generates error vector between actual SPV time series and current best model prediction
%also plots SPV and current fit every 50 iterations to check algorithm progress

%*********************************************************************




x = Data(:,1);
y = Data(:,2);

A = k(5) + k(1)*exp(k(2)*x) + k(3)*exp(k(4)*x);

f = norm(A - y)/length(x);


steps = steps + 1;
if (((steps/50) - ceil(steps/50)) == 0)
  steps
    plot (x,y,x,A)
    ax = axis;
    xt = ax(1) + (ax(2)-ax(1))/3;
    y_range = ax(4)-ax(3);
    yt = ax(3) + 9*y_range/10;
    text (xt,(yt+ .05*y_range),['k = [',num2str(k(1)),' ',num2str(k(2)), ' ', ...
            num2str(k(3)), ' ', num2str(k(4)), ' ', num2str(k(5)), ']'])
    text (xt, yt, ['count = ', num2str(steps)]);
    axis;
end  %if

if (steps > 1200)
    break_flag = 1;
    f = 0.0;
end  %if
```

```
%*******************************************************************

%get_vect
%
%given run path, calculates vection parameters for each trial:  onset time(s), maximum and
%  average vection, and dropout times if they exist
%
%*******************************************************************



max_v = 4.78;
min_v = -4.95;
max_zero = -.045;
min_zero = -.395;
null = (max_v + min_v)/2;
v2p = 100/(max_v - null);
da2v = 10/2048;
da2p = da2v*v2p;
pos_thr = (max_zero - null)*v2p + 4;
neg_thr = (min_zero - null)*v2p - 4;
break
path_specs
disp (in_path)
pre = 5*200;
if ((subject == 'M') & (pstr == 'ERECT'))
    per = pre + 45*200;
else
    per = pre + 30*200;
end
on_dur = 0.5*200;
eval (['load ', nys_path, 'pos']);
clear ppp intl fnl
num_trials = length(dome);
first_on = -ones(num_trials,1);
max_vect = first_on;
ave_vect = max_vect;
onset = [];
dropout = [];

for trial = 1:num_trials
    tr = int2str(trial);
    eval (['load ', in_path, 'JS', tr, '.matlab'])
    var_name = ['js', tr];
    eval (['js = ', var_name, ';'])
    eval (['clear ', var_name])
    post = length(js);
    vect = (js - null)*da2p;
    dome_on = [(pre + 1):per]';
    vect = vect(dome_on);
    dur = length(vect);
    drctn = sign(mean(vect) - min_zero*v2p);
```

306

```
max_vect(trial) = max(abs(vect));
ave_vect(trial) = abs(mean(vect));
old = 0;
leftover = vect;
vect_on = 0;
while (~isempty(leftover))
    if (~vect_on)
        if (drctn > 0)
            ind = find(leftover > pos_thr);
        else
            ind = find(leftover < neg_thr);
        end
    else
        if (drctn > 0)
            ind = find(leftover < pos_thr);
        else
            ind = find(leftover > neg_thr);
        end
    end
    dur = length(leftover);
    begin = find_start(ind,dur,on_dur);
    if (begin > 0)
        if (~vect_on)
            onset = [onset; [trial (begin+old)/200]];
            vect_on = 1;
        else
            dropout = [dropout; [trial (begin+old)/200]];
            vect_on = 0;
        end %if ~vect_on
    if ((begin + on_dur) < dur)
            leftover = leftover([(begin+on_dur):dur]);
            old = old + begin + on_dur - 1;
        else
            leftover = [];
        end %if
    else
        leftover = [];
    end %if (begin > 0)
end %while (~ )
if (~isempty(onset))
    ind = find(onset(:,1) == trial);
    if (~isempty(ind))
        first_on(trial) = onset(ind(1),2);
    end %if ~isempty
end %if ~isempty
end %for trial

eval (['save ', nys_path, 'vect_params onset first_on dropout ', ...
            'max_vect ave_vect dome']);
```

```
%*****************************************************************

%plot_corr
%computes unbiased cross-correlation functions between the vection trace and both eye
%   position and SPV traces.
%plots eye position, SPV, and vection traces; plots results of cross-correlations
%stores times of peaks in cross-correlation functions

%*****************************************************************




digits = [1:9]';
for i = 1:9
    digits(i) = int2str(digits(i));
end   %for
pos_cal = 50/2048;
js_cal = (10/2048)*(100/5);
[pb pa] = butter(2,.005);
df = 1;
df1 = 2;
df2 = 3;
dnf = 4;
l = 5;
cond_name = ['dark+fix  ';
                         'dark+fix1 ';
                         'dark+fix2 ';
                         'dark+nofix';
                         'light     '];
cond_len = [8 9 9 10 5]';
nysa_cond = ['d+f '; 'd+f1'; 'd+f2'; 'd+nf'; 'l   '];
nysa_cond_len = [3 4 4 4 1]';

%      ****  set these parameters  ****
date = '05-Sep-91';
subject = 'Q';
pstr = 'Sup';
cond = dnf;
pre = 5;
per = 35;
post = 65;
%post = 48.75;
%null_ind = []';
null_ind = [1:(pre*200)]';
%      *******************************

er_path = ['DungBeetleMan!:Thesis:', subject, '.ERECT:', subject, ...
                    '.erect_', cond_name(cond,[1:cond_len(cond)]), ':'];
sup_path = ['DKJ_Thesis1:Thesis:', subject, '.SUPINE:', subject, ...
                    '.supine_', cond_name(cond,[1:cond_len(cond)]), ':'];
er_nys_path = [er_path, subject, '.e_', nysa_cond(cond, ...
                    [1:nysa_cond_len(cond)]), '.nysa:'];
```

```
sup_nys_path = [sup_path, subject, '.s_', nysa_cond(cond, ...
                                    [1:nysa_cond_len(cond)]), '.nysa:'];
in_path = sup_path;
nys_path = sup_nys_path;

eval (['load ', nys_path, 'pos'])
num_trials = length(dome);
clear intl fnl
first = pre/.1 + 1;
last = per/.1;
dur = ceil((per - pre)*10)/10;
if (exist([nys_path, 'eye_vect.corr']) ~= 2)
    spv_vect = 0*ones(num_trials,2);
    pos_vect = spv_vect;
    eval (['save ', nys_path, 'eye_vect.corr spv_vect pos_vect']);
else
    eval (['load ', nys_path, 'eye_vect.corr']);
end  %if

trial = 1;
while (trial <= num_trials)
    tr = int2str(trial);
    fname = ['tor', tr, '.edited'];
    vname = 'edited';
    eval (['load ', nys_path, fname])
    eval (['spv = ', vname, ';']);
    eval (['clear ', vname])
    spv = decimate(spv,20);
    fname = ['JS', tr, '.matlab'];
    vname = ['js', tr];
    eval (['load ', in_path, fname])
    eval (['js = ', vname, ';'])
    eval (['clear ', vname])
    t_max = ceil(length(js)*.005*10)/10;
    t = [.1:.1:t_max]';
    js = js*js_cal;
    js = decimate (js,20);
    scale = ceil(max(abs(spv)));
    js_scl = js*scale/100;
    spv_corr1 = xcorr(spv([first:last]), js_scl([first:last]), 'unbiased');
 spv_corr1 = spv_corr1*sign(mean(spv_corr1));
    t_corr1 = [(.1 - dur):.1:(dur - .1)]';
    tc_max1 = t_corr1(find(spv_corr1==max(spv_corr1)));
    spv_vect (trial,1) = tc_max1;
    spv_corr2 = xcorr(spv, js_scl, 'unbiased');
 spv_corr2 = spv_corr2*sign(mean(spv_corr2));
    dur2 = ceil(post*10)/10;
    t_corr2 = [(.1 - dur2):.1:(dur2 - .1)]';
    tc_max2 = t_corr2(find(spv_corr2==max(spv_corr2)));
    spv_vect (trial,2) = tc_max2;
    hold off
 clg
    subplot (221)
    plot (t,[spv js_scl], [0;t_max], [scale scale]*sign(mean(js)), '--')
```

```
xlabel ('time (sec)')
   ylabel ('SPV & vection')
   title(['Subj. ',subject,':   ',pstr,', ', ...
               cond_name(cond,([1:cond_len(cond)])), ...
               '    Tr #', tr, ' ', num2str(round(dome(trial))), ...
               ' d/s'])
   grid
   subplot (222)
   plot (t_corr1, spv_corr1, t_corr2, spv_corr2)
   ax = axis;
   subplot (222)
   plot ([tc_max1 tc_max1]', ax([3 4])', '-', [tc_max2 tc_max2]', ...
               ax([3 4])', '--')
   title (date)
   xlabel ('time (sec)')
   ylabel ('X-corr: SPV, vection')
   grid
   axis;

   fname = ['LEFT', tr, '.matlab'];
   vname = ['left', tr];
   eval (['load ', in_path, fname])
   eval (['pos = ', vname, ';'])
   eval (['clear ', vname])
   pos = pos*pos_cal;
   null = mean(pos(null_ind));
   pos = pos - null;
   pos = filtfilt(pb,pa,pos);
   pos = decimate(pos,20);
   subplot (223)
 scale = ceil(max(abs(pos)));
   js_scl = js*scale/100;
   plot (t, [pos js_scl],[0 t_max],[scale scale]*sign(mean(js)), '--')
   xlabel ('time (sec)')
   ylabel ('eye position & vection')
 grid
%do correlation for whole trial
 pos_corr2 = xcorr(pos,js_scl,'unbiased');
   pos_corr2 = pos_corr2*sign(mean(pos_corr2));
   dur2 = ceil(post*10)/10;
   t_corr2 = [(.1 - dur2):.1:(dur2 - .1)]';
   tc_max2 = t_corr2(find(pos_corr2==max(pos_corr2)));
   pos_vect (trial,2) = tc_max2;
%do correlation for dome rotation segment only
   ind = find(t <= per);
   ind = find(t(ind) > pre);
 pos_corr1 = xcorr(pos(ind),js_scl(ind),'unbiased');
   pos_corr1 = pos_corr1*sign(mean(pos_corr1));
   t_corr1 = [(.1 - dur):.1:(dur - .1)]';
   tc_max1 = t_corr1(find(pos_corr1==max(pos_corr1)));
   pos_vect (trial,1) = tc_max1;
   subplot (224)
   plot (t_corr1,pos_corr1,t_corr2,pos_corr2)
 ax = axis;
```

310

```
        subplot (224)
    plot ([tc_max1 tc_max1], ax([3 4]), '-', [tc_max2 tc_max2], ax([3 4]), '--')
        xlabel ('approx. time (sec)')
        ylabel ('X-corr: eye pos., vection')
        grid
        axis;
        prtsc


%   hold on
%   subplot (111)
%   title(['Subject ',subject,':  ',pstr,', ', ...
%                   cond_name(cond,([1:cond_len(cond)])), '            ', ...
%                   '    Trial #', tr, '       ', num2str(round(dome(trial))), ...
%                   ' deg/sec'])


%   title (['Trial #', tr, '        Dome Speed: ', ...
%                   int2str(round(dome(trial))), ' deg/sec'])
%   xlabel ('time (sec)')
%   ylabel ('eye position (deg)')
%   hold off
%   [x,y,s] = ginput(1);
    s = 13;
    s = setstr(s);
    a = find(digits==s);
    if (~(isempty(a)))
        if ((a <= num_trials) & (a > 0))
            trial = a - 1;
        else
            trial = trial - 1;
        end   %if 2
    end   %if 1
    if ((s == 'b') & (trial > 1))
        trial = trial - 1;
    elseif (s == 'q')
        trial = num_trials + 1;
    else
        trial = trial + 1;
    end %if
end

eval (['save ', nys_path, 'eye_vect.corr spv_vect pos_vect'])
trials = [1:num_trials]';
hold off
clg
subplot (121)
plot (trials, spv_vect(:,1), '*', trials, spv_vect(:,2), '+')
ax = axis;
m = mean(spv_vect);
subplot (121)
plot (ax([1 2]), [m(1) m(1)], '-', ax([1 2]), [m(2) m(2)], '--')
grid
title (['Subject ', subject, ':  ', pstr, ' ', cond_name(cond,:)])
xlabel ('trial')
```

311

```
ylabel ('peak correlation time--spv, vection (*=per; +=all)')
axis;
subplot (122)
plot(trials, pos_vect(:,1), '*', trials, pos_vect(:,2), '+')
ax = axis;
m = mean(pos_vect);
subplot (122)
plot (ax([1 2]), [m(1) m(1)], '-', ax([1 2]), [m(2) m(2)], '--')
grid
xlabel ('trial')
ylabel ('peak correlation time--position, vection (*=per; +=all)')
title (date)
axis;
prtsc
```

```
%************************************************************

%state_spv    (based on get_vect)
%
%given path, loads onsets and dropouts for each trial; calculates ratio of mean SPVs
%   and difference in mean eye position for States 1 and 2
%State 1 = vection
%State 2 = no vection (before onset, during dropouts)


%************************************************************




pos_cal = 50/2048;
pre = 5*200;
if ((subject == 'M') & (pstr(1:5) == 'ERECT'))
    per = pre + 45*200;
else
    per = pre + 30*200;
end
on_dur = 0.5*200;
eval (['load ', nys_path, 'vect_params'])
clear max_vect ave_vect
num_trials = length(dome);
run_data = 0*ones(num_trials,20);

for trial = 1:num_trials
  run_data(trial,1:5) = [abs(subject) p_num cond trial dome(trial)];
  if (first_on (trial) > 0)
    tr = int2str(trial);
    eval (['load ', in_path, 'LEFT', tr, '.matlab'])
    var_name = ['left', tr];
    eval (['pos = ', var_name, ';'])
    eval (['clear ', var_name])
    pos = pos*pos_cal;
    post = length(pos);
    if ((subject == 'M') & (pstr(1:5) == 'ERECT'))
        null = mean(pos([(post - pre + 1):post]));
    else
        null = mean(pos(1:pre));
    end  %if M ERECT
    pos = pos - null;
    eval (['load ', nys_path, 'tor', tr, '.edited'])
    var_name = ['edited'];
    eval (['spv = ', var_name, ';'])
    eval (['clear ', var_name])
    dome_on = [(pre + 1):per]';
    pos = pos(dome_on);
    spv = spv(dome_on);
    dur = length(pos);
    drctn = sign(dome(trial));
    pos = pos*drctn;
```

313

```
ons = 200*onset(find(onset(:,1) == trial),2);
drops = [];
if ~isempty(dropout)
    drops = 200*dropout(find(dropout(:,1) == trial),2);
end %if no dropouts
%state 1 == vection;  state 2 == no vection
num_ons = length(ons);
num_drops = length(drops);
sched = 0*ones((num_ons + num_drops + 2),1);
sched(1) = 1;
s_ind = 2*[1:num_ons]';
sched(s_ind) = ons;
s_ind = 1 + 2*[1:num_drops]';
if num_drops>0
    sched(s_ind) = drops;
end  %if no drops
sched(length(sched)) = dur + 1;
s2_ind = [];
s1_ind = [];
while (length(sched) > 1)
    s2_ind = [s2_ind; [sched(1):(sched(2) - 1)]'];
    sched = sched(2:length(sched));
    if (length(sched) > 1)
        s1_ind = [s1_ind; [sched(1):(sched(2) - 1)]'];
        sched = sched(2:length(sched));
    end %if
end  %while

pc_s1 = 100*length(s1_ind)/dur;
p = mean(pos);
pv = std(pos);
s1_p = mean(pos(s1_ind));
s1_pv = std(pos(s1_ind));
s2_p = mean(pos(s2_ind));
s2_pv = std(pos(s2_ind));
diff_p12 = s1_p - s2_p;
v = mean(spv);
vv = std(spv);
s1_v = mean(spv(s1_ind));
s1_vv = std(spv(s1_ind));
s2_v = mean(spv(s2_ind));
s2_vv = std(spv(s2_ind));
rat_v12 = s1_v/s2_v;

run_data(trial,6:20) = [pc_s1 p pv s1_p s1_pv s2_p s2_pv diff_p12 ...
                v vv s1_v s1_vv s2_v s2_vv rat_v12];

clear pos spv
end  %if onset

end  %for trial
```

```
function [dev, t_hyp, df, prb] = T_1mean(Data, null_hyp, show)

%:*********************************************************

%T_1mean
%Program written by Jock R. I. Christie in ongoing effort to make the world a better place
%Modified by Keoki Jackson

%Designed to test whether a population mean is significantly different from the "null
%   hypothesis" value
%Takes a population column vector and a null hypothesis constant as inputs
%Returns the difference between the mean and the null hypothesis; also the t statistic,
%   the degrees of freedom, and the probability that the null hypothesis is correct
%Returns probabilities at levels of 0.1, 0.05, 0.01, and 0.001

%  SHOW = 'n' or SHOW = 'N' suppreses display statements.
%  NOTE:  These values for 2 sided test.  See CRC (1983) p.547

%*********************************************************



prob = [0.100; 0.050; 0.010; 0.001];
if ~isempty(Data)
x = Data(:,1);
n = length(x);
dev = mean(x) - null_hyp;
t_hyp = dev/(std(x)/sqrt(n));
df = n-1;

if ~exist('show')
   show = 'n';
end

t(1,:) = [  1, 6.314, 12.706, 63.657, 636.619];
t(2,:) = [  2, 2.920, 4.303, 9.925, 31.598];
t(3,:) = [  3, 2.353, 3.182, 5.841, 12.924];

t(4,:) = [  4, 2.132, 2.776, 4.604, 8.610];
t(5,:) = [  5, 2.015, 2.571, 4.032, 6.869];
t(6,:) = [  6, 1.943, 2.447, 3.707, 5.959];
t(7,:) = [  7, 1.895, 2.365, 3.499, 5.408];
t(8,:) = [  8, 1.860, 2.306, 3.355, 5.041];
t(9,:) = [  9, 1.833, 2.262, 3.250, 4.781];
t(10,:) = [ 10, 1.812, 2.228, 3.169, 4.587];
t(11,:) = [ 11, 1.796, 2.201, 3.106, 4.437];
t(12,:) = [ 12, 1.782, 2.179, 3.055, 4.318];
t(13,:) = [ 13, 1.771, 2.160, 3.012, 4.221];
t(14,:) = [ 14, 1.761, 2.145, 2.977, 4.140];
t(15,:) = [ 15, 1.753, 2.131, 2.947, 4.073];
t(16,:) = [ 16, 1.746, 2.120, 2.921, 4.015];
t(17,:) = [ 17, 1.740, 2.110, 2.898, 3.965];
```

```
t(18,:) = [ 18, 1.734, 2.101, 2.878, 3.922];
t(19,:) = [ 19, 1.729, 2.093, 2.861, 3.883];
t(20,:) = [ 20, 1.725, 2.086, 2.845, 3.850];
t(21,:) = [ 21, 1.721, 2.080, 2.831, 3.819];
t(22,:) = [ 22, 1.717, 2.074, 2.819, 3.792];
t(23,:) = [ 23, 1.714, 2.069, 2.807, 3.767];
t(24,:) = [ 24, 1.711, 2.064, 2.797, 3.745];
t(25,:) = [ 25, 1.708, 2.060, 2.787, 3.725];
t(26,:) = [ 26, 1.706, 2.056, 2.779, 3.707];
t(27,:) = [ 27, 1.703, 2.052, 2.771, 3.690];
t(28,:) = [ 28, 1.701, 2.048, 2.763, 3.674];
t(29,:) = [ 29, 1.699, 2.045, 2.756, 3.659];
t(30,:) = [ 30, 1.697, 2.042, 2.750, 3.646];
t(31,:) = [ 40, 1.684, 2.021, 2.704, 3.551];
t(32,:) = [ 60, 1.671, 2.000, 2.660, 3.460];
t(33,:) = [120, 1.658, 1.980, 2.617, 3.373];

t_inf  =  [1.645, 1.960, 2.576, 3.291];


if (df < 1)
  fprintf('\nSorry you lose.  Not enough Data.');
elseif (df >= 1)&(df <= 30)
   z = t(df,2:5);
elseif (df > 30)&(df <= 120)
   r = abs(t(:,1) - df);
   p = min(find(r == min(r)));
   if min(r) == 0
      z = t(p,2:5);
   else
      if (df < t(p,1))
         p = p-1;
      end
      z = t(p,2:5) + (df-t(p,1)) * (t(p+1,2:5) - t(p,2:5)) / (t(p+1,1) - t(p,1));
   end
else
   z = t_inf;
end

p = max(find(z <= abs(t_hyp)));
prb = prob(p);

if (show == 'y')|(show == 'Y')
    if isempty(p)
        ps = 'ns';
    else
        ps = num2str(prb);
    end  %if isempty
    disp(['t = ', num2str(t_hyp), '    df = ', int2str(df), ...
             '    p = ', ps])
end

else  %if isempty data
  prb = 1;
```

316

```
    t_hyp = 0;
    df = 0;
end  %if isempty data
```

```
function [md, t_m, df, prb] = T_2means(Data1, Data2, show)

%:*************************************************************

%T_2means
%Program written by Jock R. I. Christie in ongoing effort to make the world a better place
%Modified by Keoki Jackson

%Designed to test whether a two population means are significantly different from each
%   other using 2-sided t-test
%Takes two population column vectors as inputs
%Returns the mean difference; also the t statistic, the degrees of freedom, and the probability
%   that the two populations means are the same
%Returns probabilities at levels of 0.1, 0.05, 0.01, and 0.001

% SHOW = 'n' or SHOW = 'N' suppreses display statements.
% NOTE:  These values for 2 sided test.  See CRC (1983) p.547

%*************************************************************



prob = [0.100; 0.050; 0.010; 0.001];
if ~(isempty(Data1) | isempty(Data2))
m1 = mean(Data1);
m2 = mean(Data2);
md = m1 - m2;
n1 = length(Data1);
n2 = length(Data2);
df = n1 + n2 - 2;
t_m = md/sqrt((sum((Data1 - m1) .^ 2) + sum((Data2 - m2) .^ 2)) * ...
                    (1/n1 + 1/n2) / df);

if ~exist('show')
    show = 'n';
end

t(1,:) = [  1, 6.314, 12.706, 63.657, 636.619];
t(2,:) = [  2, 2.920, 4.303, 9.925, 31.598];
t(3,:) = [  3, 2.353, 3.182, 5.841, 12.924];

t(4,:) = [  4, 2.132, 2.776, 4.604, 8.610];
t(5,:) = [  5, 2.015, 2.571, 4.032, 6.869];
t(6,:) = [  6, 1.943, 2.447, 3.707, 5.959];
t(7,:) = [  7, 1.895, 2.365, 3.499, 5.408];
t(8,:) = [  8, 1.860, 2.306, 3.355, 5.041];
t(9,:) = [  9, 1.833, 2.262, 3.250, 4.781];
t(10,:) = [ 10, 1.812, 2.228, 3.169, 4.587];
t(11,:) = [ 11, 1.796, 2.201, 3.106, 4.437];
t(12,:) = [ 12, 1.782, 2.179, 3.055, 4.318];
t(13,:) = [ 13, 1.771, 2.160, 3.012, 4.221];
t(14,:) = [ 14, 1.761, 2.145, 2.977, 4.140];
```

```
t(15,:) = [ 15, 1.753, 2.131, 2.947, 4.073];
t(16,:) = [ 16, 1.746, 2.120, 2.921, 4.015];
t(17,:) = [ 17, 1.740, 2.110, 2.898, 3.965];
t(18,:) = [ 18, 1.734, 2.101, 2.878, 3.922];
t(19,:) = [ 19, 1.729, 2.093, 2.861, 3.883];
t(20,:) = [ 20, 1.725, 2.086, 2.845, 3.850];
t(21,:) = [ 21, 1.721, 2.080, 2.831, 3.819];
t(22,:) = [ 22, 1.717, 2.074, 2.819, 3.792];
t(23,:) = [ 23, 1.714, 2.069, 2.807, 3.767];
t(24,:) = [ 24, 1.711, 2.064, 2.797, 3.745];
t(25,:) = [ 25, 1.708, 2.060, 2.787, 3.725];
t(26,:) = [ 26, 1.706, 2.056, 2.779, 3.707];
t(27,:) = [ 27, 1.703, 2.052, 2.771, 3.690];
t(28,:) = [ 28, 1.701, 2.048, 2.763, 3.674];
t(29,:) = [ 29, 1.699, 2.045, 2.756, 3.659];
t(30,:) = [ 30, 1.697, 2.042, 2.750, 3.646];
t(31,:) = [ 40, 1.684, 2.021, 2.704, 3.551];
t(32,:) = [ 60, 1.671, 2.000, 2.660, 3.460];
t(33,:) = [120, 1.658, 1.980, 2.617, 3.373];

t_inf  =  [1.645, 1.960, 2.576, 3.291];


if (df < 1)
  fprintf('\nSorry you lose.  Not enough Data.');
elseif (df >= 1)&(df <= 30)
  z = t(df,2:5);
elseif (df > 30)&(df <= 120)
  r = abs(t(:,1) - df);
  p = min(find(r == min(r)));
  if min(r) == 0
    z = t(p,2:5);
  else
    if (df < t(p,1))
      p = p-1;
    end
    z = t(p,2:5) + (df-t(p,1)) * (t(p+1,2:5) - t(p,2:5)) / (t(p+1,1) - t(p,1));
  end
else
  z = t_inf;
end

p = max(find(z <= abs(t_m)));
prb = prob(p);

if (show == 'y')|(show == 'Y')
    if isempty(p)
        ps = 'ns';
    else
        ps = num2str(prb);
    end %if isempty
    disp(['t = ', num2str(t_b), '      df = ', int2str(df), ...
          '       p = ', ps])
end
```

```
else  %if isempty data
 prb = 1;
    t_b = 0;
    k = [0 0];
    df = 0;
end  %if isempty data
```

```
function [k, conf_k, df] = T_line_conf(Data, show)

%:*******************************************************************

%T_line_conf
%Program written by Jock R. I. Christie in ongoing effort to make the world a better place
%Modified by Keoki Jackson

%Performs a linear regression fit to array of x-y coordinates
%Generates 95% (or 90%) confidence intervals for slope and y-intercept of regression line
%Uses double-sided t-statistic
%Takes x-y array as input
%Returns the coefficients of the line fit; also the confidence interval and the degrees of %
   freedom

%  SHOW = 'n' or SHOW = 'N' suppreses display statements.
%  NOTE:  These values for 2 sided test.  See CRC (1983) p.547

%*******************************************************************




prob = [0.100; 0.050; 0.010; 0.001];
%confidence level = 0.05
c_level = 2;
if ~isempty(Data)
x = Data(:,1);
y = Data(:,2);
k = polyfit(x,y,1);
a = k(2);
b = k(1);
y_fit = polyval(k,x);
n = length(x);
se = norm(y - y_fit)/sqrt(n-2);
c_a = (se*sqrt(1/n + (n*(mean(x)^2)/(n*sum(x .^2) - (sum(x))^2))));
c_b = se/sqrt((n*sum(x .^ 2) - (sum(x))^2)/n);
t_a = a/(se*sqrt(1/n + (n*(mean(x)^2)/(n*sum(x .^2) - (sum(x))^2))));
t_b = (b/se)*sqrt((n*sum(x .^ 2) - (sum(x))^2)/n);
df = n-2;

if ~exist('show')
   show = 'n';
end

t(1,:) =  [  1, 6.314, 12.706, 63.657, 636.619];
t(2,:) =  [  2, 2.920, 4.303, 9.925, 31.598];
t(3,:) =  [  3, 2.353, 3.182, 5.841, 12.924];

t(4,:) =  [  4, 2.132, 2.776, 4.604, 8.610];
t(5,:) =  [  5, 2.015, 2.571, 4.032, 6.869];
t(6,:) =  [  6, 1.943, 2.447, 3.707, 5.959];
t(7,:) =  [  7, 1.895, 2.365, 3.499, 5.408];
```

```
t(8,:)  = [  8, 1.860, 2.306, 3.355, 5.041];
t(9,:)  = [  9, 1.833, 2.262, 3.250, 4.781];
t(10,:) = [ 10, 1.812, 2.228, 3.169, 4.587];
t(11,:) = [ 11, 1.796, 2.201, 3.106, 4.437];
t(12,:) = [ 12, 1.782, 2.179, 3.055, 4.318];
t(13,:) = [ 13, 1.771, 2.160, 3.012, 4.221];
t(14,:) = [ 14, 1.761, 2.145, 2.977, 4.140];
t(15,:) = [ 15, 1.753, 2.131, 2.947, 4.073];
t(16,:) = [ 16, 1.746, 2.120, 2.921, 4.015];
t(17,:) = [ 17, 1.740, 2.110, 2.898, 3.965];
t(18,:) = [ 18, 1.734, 2.101, 2.878, 3.922];
t(19,:) = [ 19, 1.729, 2.093, 2.861, 3.883];
t(20,:) = [ 20, 1.725, 2.086, 2.845, 3.850];
t(21,:) = [ 21, 1.721, 2.080, 2.831, 3.819];
t(22,:) = [ 22, 1.717, 2.074, 2.819, 3.792];
t(23,:) = [ 23, 1.714, 2.069, 2.807, 3.767];
t(24,:) = [ 24, 1.711, 2.064, 2.797, 3.745];
t(25,:) = [ 25, 1.708, 2.060, 2.787, 3.725];
t(26,:) = [ 26, 1.706, 2.056, 2.779, 3.707];
t(27,:) = [ 27, 1.703, 2.052, 2.771, 3.690];
t(28,:) = [ 28, 1.701, 2.048, 2.763, 3.674];
t(29,:) = [ 29, 1.699, 2.045, 2.756, 3.659];
t(30,:) = [ 30, 1.697, 2.042, 2.750, 3.646];
t(31,:) = [ 40, 1.684, 2.021, 2.704, 3.551];
t(32,:) = [ 60, 1.671, 2.000, 2.660, 3.460];
t(33,:) = [120, 1.658, 1.980, 2.617, 3.373];

t_inf  = [1.645, 1.960, 2.576, 3.291];


if (df < 1)
  fprintf('\nSorry you lose.  Not enough Data.');
elseif (df >= 1)&(df <= 30)
  z = t(df,2:5);
elseif (df > 30)&(df <= 120)
  r = abs(t(:,1) - df);
  p = min(find(r == min(r)));
  if min(r) == 0
    z = t(p,2:5);
  else
    if (df < t(p,1))
      p = p-1;
    end
    z = t(p,2:5) + (df-t(p,1)) * (t(p+1,2:5) - t(p,2:5)) / (t(p+1,1) - t(p,1));
  end
else
  z = t_inf;
end

t_a2 = z(c_level);
conf_a = t_a2*c_a;
conf_b = t_a2*c_b;
conf_k = [conf_b conf_a];
```

```matlab
if (show == 'y')|(show == 'Y')
    if isempty(p)
        ps = 'ns';
    else
        ps = num2str(prb);
    end  %if isempty
    disp(['t = ', num2str(t_b), '     df = ', int2str(df), ...
                '   p = ', ps])
end

else  %if isempty data
 prb = 1;
    t_b = 0;
    k = [0 0];
    df = 0;
end  %if isempty data
```

# REFERENCES

Adams S (1991): <u>Build a Better Life by Stealing Office Supplies: Dogbert's Big Book of Business</u>, Pharos Books, NY.

Andersen GJ (1986): 'Perception of Self-Motion: Psychophysical and Computational Approaches,' *Psychological Bulletin* 99(1):52-65.

Andersen GJ and Braunstein ML (1985): 'Induced Self-Motion in Central Vision,' *Journal of Experimental Psychology: Human Perception and Performance* 11(2):122-132.

Andersen GJ and Dyre BP (1987): 'Induced Roll Vection from Stimulation of the Central Visual Field,' in *Proceedings of the Human Factors Society--31st Annual Meeting*, pp. 263-265.

Balkwill MD (1991): 'NysA User's Manual,' internal MIT Man-Vehicle Laboratory document.

Balliet R and Nakayama K (1978a): 'Training of Voluntary Torsion,' *Invest. Ophthalmol. Visual Sci.* 17(4):303-314.

Balliet R and Nakayama K (1978b): 'Egocentric orientation is influenced by trained voluntary cyclorotatory eye movements,' *Nature* 275:214-216.

Baloh RW, Richman L, Yee RD, Honrubia V (1983): 'The Dynamics of Vertical Eye Movements in Normal Human Subjects,' *Aviat. Space Environ. Med.* 54(1):32-38.

Benson AJ (1974): 'Modification of the response to angular accelerations by linear accelerations,' in Kornhuber, <u>Handbook of Sensory Physiology</u>, vol. 6, part 2, pp. 281-320. Springer, Berlin.

van den Berg AV and Collewijn H (1988): 'Directional Asymmetries of Human Optokinetic Nystagmus,' *Exp. Brain Res.* 70:597-604.

Brandt Th, Dichgans J, Büchele W (1974): 'Motion Habituation: Inverted Self-Motion Perception and Optokinetic After-Nystagmus,' *Exp. Brain Res.* 21:337-352.

Brandt Th, Dichgans J, Koenig E (1973): 'Differential Effects of Central Versus Peripheral Vision on Egocentric and Exocentric Motion Perception,' *Exp. Brain Res.* 16:476-491.

Brandt Th, Wist ER, Dichgans J (1975): 'Foreground and Background in Dynamic Spatial Orientation,' *Perception and Psychophysics* 17(5):497-503.

Bridgeman B (1975): 'Failure to Detect Displacement of the Visual World During Saccadic Eye Movements,' *Vision Research* 15:719-722.

Bridgeman B (1986): 'Multiple Sources of Outflow in Processing Spatial Information,' *Acta Psychologica* 63:35-48.

Cheung BSK, Howard IP, Nedzelski JM, Landolt JP (1989): 'Circularvection About Earth-horizontal Axes in Bilateral Labyrinthine-defective Subjects,' *Acta Otolaryngol.* 108:336-344.

Clément G and Lathan CE (1991): 'Effects of static tilt about the roll axis on horizontal and vertical optokinetic nystagmus and optokinetic after-nystagmus in humans,' *Exp. Brain Res.* 84:335-341.

Clément G, Vieville T, Lestienne F, Berthoz A (1986): 'Modifications of Gain Asymmetry and Beating Field of Vertical Optokinetic Nystagmus in Microgravity,' *Neuroscience Letters* 63:271-274.

Cohen B, Henn V, Raphan T, Dennett D (1981): 'Velocity Storage, Nystagmus, and Visual-Vestibular Interactions in Humans,' *Ann. NY Acad. Sci.* 374:421-433.

Cohen B, Matsuo V, Raphan T (1977): 'Quantitative Analysis of the Velocity Characteristics of Optokinetic Nystagmus and Optokinetic After-Nystagmus,' *J. Physiol.* 270:321-344.

Collewijn H, van der Mark F, Jansen TC (1975): 'Precise Recording of Human Eye Movements,' *Vision Research* 15:447-450.

Collewijn H (1977) 'Eye- and Head Movements in Freely Moving Rabbits,': *J. Physiol.* 266:471-498.

Collewijn H (1981): 'The Optokinetic System,' in Models of Oculomotor Behavior and Control, Zuber BL ed. CRC Press, Inc., Boca Raton, FL. pp. 111-137.

Collewijn H, Ferman L, Van den Berg AV (1988): 'The Behavior of Human Gaze in Three Dimensions,' in Annals of the New York Academy of Sciences, vol. 545: Representation of Three-Dimensional Space in the Vestibular, Oculomotor, and Visual Systems, Cohen B and Henn V, eds. The New York Academy of Sciences, New York, NY. pp. 105-127.

Collewijn H and Noorduin H (1972): 'Vertical and Torsional Optokinetic Eye Movements in the Rabbit,' *Pfleugers Arch.* 332:87-95.

Collewijn H, Van der Steen J, Ferman L, Jansen TC (1985): 'Human ocular counterroll: assessment of static and dynamic properties from electromagnetic scleral coil recordings,' *Experimental Brain Research* 59:185-196.

Crites TA (1980): 'Circularvection and ocular counterrolling in visually induced roll supine and in weightlessness,' SM Thesis, Department of Aeronautics and Astronautics, MIT.

Dai MJ, Curthoys IS, Halmagyi GM (1989): 'A Model of Otolith Stimulation,' *Biological Cybernetics* 60:185-194.

Diamond SG and Markham CH (1983): 'Ocular counterrolling as an indicator of vestibular otolith function,' *Neurology* 33:1460-1469.

Diamond SG and Markham CH (1990): 'Prediction of space motion sickness susceptibility by disconjugate eye torsion in parabolic flight,' *Av. Space Env. Medicine* 62:201-205.

Dichgans J and Brandt Th (1972): 'Visual-Vestibular Interaction and Motion Perception,' *Bibl. Ophthal.* 82:327-388.

Dichgans J and Brandt Th (1974): 'The Psychophysics of Visually Induced Perception of Self-motion and Tilt,' in The Neurosciences: Third Study Program, Schmidt, Worden eds., MIT Press, pp. 123-129.

Dichgans J and Brandt Th (1978): 'Visual-vestibular interaction: effects on self-motion perception and postural control,' In: Handbook of Sensory Physiology, Vol. VIII. Perception. Held R, Leibowitz H, Teuber HL, eds. Berlin-New York: Springer-Verlag, pp. 755-804.

Dichgans J, Diener HC, Brandt Th (1974): 'Optokinetic-Graviceptive Interaction in Different Head Positions,' Acta Otolaryng. 78:391-398.

Dichgans J, Held R, Young LR, Brandt Th (1972): 'Moving Visual Scenes Influence the Apparent Direction of Gravity,' Science 178:1217-1219.

Dichgans J, Nauck B, Wolpert E (1973): 'The influence of attention, vigilance and stimulus area on optokinetic nad vestibular nyatagmus and voluntary saccades,' in The Oculomotor System and Brain Function, Zikmund ed. London: Butterworths, pp. 281-294.

Doslak MJ, Dell'Osso LF, Daroff RB (1979): 'A model of Alexander's Law of vestibular nystagmus," Biological Cybernetics 34:181.

Dowling JE and Dubin MW (1984): 'The vertebrate retina,' in Handbook of Physiology, Section 1: The Nervous System, Volume III, Sensory processes, Part 1. American Physiological Society.

Dubois MFW and Collewijn H (1979): 'Optokinetic Reactions in Man Elicited by Localized Retinal Motion Stimuli,' Vision Research 19:1105-1115.

Engelken EJ and Stevens KW (1990): 'A New Approach to the Analysis of Nystagmus: An Application for Order-Statistic Filters,' Aviation, Space, and Environmental Medicine 61(9):859-864.

Ferman L, Collewijn H, Jansen TC, Van den Berg AV (1987): 'Human Gaze Stability in the Horizontal, Vertical and Torsional Direction during Voluntary Head Movements, Evaluated with a Three-Dimensional Scleral Induction Coil Technique,' Vision Res. 27(5):811-828.

Finke RA and Held R (1978): 'State Reversals of Optically Induced Tilt and Torsional Eye Movements,' Perception and Psychophysics 23(4):337-340.

Fluur E (1975): 'A Comparison Between Subjective and Objective Recording of Ocular Counter-Rolling as a Result of Tilting,' Acta Otolaryngol. 79:111-114.

Fox R, Lehmkuhle S, Leguire LE (1978): 'Stereoscopic Contours Induce Optokinetic Nystagmus,' Vision Research 18:1189-1192.

Hain TC and Buettner UW (1990): 'Static roll and the vestibulo-ocular reflex (VOR),' Exp. Brain Res. 82:463-471.

Held R (1970): 'Two modes of processing spatially distributed visual stimulation.' In F.O. Schmidt (Ed.), The Neurosciences: Second Study. New York: Rockefeller University Press. pp. 317-323.

Held R, Dichgans J, Bauer J (1975): 'Characteristics of Moving Visual Scenes Influencing Spatial Orientation,' *Vision Research* 15:357-365

Helmholz H (1966): Handbuch der Physiologischen Optik. Voss, Leipzig.

Henn V, Cohen B, Young LR ed. (1980): Visual-Vestibular Interaction in Motion Perception and the Generation of Nystagmus, *Neurosciences Research Program Bulletin* 18(4), MIT Press.

Howard IP (1990): 'Visual-Vestibular Interactions in Perceived Stability,' presented at *1990 CVS Symposium: "Orientation in Space,"* Rochester, NY.

Howard IP and Cheung B (1987): 'Influence of Vection Axis and Body Posture on Visually-Induced Self-Rotation and Tilt,' in AGARD Symposium: Brussels. "Motion Cues in Flight Simulation and Simulator Induced Sickness"

Howard IP and Evans JA (1963): 'The measurement of eye torsion,' *Vision Research* 3:447-455.

Howard IP and Gonzalez EG (1987): 'Human Optokinetic Nystagmus in Response to Moving Binocularly Disparate Stimuli,' *Vision Res.* 27(10):1807-1816.

Howard IP and Ohmi M (1984): 'The Efficiency of the Central and Peripheral Retina in Driving Human Optokinetic Nystagmus,' *Vision Res.* 24(9):969-976.

Howard IP, Ohmi M, Simpson W (1987): 'Vection and the Spatial Disposition of Competing Moving Displays,' in AGARD Symposium: Brussels. "Motion Cues in Flight Simulation and Simulator Induced Sickness"

Howard IP and Simpson W (1989): 'Human optokinetic nystagmus is linked to the stereoscopic system,' *Exp. Brain Res.* 78:309-314.

Howard IP and Templeton WB (1964): 'Visually-Induced Eye Torsion and Tilt Adaptation,' *Vision Research* 4:433-437.

Jell RM, Ireland DJ, Lafortune S (1984): 'Human Optokinetic Afternystagmus: Slow-Phase Characteristics and Analysis of the Decay of Slow-Phase Velocity,' *Acta Otolaryngologica* 98:462-471

Lafortune S, Ireland DJ, Jell RM (1990): 'Suppression of Optokinetic Velocity Storage in Humans by Static Tilt in Pitch,' *Journal of Vestibular Research* 1:39-48.

Lafortune S, Ireland DJ, Jell RM, Duval L (1986): 'Human Optokinetic Afternystagmus: Charging Characteristics and Stimulus Exposure Time Dependence in the Two-component Model,' *Acta Otolaryngologica* 101:353-360.

Leibowitz HW and Post RB (1982): 'The two modes of processing concept and some implications.' In J. Beck (Ed.) Organization and Representation in Perception. New Jersey: Erlbaum. pp. 343-363.

Leibowitz HW, Post RB, Sheehy JB (1986): 'Efference, Perceived Movement, and Illusory Displacement,' *Acta Psychologica* 63:23-34.

Leibowitz HW, Shupert-Rodemer C, Dichgans J (1979): 'The independence of dynamic spatial orientation from luminance and refractive error,' *Perception and Psychophysics* 25(2):75-79.

Leigh RJ, Maas EF, Grossman GE, Robinson DA (1989): 'Visual Cancellation of the Torsional Vestibulo-Ocular Reflex in Humans,' *Exp. Brain Res.* 75:221-226.

Lichtenberg BK (1979): 'Ocular Counterrolling Induced in Humans by Horizontal Accelerations,' ScD Thesis, Interdepartmental Program in Biomedical Engineering, MIT.

Mach E (1875): Grundlinien der Lehre von den Bewegungsempfindungen. Leipzig: Engelmann.

Malan AR (1985): 'Characteristics of Optokinetic Torsion in Upright and Supine Orientations,' SM Thesis, Department of Aeronautics and Astronautics, MIT.

Matsuo V and Cohen B (1984): 'Vertical Optokinetic Nystagmus and Vestibular Nystagmus in the Monkey: Up-down Asymmetry and Effects of Gravity,' *Exp. Brain Res.* 53:197-216.

Melcher GA and Henn V (1981): 'The Latency of Circular Vection During Different Accelerations of the Optokinetic Stimulus,' *Perception and Psychophysics* 30(6):552-556.

Merfeld, DM (1990): 'Spatial Orientation in the Squirrel Monkey: An Experimental and Theoretical Investigation,' PhD Thesis, Department of Aeronautics and Astronautics, MIT.

Merker B and Held R (1980): 'Eye Torsion and the Apparent Horizon under Head Tilt and Visual Field Rotation,' *Vision Research* 21:543-547.

Miller EF (1961): 'Counterrolling of the human eyes produced by head tilt with respect to gravity,' *Acta Otolaryng.* 54:479-501.

Miyoshi T, Pfaltz CR, Piffko P (1973): 'Effect of Repetitive Optokinetic Stimulation upon Optokinetic and Vestibular Responses,' *Acta Otolaryng.* 75:259-265.

Morrow MJ and Sharpe JA (1989): 'Torsional Optokinetic Nystagmus in Upright and Supine Positions in Humans,' *ARVO Abstracts* 30:51.

Murasugi CM and Howard IP (1989): 'Up-down asymmetry in human vertical optokinetic nystagmus and afternystagmus: contributions of the central and peripheral retinae,' *Exp. Brain Res.* 77:183-192.

Nakayama K and Balliet R (1976): 'Listing's Law, Eye Position Sense, and Perception of the Vertical,' *Vision Res.* 17:453-457.

Petrov AP and Zenkin GM (1973): 'Torsional Eye Movements and Constancy of the Visual Field,' *Vision Research* 13:2465-2477.

Purkinje JE (1820): 'Beiträge zur näheren Kenntnis des Schwindels aus heautognostischen Daten,' *Med. Jb. (Österreich)* 6:79-125.

Raphan T, Matsuo V, Cohen B (1979): 'Velocity storage in the vestibulo-ocular reflex arc (VOR),' *Exp. Brain Res.* 35:229-248.

Raphan T and Cohen B (1988): 'Organizational Principles of Velocity Storage in Three Dimensions,' *Ann. NY Acad. Sci.* 545:74-92.

Raphan T and Schnabolk C (1988): 'Modeling Slow Phase Velocity Generation during Off-Vertical Axis Rotation,' *Ann. NY Acad. Sci.* 545:29-50.

Reschke MF and Parker DE (1987): 'Effects of Prolonged Weightlessness on Self-Motion Perception and Eye Movements Evoked by Roll and Pitch,' *Aviat. Space Environ. Med.* 58(9, Suppl.):A153-158.

Robinson DA (1963): 'A Method of Measuring Eye Movement Using a Scleral Search Coil in a Magnetic Field,' *IEEE Transactions on Biomedical Electronics* 10(4):137-145.

Schiff D, Cohen B, Raphan T (1986): 'Roll OKN and OKAN: Effects of Head Position on Velocity Storage in the Monkey,' *Society for Neuroscience Abstracts* 12(2):774.

Schor CM, Lakshminarayanan V, Narayan V (1984): 'Optokinetic and Vection Responses to Apparent Motion in Man,' Vision Research 24(10):1181-1187.

Seidman SH and Leigh RJ (1989): 'The Human Torsional Vestibulo-Ocular Reflex During Rotation About an Earth-Vertical Axis,' *Brain Research* 504:264-268.

Sherrington CS (1918): 'Observations on the Sensual Role of the Proprioceptive Nerve Supply of the Extrinsic Ocular Muscles,' *Brain* 41:332-343.

Simonsz HJ, Crone RA, de Waal BJ, Schooneman M, Lorentz de Haas HAL (1984): 'Measurement of the mechanical stiffness in cyclotorsion of the human eye,' *Vision Research* 24:961-967.

Skavenski AA, Blair SM, Westheimer G (1981): 'The Effect of Habituating Vestibular and Optokinetic Nystagmus on Each Other,' *J. Neuroscience* 1(4):351-357.

Steinhausen W (1931): 'Über den Nachweis der Bewegung der Cupula in der intakten Bogengangsampulle des Labyrinths bei der natürlichen rotatorischen und calorischen Reizung,' *Pflüg. Arch. ges. Physiol.* 228:322-328.

Tschermak A (1931): 'Optischer Rumsinn," in Handbuch der normalen und pathologischen Physiologie. Bethe A, Bergmann G, Embden G, Ellinger A eds. Berlin: Springer,. Vol. XII/2, pp. 834-100.

Viéville T and Masse D (1987): 'Ocular Counter-rolling during Active Head Tilting in Humans,' *Acta Otolaryngol.* 103:280-290.

Wertheim AH (1990): 'Visual, vestibular, and oculomotor interactions in the perception of object motion during egomotion,' in Perception and Control of Self-Motion, Warren R and Wertheim AH eds. Lawrence Erlbaum Associates, Hillsdale, NJ. pp. 171-217.

Wolfe JM and Held R (1979): 'Eye Torsion and Visual Tilt Are Mediated by Different Binocular Processes,' *Vision Research* 19:917-920.

Wolfe JM and Held R (1980): 'Cyclopean stimulation can influence sensations of self-motion in normal and stereoblind subjects,' *Perception and Psychophysics* 28(2):139-142.

Wolfe JM, Held R, Bauer JA (1980): 'A Binocular Contribution to the Production of Optokinetic Nystagmus in Normal and Stereoblind Subjects,' *Vision Research* 21:587-590.

Wong SCP and Frost BJ (1981): 'The effect of visual-vestibular conflict on the latency of steady-state visually induced subjective rotation,' *Perception and Psychophysics* 30(3):228-236.

Yasui S (1974): 'Nystagmus generation, oculomotor tracking and visual motion perception,' PhD Thesis, Department of Aeronautics and Astronautics, MIT.

Yasui S and Young LR (1975): 'Perceived Visual Motion as Effective Stimulus to Pursuit Eye Movement System,' *Science* 190:906-908.

Young LR, Crites TA, Oman CM (1983): 'Brief Weightlessness and Tactile Cues Influence Visually Induced Roll,' *Adv. Oto-Rhino-Laryng.* 30:230-234.

Young LR, Dichgans J, Murphy R, Brandt Th (1973): 'Interaction of Optokinetic and Vestibular Stimuli in Motion Perception,' *Acta Otolaryng.* 76:24-31.

Young LR, Lichtenberg BK, Arrot AP, Crites TA, Oman CM, Edelman ER (1981): 'Ocular Torsion on Earth and in Weightlessness,' *Annals of the New York Academy of Sciences* 374:80-92.

Young LR, Oman CM, Dichgans JM (1975): 'Influence of Head Orientation on Visually Induced Pitch and Roll Sensation,' *Av. Space Environ. Med.* 46(3):264-268.

Young LR, Oman CM, Watt DGD, Money KE, Lichtenberg BK (1984): 'Spatial Orientation in Weightlessness and Readaptation to Earth's Gravity,' *Science* 225:205-208.

Zee DS, Yee RD, Robinson DA (1976): 'Optokinetic responses in labyrinthine-defective human beings,' *Brain Research* 113:423-428.